

Universität
Rostock



Traditio et Innovatio

Professorship for Agricultural Technology and Process Engineering

Faculty of Agricultural and Environmental Sciences

Thesis

**Investigation of the applicability of wetland biomass for producing hydrochar by
hydrothermal carbonization and its effectiveness for the adsorption of ammonia**

to obtain the academic degree of

Doctor of Engineering (Dr.-Eng.)

in the Agricultural and Environmental Sciences

at the University of Rostock

Submitted by

DipEng. Bassel Ibrahim

from Rostock, Germany

born on 26.09.1975 in Homs, Syria

Rostock, 2018

Gutachter:

1. Gutachter:

Prof. Dr Norbert Kanswohl

Professur für Agrartechnologie und Verfahrenstechnik

Agrar- und Umweltwissenschaftliche Fakultät, Universität Rostock

2. Gutachter:

Prof. Dr.-Ing. Frank Scholwin

Institut für Biogas, Kreislaufwirtschaft und Energie

3. Gutachter

Prof. Dr.-Ing Christina Dornack

Institut für Abfall- und Kreislaufwirtschaft, Technische Universität Dresden

Jahr der Einreichung: 2018

Jahr der Verteidigung: 2019

DEDICATION

I dedicate this work to
my wife Yara and my daughter Ghazal,
who have been my source of inspiration,
who continually provide their moral, spiritual and emotional support

Table of contents

List of abbreviations	vi
List of cods used of raw material and HTC-chars	vii
Symbols used	viii
Figure index	x
Table index	xiii
1 Introduction	1
1.1 Background and problem statement.....	1
1.1.1 Hydrothermal carbonization process (HTC)	1
1.1.2 Ammonia and ammonium	2
1.1.3 Raw materials for the production of HTC-char.....	3
1.2 Research objectives and hypotheses	4
1.3 Overview of the structure of the thesis	5
2 Literature review	7
2.1 Overview of biomass	7
2.2 Biomass conversion technologies	9
2.3 Hydrothermal carbonization of biomass.....	11
2.3.1 Hydrothermal carbonization compared to common biomass processes...	13
2.3.2 Importance of water in hydrothermal carbonization	14
2.3.3 Process flow.....	15
2.3.4 Process parameters	18
2.3.4.1 Reaction temperature	18
2.3.4.2 Reaction time	19
2.3.4.3 Solid load/ biomass to water (B/W) ratio	19
2.3.4.4 pH value.....	20
2.3.4.5 Pressure.....	20
2.3.4.6 Composition of the raw material used	20
2.3.5 Products of HTC.....	21
2.3.5.1 Overview.....	21
2.3.5.2 HTC-char	22
2.3.5.3 HTC-process water	23
2.3.5.4 HTC-gases	24
2.4 Ammonia und ammonium	26
2.4.1 Overview	26

2.4.2	Ammonia and Ammonium in livestock farming.....	26
2.4.3	Ammonia and ammonium equilibrium.....	27
2.4.4	Health and environmental impacts	28
2.4.5	Reduction of ammonia and ammonium emissions.....	29
2.4.5.1	Overview	29
2.4.5.2	Air stripping.....	29
2.4.5.3	Ion exchange	29
2.4.5.4	Biofiltration.....	30
2.4.5.5	Bioscrubber	30
2.4.5.6	Adsorption process	31
2.4.6	HTC-char to bind ammonia.....	31
2.4.6.1	Factors of loading or reactive factors.....	31
2.4.6.2	Intrinsic factors of HTC-char.....	34
3	Materials and methods	36
3.1	Description of raw materials.....	36
3.1.1	Reed.....	36
3.1.2	Typha.....	36
3.1.3	Carex.....	37
3.1.4	Juncus	37
3.1.5	Structural composition of raw materials.....	37
3.2	HTC-experimental apparatus and HTC-process experiments	39
3.2.1	HTC-experimental apparatus.....	39
3.2.2	HTC-process.....	41
3.2.3	Experimental section according to parameters affecting HTC-process ...	42
3.3	Raw material and HTC-char characterization methods	45
3.3.1	Overview	45
3.3.2	Yield of HTC-char and the carbon recovered	45
3.3.3	Elemental analysis	45
3.3.4	Determination of ash content.....	46
3.3.5	pH measurement.....	46
3.3.6	Specific surface area.....	46
3.3.7	Bulk density.....	48
3.3.8	Point of zero charge.....	48
3.3.9	Fourier transform infrared spectrometer.....	48

3.3.10	Preliminary tests of HTC-reactor with bi-distilled water	49
3.3.11	Tests using real substrate	50
3.4	Determination of ammonia removal performance	51
3.4.1	Overview	51
3.4.2	Batch study	51
3.4.2.1	Experimental section according to adsorption parameters	52
3.4.2.2	Quality assurance	54
3.4.2.3	Adsorption isotherm models	54
3.4.2.4	Experiments on regeneration and re-usability studies	56
3.4.2.5	Preliminary test with HTC-chars and commercial activated carbon	57
3.4.3	Fixed-bed column study	58
3.4.3.1	Experimental section of the fixed-bed column studies	58
3.4.3.2	Modelling of fixed-bed column breakthrough	61
3.4.3.3	Experiments on regeneration and re-usability studies	63
3.5	Statistical testing of significance	63
4	Results and discussion	65
4.1	Hydrothermal carbonization experiments	65
4.1.1	Qualitative parameter	65
4.1.2	Effect of the HTC-reaction temperature on HTC-char	66
4.1.2.1	HTC-char yields	66
4.1.2.2	Elemental compositions	67
4.1.2.3	Van Krevelen diagram	70
4.1.2.4	Specific surface area, pore volume and $C_{\text{recovered}}$	71
4.1.2.5	Bulk density	74
4.1.2.6	Biochar acidity/Alkalinity levels	75
4.1.2.7	Statistical testing of significance of the effect of HTC-reaction temperature	75
4.1.3	Effect of the HTC-reaction time on HTC-char	79
4.1.3.1	HTC-char yields	79
4.1.3.2	Elemental compositions	80
4.1.3.3	Specific surface areas	82
4.1.3.4	Bulk density	83
4.1.3.5	Statistical testing of significance of the effect of HTC-reaction time ..	84
4.1.4	Effect of the amount of biomass (solid load) on HTC-char	86

4.1.4.1	Yield and specific surface area of HTC-char.....	86
4.1.4.2	Statistical testing of significance of the effect of solid load	87
4.1.5	Effect of the catalyst and oxidation on HTC-char	87
4.1.5.1	Elemental compositions and yield	87
4.1.5.2	Specific surface areas.....	90
4.1.5.3	Bulk density	90
4.1.5.4	pH value and point of zero charge	91
4.1.5.5	Statistical testing of significance of the effect of the catalyst.....	92
4.1.6	Effect of the particle sizes of raw materials on HTC-char	93
4.1.6.1	Yield and elemental compositions of HTC-char	93
4.1.6.2	Statistical testing of significance of the effect of particle sizes	94
4.1.7	Fourier transform infrared spectroscopy analysis	95
4.1.8	Conclusion.....	97
4.2	Batch adsorption study.....	99
4.2.1	Effect of HTC-reaction temperature on the adsorption performance.....	99
4.2.1.1	Individually comparison between adsorbents	99
4.2.1.2	Statistical testing of significance for the groups of adsorbents	100
4.2.2	Effect of HTC-char type on the adsorption performance	101
4.2.2.1	Individually comparison between adsorbents.....	101
4.2.2.2	Statistical testing of significance for the groups of adsorbents	102
4.2.3	Effect of contact time on the adsorption performance	103
4.2.3.1	Individually comparison between adsorbents.....	103
4.2.3.2	Statistical testing of significance for the groups of adsorbents used ..	105
4.2.4	Effect of initial ammonia concentration on the adsorption performance	106
4.2.4.1	Individually comparison between adsorbents.....	106
4.2.4.2	Statistical testing of significance for the groups of adsorbents	107
4.2.5	Effect of solution pH on the adsorption performance	108
4.2.5.1	Individually comparison between adsorbents.....	108
4.2.5.2	Statistical testing of significance for the groups of adsorbents	110
4.2.6	Effect of adsorbent dosage on the adsorption performance	111
4.2.6.1	Individually comparison between adsorbents.....	111
4.2.6.2	Statistical testing of significance for the groups of adsorbents used ..	112
4.2.7	Sorption isothermes	113
4.2.8	Regeneration and reusable ability studies	117

4.2.8.1	Regeneration test using different regeneration agents	117
4.2.8.2	Regeneration tests	118
4.2.9	Conclusion	121
4.3	Adsorption process in fixed-bed column study	122
4.3.1	Effect of flow rate on the adsorption performance	122
4.3.1.1	Individually comparison between adsorbents	122
4.3.1.2	Statistical testing of significance for the groups of adsorbents	125
4.3.2	Effect of initial ammonia concentrations on the adsorption performance 126	
4.3.2.1	Individually comparison between adsorbents	126
4.3.2.2	Statistical testing of significance for the groups of adsorbents	128
4.3.3	Effect of the bed height on the adsorption performance	129
4.3.3.1	Individually comparison between adsorbents	129
4.3.3.2	Statistical testing of significance for the groups of adsorbents	131
4.3.4	Modelling of fixed-bed column breakthrough	132
4.3.4.1	Thomas model	132
4.3.4.2	Yoon-Nelson model	134
4.3.5	Column regeneration studies	137
4.3.6	Conclusion	139
5	Summary and future work	141
5.1	Background of the work	141
5.1.1	Hydrothermal carbonization of wetland biomasses	141
5.1.2	Adsorption process in batch study	142
5.1.3	Adsorption process in fixed-bed column study	143
5.2	Short review of future work	144
6	Zusammenfassung und zukünftige Arbeit	145
6.1	Hintergrund der Arbeit	145
6.1.1	Hydrothermale Karbonisierung von Moorbiomassen	145
6.1.2	Adsorptionsuntersuchungen in einem Batch-Verfahrensansatz	146
6.1.3	Adsorptionsuntersuchungen in einem Festbett-Säulenansatz	148
6.2	Kurzbetrachtung zu zukünftigen Arbeiten	149
7	References	150
8	Appendix	168

List of abbreviations

ADF	Acid detergent fiber
ADL	Acid detergent liquid
ASTM	American Society for Testing and Materials
BET	Brauner–Emmet–Teller
B/W	Biomass to water ratio
CE	Carbon efficiency
CH ₄	Methane
CO	Carbon monoxide
CO ₂	Carbon dioxide
COOH	Carboxyl groups
Daf	Dry ash-free
Db	Dry basis
FTIR	Fourier-Transform Infrared
HCl	Hydrochloric acid
GHG	Greenhouse gases
HMF	Hydroxymethylfurfural
HNO ₃	Nitric acid
HTC	Hydrothermal carbonization
H ⁺	Proton
H ₂	Hydrogen
H ₂ O	Water
H ₃ O ⁺	Acidic hydronium ions
H/C	Hydrogen-to-carbon atomic ratio
IUPAC	International Union of Pure and Applied Chemistry
MSb	Mean squares between groups
MSw	Mean square within groups
NaOH	Sodium hydroxide
NDF	Neutral detergent fiber
NH ₃	Ammonia
NH ₄ ⁺	Ammonium ion
NH ₄ OH	Ammonium solution
NO ₃ ⁻	Nitrate

OH ⁻	Hydroxide ion
OSHA	Occupational Safety and Health Administration
O/C	Oxygen-to-carbon atomic ratios
pH _{pzc}	Point of zero charge
SNK	Student-Newman-Keuls
SO ₄ ⁻	Sulfate
SSb	Sum of squared deviations between groups
SSw	Sum of squared deviations within groups
TOC	Total Organic Carbon

List of codes used of raw material and HTC-chars

These codes are detailed in materials and method item 3.2.3 Table 2

Ca, J, R, T	Carex, juncus, reed and typha
Ca _N , J _N , R _N and T _N (N= 1- 3 and c)	HTC-chars produced at different reaction temperatures (180, 200, 220 and 230 °C) using citric acid (0.50 g) as catalyst, biomass amount 30 g and particle size 4 mm
Ca _N , J _N , R _N and T _N (N= 5- 10 and c)	HTC-chars produced at 230 °C and different reaction times (1, 3, 5, 7, 12, 15 and 20 h) using citric acid (0.50 g) as catalyst, biomass amount 30 g and particle size 4 mm
Ca ₁₁ , J ₁₁ , R ₁₁ and T ₁₁	HTC-chars produced at 230 °C and 15 h using citric acid as catalyst (0.50 g), biomass amount 50 g and particle size 4 mm
Ca ₁₂ , J ₁₂ , R ₁₂ and T ₁₂	HTC-chars produced at 230 °C and 15 h using citric acid as catalyst (0.05 g), biomass amount 30 g and particle size 4 mm
Ca _p , J _p , R _p and T _p	HTC-chars produced at 230 °C and 15 h using phosphoric acid as catalyst, biomass amount 30 g and particle size 4 mm
Ca _n , J _n , R _n and T _n	Oxidation with nitric acid of HTC-chars from carex, juncus, reed and typha at 230 °C and 15 h using citric acid (0.50 g) as catalyst, biomass amount 30 g and particle size 4 mm
Ca ₁₃ , J ₁₃ , R ₁₃ and T ₁₃	HTC-chars produced at 230 °C and 15 h using citric acid (0.50 g) as catalyst, biomass amount 30 g and particle size 0.50 mm

Symbols used

Symbol	Unit	Explanation
b	$[l\text{ mg}^{-1}]$	Affinity coefficient
C_0	$[mg\text{ l}^{-1}]$	Initial ammonia concentration
C_e	$[mg\text{ l}^{-1}]$	Equilibrium concentration
C_t	$[mg\text{ l}^{-1}]$	Effluent concentration
F	$[ml\text{ min}^{-1}]$	Flow rate
H	$[mm]$	Bed height
i	$[-]$	$= 1, \dots, n$ are sample values
k_f	$[mg\text{ g}^{-1}]$	Freundlich constants in terms of the adsorption capacity
K	$[-]$	Number of groups being compared
K_{th}	$[ml\text{ mg}^{-1}\text{ min}^{-1}]$	Thomas rate constant
$K - 1$	$[-]$	Degrees of freedom between groups
K_{YN}	$[l\text{ min}^{-1}]$	Yoon-Nelson rate constant
m	$[g]$	Mass
M	$[g]$	Amount of adsorbent in the column
n	$[-]$	Freundlich constants related to the adsorption intensity
N	$[-]$	Total number of observations
n_i	$[-]$	Sample size for the i^{th} group
$N - K$	$[-]$	Degrees of freedom within groups
Q	$[mg\text{ g}^{-1}]$	Adsorption capacity
q_0	$[mg\text{ g}^{-1}]$	Adsorption capacity of the bed
q_e	$[mg\text{ g}^{-1}]$	Equilibrium adsorbate uptake
q_m	$[mg\text{ g}^{-1}]$	Monolayer maximum adsorption capacity
R	$[\%]$	Removal efficiency
R^2	$[-]$	Correlation coefficient
T_e	$[h]$	Time required for bed exhaustion
T_b	$[h]$	Breakthrough time
t	$[min]$	Sampling time
τ	$[min]$	Time required for 50 % adsorbate breakthrough
v	$[l]$	Solution volume
x_{ij}	$[-]$	Demonstrate the data from the i^{th} group (level) and j^{th} observation.

\bar{x}	[-]	Mean sample i (i= 1,2K)
\bar{x}_t		Demonstrate the grand mean
β_0	[-]	Intercept parameter, the value predicted for the response variable when the explanatory variable takes the value zero.
β_1	[-]	Slope parameter is the change in the response variable predicted when the explanatory variable is increased by one unit.

Figure index

Figure 1: Overview of the structure of the thesis	6
Figure 2: Illustration of lignocellulosic composition of biomass with cellulose, hemicellulose and building block of lignin (Alonso et al., 2012).....	7
Figure 3: Thermochemical conversion process of biomass (Zhang et al., 2010; Balat et al., 2009).....	10
Figure 4: Van Krevelen diagram based on O/C and H/C atomic ratios (adapted from Mumme et al., 2011)	12
Figure 5: Schematic composition of energy and material flows of different conversation methods based on carbon efficiency (CE) and on the stored combustion energy (Titirici et al., 2007b)	13
Figure 6: Physical properties of water with temperatures at 24 MPa (Kritzer, 2004)...	14
Figure 7: Overview of relevant reaction mechanisms of hydrothermal carbonization (Kruse et al., 2013).....	16
Figure 8: Distribution of HTC-products (comply with Libra et al., 2011).....	21
Figure 9: Effect of pH and temperature on the equilibrium of ammonia and ammonium (Sawyer and McCarty, 1978)	28
Figure 10: Factors influencing the removal of ammonia in aqueous solution using HTC-char as adsorbent	32
Figure 11: Schematic diagram of HTC-apparatus (Ibrahim et al., 2014).....	39
Figure 12: Experimental apparatus of the hydrothermal carbonization	40
Figure 13: Scheme of HTC-char production trials	41
Figure 14: IUPAC classification of adsorption isotherm (Sing et al., 1985).....	47
Figure 15: Temperature and pressure curves during the tightness test of HTC-reactor using bi-distilled water at different reaction temperatures.....	49
Figure 16: Temperature and pressure curves during the test period of HTC-process for producing of HTC-char of reed at 230 °C and 20 h using citric acid as catalyst.....	50
Figure 17: Adsorption capacities of ammonia on two commercial activated carbon (AC ₁ and AC ₂) and HTC-chars produced from reed (R), typha (T), juncus (J) and carex (Ca)	57
Figure 18: Schematic diagram for the adsorption experiments using a fixed-bed column of HTC-chars as adsorbents	59

Figure 19: Adsorption and regeneration experimental unit for adsorption using a fixed-bed column of HTC-chars	60
Figure 20: Raw material and HTC-char produced	65
Figure 21: Effect of the variation of reaction temperatures between 180-230 °C on the yield of HTC-char produced	66
Figure 22: H/C and O/C atomic ratios of the raw materials used and HTC-chars produced at 180 and 230 °C (Ibrahim et al., 2014)	70
Figure 23: Effect of the variation of reaction temperatures between 180-230 °C on the specific surface area of HTC-chars produced from reed	72
Figure 24: Adsorption/desorption isotherm of reed (A), typha (B), juncus (C) and carex (D) and their HTC-chars produced at 230 °C.....	73
Figure 25: Effect of the variation of reaction temperatures between 180-230 °C on the bulk density of HTC-chars	74
Figure 26: The yield of the HTC-chars produced at different reaction temperatures 180-230 °C and 15 h using citric acid as catalyst as boxplots.....	78
Figure 27: Effect of the variation of reaction times between 1-20 h on the yield of HTC-chars produced at 230 °C using citric acid as catalyst	79
Figure 28: Effect of the variation of reaction times on the elemental compositions of HTC-chars produced from reed (A), typha (B), juncus (C) and carex (D) .	80
Figure 29: Van Krevelen diagram based on O/C and H/C atomic ratios of the raw materials used and HTC-chars produced at different reaction times	81
Figure 30: Effect of the variation of reaction times on the specific surface area of the HTC-chars produced at 230 °C using citric acid as catalyst	82
Figure 31: Effect of the variation of reaction times on the bulk density HTC-chars produced at 230 °C	83
Figure 32: Oxygen proportion in HTC-chars produced at different reaction times 1-20 h and 230 °C using citric acid as catalyst as boxplots.....	85
Figure 33: Effect of the variation of solid load on the yield (A) and BET-measurement (B) of HTC-chars produced, biomass amount: $M_1 = 30$ g, $M_2 = 50$ g	86
Figure 34: Effect of catalyst and oxidation on specific surface area of HTC-chars produced at 230 °C and 15 h	90
Figure 35: Effect of catalyst and oxidation on bulk density of HTC-Chars produced at 230 °C and 15 h.....	91
Figure 36: Effect of the particle size on the elemental analysis of HTC-chars	94

Figure 37: FTIR of HTC-chars from reed and typha produced at 15 h using citric acid as catalyst at different reaction temperature (180-230 °C).....	96
Figure 38: Effect of the variation of HTC-reaction temperature on the adsorption capacity of HTC-chars (Ibrahim et al., 2018).	99
Figure 39: Adsorption capacity of the groups of adsorbents containing HTC-chars produced at different HTC-reaction temperatures as boxplots	101
Figure 40: Effect of contact time on the removal efficiency rate of HTC-chars.....	104
Figure 41: Effect of initial ammonia concentration on the removal efficiency rate of HTC-chars (Ibrahim et al., 2018).....	106
Figure 42: Effect of solution pH on the removal efficiency rate (Ibrahim et al., 2018).....	108
Figure 43: Removal efficiency at different solution pH for adsorbents before oxidation with nitric acid as boxplots	111
Figure 44: Adsorption isotherm for adsorbents prepared from HTC-chars produced from reed (A), typha (B), juncus (C) and Carex (D)	115
Figure 45: Effect of different regeneration agents on the adsorption capacity of adsorbents used	117
Figure 46: Effect of number of regeneration cycles on the adsorption capacity	119
Figure 47: Effect of the flow rate on the removal efficiency of adsorbents prepared from reed (A) and typha (B) while using phosphoric acid as catalyst and from reed (C) and typha (D) after oxidation with nitric acid.....	123
Figure 48: Effect of initial ammonia concentrations on the breakthrough curves for ammonia removal on R_p and T_p (A), R_n and T_n (B).....	126
Figure 49: Breakthrough capacity at different initial ammonia concentrations	127
Figure 50: Effect of the bed height on the length of unused bed of adsorbents	130
Figure 51: Thomas model at different flow rates for adsorbents produced using phosphoric acid as catalyst R_p (A) and T_p (B) and after oxidation with nitric acid R_n (C) and T_n (D).....	132
Figure 52: Yoon-Nelson model at different flow rates for adsorbents produced using phosphoric acid as catalyst R_p (A) and T_p (B) and after oxidation with nitric acid R_n (C) and T_n (D).....	135
Figure 53: Profiles of three regeneration cycles of the exhausted adsorbent	137
Figure 54: Breakthrough curves for ammonia adsorption using adsorbent before and after regeneration	138

Table index

Table 1: Structural composition of the biomass used (Ibrahim et al., 2018).....	38
Table 2: Process parameters and HTC-char codes for studying the effect of the variation of each HTC-process parameter on the properties of HTC-chars.....	44
Table 3: Characteristics of commercial activated carbon used	52
Table 4: Basic one-way ANOVA table (Ostertagová and Ostertag, 2013).....	64
Table 5: Characterizations of the raw material and HTC-chars produced at different reaction temperatures	68
Table 6: Surface area, pore volume and $C_{\text{recovered}}$ of raw materials and their HTC-chars.....	71
Table 7: Analysis of variance and lack of fit test for the influence of the reaction temperatures on the properties of HTC-chars produced	76
Table 8: Means and standard error (SNK method) of different terms for the influence of reaction temperature on the properties of HTC-chars produced at 15 h using citric acid as catalyst	77
Table 9: Means and standard error (SNK method) of different terms for the influence of reaction time on the properties of HTC-chars produced at 230 °C using citric acid as catalyst	84
Table 10: Means and standard error of different terms for the influence of solid load ($M_1= 30$ g, $M_2= 50$ g) on the properties of HTC-chars produced at 230 °C and 15 h using citric acid as catalyst.....	87
Table 11: Effect of catalyst used and oxidation on the properties of HTC-chars produced at 230 °C and 15 h	89
Table 12: The pH value of HTC-chars produced at 230 °C and 15 h.....	91
Table 13: Point of zero charge of HTC-chars of reed and typha produced at 230 °C....	92
Table 14: Means and standard error of different terms for the influence of the catalyst used on the properties of HTC-chars produced at 230 °C and 15 h.....	93
Table 15: Effect of the particle size of raw materials on the yield of HTC-chars produced at 230 °C and 15 h	93
Table 16: Means and standard error of different terms for the influence of the particle size on the properties of HTC-chars produced at 230 °C and 15 h using citric acid as catalyst	94
Table 17: Functional groups of HTC-char samples according to the FTIR spectrum ...	95

Table 18: Means and standard error (SNK method) of the adsorption capacities of the groups of adsorbents containing HTC-chars produced at different HTC-reaction temperatures using citric acid as catalyst	100
Table 19: Effect of the variation of the adsorbents prepared from different HTC-char types on the ammonia removal efficiency rate (R [%]) of HTC-chars	101
Table 20: Means and standard error (SNK method) of different terms for the effect of HTC-char type on the adsorption performance of the groups of adsorbents used	103
Table 21: Means and standard error (SNK method) of different terms for the effect of the contact time on the adsorption performance of adsorbents before and after oxidizing with nitric acid	105
Table 22: Means and standard error (SNK method) of different terms for the effect of ammonia concentration on the adsorption performance of adsorbents before and after oxidizing.....	107
Table 23: Means and standard error (SNK method) of different terms for the effect of the solution pH on the adsorption performance of adsorbents before and after oxidizing with nitric acid	110
Table 24: Effect of the variation of the adsorbent dosage on the ammonia removal efficiency rate (R [%]) and the adsorption capacity (q_e).....	111
Table 25: Means and standard error (SNK method) of different terms for the effect of the adsorbent dosage on the adsorption performance of adsorbents before and after oxidizing.....	113
Table 26: Parameters obtained from Langmuir and Freundlich isotherms for the adsorbents used (Ibrahim et al., 2018)	114
Table 27: Effect of different regeneration agents on the regeneration ratios of the adsorbents produced.....	118
Table 28: Effect of number of regeneration cycles on the regeneration ratios.....	119
Table 29: Breakthrough time (T_b) and breakthrough capacity ($Q_{0.5}$) at different flow rates	122
Table 30: Means and standard error (SNK method) of breakthrough time (T_b), breakthrough capacity ($Q_{0.5}$) and time required for bed exhaustion (T_e) at different flow rates	125
Table 31: Means and standard error (SNK method) of breakthrough time (T_b), breakthrough capacity ($Q_{0.5}$) and time required for bed exhaustion (T_e) at different initial ammonia concentrations	128
Table 32: Predicted breakthrough times (T_b), breakthrough capacity ($Q_{0.5}$) and time required for bed exhaustion (T_e) for adsorbents used with different bed heights	129

Table 33: Means and standard error of breakthrough time (T_b), breakthrough capacity ($Q_{0.5}$) and time required for bed exhaustion (T_e) for the effect of bed height on the adsorption performance of adsorbents	131
Table 34: Parameters predicted by Thomas model for different adsorbents at different initial concentrations of ammonia	133
Table 35: Parameters predicted by Yoon-Nelson model at different initial concentrations	136
Table 36: Predicted time required for breakthrough times (T_b), breakthrough capacity ($Q_{0.5}$) and bed exhaustion time (T_e) for adsorbents used before and after regeneration.....	139

1 Introduction

1.1 Background and problem statement

1.1.1 Hydrothermal carbonization process (HTC)

Some properties of biomass make it unsuitable for use as energy feedstock, in carbon sequestration or improvement of soil fertility (Libra et al., 2011). However, not only does biomass have an interesting internal structure, it also has the advantage of being available in large quantities at low cost. Therefore, pre-treatment technologies can be used to develop the characteristic of biomass and convert it into useful and homogenous products, more efficient energy carriers or carbon storage deposits (Pala et al., 2014). Different biological or thermo-chemical processes can be used to convert biomass into materials with higher carbon content than the original biomass.

Hydrothermal carbonization process (HTC) is a thermo-chemical process at temperatures ≥ 180 °C for the conversion of organic material, which can improve the properties of biomass. Wet biomass can be transformed into carbonaceous materials with no request to be dried before or during HTC-process (Libra et al., 2011).

During HTC, the solid material is surrounded by water, which is heated up to more than 180 °C (Mumme et al., 2011; Schneider et al., 2011; Funke and Ziegler, 2010; Heilmann et al., 2010). Recently, HTC-process has attracted a great attention as it uses water, which is naturally present in biomass. Water is a non-toxic, environmentally, friendly and inexpensive medium (Libra et al., 2011).

When HTC-char is used in heating, large amounts of greenhouse gases (GHG) emissions can be mitigated compared with the fossil-derived sources of energy. Due to its reaction temperature, HTC-process is seen as a potential and an innovative method to convert problematic biomass like bio-waste, sewage sludge and fermentation residue in a renewable, sterile and hygienic solid product (Dea Marchetti, 2009). Under certain condition, HTC can become profitable and be economically in competition with fossil energy sources. The technological development of HTC-process and the potential for cost reduction will have an essential role in this respect (Zeymer et al., 2017). Moreover, non-fossil carbon sources such as biomass present promising renewable energy carrier. HTC-char is a low-cost adsorbent with many potential environmental applications. The exhausted HTC-char can be applied directly as fertilizer with no need to be regenerated.

1.1.2 Ammonia and ammonium

The public interest in environmental damage caused by air and water pollutants has increased in the recent years. The common term of pollutants is disputed, whether a gas causes a damage is depended on its concentration and duration of action as well as the interaction with other existing components (Hillinger, 1990).

Air and water pollutants affect human and animal health and their well-being; they contribute also to environmental pollution. The current air pollution policy in Europe has set the objective of limiting the so-called "critical loads" (Eurich-Menden et al., 2003) for numerous substances, including ammonia. Water is a valuable natural resource, so that it is a relatively recent concern and becomes more attention on its purification.

Ammonia (NH_3) is one of the most abundant found nitrogen-containing compounds in the atmosphere, it is an undesirable contaminant because of its negatively impact on air and water quality and its potential to create odors (Chung et al., 2005; Gue et al., 2004). The relative proportion of ammonia emissions from animal husbandry to the total emissions of nitrogen compounds has been increasing (Eurich-Menden, et al., 2003). Therefore, emissions reductions of ammonia from livestock production plants can make an ecologically relevant and economically effective contribution.

Ammonium (NH_4^+) is an inorganic nitrogen contamination. It is discharged in context of agricultural wastes and industrial or municipal effluents; it is responsible for harmful effects and toxicity to aquatic life (Yusof et al., 2010; Balci and Dince, 2002).

NH_3 and NH_4^+ are familiar by-products of animal and agriculture waste as well as the industrial activities. About 99 % of ammonia in the atmosphere releases by the decomposition of organic waste (WHO, 1986). Organic substances such as urine releases ammonia during its biological degradation by microorganisms (Aneja et al., 2000; Allen et al., 1988).

In an aqueous solution, equilibrium exists between ionized form (NH_4^+) and unionized form (NH_3) depending on pH-value and temperature. Ammonia and ammonium ions belong to the major impurities that pollute the ecosystem, so that there is a need to treatment air and effluents containing ammonia and ammonium. In order to reduce the environmental impacts of animal production, both national and international regulations dealing with these issues have come into force.

Some traditional techniques are available for water treatment applications, particularly for the removal of ammonia and ammonium ions, including air stripping, ion exchange (Lim et al, 2004; Hung et al, 2003; Jorgensen and Weatherley, 2003; Ilies and Mavinic, 2001), bio-scrubber, bio-filtration, membrane filtration, adsorption by solids (Padmesh and Sekaram, 2005; Parkash and Velan, 2005). However, associated operational and technical maintenance problems, strict monitoring and control of operating conditions and the high costs of these methods restrict their applicability.

Adsorption processes using dry adsorbents is estimated as superior to other methods and is regarded as one of the most effective method because of its selectivity, simplicity of design, flexibility, ease of operation and efficiency (Gue et al., 2004; Sepulveda et al., 2004; Ilies and Mavinic, 2001). Nevertheless, the difficulty of the use of commercially synthetic sorbents such as activated carbon and its regeneration problem (Crini, 2006; Cheremisinoff, 2002; Wilderer, 2002) requested to investigate and develop alternative effective and cheaper adsorbents synthesized of cheap natural or raw agricultural materials. Such materials can be as potential replacements of the expensive commercial adsorbents and can improve the efficiency of ammonia removal.

1.1.3 Raw materials for the production of HTC-char

Due to the increasing demand, the supply of biomass for different utilizations is becoming limited. This is reflected in rising prices of biomass as well as in an area competition between food, feed and energy production.

From a global perspective, Germany is one of the regions rich in wetland areas. They concentrate on the northern and southern states. The surface area covers in Mecklenburg-Western Pomerania approximately 280,000 ha and thus 12 % of the land area (Zeitz et al., 2011). However, the production of biomass from re-wetted or wetland is not in competition with other agricultural products. Biomasses from wetlands are generally of a little use, but have great potential as a renewable energy source.

Besides their use for feed and direct combustion, wetland biomasses can also be applied as a feedstock for industrial biochemistry (Wichtmann et al., 2010). The production of HTC-char from biomasses growing in wetland is a possibility to the use of these biomasses. They are abundant at low costs and their properties can be improved using treatment technologies, which may give them a higher value.

Rapidly growing grassy plants, such as, reed, typha, juncus and carex, belong to the promising sources of plant biomasses. Their short rotation period and abundant content

give favorable application possibilities. In this study, reed (R), typha (T), juncus (J) and carex (Ca) should be selected as a representative of wetland biomasses as substrates for HTC-chars production.

There are very few practical uses of wetland biomasses, other than in HTC, which makes them of particular importance for this process. HTC can be used for the treatment of such biomasses to generate sustainable carbonaceous materials with higher carbon content than the original biomasses. To date, there have been no other comparable studies concerning the carbonization of wetland biomasses and using them as adsorbent especially for ammonia removal (Ibrahim et al., 2018).

Furthermore, these four wetland biomasses were selected because they are widespread and prevailing. Moreover, they are high wetland-adapted flora, which are tolerant of chemically diverse environments (Rogers, 2003).

1.2 Research objectives and hypotheses

The objective of this work was to investigate the applicability of wetland biomass for producing HTC-chars. Another objective was to investigate the application of these HTC-chars as adsorbents for ammonia removal in aqueous solution in order to investigate a value-added utilization approach for these biomasses and their products.

The following three principal questions were in the focus of interest in this study:

Is it available to transform wetland biomasses into a higher value carbonaceous product, which could be designed as a filter that removes pollution in aqueous solution?

How do the type of biomass and the process parameters affect the potential products and their properties?

How do the hydrothermal treatment, oxidation with acid and other adsorption parameters affect the enhancing the ammonia adsorption capacity of HTC-chars?

In this context, the following general hypotheses will guide this study:

- HTC-chars produced from different raw materials can be differentiated from each other because their raw materials contain different proportions and forms of organic biomass building blocks (cellulose, hemicellulose and lignin).
- HTC-chars properties depend significantly on HTC-parameters because of the alteration of the kinetic of the hydrothermal carbonization reactions. Higher reaction temperatures and longer reaction times enhance the reaction severity and develop the properties of HTC-chars produced.

- HTC-chars have a high efficiency for ammonia removal in aqueous solution. Their adsorption performances will be significantly affected by the adsorption process parameters in both batch study and a fixed-bed column study.
- HTC-chars after oxidation with acids have a developed adsorption performance, which could be because the change in the chemical structure of HTC-chars and the increase of adsorption sites on their surfaces.
- The exhausted HTC-chars are regenerable. Due to the desorption of ammonia and the rejuvenation of the activity, the exhausted HTC-chars can be reused their adsorption performances after regeneration several times without loss of.

This work will provide an understanding into the changes in wetland biomass during HTC-process into a useful form. To examine these questions and achieve these aims, the following steps were set:

- Using HTC as a technique for converting the wetland biomasses into HTC-char.
- Investigate the influences of HTC-parameters (reaction temperature, reaction time, raw material type, particle size and catalyst) on the HTC-char properties.
- Implementation of ammonia adsorption in a batch study using different HTC-chars produced and estimating the adsorption parameters (HTC-reaction temperature, the type of HTC-char, adsorption contact time, adsorbent dosage and solution pH value as well as the ammonia concentration on the adsorption performances.
- Implementation of ammonia adsorption in a fixed-bed column for those types of HTC-char samples, which had high adsorption performance and estimating the effect of adsorption parameters (flow rate, initial ammonia concentration and bed height) on the adsorption performances.
- Regeneration of the exhausted adsorbents using different regeneration agents and choice the best one, which ensure the heights regeneration ratio for reusing the adsorbent in adsorption-regeneration cycles.

A key feature of this study is the production of HTC-chars, which has potential value for real application on a larger scale as they are effective for pollutant sequestration.

1.3 Overview of the structure of the thesis

The general overview of the structure of this thesis is illustrated in Figure 1.

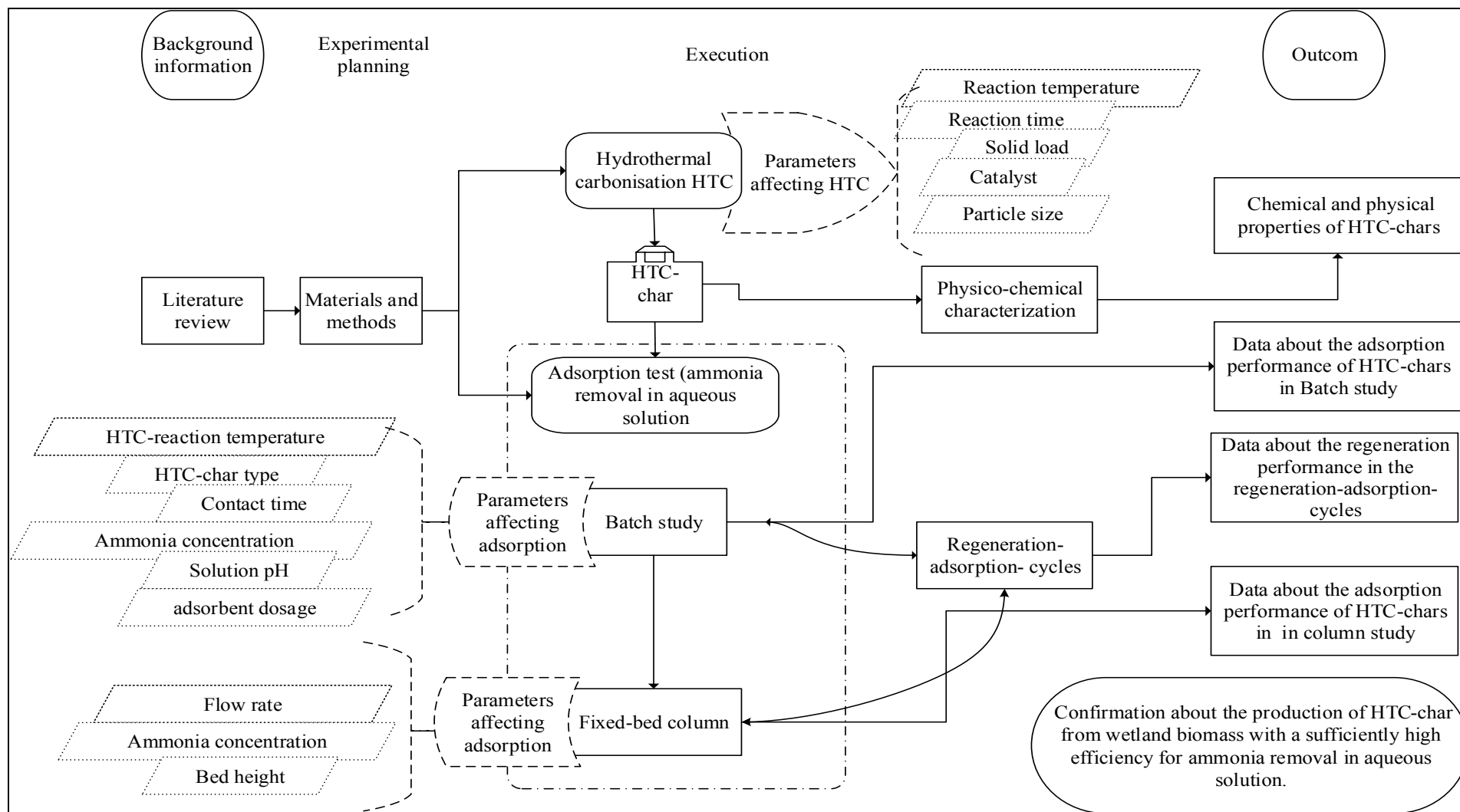


Figure 1: Overview of the structure of the thesis

2 Literature review

2.1 Overview of biomass

Biomass is a renewable resource derived from plants or animals. Biomass is available in many forms as lignocellulosic material like agricultural crops, woody crops and forestry products or non-lignocellulosic materials like municipal solid wastes.

Plant biomass transforms solar radiation into organic matter through the process of photosynthesis. Therefore, biomass can be considered as a stored solar energy (Kaltschmitt et al., 2000). In this case, inorganic compounds with low chemical energy levels (mainly carbon dioxide and water) are synthesized into chemically higher molecular weight organic compounds such as carbohydrates (Lehmann and Joseph, 2009; Neubarth and Kaltschmitt, 2000). Plant biomass, following as raw material, contains various components with different properties. The three main components are cellulose, hemicellulose and lignin as shown in Figure 2. They make together more than 95 % of the plant dry matter (Kaltschmitt et al., 2009).

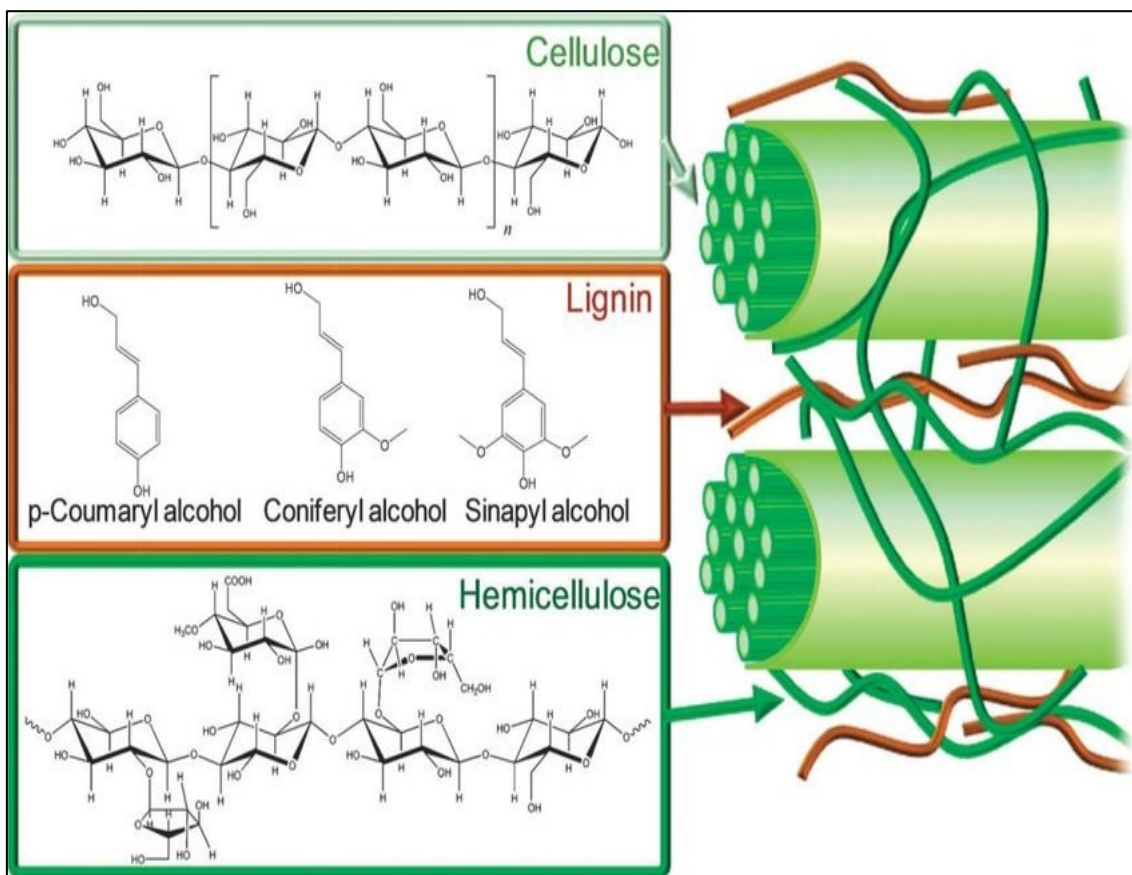


Figure 2: Illustration of lignocellulosic composition of biomass with cellulose, hemicellulose and building block of lignin (Alonso et al., 2012)

Cellulose is among all organic substances the most common in nature; it represents most of the plant cell wall. Depending on the type of biomass, cellulosic composition can range, based on the dry mass, from about 20-35 % in grass to about 38-55 % in wood (Harmsen et al., 2010, Kaltschmitt et al., 2009, Lehmann and Joseph, 2009).

Cellulose is often also considered as polymer of glucose. It consists of a very large number of glucose compounds (several thousands), which form a long unbranched multiple sugar chain. Cellulose can be found in amorphous or crystalline phases (Harmsen et al., 2010; Kaltschmitt et al., 2009). In addition, it is the least complicated and best-defined component of biomass. Cellulose is the main source of combustible volatile fuel of fuel-burning combustion. The crystalline structure makes cellulose more resistant to decomposition than hemicellulose (Lehmann and Joseph, 2009).

Hemicellulose is the second major component of lignocellulosic biomass and has generally lower molecular weight than cellulose. Unlike cellulose, hemicellulose is chemically heterogeneous and readily hydrolyzed to its monosaccharide components (Kaltschmitt et al., 2009; Ezeji et al., 2007). In plant material, hemicellulose makes about 20-30 % based on the dry matter and is responsible of supporting and strengthening plant cells (Kaltschmitt et al., 2009). Hemicellulose is the most active component and is a highly soluble polymer in water. The chemical and thermal stability of the hemicelluloses is lower than that of cellulose due to the lack of crystallinity and lower polymerization degree.

Lignin is the largest non-carbohydrate content of lignocellulose and is the actual filler of lignocellulosic materials. It is an amorphous, high molecular weight polymer.

Lignin is phenolic in nature, very stable and difficult to isolate. It occurs between the cells and cell walls and serves as cement between the wood fibers (Blaschek and Ezeji, 2007; Boerjan et al., 2003; Plomion et al., 2001). Lignin shows the highest energy content of the three fractions (Belderok, 2007). It also has relatively large carbon content against cellulose and hemicellulose (Van de Weerdhof, 2010).

It does not have a well-defined crystalline structure, such as cellulose, but it is amorphous and strongly cross-linked (Harmsen et al., 2010; van de Weerdhof, 2010). Lignin content is usually in the range of 20-30 % in the wood-like biomass, based on the dry mass (Lehmann and Joseph, 2009).

2.2 Biomass conversion technologies

Biomass is a promising renewable resource for energy production by using different processes depending on the requested energy type and variations in biomass characteristics as moisture content and composition (Özbay et al., 2001).

Biochemical processing techniques as fermentation or anaerobic digestion can be used to convert biomass to biofuels throughout a chemical reaction. Biomass with high sugar or starch content is suitable as raw material for fermentation. Lignin is not fermentable, so that acid or enzyme treatments are required while using biomasses like straw or wood as raw materials. In addition to methane formation, bioethanol from biomass can be fermentative formed that can be used as a fuel additive.

Anaerobic digestion is a type of fermentation that convert organic material in an anaerobic and microbial degradation to biogas, which is a mixture of methane and carbon dioxide (Dea Marchetti, 2009). The disadvantage is the limited applicability of biomass. Cellulose- or lignin-containing materials cannot be degraded. Furthermore, these types of conversions need long residence times (several days to months).

Thermochemical conversion is the main process to produce power and heat from biomass. These types of the conversions of biomass have many benefits such as reducing its volume, improvement of transportation abilities, producing renewable energy and reducing greenhouse gas emissions.

The major thermochemical processes are direct combustion, gasification, pyrolysis and liquefaction. Figure 3 shows the thermochemical conversion processes of biomass (Zhang et al., 2010; Balat et al., 2009) and displays that the energy in biomass could be converted into heat by direct use as in combustion, it could also be transformed into gaseous, liquid and solid (carbon rich material) fuels via gasification, pyrolysis and liquefaction.

Combustion may be assigned as fast oxidation of biomass that produces heat at high temperatures. The high moisture content of the feedstock affects the rates of combustion, and increases the pollutant emissions due to the emission of carbon monoxide (Khan et al., 2009). Biomass combustion using conventional combustion technology is principled possible, but requires additional measures and reduces the plant efficiency compared to fossil fuels. Furthermore, the biomass must be dried before combustion.

Gasification is a thermochemical decomposition of biomass at elevated temperatures range of 800-1300 °C in the absence of enough oxygen so that partial combustion may develop resulting in production of gaseous fuel. Biomasses that contain less than 10 % moisture are suitable for gasification. This process likes to be as a combination of combustion and pyrolysis (Rathore et al., 2008).

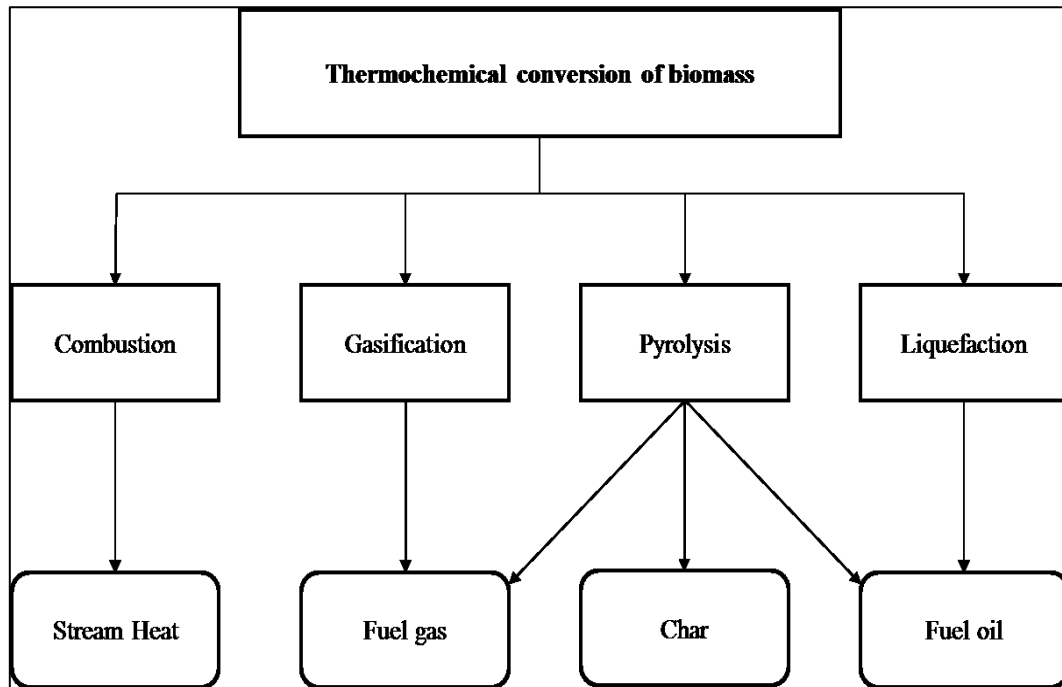


Figure 3: Thermochemical conversion process of biomass (Zhang et al., 2010; Balat et al., 2009)

Pyrolysis is a thermochemical process in which the biomass decomposes at elevated temperatures in the lack of oxygen or when the presented oxygen amount is considerably less than needed for complete combustion. Dry biomasses are usually used for pyrolysis processes, which will be heated at a temperature range of 300-650 °C.

The pyrolysis products strongly depend on the process parameters and biomass composition. The main products are carbon-rich material (biochar) condensable vapors (bio-oil) and “non-condensable” gases (Brownsort, 2009; Mohan et al., 2006).

Liquefaction is a thermochemical process to convert biomass into bio crude or bio oil using water. At reaction temperature of 280-380 °C and pressure of 7-36 MPa (Peterson et al., 2008). A black organic liquid called bio crude or bio oil is the main product of liquefaction. Where solid residue (biochar), water-soluble product and gases are by-products. The products yield of liquefaction of biomass depend on various parameters such as lignin content, the catalyst, the reaction temperature and the reaction time.

Most of these thermochemical processes requires drying the biomass prior to conversion. Energy required to dry biomasses depends obviously on their moisture content. Environmental safety, minimal production of waste, time requirements, energy requirements, investment cost and minimal pre-processing requirements such as drying and process efficiency are important factors while choosing the pretreatment type (Reza, 2011). A new renewable thermochemical technology, which is considered as environmentally friendly process and clean sources of energy, is the hydrothermal carbonization process.

2.3 Hydrothermal carbonization of biomass

In nature, the coal is made of burned materials undergoing heat and pressure treatment over millions of years. Hydrothermal carbonization (HTC) mimics the natural conversion process of biomass into coal, whereby the reaction time here is in the range of a few hours depending on the other process parameters such as pressure, temperature and catalyst (Bergius, 1928).

HTC can be a considerable technical aspect for an interesting alternative for carbon production because it achieves an acceleration of coalification by a factor of 10^6 to 10^9 under rather mild process conditions (Titirici et al., 2007a).

Friedrich Bergius discovered the hydrothermal carbonization in the early 20th century (Bergius and Specht, 1913; Bergius, 1928). Already in 1913, Bergius and Specht described the hydrothermal conversion of cellulose into coal materials. It differs from the above-mentioned processes in that HTC occurs at comparatively lower temperatures ranging from 180-250 °C in a hot compressed water environment.

Since HTC uses water as a reaction medium, wet biomass is particularly suitable as a starting substrate with avoiding any drying pretreatment (Mumme et al., 2011; Schneider et al., 2011; Funke and Ziegler, 2010; Heilmann et al., 2010).

Water splitting under HTC-conditions is considered to play an important role in catalyzing the reaction (Peterson et al., 2008). The biomass components in the hydrothermal medium are less stable. The decomposition of cellulose carried out over approximately 220 °C, hemicelluloses between 180 and 200 °C and most of the lignin between 180 and 220 °C (Libra et al., 2011; Bobleter, 1994).

The reaction mechanism comprises a dehydration of the carbohydrate and polymerization of the dehydration products (e.g. 5-Hydroxymethylfurfural) to produce carbon particles with polar functional groups (Schüth, 2003).

The execution of HTC-process by temperature up to 300 °C or higher was reported by some authors (Liu et al., 2012; Kumar et al, 2011). In HTC-process, decomposition of biogenic material takes place under the influence of heat in the surrounding of water in a closed container under pressure. The reaction pressure is autogenic with the saturation vapor pressure of water correspond with the reaction temperature (Heilmann et al., 2010). HTC is a favorable way to convert biomass in carbonaceous materials under moderate conditions. Moreover, the carbon product can be easily separated by filtration. HTC-char has a chemical structure that is similar to natural coal with lower oxygen-to-carbon atomic ratios (O/C) and hydrogen-to carbon atomic ratio (H/C) than those are of the raw material. The changes of theses atomic ratios during HTC can be clearly examined in the Van Krevelen diagram (Figure 4).

The Van Krevelen diagram cross plots H/C atomic ratio in relation to O/C atomic ratio and presents the typical ranges for biomass, peat, lignite, coal, and anthracite (Van Krevelen, 1950). This diagram was developed to describe the changes of elemental composition during coal formation.

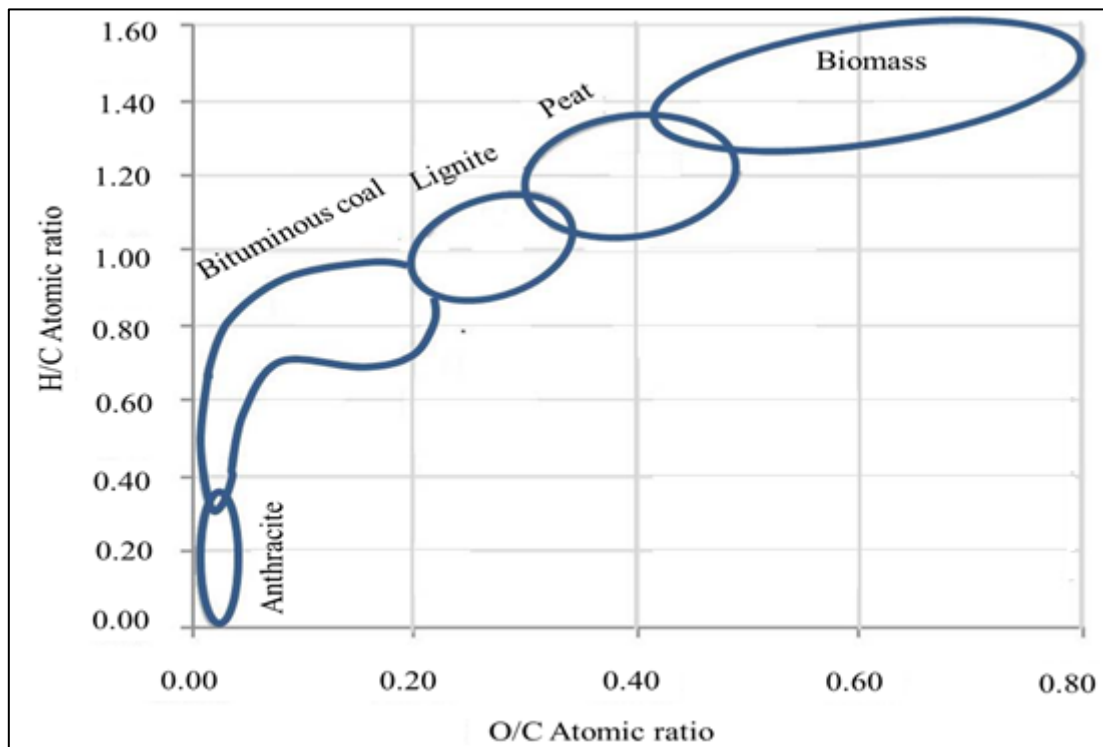


Figure 4: Van Krevelen diagram based on O/C and H/C atomic ratios (adapted from Mumme et al., 2011)

HTC-chars are attractive for use in many different applications including soil improvement, catalysis, surface adsorption and energy storage (Titirici and Antonietti,

2010). It can also be used as solid fuels to replace brown coal and is suitable for use in wastewater treatment and recycling. Therefore, HTC can act as a model system for a green and sustainable process to transfer low value and widely available biomass in carbon-neutral materials (Titirici and Antonietti, 2010).

2.3.1 Hydrothermal carbonization compared to common biomass processes

HTC is an exothermic process. Up to a third of the combustion energy stored in the carbohydrate will be liberated through dehydration during HTC (Titirici et al., 2007b). Figure 5 shows a schematically comparison of the energy and material flows (expressed by a carbon efficiency) of HTC with those of the prevalent biomass conversion processes. HTC has the highest efficiency for carbon fixation; the described path of HTC binds in a chemical process nearly 100 % of the original carbon, while the carbon efficiencies (CEs) of fermentation and anaerobic digestion are 66 % and 50 %, respectively. The derived energy from HTC-char used as a solid fuel can be more than it is from the gases resulting from anaerobic digestion. In addition, the reaction time of HTC only takes hours to one day compared to days or months required for biological processes. Furthermore, the process temperatures inactivate potential contaminants making the outputs products hygienic (Libra et al., 2011).

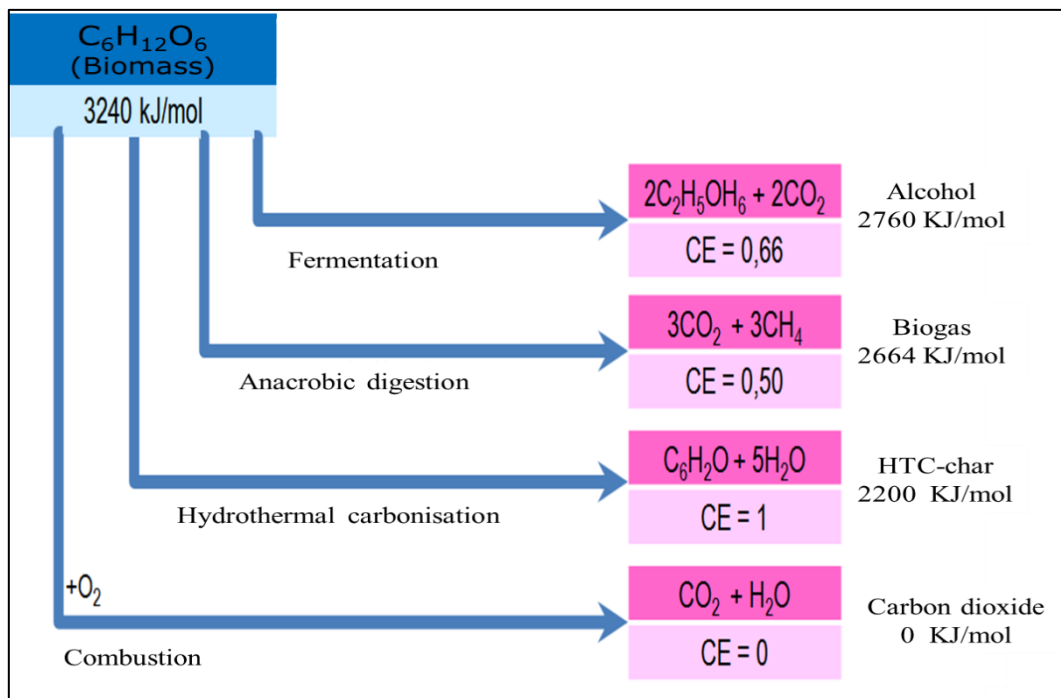


Figure 5: Schematic composition of energy and material flows of different conversion methods based on carbon efficiency (CE) and on the stored combustion energy (Titirici et al., 2007b)

Considering the relatively high-energy consumption in dry carbonization processes as pyrolysis, hydrothermal reaction is principally more favorable for biomasses containing moisture (Libra et al., 2011; Erlach and Tsatsaronis, 2010), which is because HTC-process needs lower reaction temperature and the energy intensive drying before the reaction can be avoided.

In contrast to pyrolysis, HTC generates higher char yields and more water-soluble organic components. A little gaseous oxidation results from HTC due to a limited exposure to oxygen. Therefore, HTC is more environmentally friendly; it can be applied for a wide range of biomasses with no competition with food production. HTC can also treat the wastes problems that presently need expensive disposal.

2.3.2 Importance of water in hydrothermal carbonization

Water is a non-toxic and abundantly universal solvent in nature and is intrinsically existent in the wet biomass. The critical point of water (374 °C and 22.1 MPa) is relatively high due to the forceful interaction between the molecules. Subcritical water is the liquid water below the critical point, whereas is supercritical water is that above the critical point. Increasing the temperature leads to a significant change in the physical and chemical properties of water. Its density, surface tension and viscosity drop at elevated temperatures. At reaction temperatures of 200, 300, 370 and 500 °C (Figure 6) water has a similar dielectric behavior to that of ambient methanol, ambient acetone, methylene chloride, ambient hexane, respectively, which improves the solubility of organic components of biomass.

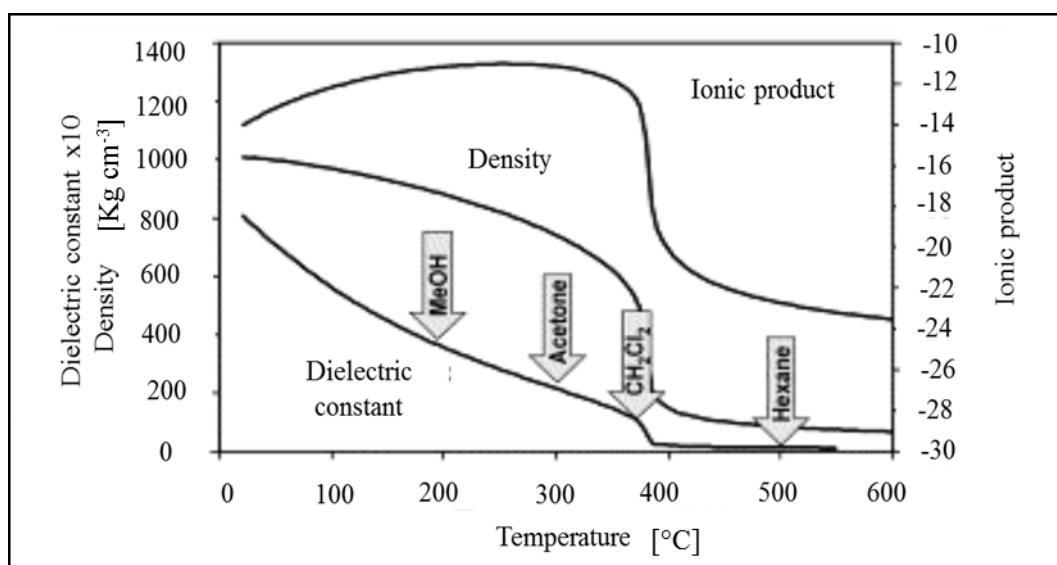


Figure 6: Physical properties of water with temperatures at 24 MPa (Kritzer, 2004)

Hot pressurized water works both as a catalyst and as a reactant (Yu et al., 2008). Water molecules can act as both base and acid catalyst for biomass component reactions. Heating the water results in weakening the H-bonding allowing dissociation of water into basic hydroxide ions (OH^-) and acidic hydronium ions (H_3O^+).

Moreover, Water is useful in the dissolution of hemicelluloses, especially at temperatures above 180 °C. Under wet conditions, hemicelluloses and cellulose conversion occurs at lower temperatures than those reported for dry processes, because of reducing of activation energy level of hemicellulose and cellulose, which enhances the degradation of these polymers (Libra et al., 2011).

The enhanced transport and soluble properties of the subcritical play an important role in the conversion of biomass to high-energy fuels and functional materials (Hu et al., 2008). Complete coverage of the biomass with water during HTC prevents air termination, which averts a reaction in the form of coking or combustion. Furthermore, the existing inorganic component in the biomass could drift in the HTC-process water and thus can reduce the ash content of the solid product.

2.3.3 Process flow

In HTC, a mixture of solid material and water is heated in a pressure resistant reactor and at a reaction time of a few hours to one day (Heilmann et al., 2011). During the HTC of biomass, organic acids are split off, which acidify the reaction medium. The pH of HTC-process reaction water is commonly low. Above 120 °C, organic materials in the biomass subjected to hydrothermal decomposition (Lehmann and Joseph, 2009).

In general, during HTC, many reactions could present at subcritical temperature as shown in Figure 7, including hydrolysis, dehydration, decarboxylation, condensation, polymerization and aromatization (Libra, et al., 2011; Funke and Ziegler, 2010) resulting in the production of gas, liquid and solid (HTC-char). These reactions cannot clearly divide into separated reaction steps.

The detailed nature of these reaction pathways depends on the type of biomasses used (Funke and Ziegler, 2010). It can only be formulated for individual pure substances such as glucose, cellulose or lignin. The hydrothermal degradation is mainly governed by hydrolysis, which has lower activation energy than most of the pyrolytic decomposition reactions (Mok et al., 1992). This reaction breaks the ester and ether bonds of hemicellulose (at $T > 180$ °C), cellulose (at $T > 220$ °C), and lignin (at $T > 200$

°C) by addition of water (Libra et al., 2011). Complete hydrolysis of both lignin and cellulose probably will not occur (Kruse et al., 2013).

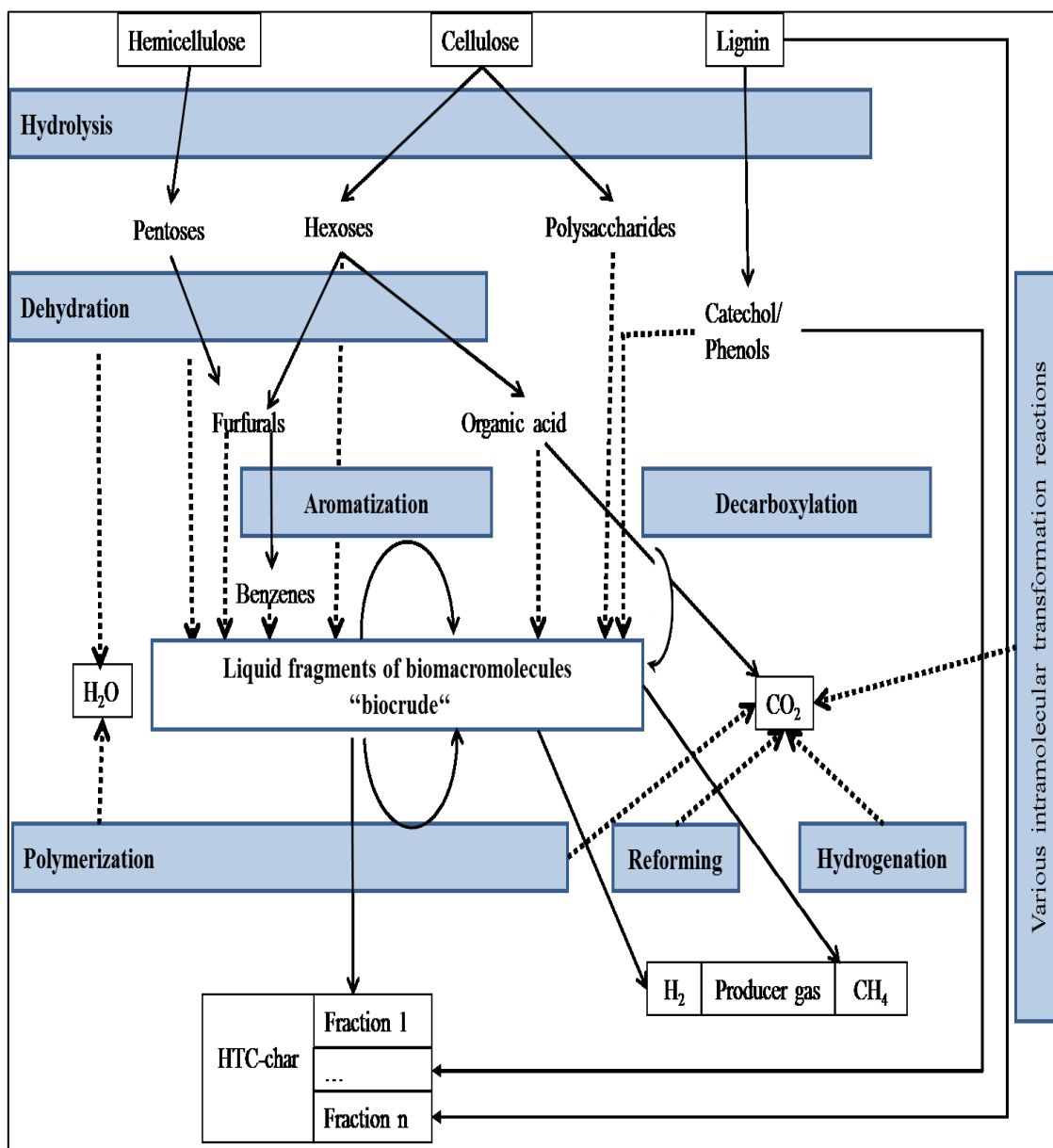


Figure 7: Overview of relevant reaction mechanisms of hydrothermal carbonization (Kruse et al., 2013)

Literature studies showed that after the hydrolysis, reactants would then undergo dehydration. In particular, the production of HMF, one of the most important precipitates of the process, is formed by dehydrogenation reactions (Knezevic et al., 2010; Yu et al., 2008). During HTC, dehydration can involve both chemical and physical reactions. The physical process is known as dewatering in which the bound water is removed from the biomass matrix without changing its chemical composition during HTC (Reza et al., 2012; Acharjee et al., 2011).

Chemical dehydration can occur due to the elimination of hydroxyl groups. During chemical dehydration, the biomass is carbonized with decreasing H/C and O/C atomic ratios (Seville and Fuertes, 2009a). It is reported that the main part of HTC-gas is CO₂ (Hoekman et al., 2011; Kobayashi et al., 2010). Hydrothermal treatment induces a partial elimination of carbonyl groups (Lau et al., 1987).

Carbonyl (C=O) and carboxyl (-COOH) groups are degraded during decarboxylation that generates CO₂ and CO, respectively. This process occurs rapidly at temperatures above 150 °C (Seville and Fuertes, 2009b).

A possible route to decarboxylation under hydrothermal conditions involves degradation of extractives, hemicellulose and cellulose into monomers such as formic acid, acetic acid and furfurals, which are further degraded to CO₂ and H₂O (Hoekman et al., 2013; Yan et al., 2009). The lowering of H/C and O/C atomic ratios during HTC is mainly explained by dehydration and decarboxylation mechanisms. These mechanisms explain the lower O/C and H/C atomic ratios by removing oxygen and hydrogen.

The generated fragments can also undergo condensation, polymerization or aromatization. Condensation is most likely predominant with the formation of H₂O. Higher reaction temperatures and longer reaction times improve poly-condensation (Funke and Ziegler, 2010). Thus, it is likely that the formation of HTC-char during hydrothermal carbonization is mainly characterized by condensation and polymerization (Kabyemela et al., 1999; Nelson et al., 1984). Although hemicellulose and cellulose consist of carbohydrates, they can form aromatic structures under hydrothermal conditions. Aromatic structures resulting from the aromatization of the polymer under hydrothermal conditions at high reaction conditions of pressure and temperature are very stable and are regarded as building blocks of HTC-chars produced (Funke and Ziegler, 2010). The crosslinking condensation of aromatic compounds also compensates for the main components of natural coal (Stach et al., 1982). This might explain the good consensus between natural and hydrothermal carbonization coalification.

Other mechanisms as demethylation, transformation reactions and pyrolytic reactions can be involved in HTC (Xiao et al., 2012; Funke and Ziegler, 2010). Demethylation involves the removal of a methyl group from the molecule and results in phenol (Hatcher et al., 1994).

Transformation reactions in lignin molecule may take place instead of hydrolysis and the subsequent condensation cannot happen, principally for stable compounds with a crystalline structure and oligomer fragments, which do not hydrolyze (Peterson et al.,

2008). In the case of using biomass with little lignin content, the original physical structure of the material is in principle completely resolved. Pyrolytic reactions may become significant at reaction temperatures above 200 °C (Kaltschmitt et al., 2009).

HTC-process is principally conducted by the following parameters: raw material composition, reaction temperature, pressure, reaction time, biomass to water (B/W) ratio and pH, which affect the structure of HTC-char (Lehmann and Joseph, 2009). These parameters play a key role in several reactions that occur in the carbonization process to produce compounds with different physical and chemical properties.

2.3.4 Process parameters

2.3.4.1 Reaction temperature

Reaction temperature is considered to play an essential role in the hydrothermal carbonization and appears to be most influencing parameter on the properties of HTC-products. High reaction temperatures result in higher reaction rates and have an important effect on the number of biomass components that can be hydrolyzed.

It was found that the presumed reference temperature of the HTC was set to 170 °C (Bergius, 1928). In the case of cellulosic biomass, no changes have been observed with HTC at temperatures below 180 °C, since hydrolysis, the first reaction of HTC-process, begins at this temperature (Titirici et al., 2007b). It can be assumed that the reference temperature, from which first reactions occur is strongly dependent on the composition of the biomass used (Funke, 2012).

Many researchers investigated the effect of the reaction temperature on the yields of HTC-chars while using different biomasses (Wiedner et al., 2013; Yan et al., 2009; Huber et al., 2006). All authors agreed that increasing the reaction temperature reduces the solid yield, since several of the biomass components are reacted at a higher reaction temperature. The mainly decomposition of the solid biomass or the further degradation of part of the char generated results in a decrease in the solid yield and generates more gaseous and liquid products.

In fact, the increase of reaction temperatures favors the dehydration and the decarboxylation reactions, which decrease the of oxygen and hydrogen proportions of the treated biomass and enhance the carbon proportion of the HTC-char produced.

Both high reaction temperatures and longer reaction times enhance the reaction severity. Higher reaction severity leads to higher carbon proportion of the HTC-char (Funke and Ziegler, 2010). Both reaction temperatures and reaction times influence the HTC-char

properties. However, HTC at higher reaction temperatures produces chars that are more aromatic consistent with their lower H/C and O/C ratios.

2.3.4.2 Reaction time

Hydrothermal carbonization of biomass is a comparatively slow process. However, typical reaction times range between 1-72 h (Mukherjee et al., 1996; Lau et al., 1987). The reaction time influences product characteristics and can have a significantly effect on the solid product yield, which means that a longer reaction time may increase the yield of HTC-char (Glasner et al., 2011; Schuhmacher et al., 1960) that might be because of the enhancement of polymerization of solved components in the liquid phase. Mumme et al. (2011) reported that both reaction time and temperature reduce the yield of HTC-char.

The carbon proportion of the HTC-char rises with an increase in the reaction time at the same reaction temperature. Attempts with reaction times less than one hour were carried out and resulted in a significant increase in the calorific value of the HTC-char (Funke and Ziegler, 2010; Leger et al., 1987). However, it is not explained whether already a certain degree of coalification has taken place.

The relationship between reaction temperature and reaction time is attributed to the slow reaction rate of the polymerization, so that with a longer reaction time more time is available for this process phase in which the solid products are formed. However, after a certain reaction time, there are no longer changes in the elemental composition of the resulting solid body.

2.3.4.3 Solid load/ biomass to water (B/W) ratio

It is assumed that the solid load plays a crucial role in the hydrothermal carbonization of biomass. Despite its important role, most of the experiments carried out with water contents between 50 % and 95 % did not deeply investigate the influence of solid load on HTC-products (Hwang et al., 2012; Liu and Balasubramanian, 2012; Kumar et al., 2011; Kruse and Dinjus, 2007). A high solid load will result in a lower reaction time, which allows earlier starting of the polymerization and higher overall char yields (Funke and Ziegler, 2010). At a very low solid load, biomass may be completely dissolved in water without the formation of significant solid residues.

The solid load must be selected at the highest grade possible therewith the char yield can be maximized of a certain size in a HTC-reactor, so that the amount of biomass used is still covered with water (Krause, 2010). On the other hand, high-loading results

in less biomass dissolving since the equilibrium concentration of TOC in the water remains unchanged and thus the whole amount decreases (Funke, 2012).

2.3.4.4 pH value

Many studies investigated the influence of various bases and acids on the properties of HTC-products. The reaction proceeds preferentially and accelerates in an acid environment. A lower pH of the starting mixture (biomass/ water) can be adjusted by adding acids (including citric acid). This is expected to result in faster dehydration of the biomass, thereby accelerating the rate of the reactions during HTC and affecting the product characteristics (Funke and Ziegler, 2010; Kubo, 2011).

Acid conditions increase both the yield of HTC-chars and their carbon proportion (Kleinert and Wittman, 2009). Although, Heilmann et al. (2011) did not find such an influence on the HTC-char while using of citric acid. In addition to the adding of citric acid, metal ions such as silver ions have also been identified as reaction accelerators (Yu et al., 2004).

During hydrothermal carbonization process, the pH value generally decreases because of the formation of a variety acidic compounds, such as formic, acetic and lactic acid, as reported by some authors (Seville and Fuertes, 2009a; Orem et al., 1996).

2.3.4.5 Pressure

Pressure is usually regarded as an indirect parameter of HTC-process, since it is mainly dependent on the reaction temperature and increases by the increment of the reaction temperature. The increased pressure of the reaction medium keeps water in the liquid phase and mainly influences the density-dependent physical properties of the water. Therefore, exposure to pressure in this reaction temperature ranges is not pronounced, but it helps to improve the contact between biomass components and water molecules and develop HTC-process (Hashaikeh et al., 2007; Afonso and Crespo, 2005).

The high pressure at a reaction temperature around 200 °C ensures the remaining of water in a liquid state in which the most of HTC-products are solid. Whilst more liquid hydrocarbons and gases are created by increasing the temperature up to 400 °C.

The supercritical state of water will be reached by more increase of reaction temperature and pressure in which the mainly product is gaseous (Libra et al., 2011).

2.3.4.6 Composition of the raw material used

Depending on the origin of the biomass, their composition of e.g., lignin and carbohydrates varies significantly. The water and ash content as well as the composition

have an influence on the conversion results. HTC is an effective treatment and has a high flexibility in the selection of the biomass as a starting material. In principle, HTC-process can carbonize any type of biomass such as sewage sludge, manure, settling waste, agriculture residues and algae (Libra, et al., 2011). It can treat the biomass used as it is, and it is not influenced by the existence of toxic compounds. Therefore, the composition of the biomass used is not subject to any particular requirements using HTC, so that any type of biomass can be used (Titirici et al., 2007b).

2.3.5 Products of HTC

2.3.5.1 Overview

At the end of the reaction, sludge of HTC-char, reaction water and a gaseous mixture are present in the reactor, from which the char fraction is obtained as a valuable product after appropriate dewatering and optionally drying (Glasner et al., 2011).

Principally, the relative proportions and characteristics of HTC-products depend on the biomass used and on the process conditions.

Figure 8 represents a qualitative illustration of the distribution of product groups and corresponds only in its magnitude to the actual conditions.

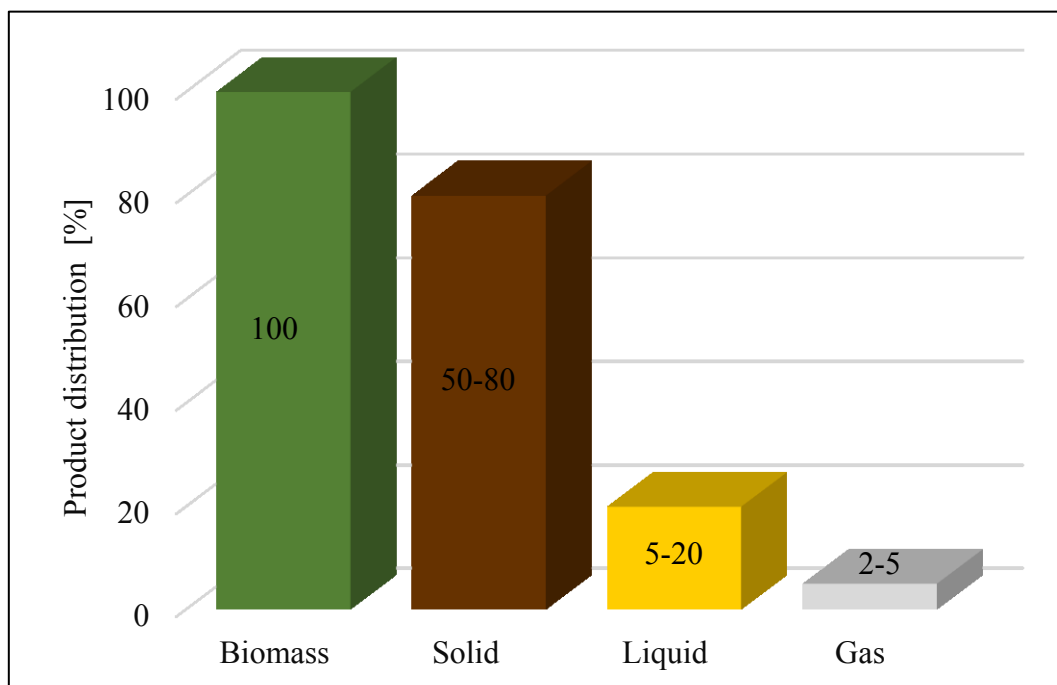


Figure 8: Distribution of HTC-products (comply with Libra et al., 2011)

2.3.5.2 HTC-char

The solid fraction referred to as HTC-char is similar to natural coal, approaching specifically to lignite with regard to its carbon content, type of chemical bonds and calorific value (Glasner et al., 2011; Libra et al., 2011). HTC-char is the main product in the hydrothermal carbonization; it distributes in the reaction water as fine particles and can be separated easily from it.

The carbonaceous materials collected directly after hydrothermal carbonization have only a small number of micro pores and therefore, a small area compared to activated carbon (Titirici and Antonietti, 2010). Compared to both the gas and liquid portions, most of the carbon present in the biomass remains up to 80 % by weight within HTC-char (Hwang et al., 2012; Berge et al., 2011).

The main property of HTC-char is that it has higher carbon proportion and lower H/C and O/C atomic ratio than the original biomass used due to the evolution of H₂O and CO₂ in the dehydration and decarboxylation reactions during HTC (van Krevelen, 1993). The elimination of the hydroxyl and carboxyl groups in the HTC-process results in a product with a lower hydrophilicity than the biomass used. Furthermore, HTC-char exhibits a considerable quantity of functional groups in comparison to natural bituminous coal (Unur, 2013; Bernardo et al., 2012; Kumar et al., 2011).

The specific surface area of HTC-chars ranges between 25 and 30 m² g⁻¹ (Bernardo et al., 2012). Increasing the HTC-process severity will decrease solid yields, in addition to the decrease of H/C and O/C atomic ratios, resulting in higher heating values (Berge et al., 2011; Hoekman et al., 2011).

Potential applications of HTC-char

The HTC-chars produced are easier to transport, store because of improving their material properties and reducing the water content, so that they have the potential to be used in a wide range of applications such as energy source, soil improver, carbon fixation carbon, catalysts and activated carbon adsorbents (Heilmann et al., 2010; Hu et al., 2010; Rillig et al., 2010). However, the applications of HTC-char in the last years were as energy carrier, carbon sequestration and soil fertilizer.

Compared to the raw materials, HTC-char produced has a higher heating value and energy density, which enhances its use as combustible materials for the energy production replacing usual fossil fuels (Dea Marchetti, 2009).

HTC-char is homogeneous and has low moisture content, which makes it suitable for the co-combustion with coal (Lu et al., 2011). It is regarded as a carbon neutral energy source because it does not generate new CO₂. Another potential application of HTC- is as soil fertilizer and carbon storage that is because of its physical and chemical characteristics and the high carbon content (Libra et al., 2011). Converting of biomass to char and then storing it in a soil is a method to capture and storage of carbon that can prevent releasing it in form of CO₂ and result in carbon-negative environment, which reduce the emission of greenhouse gas.

Recently, it is reported that using HTC-char in the soil reduce the nitrogen availability for plant in the first week (Bargmann et al., 2014). The existence of heavy metals while applying HTC-char in soil can interrupt the food chains and pollute the soil.

On the other hand, HTC-char has a lower stability in soils, when used as soils amendment because of its higher proportion of labile carbon species and less aromatic structure; therefore, it may be decomposed more quickly than biochar from dry pyrolysis (Cao et al., 2011). The less stability of HTC-char in soil will not favor its application for carbon sequestration (Berge et al., 2013; Rillig et al., 2010). Therefore, further study of using HTC-char as both a soil amendment and carbon storage is needed. Another potential is the application of HTC-chars as catalysts or as catalyst supports. HTC-chars have here an advantage due to their polarity and the presence of functional groups on their surface, in addition to their high stability by elevated temperatures so that they can replace non-renewable catalysts, which are generated at higher costs.

It is of great importance, to investigate the potentially use of relatively low-cost and environmentally friendly HTC-chars as adsorbents or as a precursor for activated carbons because of the ability to adjust their porosities and surface areas (Roman et al., 2013). Some attempts are known about the effectiveness of HTC-char for selectively adsorption of pollutants from both water and air. However, HTC-chars have low specific surface area, which may influence their adsorption performance.

On the other hand, some investigations have reported that HTC-chars have a relatively large number of oxygen-containing functional groups on their surface that can increase their adsorption performance.

2.3.5.3 HTC-process water

The liquid phase or so-called process water remains after the filtration of HTC-char suspension produced. The liquid phase, the HTC process water, is composed of the

initially added water, the water released from the biomass, the particles that could not be separated from the liquid phase, the dispersed substances and the substances that are in solution in the water. Principally, HTC-process water is predominantly acidic and contains a high proportion of dissolved organic and inorganic compounds, in addition to aromatics such as phenolic and furanic compounds (Funke and Ziegler, 2010).

However, an enrichment of minerals or any heavy metals from the biomass in the reactor must be monitored (Ramke et al., 2010). The mix of solutes is temperature- and biomass-dependent.

HTC-reaction severity influences the nature and yield of liquid products. At higher reaction severity, there is a high water formation by dehydration as well as higher levels of acetic acids (Hoekman et al., 2011; Yan et al., 2010). Many significant quantities of organic compounds founded in the process water represent potentially valuable materials to be recovered (Greve, 2016).

Process water is expressed in units of either chemical oxygen demand (COD), biological oxygen demand in five days (BOD₅) or total organic carbon (TOC). It is stated to be between 14000 and 70000 mg l⁻¹ for COD (Ramke et al., 2010), where domestic effluents are between 300 and 600 mg l⁻¹. Disposal is therefore cost-intensive, so that alternative treatment or recycling routes are of great interest.

Recent investigations reported that the recirculation of process water in HTC improves the solid product yields and its carbon content (Stemann et al., 2013). In fact, the success was that it increased the acetic acid concentration and lowered the concentration of 5-hydroxymethyl -2-furaldehyde (HMF). This approach aims to shift the composition of process water towards less problematic compounds.

Purification of HTC-process water by anaerobic process offers the possibility to produce high quality methane gas. In this way, a reduction of 85 % of BOD could be achieved (Wirth and Mumme, 2013). This combination between hydrothermal carbonization and anaerobic process culminates in a promising one synergy in the context of municipal wastewater treatment plants. However, the digestate produced from anaerobic process requires further treatment.

2.3.5.4 HTC-gases

During HTC-process, a small amount of gaseous phase will be produced, where the reaction severity and the biomass used can influence the composition of the gas phase.

Compared to combustion, pyrolysis, and gasification, HTC produced lower yield of gaseous compounds because of the limited amount of oxygen available.

HTC-gas can be considered as steam-saturated hot gas mixture. The resulting gas can lead to an increase in the pressure in the reactor. In addition, since the process gas is saturated with water vapor, it can be assumed that corresponding proportions of steam-volatile constituents (for example acetic acid) from the liquid phase are present.

After cooling the HTC-reactor, a pressure is measurable before opening, which varies by the outgassing depending on the reaction parameters. Gas phase mainly consists of carbon dioxide (CO_2) because of the process of decarboxylation. Traces of carbon monoxide (CO), methane (CH_4) and hydrogen (H_2) are present (Berge et al., 2011; Dinjus et al., 2011). A detection of other hydrocarbons (ethane and propene) in significant concentrations is also reported (Lu et al., 2012).

Decarboxylation is temperature sensitive. Therefore, increasing the reaction temperatures results in an increase in gaseous yield. Ramke et al. (2009) reported that the concentration of CO_2 in the gas phase was between 70-90 % depending on the process parameter and the raw material used. On the other hand, Berge et al. (2011) suggested that the gas composition did not vary significantly with raw materials.

Depending on the raw material used and the pH in the process, ammonia (NH_3) or hydrogen sulfide (H_2S) may also be present. Depending on the procedural design of the discharge from the pressure range of the reactor, aerosols may occur, which contain the finest particles and can lead to corresponding fine dust emissions.

HTC-gases must be treated or cleaned accordingly. Depending on the cleaning objective, chemical-physical, biological and thermal-catalytic processes for exhaust gas can be used. Several of the trace compounds detected in gaseous phase as methane and hydrogen could be applied for subsequent energy generation.

2.4 Ammonia und ammonium

2.4.1 Overview

Ammonia (NH_3) is under normal conditions a colorless gas, which has a pungent and irritating odor. The residence time of ammonia in the atmosphere is in the range from 2-56 h. It can be compacted without difficulty into a liquid (Nefel et al., 1990).

Ammonia (NH_3) and its conversion product ammonium (NH_4^+) in the industrial, municipal and agricultural wastewater are crucial air and water pollutants contributing to soil acidity, odor emission and aerosol formation (McNaughton and Vet, 1996).

Their entry is problematic in many respects. They impair nutrient-poor soil and can lead to direct damage to the vegetation near large animal stables. If humans or animals absorb ammonia, even small concentrations have an irritating effect on the mucous membranes (Frosch, 2004). If the atmosphere contains more than 50 ppm, it even may cause breathe problems (Gue et al., 2004). In this way, levels of 50-100 ppm can cause irritation of nose, eye and throat (Huang et al., 2008).

Ammonia reacts relatively quickly with acidic air pollutants (for example sulfur dioxide, nitrogen oxides) to form ammonium salts. The particles of these salts bind together and form suspended particles, which are distributed in the surrounding air, so-called aerosols. Deposition of excess nitrogen compounds in environments where natural N-supply is low or in N-sensitive ecosystems can negatively affect these systems (Arogo et al., 2006).

2.4.2 Ammonia and Ammonium in livestock farming

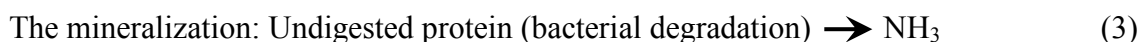
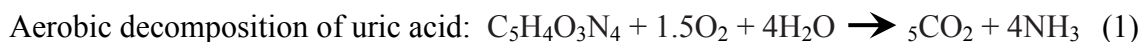
It is estimated that 80-90 % of the German ammonia emissions are derived from agriculture activities. McCrory and Hobbes (2001) identified that animal production is a major contributor to ammonia in Europe (80 %). The main sources of NH_3 and NH_4^+ in livestock and poultry production are urea and uric acid. Their formation begins immediately after excretion of urine and feces (Hristov et al., 2011).

Farm animals consume a considerable amount of protein and other nitrogenous substances in their feed. Nitrogen taken up by animals via the feed can only be utilized to about 20-30 %. The rest is excreted again through urine and feces.

The precipitated nitrogen compounds (urea, cellular nitrogen) are the starting substrate for NH_3 and its equilibrium partner ammonium ion (NH_4^+). These two compounds are summarized under the term total ammonia nitrogen (TAN). The hydrolysis of uric and

acid urea occurs very quickly, it requires only hours for the basic conversion and days for the complete reaction (Meda et al., 2011). This conversion is dependent on pH, moisture and temperature.

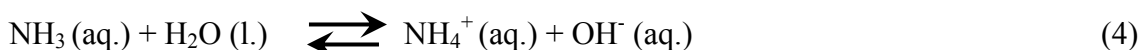
Ammonia is generally produced from manure and animal waste in accordance with the following reactions (Koerkamp et al., 1998).



2.4.3 Ammonia and ammonium equilibrium

Ammonia volatilization is the main pathway for nitrogen loss from animal production (Harper et al., 2000; McGinn and Janzen, 1998). Ammonium is itself non-volatile, but is prone to volatilization by its substitute species. Ammonia and ammonium are in dynamic equilibrium in surroundings, where water normally exists such as soil, plants and water itself.

Several environmental factors such as temperature, moisture, physical and surface conditions influence the deposition of ammonia from the atmosphere to land and water. The polarity of NH_3 molecules and their ability to form hydrogen bonds partly explains the high solubility of ammonia in water. However, a chemical reaction occurs even when ammonia dissolves in water. Ammonia acts as a base in an aqueous solution, and it acquires hydrogen ions of H_2O and generates ammonium ions and hydroxide ions.



In general, the physical and chemical properties of ammonia and ammonium and their environmental behaviors are both temperature and pH-dependent. At environmentally relevant pH values, ammonium ion is the dominant form of ammonia in water.

Figure 9 shows the effect of pH and temperature on the equilibrium of ammonia. Increasing the temperature lead to an increase in the dissociation of NH_4^+ to NH_3 and thus the ammonia volatilization is improved. Ammonia evaporation rate from an aqueous solution enhances with temperature because the solubility of ammonia decreases when the temperature rises. At a given pH, the proportion of the ionized $NH_3(aq.)$ increases in solution with temperature. The higher temperatures increase the mineralization of the organic substances, which can increase the NH_3 production (Arogo et al., 2006). With increasing pH, more than seven, the equilibrium between ammonium

and the dissolved ammonia shifts disproportionately in favor of the ammonia (Zürcher, 2004; Hartung, 2001).

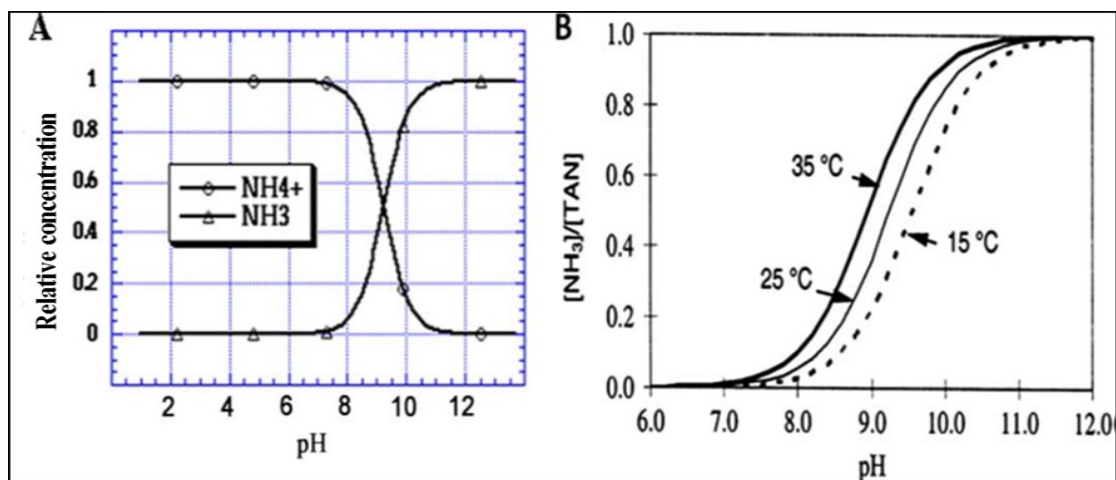


Figure 9: Effect of pH and temperature on the equilibrium of ammonia and ammonium (Sawyer and McCarty, 1978)

2.4.4 Health and environmental impacts

The current threshold level volume for ammonia according to United States Occupational Safety and Health Administration (OSHA) is 25 ppm with a short-term exposure limit of 35 ppm. 30-60 min exposure to 300-500 ppm can be harmful to the health (ATSDR, 1990).

Ammonia is an active gas and easily combines chemically with nitrate (NO_3^-) and sulfate (SO_4^-) in the atmosphere and can negatively affect the environment by forming particles with a mean mass diameter of 2.50 microns (atmospheric particulate matter) that can cause respiratory system diseases in humans and animals and contribute to air pollution (Heber et al., 2001).

Ammonia dissolves in contained water in skin, mucous membranes and eyes and forms ammonium hydroxide, a weak base that interferes with cell membrane and extracts water from the cells, which leads to irritation, inflammation and cellular destruction (ATSDR 2004). The deposition of $\text{NH}_3/\text{NH}_4^+$ influences the growth of forests, plants and other types of vegetation (Kurvits and Marta, 1998). If NH_3 and NH_4^+ are deposited on the ground, NH_4^+ nitrification may occur. This oxidation process can lead to soil acidification.

2.4.5 Reduction of ammonia and ammonium emissions

2.4.5.1 Overview

Ammonia emission reductions are an important issue. Methods in which the formation of ammonia can be influenced and others in which ammonia can be selectively removed are discussed in the literature. Some of the important methods for ammonia removal are briefly described below.

2.4.5.2 Air stripping

In this process a liquid, usually Municipal or industrial wastewater is brought into contact with a gas, usually air, therefore, some undesirable components existing in the liquid phase can be released and carried away by the gas. Influent streams downward over packing material (Wang et al., 2006). Clear air is blown from the bottom and travels upward through the packing. It strips ammonia, which is partially existed as a dissolved gas. Then the loaded air exits the top of the packed column and the treated liquid is collected in the bottom. The most important parameters, which influence the efficiency of this method, are temperature and pH value due to their effect on the equilibrium relationship between the gaseous ammonia and ammonium ion. Lime or caustic is added in this process to increase the pH of the effluent to 10.80-11.50 (Liu et al., 2015), which converts ammonium hydroxide ions to ammonia gas.

This method has a low capital and operating costs. The addition of basic substances may generate operation problems. Moreover, ammonia stripping cannot be done in freezing conditions without using heated air. In addition, ammonia released into atmosphere may react sulfur dioxide and causes air pollution problems.

2.4.5.3 Ion exchange

This process is a reversible reaction. The undesirable ions in a solution are exchanged for a similarly charged ion attached to an immobile solid phase in which the removal of undesirable ions is practically concluded. The effluent passes through a bed of solid phase as natural zeolite, which has a high affinity for ammonium ion (Davis, 2010).

The loaded ion exchange system needs regeneration, when they are saturated. This technology was applied for the removal of nitrogen compound and heavy metals of wastewater applications. Although this technology is environmental friendly, it has some disadvantages such as relatively high capital and operating costs and the need of pretreatment such as filtering and clarification by high concentration of the total suspended solids in the effluent and depends on relatively high-energy consumption

(Gupta et al., 2015). In addition, the adsorbent structure can be destroyed while reacting with NH_4OH , which increases pressure drop and cause the impossibility of the operation itself.

2.4.5.4 Biofiltration

Biofilters usually rely on a biological filter material that is normally organic in nature with a microbial film that is involved in the degradation of gases and odors in addition to its trapping function. Biofilters are made of materials such as compost, straw, peat, or mixtures of these materials, which can effectively purify the air of odors compounds (Ogink and Aarnink, 2003). Ambient conditions such as ammonia concentration, temperature and acidity of the biofilter medium normally affect the performance of biofilter (Pagans, et al., 2005). In most cases, its practical applications are limited because of relatively high capital costs, technical problems and the risk of higher ammonia concentrations in the supply air that ultimately leads to contamination of the filter. In addition, biofilter can also be expensive to install, operate and maintain. It requires frequent monitoring to achieve optimum operating conditions.

2.4.5.5 Bioscrubber

The exhaust air flows from the bottom to the top through a packed bed that is sprinkled from above with water. Bioscrubber is a two-stage process consisting of a scrubber as a first stage in which the pollutants are transferred from the gas phase to the aqueous phase. Clean air is discharged from the scrubber and the polluted water phase is fed into the second stage, a bioreactor, where a biological degeneration of the pollutants occurs (Atia et al., 2004). In bioscrubber, it is not necessary to wet the stream before treatment. This can save the cost of building in a humidifier. The rate of microbial oxidation is affected by the temperature and variations in pollutant concentrations. Some operation parameters must be met while using this method. The temperature must be maintained above 15 °C. The biologically active zone must be sufficiently humidified. In addition, a pH values in the range 6.50-7.50 are to be applied in the circulation water, which must be regularly replaced to prevent undesirable salinity. Bioscrubber is less suitable for less water-soluble compounds. Careful maintenance with appropriate monitoring is required to meet these requirements all the time. Bioscrubber is more expensive to install than other bioreactors. Moreover, the operating costs can be higher than in the other bioreactor processes (Mudliar et al., 2010).

2.4.5.6 Adsorption process

Among the mentioned technologies methods for removal of pollutants, adsorption process becomes an important position over other methods used for ammonia removal because of its affectivity and for the possibility of the recovery of the substances adsorbed through desorption. Adsorption method is a process where molecules from the liquid phase or gas are concentrated on a solid or liquid surface. Adsorbate is the molecules that contacting to the surface, while adsorbent is the surface of the solid or liquid material, which holds the adsorbate. The molecules in the bulk phase are called adsorptive. In addition, desorption is the process for the recovery of adsorbate from the adsorbent surface (Butt et al., 2003).

The adsorption process applies in the area of gaseous separation to remove pollutants and odors from air and industrial gases (Parkash and Velan, 2005). In water treatment or liquid separations, adsorption process is normally one of the most effective methods because of many advantages such as simplicity of design and operation.

Activated carbon is one of the most successful and widely used adsorbents for different purification processes due to its good adsorptive ability and good adsorption capacity (Okoniewska et al., 2007). However, the utilization of commercially available adsorbents, such as polymeric resins, or activated carbon in a large-scale application is restricted due to its costly in design and maintenance.

In recent times, using low cost natural materials, agricultural residue and waste products to produce potential replacements for the expensive commercial adsorbents for the removal of pollutants is a promising approach.

2.4.6 HTC-char to bind ammonia

The ammonia removal using HTC-chars, in batch study or fixed-bed column, depends on various factors, which can be divided into two categories. Firstly, factors of loading or reactive factors (brown color) during loading. Secondly, intrinsic factors that are based on the HTC-char itself and its chemical, physical and adsorptive properties (gray color) as seen in Figure 10.

2.4.6.1 Factors of loading or reactive factors

Contact time

It refers to the time required for the solution to flow from the beginning to the end of the bed, or for the contact between the adsorbate and the adsorbent in which adsorption

takes place. Contact time is a crucial factor since it can reveal the adsorption kinetics of an adsorbent for a specific concentration of an adsorbate; it depends on the nature of the reactions taking place and the frequency of these reaction cycles. In the case of short contact times, only rapid reactions can proceed efficiently. Adsorption resumes until equilibrium is established between adsorbate and adsorptive. In equilibrium, there is a relationship between the concentration of the species in the adsorbed state and their concentration in the solution.

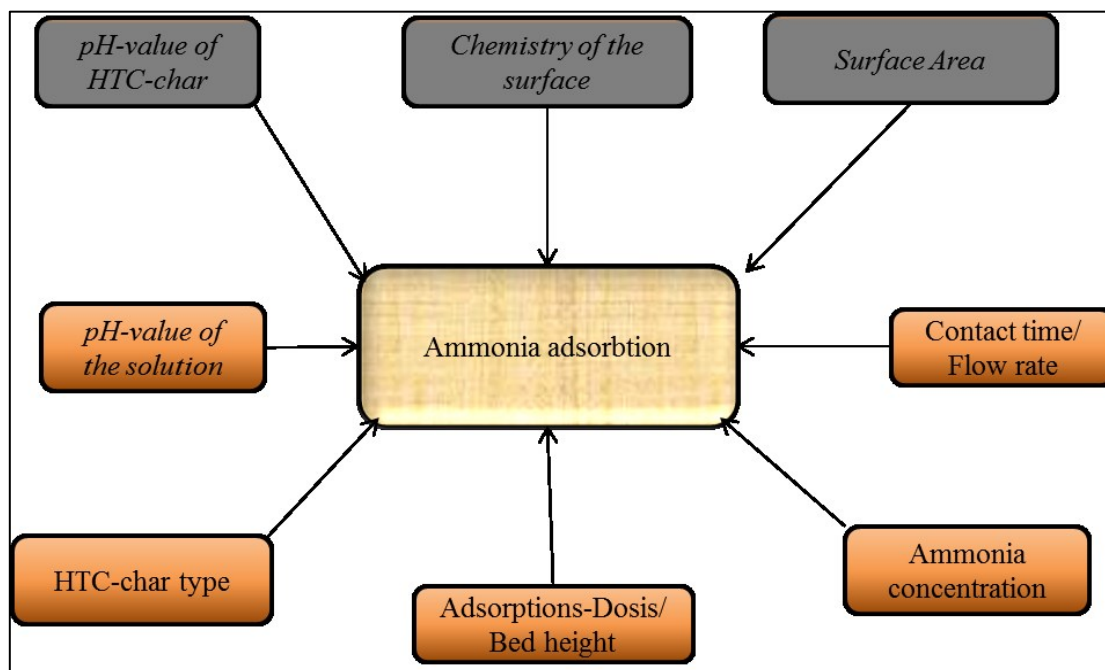


Figure 10: Factors influencing the removal of ammonia in aqueous solution using HTC-char as adsorbent

In a fixed bed column study and as the contact time increases, the adsorbate ions migrate continuously from the entry point to the outlet point of the fixed-bed. The adsorbed amount of the substance increases with the increase in the adsorption time. However, it remains constant after an equilibrium time, which indicates that adsorption tends to saturate at this time. Wang et al. (2011) found that adsorption of ammonium using vermiculite increased rapidly in the first 60 min, slowed stepwise with time and reached the equilibrium time after 3 h. These results supposed the fact that other adsorption parameters influenced the adsorption performance.

Ammonia Concentration

The adsorbate concentration plays a significant role in the adsorption process. At lower initial concentrations, the adsorption behaves independently of the initial concentration

of adsorbate because the ratio of total number moles of adsorbate to the available surface area of the adsorbent is low. The total number of moles of adsorbate at higher concentration can exceed the available sites of adsorption, which can cause a reduction in the adsorption efficiency. It was reported that higher ammonia concentration resulted in a greater amount of adsorbed ammonia. That can be explained by the fact that higher ammonia concentration in solution leads to increase the solute gradient that provides the required driving force for ammonia, which indicates that the adsorption process greatly depends on the initial concentration of ammonia (Long et al., 2008).

pH value

The pH value of a solution is an important parameter that affects the adsorption process. Since it leads to a change in the effective charge on the adsorbent surface as well as to the degree of ionization of an adsorbent (Terzyk et al., 2003). The pH of a solution can affect both the property of adsorbate and adsorbent itself. Therefore, it is supposed that it influences ammonia removal. There is usually an optimum pH value for ammonia adsorption, at which a maximum adsorption capacity is found (Ji et al., 2007; Maraňón et al., 2006). However, lower pH values of solutions decrease the ammonia adsorption capacity due to the competition between ammonium ions and H^+ for occupation of the available active sites on the adsorbent surface in low pH values, which results in a decreasing in the adsorption capacity of ammonium ion.

Application of activated carbon from coconut husk to remove NH_4^+ was performed in batch experiments with optimum conditions of pH 9, temperature 283 K and contact time of 120 min (Boopathy et al., 2013). Other investigators in the range of 5-8 (Liu et al., 2010; Yusof et al., 2010; Ji et al., 2007) reported the optimal pH ranges for ammonium adsorption.

Adsorbent dosage

The increase of adsorbent amount enhances the adsorption efficiency due to the increase of available active sites with higher adsorbent concentration. After a given adsorbent dosage, a very slow increase in removal efficiency can be happened; it may be attributed to the achievement of equilibrium between adsorbate and adsorbent at the operating conditions. So that, the amounts of free ions and those bound to the adsorbent remain constant upon a further increase of adsorbent dosage.

Wang and Lin (2008) reported that the adsorbed amount per unit of mass decreased as the adsorbent dosage increased. This could be achieved by increasing the unsaturated

activated sites or particle interaction, such as aggregation, which resulted in a reduction in the total surface area of the adsorbent (Shukla et al., 2002).

Ghauri et al. (2012) found that the ammonia removal efficiency increased by increasing the amount of the adsorbent used, and increasing the adsorbent dosage more than 1 g, the change of removal efficiency was not remarkable.

Flow rate

This parameter is important for estimating the effectiveness of an adsorbent in a continuous industrial scale fixed-bed column operation. It was reported by various researchers (Sadaf and Bhatti, 2014; Cruz-Olivares et al., 2013) that a high flow rate led to faster breakthrough and shorter column exhaustion.

Increasing the flow rate results in lower residence time in the fixed-bed column and the adsorption process cannot take place at short contact time. This may be because of the increase in speed of adsorption zone at high flow rates and the solutes have no sufficient time to go through the pores of adsorbents. Moreover, a very low flow rate reveals a poor liquid distribution across the fixed-bed and results in dead zones. That can be because the fact that liquid always follows the way of least resistance through the fixed-bed. Thus, flow rate has to be optimized considering the properties of the fixed-bed and the other process parameter.

Bed height

The increase in bed height corresponds identically more amount of adsorbent in the column. The contact time increases by increment of the adsorbent loading, also more number of sorption sites are available (Sivakumar and Palanisamy, 2009), which enhances the adsorption process and results in higher adsorption capacity.

Moreover, increasing the bed height results in the possibility of higher solution treated, which is useful for adsorption bed operation. As a result, a decrease in the effluent concentration at the same service time will be achieved by higher fixed-bed column (Tan et al., 2008).

2.4.6.2 Intrinsic factors of HTC-char

Appearance properties and chemistry of the surface

The adsorption capacity of HTC-char is affected by some parameters such as the composition of HTC-char, its specific surface area, surface functional groups and pore structure. These parameters can be influenced by the chemical composition of different

raw materials and the conditions of HTC-process, especially, the reaction temperature. Li et al. (2015) found that the adsorption capacity of rice husk derived biochar increased with the increase of pyrolysis temperature.

Surface functional groups of HTC-char are mainly divided into basic groups and acidic groups. Depending on the dominating conditions during the carbonization, mainly basic or acidic surface oxides are formed that can influence the pH of the HTC-char. Functional groups are variable charge, so that and depending on the pH, they can donate or receive a proton (H^+). Fuertes et al. (2010) suggested that the acidity of HTC-char might be because of a high content of carboxyl functional groups.

Surface oxides such as carboxyl, carbonyl and phenolic hydroxyl groups are representatives of acidic groups. It has been investigated that the acidic surface oxides improve the adsorption capacity for polar alkaline molecule, such as ammonia (Le Leuch and Bandosz, 2007; Guo et al., 2005).

pH value of the HTC-char

The pH value of HTC-char is helpful for the investigation of the surface charge, which is very important in the adsorption processes. Thermo-chemical conversion of the raw materials influences the pH of HTC-char, which can be affected by the properties of the raw materials used, the operating conditions and/ or by synthetic additives (e.g. impregnating substances). This factor can develop and affect the adsorption process only in combination with water.

It is important to determine the state of the particle surface charge introduced in an aqueous medium to be in the desired pH adsorption conditions. These conditions lead to the elimination of an ion present on the solid, or vice versa to the adsorption of ions at the solid (Reymond and Kolenda, 1999). The surface charge of carbon is a function of the pH of the solution. The point of zero charge (pH_{pzc}) represents the pH value at which the net surface charge is zero. The surface is positively charged at pH below pH_{pzc} , which means that it attracts anions from the solution, and negatively charged at a pH above pH_{pzc} in which it attracts cations from the solution (Liu et al., 2012).

3 Materials and methods

3.1 Description of raw materials

In order to fulfill the condition of an adsorbent, which must be inexpensive, wetland biomasses were selected for this study. For these investigations, four types of wetland biomass (reed, typha, juncus and carex) were used.

3.1.1 Reed

Reed (*Phragmites australis*) is a large perennial grass, which can grow in the range from 1.50-4 m in height at maturation (Ailstock et al., 2001). It has a rapid growth rate and is appreciate to be the most widely distributed flowering plant in the world.

Reed is abundantly available in most wetlands and is often cheap and available as a raw material because of its fast-growing properties. The composition of this plant is dependent on environmental factors. Its core distribution region is Europe, Middle East and America (Haslam, 2010). The lignin content ranged from 17.20-26.50 %, where hemicellulose content could range from 16.40-19 % and the cellulose content (29.70-37.30 %) is relatively high (Kim et al., 2015). This plant can be used for handicrafts such as roofs and baskets (Sathitsuksanoh et al., 2009). Reed is recognized as a promising source of renewable energy due to its worldwide dominance and it can be used in industrial, energy, agricultural and water treatment field (Cotana et al., 2015).

3.1.2 Typha

Typha is one of the most common perennial aquatic plants presented in marshes and shallow waters worldwide (Dahlgren et al., 1985). It is abundant in most wetlands and its composition is affected by environmental factors. Zhang et al. (2011) reported that the cellulose, hemicellulose and lignin contents were 32.30, 18.60 and 20.70 %, respectively. Because of its interesting chemical composition and high yield, typha can be considered as a particularly viable energy crop. Typha is weather resistant and biologically resistant because of its high polyphenol content. The cultivation of typha plants will present environmental assistance regarding the stabilization and renaturation of re-wetted fenlands. Typha is particularly suitable for the production of building materials because of the specific structure of their leaves (Krus et al., 2014).

3.1.3 Carex

Carex is one of the most common vascular plant groups in the world, it is with around 1800 kinds very wide and it is substantial for wetlands and is commonly used (Mabberley, 2008). It exists in very different habitats as in wet and moist, but fewer species occur in dry locations (Bogucka-Kockaa and Fatty, 2010). With around 120 species, the genus in the German flora is one of the most species-rich groups (Düll and Kutzelnigg, 2011). Florio (2014) reported different constituents of fiber (hemicellulose, cellulose and lignin) of three species of carex, where cellulose content had median values ranging from 26.70-29.70 %, hemicellulose from 29.50-36 % and lignin from 5.60-7.90 %. The cell wall characteristics (lignin content) restrict the conversion of cell wall to energy. Some arts of carex were previously used as a bedding (Düll and Kutzelnigg, 2011). Today, carex plays lower role in agriculture but are rather important elements in garden culture.

3.1.4 Juncus

Juncus effusus L. is a multi-year plant that grows in wetlands in wet locations. This specie has become problematic. Per plant, over 500,000 seeds are produced; most of them remain germinative for more than twenty years. Due to the low feed value, juncus is eaten, if at all, by only a few animals. It is generally regarded as the greatest challenge in grassland areas and it can often displace other plants (Kaczmarek-Derda et al., 2014). Therefore, new technologies of biomass use are requested urgently.

Hydrothermal carbonization could be a promising alternative for the usage of this kind of wetland biomasses. Kuehn et al. (2000) reported different constituents of fiber (hemicellulose, cellulose and lignin) of juncus effusus L. in different periods. Cellulose content had median values ranging from 36.71-41.39 %, hemicellulose from 28.94-30.73 % and lignin from 10.48-13.12 %.

3.1.5 Structural composition of raw materials

The biomasses under investigation were harvested in Mecklenburg-Western Pomerania, near the small town Triebsees, in autumn 2011. Moisture content is an important parameter, which affects the storage stability of the samples used in this work, since the biomass between harvest and use in the research had to be stored for months. This can lead to unwanted biological reactions that lead to get mouldy or composting.

Good dried raw materials are easier to be stored and processed. So that the collected raw material samples were freed of foreign matter as stones and dust, then were cut, dried at temperature 60 °C, for 48 h. After that, the dried raw materials were milled and sieved using Fritsch Analysette under 4 mm size and then the biomasses were further dried to have a moisture content of about 6 %. The dried raw materials were then packed in plastic bags and stored in a box until being used in the experiments (Ibrahim et al., 2014). The moisture content of the dried raw material can affect the calorific value and combustion temperature, which were not in the focus of interest in this study.

The main elements carbon, oxygen, hydrogen and nitrogen as well as the lignocellulosic composition of the dried raw material samples were analyzed, the quantitative analysis gives information on ash content were also performed. All these data help to compare a certain biomass to another and to determine a suitable application of this biomass.

Table 1 shows the structural composition of the biomasses used. The percentage of hemicellulose, cellulose, and lignin in biomass used were calculated from the difference of NDF, ADF, ADL and ash (Goering and Van Soest, 1970).

Table 1: Structural composition of the biomass used (Ibrahim et al., 2018)

Parameter	Reed	Typha	Juncus	Carex
Moisture [%, db] ^{1,2}	6.26	6.17	6.15	6.08
Ash content [%, db] ²	4.15	3.82	4.23	5.64
Carbon [%, daf] ³	43.82	42.74	43.27	42.24
Hydrogen [%, daf] ³	5.82	5.58	5.85	5.86
Nitrogen [%, daf] ³	0.54	0.78	1.42	2.17
Oxygen [%, daf] ³	45.66	47.08	45.23	44.09
Cellulose [%]	42.60	45.70	31.52	41.64
Hemicellulose [%]	31.70	24.60	33.00	36.30
Lignin [%]	14.10	12.60	5.28	5.16

¹According to DIN 51 718 (1995). ²db: dry basis. ³daf: dry ash-free

Typha had the highest cellulose content, while juncus had the lowest one. On the other hand, carex contained higher amounts of hemicelluloses compared to the other biomass. The highest lignin content was observed in reed, the lignin content for juncus was similar to that was for carex. In terms of ash content, typha had the lowest ash content. However, the structure of biomass can also affect HTC-products and their characters even when the HTC-parameters are similar.

3.2 HTC-experimental apparatus and HTC-process experiments

3.2.1 HTC-experimental apparatus

The experiments using wetland biomasses were performed in a stainless steel reactor, which has an inner volume of 600 ml, and is hermetically sealed. This reactor has been designed, realized and tested in cooperation with the company Technology and Plant Construction in Rostock (TAB GmbH). The design of the experimental apparatus took in consideration the temperatures and pressures involved in HTC-process (Figure 11 and 12). The reactor could be used for HTC of biomass of different origin.

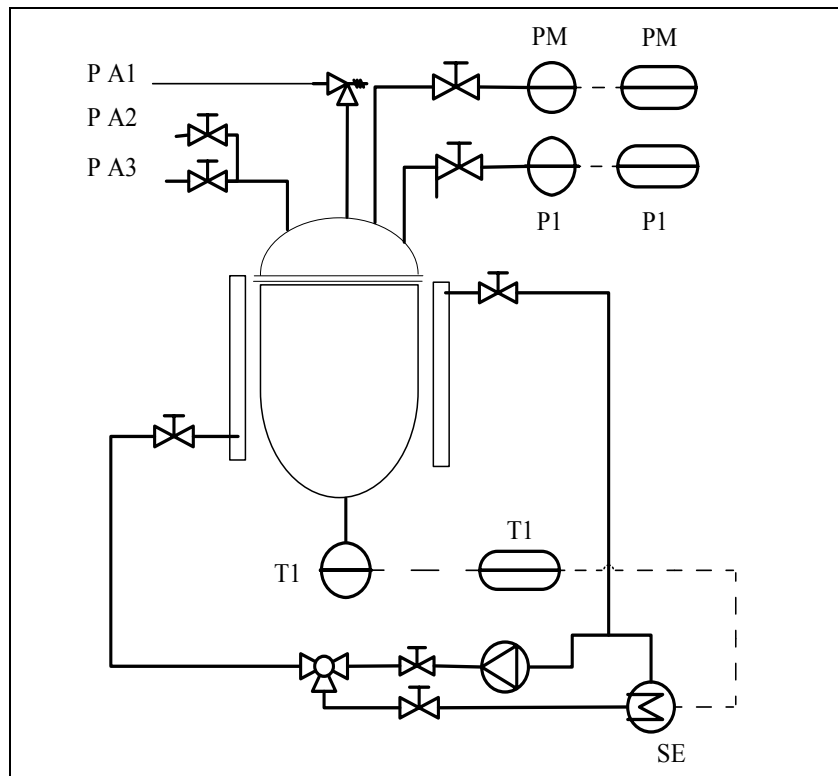


Figure 11: Schematic diagram of HTC-apparatus (Ibrahim et al., 2014)

The entire system (laboratory construction) with vent line is made of corrosion-resistant stainless steel of grade 1.4571. The installation took place vertically in the entire system. Due to its material properties, the apparatus has excellent corrosion resistance to a variety of fluids and gases in the specified pressure and temperature spectrum.

The cover is equipped with a pressure gauge (PM), a pressure sensor (P1) and a pressure relief valve (PA1) as well as gas inlet (PA2) and gas outlet (PA3). The Julabo heater (SE) is used as a heating circuit to provide the required heat in the process. The temperature of the medium is detected by a temperature sensor (T1) installed in the reactor vessel. These sensors register values every 10 sec (the register time can be

chosen) and transfer the data via USB to the computer. During the entire test period, both the internal temperature and the corresponding pressure in the reactor were measured every 10 sec. During the experiment, a HTC-controller continuously checked the temperature, if the temperature was lower than the set point; the HTC-controller would switch on the pump to provide additional heated oil. When the temperature was equal or higher than the set point, the pump would switch off.



Figure 12: Experimental apparatus of the hydrothermal carbonization

Heating circuit

In the heating circuit, the heating power required for the process is provided by means of a Julabo heating device. The reactor has a double jacket, through which hot medium oil thermal HS, acting as heating medium, is circulated. The temperature is controlled using a temperature sensor that reveals the media temperature. The container space of the reactor is designed for the following operating and conditions of use:

Pressure range 0-200 bar and temperature range 0-350 °C. The components of the heating circuit are:

- Julabo SL-6

- Hand shut-off valves
- Temperature sensors
- Circulator pump
- Safety valve
- Filling and emptying fittings

3.2.2 HTC-process

Figure 13 presents the scheme of production trials of HTC-process. In each test, a desired amount of wetland biomass was dispersed in bi-distilled water with addition of acid catalysts.

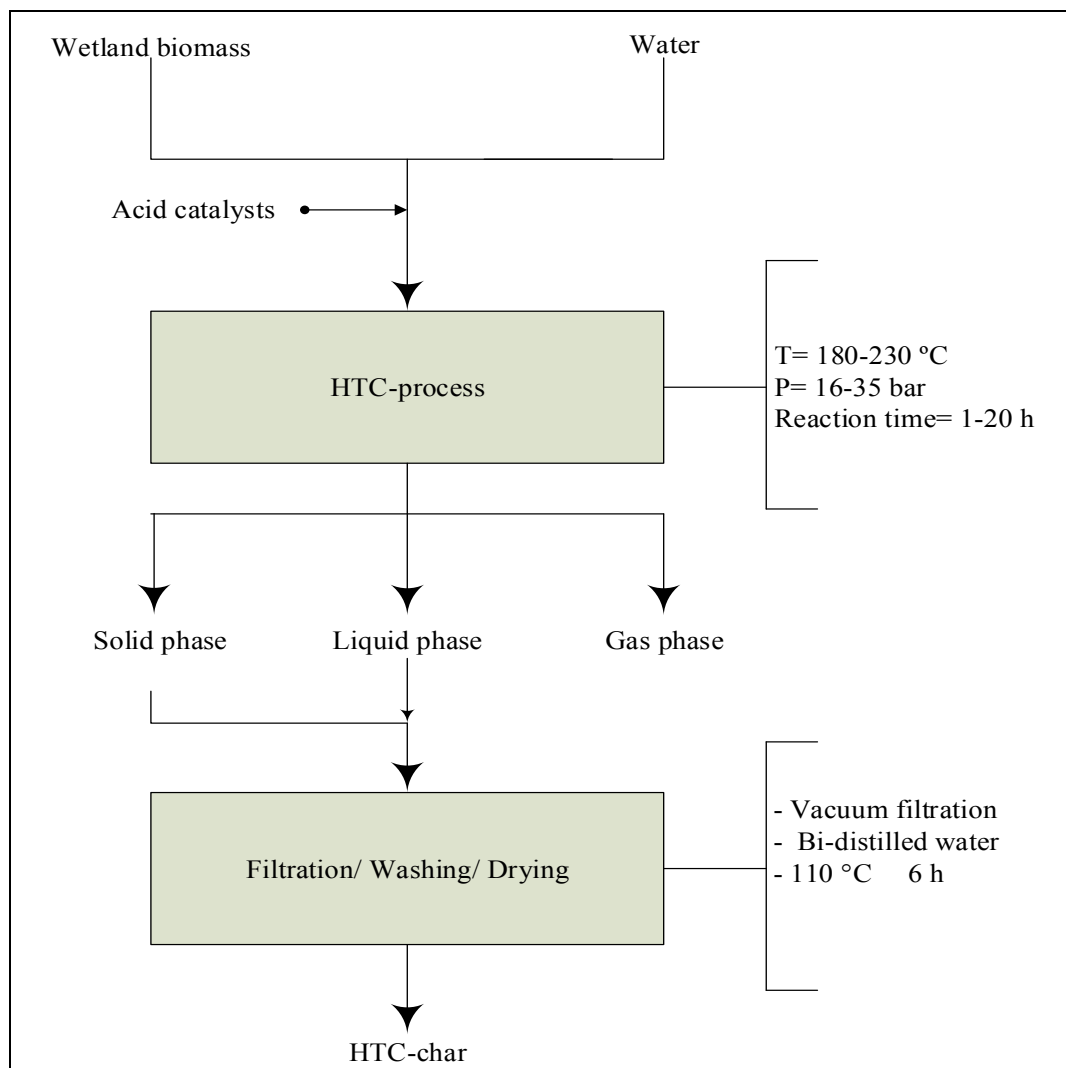


Figure 13: Scheme of HTC-char production trials

The mixture was stirred for two hours before starting the experiment, so that a complete wetting of the substrate with water took place. The mixture transferred then to the

reactor and sealed. The reactor was filled at about 90 % of its inner volume. It was then heated up to the desired reaction temperature (set point temperature) in the range of 180-230 °C and left at this temperature for the designated reaction time from 1-20 h. After reaching this time, the heating was automatically switched off and the reactor was manually cooled using water. After the internal temperature of the reactor had cooled to about 40 °C. Then, the reactor could be opened.

First, the pressure valve was opened slowly and the residual pressure was released. The solid-liquid mixture was filtered under vacuum with a Buchner funnel and Whatman filter paper and the filter cake washed with bi-distilled water in order to remove the soluble intermediates deposited on the HTC-char. Subsequently, the filter cake was dried at 110 °C for 6 h, cooled in a desiccator and weighed.

3.2.3 Experimental section according to parameters affecting HTC-process

Series of HTC-trials were conducted to determine the effects of the process parameters such as biomass type, reaction temperature, reaction time, catalyst and the amount of biomass on the composition and properties of HTC-chars produced.

In the **first series of experiments, reaction temperatures** were varied in the range of 180-230 °C, the other parameters were constant. The different HTC-chars were designated as R_N , T_N , J_N and Ca_N ($N=1, 2, 3\dots$), where $N=1$ indicated the influence of the reaction temperature of 180 °C, $N=2$ indicated the influence of the reaction temperature of 200 °C, etc. (Ibrahim et al., 2014). The study was carried out as presented in the process parameters and the codes of HTC-chars were listed in Table 2. Furthermore, the analysis of variance was performed to detect the significance effect of the variation of the reaction temperatures during HTC-process on the properties of HTC-chars in each group, which contained HTC-chars produced from the four types of the raw materials used at each reaction temperature.

In the **second series of experiments, reaction times** were varied in the range of 1-20 h, while the other process parameters were constant as shown in Table 2.

Furthermore, the analysis of variance was performed to detect the significance effect of the variation of the reaction times during HTC-process on the properties of HTC-chars in each group, which contained HTC-chars produced from the four types of the raw materials used at each reaction time.

In the **third series of experiments**, the **amount of biomass (solid load)** used was varied using 30 and 50 g of the dried biomass (6 % and 9 % solid load), while the other process parameters were constant as presented in Table 2.

Furthermore, the analysis of variance was performed to detect the significance effect of the variation of the solid loads during HTC-process on the properties of HTC-chars in each group, which contained HTC-chars produced from the four types of the raw materials used at each solid load.

In the **fourth series of experiments**, the **catalyst** used was varied, while the other process parameters were constant (Table 2). Citric acid was used with two different amounts 0.50 g and 0.05 g. Phosphoric acid was also used as catalyst (6.50 g) in order to compare its effect on the properties of HTC-chars with those while using citric acid.

In this series of experiments, the effect of the oxidation of HTC-chars was also studied. Furthermore, the analysis of variance was performed to detect the significance effect of the variation of the catalyst during HTC-process and the oxidation on the properties of HTC-chars in each group, which contained HTC-chars produced from the four types of the raw materials used.

Oxidation with nitric acid: In this set, HTC-chars produced at reaction temperature of 230 °C and reaction time of 15 h using citric acid as catalyst were oxidized (impregnated) with 10 % nitric acid at room temperature (20 °C) to investigate how oxidation might influence the properties of HTC-chars and might improve their adsorption efficiency. For the oxidation (impregnation) of HTC-chars, 10 g of HTC-char with 100 ml nitric acid 10 % were stirred for seven days. The reaction took place at room temperature. The oxidized HTC-chars were filtered, washed with bi-distilled water until attaining a constant pH value of the effluent water, and then dried at 110 °C.

In the **fifth series of experiments**, the **particle sizes** of the raw materials used were varied. Particle sizes of 4 mm and 0.50 mm of the biomasses used, while the other parameters were constant as presented in Table 2. Furthermore, the analysis of variance is performed to detect the significance effect of the variation of the particle size on the properties of HTC-chars in each group, which contains HTC-chars produced from the four types of the raw materials used at each particle size.

Table 2: Process parameters and HTC-char codes for studying the effect of the variation of each HTC-process parameter on the properties of HTC-chars

The examined process parameter	Reaction temperature [°C]	Biomass amount [g] (solid load [%])	Catalyst [g]	Particle size [mm]	Reaction time [h]	HTC-char			
						Reed	Typha	Juncus	Carex
First series/ Reaction temperature	180	30 (6)	Citric acid (0.50)	4	15	R ₁	T ₁	J ₁	Ca ₁
	200					R ₂	T ₂	J ₂	Ca ₂
	220					R ₃	T ₃	J ₃	Ca ₃
	230					R_c	T_c	J_c	Ca_c
Second series/ Reaction time	230	30 (6)	Citric acid (0.50)	4	1	R ₅	T ₅	J ₅	Ca ₅
					3	R ₆	T ₆	J ₆	Ca ₆
					5	R ₇	T ₇	J ₇	Ca ₇
					7	R ₈	T ₈	J ₈	Ca ₈
					12	R ₉	T ₉	J ₉	Ca ₉
					15	R_c	T_c	J_c	Ca_c
					20	R ₁₀	T ₁₀	J ₁₀	Ca ₁₀
Third series/ Biomass amount (solid load)	230	30 (6)		4	15	R_c	T_c	J_c	Ca_c
		50 (9)				R ₁₁	T ₁₁	J ₁₁	Ca ₁₁
Fourth series Catalyst/ Oxidation	230	30 (6)	Citric acid (0.50)	4	15	R_c	T_c	J_c	Ca_c
			Citric acid (0.050)			R ₁₂	T ₁₂	J ₁₂	Ca ₁₂
			Phosphoric acid (6.50)			R_p	T_p	J_p	Ca_p
	20	-	Nitric acid (10 %)	-	168	R_n	T_n	J_n	Ca_n
Fifth series/ Particle size of the biomass	230	30 (6)	Citric acid (0.50)	4	15	R_c	T_c	J_c	Ca_c
				0.50		R ₁₃	T ₁₃	J ₁₃	Ca ₁₃

3.3 Raw material and HTC-char characterization methods

3.3.1 Overview

During the hydrothermal carbonization process, a thermochemical transformation takes place; therefore, it is important to analyze the main elements in HTC-char to understand the chemical changes.

The characteristics of the HTC-char were investigated with the objectives of qualitatively evaluating the carbonization process and identifying the changes in the solid material during HTC-process as well as determining the effects of the reaction process parameters on the properties of the HTC-char.

3.3.2 Yield of HTC-char and the carbon recovered

The yield is defined as the quotient of the mass of solid product relative to the mass of the biomass used (indicated in percent). In term of carbon sequestration potential, the carbon recovered was determined. It indicates the percent of the carbon content in the biomass that is preserved in the final product. Calculations of the yield of HTC-char and the carbon recovered were defined on a dry basis according to equations 5 and 6 (Aydincak et al., 2012).

$$Yield [\%] = \frac{\text{mass of dried trated biomass}}{\text{mass of dried biomass}} \times 100 \quad (5)$$

$$C_{recovered} = \frac{[g] \text{ biomass} \times \text{yield} \times \text{treated biomass carbon} [\%]}{[g] \text{ biomass} \times \text{carbon content} [\%]} \quad (6)$$

3.3.3 Elemental analysis

The elemental analysis of carbon, hydrogen and nitrogen of raw materials used and HTC-char produced was performed using a microanalyzer TruSpec CHNS Micro Company Leco to determine the degree of carbonization. The analysis was carried out in cooperation with Leibniz Institute for Catalysis (Rostock)

The speed and analytical performance of the TruSpec CHNS microanalyzer is created by the combination of the combustion with the optimum measuring cells for the corresponding combustion gases. As a result, the characteristics of the gases can be optimally utilized and in addition to high accuracy, a short analysis time and high user friendliness can be achieved.

Oxygen proportions were calculated from the difference of loss on ignition and the sum of organic carbon, hydrogen and nitrogen proportions (Jamari and Howse, 2012; Ramke

et al., 2009). H/C and O/C atomic ratios were computed for both raw materials and HTC-chars and were analyzed using the carbonization diagram (van Krevelen, 1950).

3.3.4 Determination of ash content

Ash is the residue remaining after burning the HTC-char. The Ash content was measured to determine the amount of non-combustible solid remaining after the combustion process. First, the samples were homogenized in an analytical mill (Fritsch Rotor Speed Mill Pulverisette 14) for 2 min per sample. The homogenized samples were stored until analysis in capped glass vials at room temperature. Ash content was determined by combusting the dried raw materials and HTC-chars at 600 °C, based on ASTM D3172 (2013)

3.3.5 pH measurement

The measurement of the pH value of a material gives an idea of its acid content. These measurements were detected according to the method of CEFIC 3.6 (1986). In this study, about 4 g of the crushed HTC-char sample was weighed and added to 100 ml of bi-distilled boiled (CO₂-free) water into a beaker (250 ml). The beaker was covered with a watch glass and then cooked on the heating plate for 5 min (IKA Magnetic Stirrer RCT Classic). After inserting a thermometer, the char suspension was allowed to settle and decant the supernatant liquid before it was cooled below 60 °C. The decanted liquid was cooled to room temperature and the pH was accurately measured to two decimal places.

3.3.6 Specific surface area

The specific surface area of HTC-char is an important physical property that affects the adsorption capacity. The specific surface area and the pore volume of the raw material and HTC-char samples were estimated using the standard Brunauer–Emmett–Teller (BET) method (Brunauer et al., 1938) based on the principles of physical adsorption and desorption of nitrogen. Accelerated Surface Area and Porosimetry analyzers (ASAP 2010) were used.

The specific surface area were detected using the nitrogen adsorption and desorption isotherms. The measurements were carried out in cooperation with Leibniz Institute for Catalysis (Rostock). Assuming, that the pores were filled with liquid nitrogen, the amount of vapor adsorbed at a relative pressure close to unity was used to derive the total pore volume (Brunauer et al., 1938).

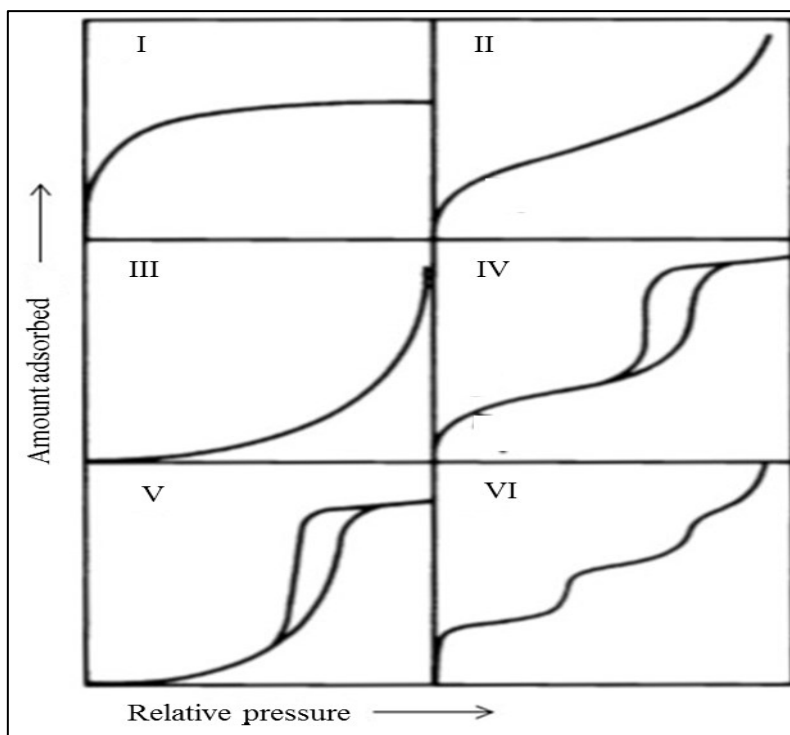


Figure 14: IUPAC classification of adsorption isotherm (Sing et al., 1985)

Adsorption isotherm was used to describe the adsorption process quantitatively, the amount adsorbed (gas or liquid) by the material at a fixed temperature as a function of pressure. IUPAC conventions have been submitted for classifying pore sizes and sorption isotherms.

Figure 14 shows the IUPAC classification of the sorption isotherm (Sing et al., 1985). As the relative pressure approaches one, the amount of adsorbate reaches a limiting value in the type I or Langmuir isotherm. This happens with microporous adsorbents that possess relatively small external surfaces such as molecular sieve zeolites and activated carbons. Nonporous or macro porous solid adsorbents are described using type II, which presents unrestricted monolayer-multilayer adsorption (Lowell et al., 2004). Type III isotherm is rarely encountered, it presents the relatively weak interactions between a nonporous or macro porous solid adsorbent and adsorbate.

Type IV isotherm happens with mesoporous adsorbents and is associated with capillary condensation. The initial part of this isotherm takes the same path as corresponding part of the type II. Type V isotherm is detected for water adsorption on hydrophobic microporous and mesoporous adsorbents. Type V isotherm is very similar to Type III in the range of low relative pressure in which the adsorbent-adsorbate interactions are weak. Type VI isotherm represents gradually multilayer adsorption on a uniform non-porous surface (Thommes et al., 2015).

3.3.7 Bulk density

The bulk density presents structural and pore space volume, where the particle density including only the volume occupied by solid molecules. This parameter will be used while designing adsorption columns in the industry, it influences the overall cost of the adsorption process. The method of Ahmedna et al. (1997) was used to measure the bulk density and calculated using equation 7.

$$\text{Bulk density } [g \text{ cm}^{-3}] = \frac{\text{weight of dry sample } [g]}{\text{volume of packed dry sample } [\text{cm}^3]} \quad (7)$$

3.3.8 Point of zero charge

The point of zero charge (pH_{pzc}) is one of the main surface properties of an adsorbent. It relies on the electronic and chemical properties of the functional groups on the surface of HTC-char. pH_{pzc} corresponds to pH of the surrounding liquid of adsorbent particles, at which the pH of the adsorbent surface in the aqueous solution has a net neutral charge (Liu et al., 2012; Reymond and Kolenda, 1999). This means that the sum of the surface positive charges is equilibrium of the sum of surface negative charges (the net surface charge is zero).

The pH_{pzc} was determined as following: 0.1 M (molarity) NaCl solutions with different pH values (2-11) were prepared using deionized water, which was boiled to remove CO_2 . Solutions of 0.50 N (normality) HCl or NaOH were used to adjust pH. HTC-char samples (100 mg) were added with 20 ml of 0.1 M NaCl solutions with different initial pH values in 25 ml vials and equilibrated for 48 h by constant stirring in capped glass vials at room temperature, and then left for settling of HTC-chars (Dastgheib et al., 2004). Blank samples with no HTC-char were also prepared. Duplicate experiments were performed. The final pH value of the solution was measured. The pH_{pzc} of char was determined as the pH at which the initial and final pH is equal (Dastgheib et al., 2004). In the present investigation, the point of zero charge was determined for only HTC-chars with the best adsorptions efficiency, which were identified in preliminary tests. The pH value was measured using pH 330i/340i Meter (WTW).

3.3.9 Fourier transform infrared spectrometer

Fourier transform infrared spectrometer (FTIR) analysis represents the fundamental absorbance of functional groups and provides information on molecular structure through the frequencies of the natural molecular vibration. It gives direct information on

the presence of functional groups on the solid surface by their characteristic spectrum (Cheng et al., 2006; Sharma et al., 2004).

FTIR were implemented in the range of $400\text{--}4000\text{ cm}^{-1}$ to identify the surface functional groups by showing the bond energies of these groups and were recorded on a Bruker-Alpha spectrometer by ATR technique with a diamond crystal. The dried samples were again finely ground and measured without further preparation. The measurement was carried out in cooperation with Leibniz Institute for Catalysis (Rostock).

3.3.10 Preliminary tests of HTC-reactor with bi-distilled water

The HTC-reactor was tested using bi-distilled water to observe its behavior by enhancing the reaction temperature and to investigate a heating curve using only bi-distilled water.

Figure 15 shows the measurement of the internal reaction temperature (continued line) and the corresponding pressure (dashed line) during the entire test period at regular intervals of 10 min.

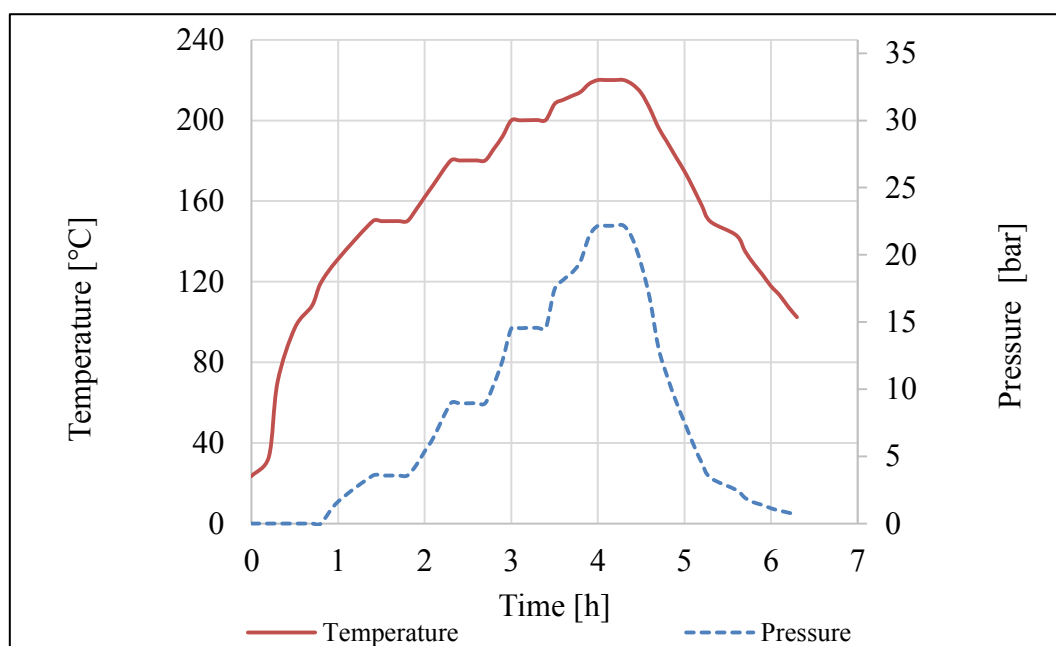


Figure 15: Temperature and pressure curves during the tightness test of HTC-reactor using bi-distilled water at different reaction temperatures

The test was implemented using 500 ml of bi-distilled water, warming the reactor up to several different reaction temperature 150, 180, 200 and 220 °C, and then leaving the reactor at each reaction temperature for 20 min. By monitoring the recorded pressure, it was found that no leaching occurred during this test.

3.3.11 Tests using real substrate

Reed was chosen as a model compound representing wetland biomass to perform this test in order to evaluate the behavior of the reactor in real HTC-conditions.

Figure 16 shows the carbonization process of reed at 230 °C and a reaction time of 20 h using citric acid as catalyst. It shows also the approximate times for each reaction phase.

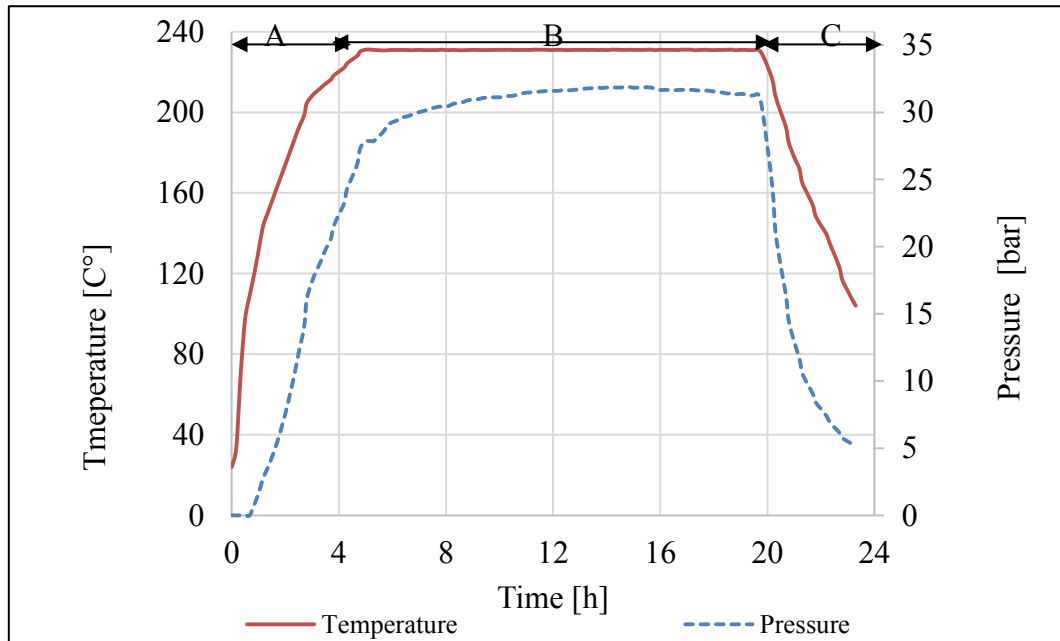


Figure 16: Temperature and pressure curves during the test period of HTC-process for producing of HTC-char of reed at 230 °C and 20 h using citric acid as catalyst

The reaction time was defined as the time at the reaction temperature „B” without heating „A” and cooling time „C”. The recorded results show that the heating controller was able to control the reaction temperature and the pressure within a small fluctuation range during the reaction time.

The reactor pressure was higher than the vapor pressure of water (Figure 15) because of the formation of gaseous products. Compared with the heating curve using only water, the reactor pressure did not considerably exceed the steam saturation pressure before the temperature reached 210 °C, indicating the production of only small amounts of gaseous products during the preheating period. Hoekman et al. (2011) noted the same behavior at temperatures above 200 °C. After cooling down the reactor, there was only a slight overpressure inside the vessel, suggesting that only minimal amounts of gas were generated during the HTC-process. In all HTC-experiments, the reactor was cooled down using cold-water. The primary goal was to shorten as much as possible the cooling time to be considered irrelevant when compared to the reaction time.

3.4 Determination of ammonia removal performance

3.4.1 Overview

Batch study and fixed-bed column study using ammonia solution as a model compound were used to measure the adsorption performance of ammonia in aqueous solution onto HTC-chars.

The measurement of the equilibrium concentration in a batch experiment is an uncomplicated process. Equilibrium states will be only used to measure the adsorption isotherms while using static methods. In this case, no need to analyze the concentration-time curves. Dynamic fixed-bed column experiments determine the change in removal efficiency with the time. They are requested to attain basic data for direct applications in industrial systems. The overall goal of this work is to investigate the use of HTC-chars as an alternative for activated carbon to serve as a filter material for ammonia purification in an aqueous solution.

3.4.2 Batch study

In order to achieve the best removal of ammonia in aqueous solution, the affecting factors, including HTC-reaction temperatures, HTC-char type (using different catalysts and also after oxidation), adsorption contact time, adsorbent dosage, solution pH value and the effect of ammonia concentration on the adsorption performance were investigated in this study. The analysis of variance was performed to detect the significance effect of the variation of the adsorption parameters on the adsorption performance of each group of adsorbents, which contained HTC-chars produced from reed, typha, juncus and carex.

The adsorption experiments were carried out in a stirred system using a rotary shaker (VWR Advanced Digital Shaker 3500) at 220 rpm at room temperature. Different concentrations of ammonia solution ranging from 25-200 mg l⁻¹ were prepared by stepwise dilution of stock solutions using bi-distilled water. Different amounts (m) of HTC-chars used as adsorbents and 75 ml of the NH₄OH solution (v) were added to glass-stoppered Erlenmeyer flasks with 100 ml capacity. At the designated time, the solid and liquid phases of mixture were separated by filtration through Millipore (0.20 µm) filter. The initial ammonia concentrations (C₀) and the equilibrium ammonia concentration (C_e) were determined spectrophotometrically using Spekol 11 Carl Zeiss Jena, GDR single beam spectrophotometer at a wavelength absorbance of 625 nm.

A calibration curve was developed with NH_4OH standard solution. The amount of ammonia removed was determined by measuring the ammonia concentration difference in solutions before and after adsorption. The adsorption capacity (Q) by one unit weight of adsorbent was defined as seen in equation 8 (Lebedynets et al., 2004).

$$Q = \frac{(C_0 - C_e)v}{m} \quad (8)$$

The removal efficiency rate (R [%]) was defined as the ratio of difference in the solute before and after adsorption to its initial concentration in the solution and calculated as seen in equation 9.

$$R [\%] = \frac{(C_0 - C_e)}{C_0} \times 100 \quad (9)$$

3.4.2.1 Experimental section according to adsorption parameters

Different types of HTC-chars were produced in order to investigate their adsorption performance. The HTC-chars produced were washed with bi-distilled water to remove any substances physically adhered to the surface, and were then dried at 110°C for 6 h. Thereafter, the dried samples of HTC-char were ground and passed through a 2 mm sieve to ensure a consistent particle size.

Two commercial activated carbons were used in the preliminary test for comparison purpose. The properties of the activated carbons are recorded in Table 3.

Table 3: Characteristics of commercial activated carbon used

Sample	BET [$\text{m}^2 \text{g}^{-1}$]	Bulk density [g cm^{-3}]	pH	Ash [%]
Ac ₁	300	0.47	N.A	9
Ac ₂	1000	0.55	basic	10

In the **first adsorption set**, the adsorption performances of HTC-chars produced from reed, typha, juncus and carex at different HTC-reaction temperatures were investigated in order to study the effect of this parameter on the adsorption performance. The raw materials and HTC-chars of reed, typha, juncus and carex produced at different carbonization reaction temperatures (first series of HTC-experiments in Table 2) were chosen for these experiments. HTC-char (0.25 g) was added in 75 ml NH_4OH solution (100 mg l^{-1}). All samples were shaken for 1 h. Furthermore, the analysis of variance was performed to detect the significance effect of the variation of the reaction temperatures during HTC-process on the adsorption performance of HTC-chars produced. Each

group contained HTC-chars produced from the four types of the raw materials at each reaction temperature.

In the **other adsorptions sets** (second set till the sixth set), three types of HTC-chars of the fourth series of HTC-experiments (Table 2) were used. HTC-chars produced using citric acid (0.50 g) and phosphoric acid (6.50 g) as catalysts while keeping the HTC-reaction temperature at 230 °C as well as the oxidized HTC-chars, produced using citric acid as catalyst, with 10 % nitric acid (the last one in the fourth series in Table 2).

In the **second adsorption set**, the effects of the type of HTC-chars depending on the raw materials, catalysts and oxidation on their adsorption performance was investigated. Experiments were carried out using initial ammonia concentration of 75 mg l⁻¹, 0.25 g of HTC-char and contact time of 1 h. Furthermore, the analysis of variance was performed to detect the significance effect of the variation of raw materials type used on the adsorption performances of adsorbents. Each group contained HTC-chars produced from a certain raw material while using citric acid or phosphoric acid during HTC as well as after oxidation. Another significance test was performed to study the effect the catalyst during HTC-process and the oxidation after production on the adsorption performance of HTC-chars. Each group contained HTC-chars produced from the four types of the raw materials at each catalyst or after oxidation.

In the **third adsorption set**, the equilibrium studies were done at different contact time intervals 15, 30, 45 min and 1.h, 1.5 h then 2 h using 0.25 g of HTC-char at the initial concentration of ammonia 75 mg l⁻¹ to investigate the effect of contact time on the adsorption performance of HTC-chars used. Furthermore, the analysis of variance was performed to detect the significance effect of the variation of the contact times during adsorption. Each group contained HTC-chars produced from the four types of the raw materials at each contact time.

In the **fourth adsorption set** and in order to study the influence of the initial concentration, adsorption experiments were carried out using initial ammonia concentrations of 25, 50, 75, 100, 150 and 200 mg l⁻¹. Furthermore, the analysis of variance was performed to detect the significance effect of the variation of the initial concentrations. Each group contained HTC-chars produced from the four types of the raw materials at each initial concentration.

In the **fifth adsorption set**, the initial solution pH values were previously adjusted between 5.84 and 11 using 0.1 M HCl and NaOH. The initial concentration of ammonia was 75 mg l⁻¹. HTC-chars with the highest adsorption of ammonia in the initial

evaluation were used to test the effects of the variation of the solution pH on their adsorption performance. Furthermore, the analysis of variance was performed to detect the significance effect of the variation of the initial pH values during adsorption. Each group contained HTC-chars produced from the four types of the raw materials at each solution pH value.

In the **sixth adsorption set**, experiments were performed over the adsorbent dosage range from 0.15, 0.25, 0.5 and 1 g. Ammonia solution 75 mg l^{-1} was equilibrated with HTC-chars of reed and typha. Furthermore, the analysis of variance was performed to detect the significance effect of the variation of the adsorbent dosages during adsorption. Each group contained HTC-chars produced from the four types of the raw materials at each adsorbent dosage.

3.4.2.2 Quality assurance

The data presented in this study constituted average values as experiments were repeated three times over for reliability. Bi-distilled water and analytical grade reagents were used for adsorption experiments. A preliminary control test using only NH_4OH solution had shown no indication of the adsorption of the glass wall of the flask, and no concentration changes due to the volatilization during the experimental period. The losses by filtration were not considerable (Ibrahim et al., 2018).

3.4.2.3 Adsorption isotherm models

At the beginning of adsorption, the concentration of solutes are changing until the reaching a steady state. Adsorption equilibrium describes the state in which the adsorbent has adsorbed the maximum available amount of the solutes under the conditions used and therefore, the concentrations remain constant over time (Werner, 2003). An isotherm equation is usually used to express the adsorption equilibrium; its parameters present the surface characteristics and affinity of an adsorbent at a certain pH and temperature. This can present further perception onto the type of adsorption process and support by designing and optimizing the adsorption systems and design of the adsorption equipment (Limousin et al., 2007; Allen et al., 2004).

The application of the amount of adsorbate accumulated on the surface of an adsorbent after reaching equilibrium at constant temperature against the equilibrium concentration of the solution results in the so-called adsorption isotherm. Different types of isotherm models are available to express mathematically the equilibrium behavior and to facilitate estimation of the adsorption process such as Freundlich, Langmuir, Brunauer-

Emmett-Teller and Redlich-Peterson (Zhao et al., 2010; Zheng et al., 2008). The two well-known isotherm models, Freundlich (Freundlich, 1906) and Langmuir (Langmuir, 1918) are the most commonly used method for investigation the equilibrium study.

Freundlich isotherm model

In 1906, Freundlich submitted the earliest known adsorption isotherm equation. This empirical model could be used with multilayer adsorption with non-uniform distribution over the heterogeneous surface. It is convenient in correlating data collected over a wide range of concentration.

The expression of Freundlich isotherm and its linearized form to determine Freundlich constants K_f in terms of the equilibrium adsorption capacity (q_e) at the equilibrium concentration (C_e) are shown in equations 10 and 11.

$$q_e = K_f \cdot C_e^{\frac{1}{n}} \quad (10)$$

$$\log q_e = \log k_f + \frac{1}{n} \cdot \log C_e \quad (11)$$

Values of n (related to the adsorption intensity) are ranging between 1 and 10 ($1/n < 1$) represents favorable adsorption (Vassileva et al., 2008). The higher values of $1/n$ indicate a weak adsorption bond, while the smaller values mean that adsorption bond is strong. The large K_f values represent a high adsorption capacity of adsorbents. Freundlich isotherm has been proved a suitable adsorption isotherm for the description of the adsorption in many cases, especially in aqueous solutions (Werner, 2003).

Langmuir isotherm model

Langmuir (1918) isotherm is one of the most widely used models. It suspects monolayer coverage of adsorbate on a homogeneous adsorbent. The adsorbent is assumed to have a limited uptake capacity, where each site can accommodate only one molecule (Demirbas et al., 2008; Limousin et al., 2007; Allen et al., 2004).

The Langmuir isotherm, when fitted to experimental data, helps to evaluate the maximal adsorption capacity (q_m) and the affinity coefficient (b). Langmuir isotherm can be written as in equation 12 (Allen et al., 2004; Ghiaci et al., 2004).

$$q_e = \frac{b q_m C_e}{1 + b C_e} \quad (12)$$

Langmuir equation can be assigned into the following liner form as in equation 13 (Zhao et al., 2010).

$$\frac{C_e}{q_e} = \frac{1}{q_m \cdot b} + \frac{C_e}{q_m} \quad (13)$$

By applying C_e/q_e to C_e , it is possible to obtain the values of q_m and b . Langmuir adsorption isotherm has also been applied to many pollutant sorption processes.

The separation factor (R_L) expresses the favorability or unfavorability of the Langmuir isotherm and it can be calculated as in equation 14 (Nguyen and Lee, 2015).

$$R_L = \frac{1}{1 + b \cdot C_0} \quad (14)$$

Where, C_0 is the initial ammonia concentration.

This dimensionless factor presents the isotherm shape, which is suggested to be unfavorable ($R_L > 1$), linear ($R_L = 1$), favorable ($R_L < 1$) or irreversible ($R_L = 0$)

3.4.2.4 Experiments on regeneration and re-usability studies

In addition to its high adsorption capacity, a good adsorbent must also present a good ability of reuse during multiple adsorption-regeneration cycles, which is substantial importance in the economic development. Some solutions can be used to regenerate the exhausted adsorbents in order to reuse them in new adsorptions experiments.

Preliminary experiments proved that each of sodium hydroxide (NaOH), hydrochloric acid (HCl) or sodium chloride (NaCl) could be used as regenerant for the desorption of adsorbed ammonia on the surface of different adsorbents (Abdul Halim et al., 2013; Du et al., 2012; Zheng and Wang, 2009)

Three regeneration agents 1 M NaCl (adjusted with NaOH to pH= 11.77), 0.1 M NaOH (pH= 13.44) and 0.1 M HCl (pH= 1.14) were selected for the preliminary test at room temperature. Only one type of the exhausted adsorbent was used in order to investigate the influence of using these agents on the development of the adsorption capacity and choose the best one for other regeneration trials.

A fixed amount (0.25 g) of adsorbent was contacted separately with 100 ml of regeneration agent and then it kept stirring at room temperature for 30 min. The regenerated adsorbent was washed with bi-distilled water several times for another adsorption. After choosing the best regeneration agent, the same regeneration procedure was repeated for three times.

The adsorption capacity, removal efficiency rate and regeneration ratio were determined after each process. The regeneration ratio is defined as the ratio of adsorption capacity of the regenerated HTC-char at equilibrium to the original adsorption capacity of the

virgin HTC-char at equilibrium (Goel et al., 2005). The same adsorption parameter were used for all experiments.

3.4.2.5 Preliminary test with HTC-chars and commercial activated carbon

In this preliminary test, HTC-chars produced from reed, typha, juncus and carex at reaction temperature 230 °C and reaction time 15 h using citric acid as catalyst in addition to two commercial activated carbon were used in order to investigate the possibility of using HTC-chars as adsorbents for ammonia removal in aqueous solution. The test was executed by adding 0.25 g of the adsorbent in 75 ml NH_4OH solution (75 mg l^{-1}) and all samples were shaken for 1 h.

The results presented in Figure 17 show that all used adsorbents have the possibility to adsorb ammonia. Interestingly, HTC-chars produced from reed and typha had higher adsorption capacity than the commercial carbon samples used, where HTC-char from reed had the highest one compared with all adsorbents used.

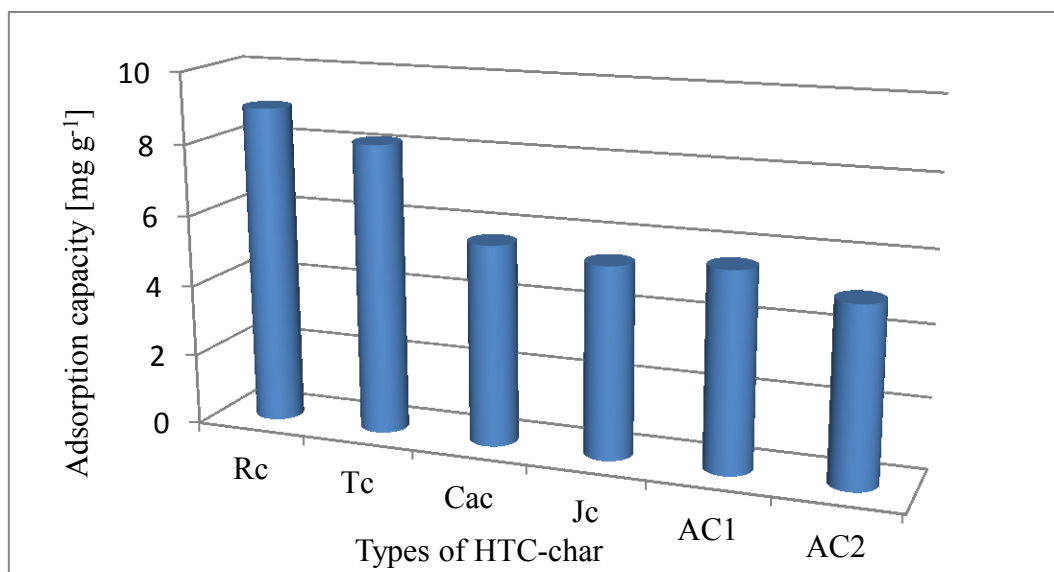


Figure 17: Adsorption capacities of ammonia on two commercial activated carbon (AC_1 and AC_2) and HTC-chars produced from reed (R), typha (T), juncus (J) and carex (Ca)

The adsorption capacities of HTC-char from reed and typha were more than those of the commercial carbon samples AC_1 and AC_2 , respectively. The adsorption capacities of HTC-chars from carex and juncus as well as the commercial carbon samples were similar. With respect to the removal efficiency of the tested samples, the following order can be determined: $\text{AC}_1 < \text{Jc} < \text{AC}_2 < \text{Ca}_c < \text{Tc} < \text{Rc}$.

Other preliminary tests were also performed in batch study for adsorbents prepared by the oxidation/ impregnation HTC-chars produced from reed with phosphoric acid or

nitric acid (25 % and 50 %). The tests were performed using 0.25 g of the adsorbent, initial ammonia concentrations of 75 mg l⁻¹ and contact time of 1 h.

The adsorption capacities were 4.22, 7.66 and 2.23 mg g⁻¹ for adsorbents oxidized with phosphoric acid, nitric acid (25 %) and nitric acid (50 %), respectively. These adsorption capacities were lower than that for adsorbent produced from reed before oxidation, so that no further tests or analyses were performed.

3.4.3 Fixed-bed column study

During the continuous column adsorption, a mass transfer zone will be built due to the contact between a contaminated solution stream and a fixed-bed adsorbent. Most of the contaminated adsorbate species will be adsorbed near the bed inlet. When the inlet portion of the adsorbent becomes saturated, the adsorption will be deeper within the bed and the mass transfer zone moves along and reaches its discharge limit by indicating of contamination in the outflow. This state is classified as breakthrough and the amount of the adsorbed material is taken into account as the breakthrough capacity.

When the solution stream is continued, the exit concentration increases slowly from the bed until it reaches the same level of the input concentration. That indicates a complete saturation of the bed at this point. The lifetime of the fixed-bed is considered the time when the exit concentration has reached an unacceptable level.

3.4.3.1 Experimental section of the fixed-bed column studies

The adsorption experiments of ammonia under a dynamic column adsorption study were carried out in a cylindrical Plexiglas column (2.50 cm in outside diameter, 1.80 cm inside diameter, 40 cm in height and a total volume of 102 ml) as shown in Figure 18.

A metallic mesh was set at the bottom of the bed as distributor; up and down the bed were filled with glass wool (inert bed with a height of 5 cm). Concentrations of ammonia in the effluent were determined as a function of time where a sample would be taken at regular intervals for analysis using auto sampler (ETG, Germany).

The fixed-bed column study was carried out using four types of HTC-chars including HTC-chars produced from reed and typha using phosphoric acid during HTC as well as after oxidation, namely HTC-chars that had the best ammonia removal efficiency in the already performed batch study. The adsorbent was charged with different concentrations of ammonia solution (NH₄OH) using a peristaltic pump (Heidolph Pumpdrive 5201) to

keep a desired constant flow rate. The fixed-bed column was exhausted by up-flow mode in order to ensure a uniform streaming and avoid channeling.

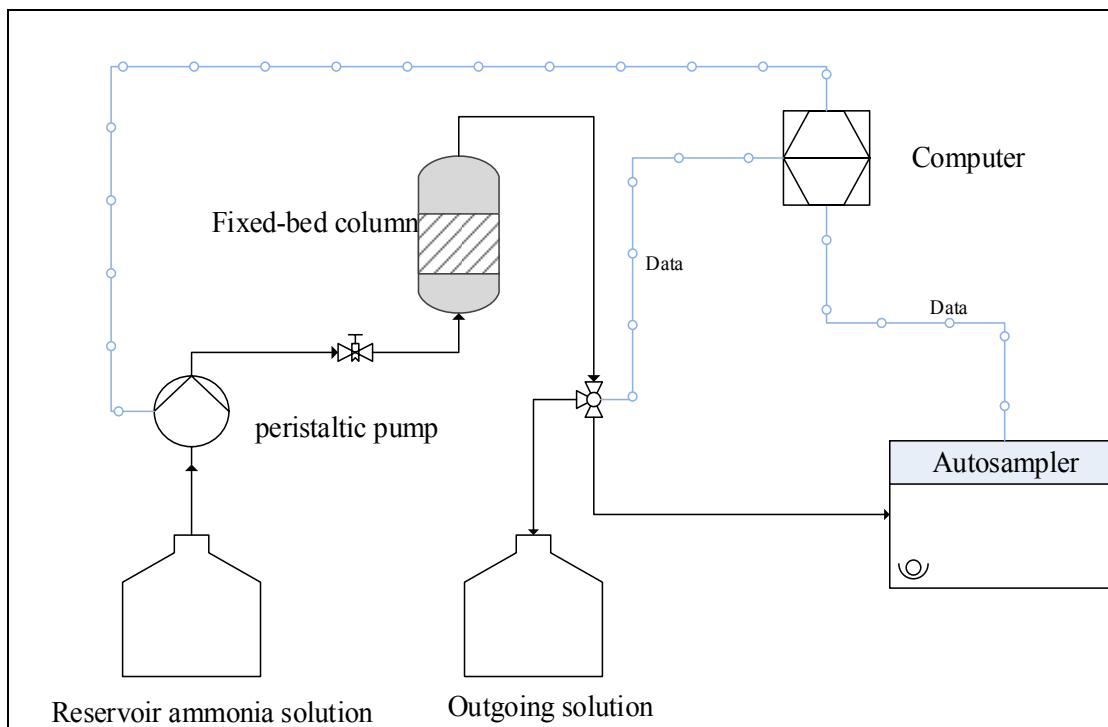


Figure 18: Schematic diagram for the adsorption experiments using a fixed-bed column of HTC-chars as adsorbents

The inlet was given from the bottom of the column, in this case the flow moved upwards, interacting with the particles present in the column. Particle sizes of 1-2 mm were used so that the column-to-particle diameter is ≥ 10 . This can help to reduce the influence of pressure drop (Worch, 2012).

The analysis of variance is made in order to investigate the effect of the variation of adsorption parameters on the adsorption performance in column study.

In the **first adsorption set**, the effect of flow rates on the adsorption performances of adsorbents used was investigated. Flow rates (F) of 1, 3.50 and 7 ml min^{-1} were chosen to prevent bed lifting. After the adjusting of the peristaltic pump, it was found that the actual flow rates were 0.75, 3.30 and 6.60 ml min^{-1} , respectively. Bed lifting was observed during the tests using a flow rate of 9 ml min^{-1} , so that tests were stopped.

The experiments were executed using bed height 20 cm and initial ammonia concentration 75 mg l^{-1} . Furthermore, the analysis of variance was performed to detect the significance effect of the variation of the flow rates on the adsorption performance. Each group contained HTC-chars produced from the reed and typha at each flow rate.

In the **second adsorption set**, the influence of the initial ammonia concentration (C_0) was studied. Initial ammonia concentrations of 50, 75 and 100 mg l⁻¹ were used in this test. Experiments were executed using bed height 20 cm and flow rate 3.30 ml min⁻¹. Furthermore, the analysis of variance was performed to detect the significance effect of the variation of the initial concentrations during adsorption. Each group contained HTC-chars produced from the reed and typha at each initial ammonia concentration.

In the **third adsorption set**, experiments were performed over bed heights (H) of 20 cm and 30 cm, which met a certain amount (M) of adsorbent in the column. The experiments were executed at initial ammonia concentration 75 mg l⁻¹ and flow rate 3.30 ml min⁻¹. The analysis of variance was performed to detect the significance effect of the variation of the bed heights during adsorption. Each group contained HTC-chars produced from reed and typha at each adsorbent dosage.

The experimental unit for adsorption and regeneration tests was manufactured as shown in Figure 19. The effect of each operating variable on the adsorption efficiency of HTC-chars was studied. The concentration of ammonia in the effluent was determined as a function of time where a sample would be taken at regular intervals for analysis



Figure 19: Adsorption and regeneration experimental unit for adsorption using a fixed-bed column of HTC-chars

After beginning the adsorption, the effluent concentration grows with time that is termed as break point, while the breakthrough time (T_b) is the time taken for reaching the effluent concentration a specific breakthrough concentration of interest. In this study, T_b was assigned as the time when the effluent concentration (C_e) of ammonia reached 50 % of the initial concentration (C_0). Breakthrough curves were developed for presumption the column efficiency in the recovery of ammonia. These curves were plotted-giving (C_e/C_0) and time (h) for varying operating conditions.

The experiments were stopped when the effluent concentration of ammonia (C_t) was equal to 90 % of the initial ammonia concentration (C_0) and this time was expressed as the time required for bed exhaustion (T_e at $C_t/C_0 = 0.9$). After stopping the experiments, the liquid in the column was drained, and the column was subjected to regeneration test. Equation 15 was used to calculate the breakthrough capacity $Q_{0.5}$ (at $C_t/C_0 = 0.50$) in mg of ammonia adsorbed at the breakthrough time (T_b at $C_t/C_0 = 0.50$) per gram of adsorbent (Goel et al., 2005).

$$Q_{0.5} = \frac{T_b F C_0}{M} \quad (15)$$

At the breakthrough point, the bed is not fully used for the effluent uptake. The length of the unused bed (LUB) describes this situation; it is calculated as described in equation 16 (Karunaratheya and Amarasinghe, 2013).

$$LUB = \frac{H}{T_e} (T_e - T_b) \quad (16)$$

The fraction equivalent length of unused bed (FLUB) is defined as in equation 17.

$$FLUB = \frac{LUB}{H} \times 100 \quad (17)$$

3.4.3.2 Modelling of fixed-bed column breakthrough

Various models have been developed to analyze and describe the performance of the fixed-bed column and to scale it up for industrial applications. In this study, two models were used to predict the column dynamic behavior by determining breakthrough performance, adsorption capacity and the kinetic parameters of the fixed-bed column.

Thomas model

The Thomas model is one of the most generally and a widely used methods in column performance theory. It suggests that the rate of the adsorption is controlled by the surface reaction between the unused capacity of the adsorbent and the adsorbate. Thomas model helps to determine maximum adsorption capacity of an adsorbent, which

is also required in design. Adsorption rate constant (K_{th}) and adsorption capacity of the column (q_0) in a continuous adsorption process are calculated using equations 18 and 19 (Baek et al., 2007).

$$\frac{C_t}{C_0} = \frac{1}{1 + \exp\left[\frac{K_{th}}{F}(q_0M - C_0V)\right]} \quad (18)$$

The linearized form is given as described in equation 19.

$$\ln\left(\frac{C_0}{C_t} - 1\right) = \frac{K_{th}q_0M}{F} - \frac{K_{th}q_0C_0}{M}V \quad (19)$$

K_{th} and q_0 are defined from the plot of $\ln(C_0/C_t - 1)$ versus the sampling time (t) at a given flow rate (F). Where C_t and C_0 are the effluent and initial ammonia concentrations, V is the solution volume and M is the amount of adsorbent in the column. Thomas model was applied to determine the effect of the change in each of flow rates (0.75, 3.30 and 6.60 ml min⁻¹) and initial ammonia concentrations (50, 75 and 100 mg l⁻¹) at a fixed bed height of 20 cm.

Yoon–Nelson model

The Yoon-Nelson model supposes that the probability of adsorption for an adsorbate molecule decreases at a rate, which is proportional to both the adsorbate breakthrough and the probabilities of adsorbate adsorption (Yoon and Nelson, 1992). This model is usable for a single component system and demands with no detailed column parameters in connection with the type of adsorbent and the properties of adsorbate (Aksu and Gönen, 2004) and is expressed in equation 20.

$$\frac{C_t}{C_0 - C_t} = \exp(K_{yn}t - \tau K_{yn}) \quad (20)$$

The linearized form of equation 20 is given in equation 21.

$$\ln\left(\frac{C_t}{C_0 - C_t}\right) = K_{yn}t - \tau K_{yn} \quad (21)$$

The plot of $\ln(C_t/(C_0 - C_t))$ versus t will lead to a straight line with slope of Yoon-Nelson rate constant (K_{yn}) and intercept τK_{yn} . Where τ is the time required for 50 % adsorbate breakthrough. This model was used to evaluate the adsorption performance and predict the adsorption behavior in aqueous solution in HTC-char-fixed bed column at different flow rates (0.75, 3.30 and 6.60 ml min⁻¹) and initial ammonia concentrations (50, 75 and 100 mg l⁻¹) at a fixed bed height of 20 cm.

3.4.3.3 Experiments on regeneration and re-usability studies

Regeneration and reuse of the adsorbent material is a crucial aspect to make it more environments friendly and economical. The aim of the regeneration and re-usability studies was to remove the loaded ammonia from the column and regenerate the exhausted adsorbent to study the availability of multi-use of the adsorbent.

In the current study, the exhausted adsorbent was regenerated with 0.1 M HCl under flow rate 4.50 ml min^{-1} and adsorbent bed height of 20 cm for reuse in the next adsorption cycle. Each adsorption-regeneration stage was considered as one cycle. Three loading and two regeneration cycles were carried out. The concentration of ammonia in the effluent was measured at different time interval to show the completion of regeneration.

The adsorptions experiments were terminated when the effluent concentration approached about 95 % of the feed concentration and desorption steps were stopped when the effluent concentration was about 0.05 % of the feed concentration. All regeneration tests were carried out at room temperature. Breakthrough, exhausted times and adsorption capacity for adsorbents used before and after regeneration were determined.

3.5 Statistical testing of significance

The statistical analysis to measure the effects of varying process parameter on each of the characterization of HTC-chars and their adsorption performance in batch study and fixed-bed column study were studied via a statistical program IBM SPSS Statistics 22.

IBM SPSS Modeler is a comprehensive predictive data management system for analyzing data, which presents a mechanism for taking quantitative decisions about processes (Sabine and Everitt, 2004). It is based on comparing the variance between different groups to the variability within each particular group (Sabine and Everitt, 2004; Montgomery and Runger, 2003).

The analysis of variance One-Way ANOVA, which is hypothesis-testing technique, was used to compares the statistical differences among means between different groups to determine whether there was statistical difference. Significance levels were defined as highly significant ($p < 0.01$), significant ($0.01 < p < 0.05$), and not significant ($p > 0.05$).

Table 4 shows the ANOVA table, which summarized the computations that make for the F-statistic. F-test analysis of variance was used to verify the statistically significant of the sample at 95 % confidence level.

Table 4: Basic one-way ANOVA table (Ostertagová and Ostertag, 2013)

Variance source	Sum of squares (SS)	Degrees of freedom (df)	Mean square (MS)	F-value	Tail area above F
Between	SSb	K-1	MSb	MSC/MSW	p-value
Within	SSw	N-K	MSw	—	—
Total	SS _t	N-1	—	—	—

Where (Ostertagová and Ostertag, 2013),

$$SSb = \sum_{i=1}^K \sum_{j=1}^{n_i} (\bar{x}_i - \bar{x})^2 \quad (22)$$

$$SSw = \sum_{i=1}^K \sum_{j=1}^{n_i} (x_{ij} - \bar{x}_i)^2 \quad (23)$$

$$SS_t = \sum_{i=1}^K \sum_{j=1}^{n_i} (x_{ij} - \bar{x})^2 \quad (24)$$

$$SS_t = SSb + SSw \quad (25)$$

$$N = n_1 + n_2 + \dots + n_K \quad (26)$$

$$MSb = \frac{SSb}{K - 1} \quad (27)$$

$$MSw = \frac{SSw}{N - K} \quad (28)$$

4 Results and discussion

4.1 Hydrothermal carbonization experiments

4.1.1 Qualitative parameter

HTC from wetland biomasses produced a hydrophobic char, which was easy to be dried and pelleted. The palletization could help to avoid some of the major problems like transportation difficulties, low bulk density. The color of biomass changed through HTC-process because of the losses of the moisture and light volatile gases at different stages of HTC depended on the process parameters. The changes in color can be as an indicator of the degree of conversion. For example, the color changed from brownish to dark when the reaction temperature and time were increased.

As seen in Figure 20 the color of HTC-char produced at reaction temperature of 230 °C was dark brown. HTC-chars produced at higher reaction temperatures retained less moisture, more fragile and could be easily powdered by hand. The evaluation of the fragility was qualitative and no quantitative analysis for this property was performed.



Figure 20: Raw material and HTC-char produced

The plant structures were often still recognizable after the carbonization of wetland biomasses, although a substantial material conversion had occurred.

Wiedner et al. (2013) proposed that most of the polysaccharides did not degrade at lower reaction temperatures, leading to a char more similar to the original raw materials. Actually, the lignin content generally reduced with increasing reaction temperature, while the content of black carbon increased (Du et al., 2012).

Dissolving of organic substances in the process water during the cleavage reactions resulted in yellowish to brownish HTC-process water. On the other hand, decreasing the reaction temperature created darker process water.

4.1.2 Effect of the HTC-reaction temperature on HTC-char

4.1.2.1 HTC-char yields

As presented in Figure 21, a higher yield of HTC-char was observed at lower reaction temperatures. As expected, the yield of HTC-char decreased with increasing the reaction temperature. By increasing the reaction temperature from 180-230 °C there was a reduction of more than 30 % of the HTC-chars produced for all raw materials used.

The highest char yields were found in the HTC of reed at all reaction temperatures used, while the smallest was that associated with the carbonization of carex suggesting that the yield of HTC-char also showed some variation with the kind of biomass, similar results were recorded by others (Aydincak et al., 2012; Xiao et al., 2012).

These results were consistent with the suggestion of previous studies about the influence of the reaction temperature on the yield while using other kinds of biomass (Hoekman et al., 2011; Kumar, 2011; Yan et al., 2010).

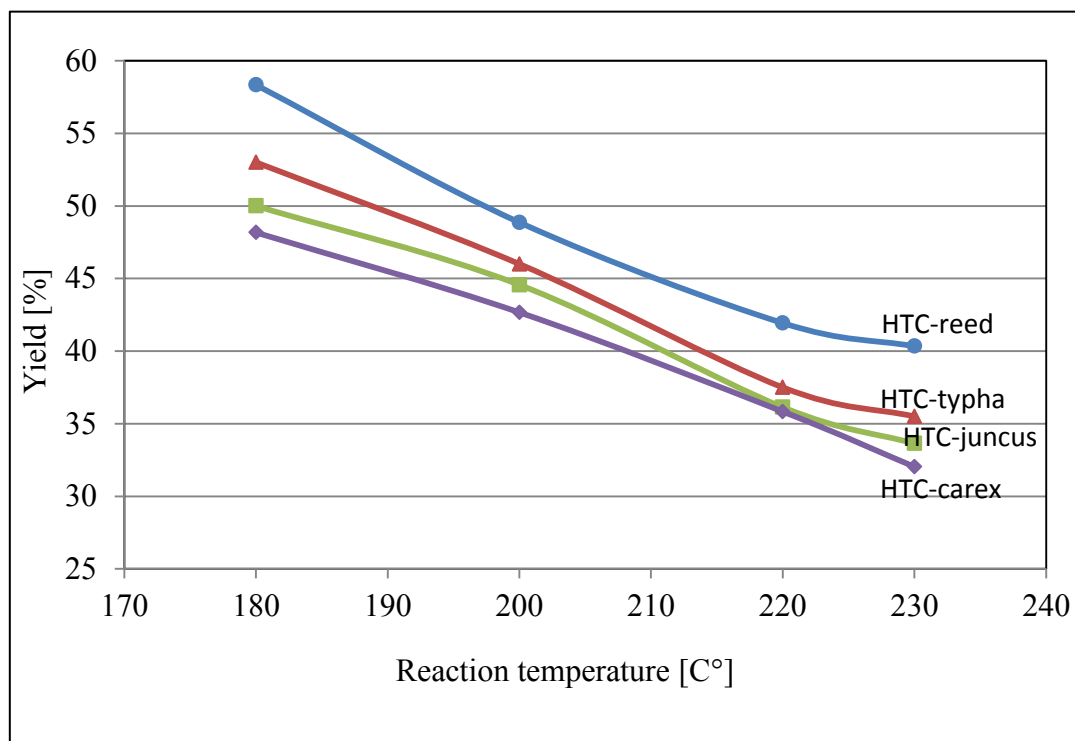


Figure 21: Effect of the variation of reaction temperatures between 180-230 °C on the yield of HTC-char produced

The yield is the proportion of the solid product, which remains after HTC. Higher weight loss during HTC resulted in lower yields of HTC-chars; this weight loss was attended with an enhancement in the molecular weight.

The impact of the reaction temperature on polymeric compositions, and devolatilization rate could explain the different solid yields or mass losses at different reaction temperatures. Therefore, the mass loss during HTC depends on the devolatilization of hemicellulose. Similar results were also observed by different pyrolysis reactions (Rousset et al., 2011). At reaction temperatures 180-200 °C, hemicellulose (the most active component in the biomass) degrades and forms water-soluble pentose that can explain the lower yield of HTC-chars produced from carex, which had the higher content of hemicellulose (Table 1). The crystalline structure of the cellulosic fibrils makes them relatively stable to the temperature than the hemicellulose. Cellulose is relatively inert and begins to hydrolyze at 220 °C to produce hexoses. Lignin is more heat-resistant compared to hemicellulose and cellulose. Higher lignin content in the biomass favor the solid yield, therefore, higher lignin content in reed (Table 1) led to higher HTC-char yield in comparison with the others HTC-chars produced.

4.1.2.2 Elemental compositions

Table 5 lists the data about the average values of the proportions of carbon, hydrogen, nitrogen, oxygen and ash content of the raw materials used and HTC-chars produced as well as the atomic ratio of oxygen-to-carbon (O/C) and hydrogen-to carbon (H/C).

The results show that the elemental composition (C, H, N and O) of the solid materials changed because of HTC. Increasing the reaction temperature led to an increase in the carbon proportion for all HTC-chars produced. In contrast to the reaction temperatures of 180, 200, and 220 °C, higher carbon proportions were obtained at 230 °C.

HTC-chars produced from the four raw materials at 230 °C showed an increase in the carbon proportion in the range of about 52-66 % compared with the raw materials.

For all HTC-chars produced, there was a slightly change in the hydrogen proportion with the variation of reaction temperatures remaining under the hydrogen proportion of the raw material. The nitrogen proportion tended to increase with the reaction temperature between 180 and 220 °C remaining averagely over the nitrogen mass percentage of the raw material, a slightly decrease in the nitrogen proportions was found by increasing the reaction temperature from 220 to 230 °C.

Table 5: Characterizations of the raw material and HTC-chars produced at different reaction temperatures

Parameter	Unit	Materials				
		Raw material	HTC-char			
			Reaction temperature [°C]			
			180	200	220	230
		Reed	R ₁	R ₂	R ₃	R _c
C	[%]	43.82	52.32	56.97	63.79	66.71
H	[%]	5.82	4.22	4.24	4.68	4.85
N	[%]	0.54	0.95	1.37	1.61	1.53
O ^[a]	[%]	45.67	39.24	34.21	27.22	23.41
Ash	[%]	4.15	3.26	3.22	2.70	3.50
O/C ^[b]	[-]	0.78	0.56	0.45	0.31	0.26
H/C ^[b]	[-]	1.59	0.97	0.89	0.88	0.87
		Typha	T ₁	T ₂	T ₃	T _c
C	[%]	42.74	52.69	56.73	64.08	67.30
H	[%]	5.58	5.45	5.03	5.29	5.09
N	[%]	0.78	0.46	0.72	0.88	0.78
O ^[a]	[%]	47.08	38.48	34.58	26.08	23.15
Ash	[%]	3.82	2.92	2.94	3.67	3.68
O/C ^[b]	[-]	0.82	0.55	0.46	0.31	0.29
H/C ^[b]	[-]	1.57	1.24	1.06	0.99	0.91
		Juncus	J ₁	J ₂	J ₃	J _c
C	[%]	43.27	54.35	60.87	68.35	70.95
H	[%]	5.85	5.05	5.59	5.35	5.25
N	[%]	1.41	1.73	1.95	2.93	2.92
O ^[a]	[%]	45.23	37.72	30.31	21.86	19.54
Ash	[%]	4.24	1.15	1.28	1.51	1.34
O/C ^[b]	[-]	0.78	0.52	0.37	0.24	0.21
H/C ^[b]	[-]	1.62	1.13	1.10	0.94	0.89
		Carex	Ca ₁	Ca ₂	Ca ₃	Ca _c
C	[%]	42.24	51.57	57.44	66.94	70.28
H	[%]	5.86	5.09	5.44	5.49	5.57
N	[%]	2.17	1.60	2.54	3.93	3.76
O ^[a]	[%]	44.09	40.89	33.67	22.22	19.25
Ash	[%]	5.64	0.85	0.91	1.42	1.14
O/C ^[b]	[-]	0.78	0.59	0.44	0.25	0.21
H/C ^[b]	[-]	1.66	1.18	1.14	0.99	0.95

^[a] Content by difference ^[b] Atomic ratio (Ibrahim et al. 2014).

The different HTC-chars were designated as R_N, T_N, J_N and Ca_N, where N= 1, 2, 3 and c indicated to chars produced at 180, 200, 220 and 230 °C, respectively

On the other hand, increasing the reaction temperatures resulted in an obvious reduction in the oxygen proportions for all HTC-chars produced compared with the raw materials. Ash content in HTC-chars changed only slightly when the reaction temperature was increased. In comparison with the raw materials used, all HTC-chars produced had lower ash contents, where HTC-chars from juncus and carex had lower ash content than those from reed and typha.

Interestingly, HTC-chars produced from reed and typha had similar carbon and oxygen proportions as well as ash content. The same observation was found related to HTC-chars produced from juncus and carex. HTC-chars had an increase in the carbon proportion as lower O/C and H/C atomic ratios compared with the raw materials. These rates decreased with increasing process severity. For operating conditions of 230 °C, a reduction of about 42-45 % of H/C atomic ratios and about 66-73 % of O/C atomic ratios were calculated.

The reaction temperature was regarded as the most influential parameter. The obtained results in this study were an indication that the elemental composition (C, H, N and O) of the solid materials altered perceptibly through HTC, which was also reported by other Authors (Xiao et al., 2012; Dinjus et al., 2011). These variations became greater as the reaction temperature increased, which was consistent with a carbonization process (Sevilla and Fuertes, 2009b). The results presented that the properties of HTC-chars produced depended on the type of the raw materials as well as the reaction temperature, which corroborated the research hypothesis related to these parameters.

The raw materials used contained more than 40 % by weight of oxygen. HTC-process actually led to the deoxygenation of biomass. The removal of oxygen is most easily accomplished by dehydration and decarboxylation reactions in which oxygen is removed in the form of water or carbon dioxide (Peterson et al., 2008). Authors agreed that generally an increase of the reaction temperature led to an increment in the carbon proportion of the HTC-char produced, while the oxygen proportions decreased (Heilmann et al., 2011; Mumme et al., 2011).

The reduction in the ash proportion after carbonization might be due to the dissolution of some minerals substances in the water during HTC-process.

The atomic ratios of H/C and O/C are as indicators of the degree of carbonization of HTC-chars. High atomic ratios show the existence of incipient plant macromolecules (e.g. cellulose), while the low ones are representative of more condensed (aromatic) structures (Schimmelpfennig and Glaser, 2012; Chun et al., 2004).

4.1.2.3 Van Krevelen diagram

H/C and O/C atomic ratios for the raw materials used and HTC-chars produced at reaction temperatures 180 and 230 °C are presented in Figure 22 for comparative purposes. The dotted lines indicated the dehydration process and the dashed lines represented the decarboxylation processes (Ibrahim et al., 2014; Aydincak et al., 2012; Berge et al., 2011). The atomic ratios for bituminous coal and lignite coals were included for comparative purposes (Berge et al., 2011). The starting raw materials were shown in the biomass area (A) in the upper right corner of the diagram.

The different HTC-chars were designated as R_N , T_N , J_N and Ca_N , where $N=1$ and c indicated to chars produced at 180 and 230 °C

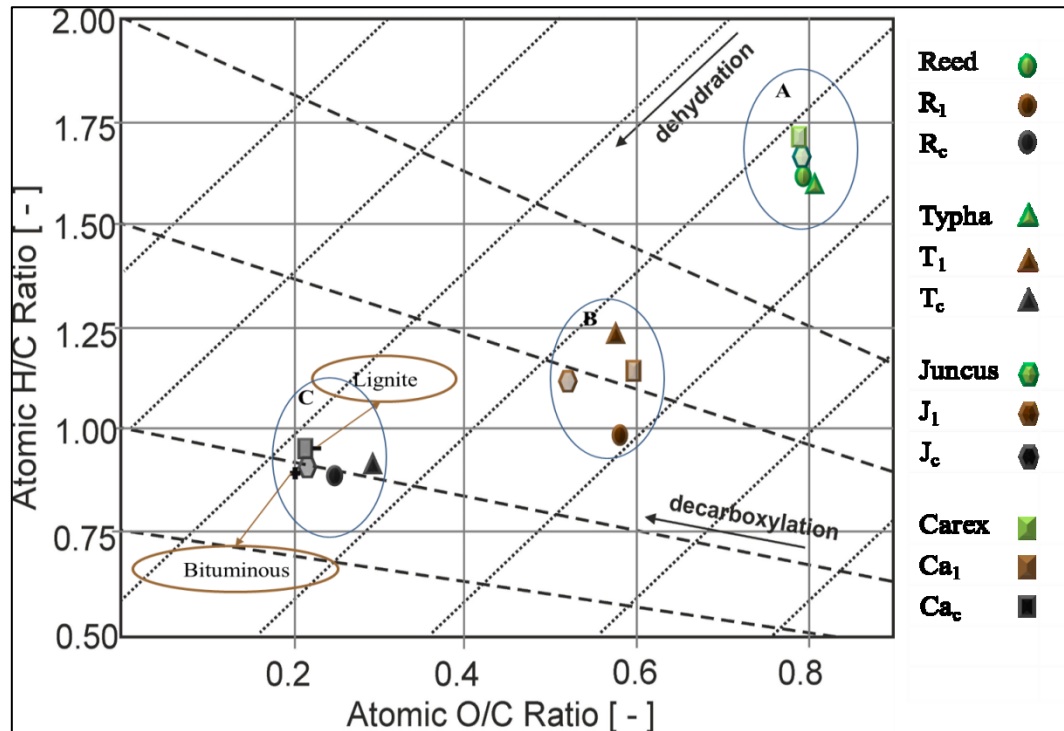


Figure 22: H/C and O/C atomic ratios of the raw materials used and HTC-chars produced at 180 and 230 °C (Ibrahim et al., 2014)

In general, both the H/C and O/C atomic ratios decreased when the reaction temperature was raised. HTC-chars produced at reaction temperatures 180 °C were in the peat area (B) and HTC-chars produced at 230 °C were in the brown coal area (C).

At higher HTC-reaction temperatures, HTC-chars produced were increasingly more similar to those associated with lignite and bituminous coal than those of their raw materials. Ruyter (1982) reported that O/C atomic ratios of 0.20-0.30 are indicative of low-grade coals. This diagrammatic overview presents a distinct view on the chemical transformation of the carbonaceous material whilst providing information about the potential reaction routes.

The conversion of wetland biomasses was mainly dominated by the dehydration process (lower H/C), which explained why the HTC-chars produced were mainly located on the bottom left. Anywise, there was a deviation from the diagonal line, which proposed the present of a side reaction, decarboxylation, occurred during HTC because a complete dehydration reaction removed water molecules from the samples.

4.1.2.4 Specific surface area, pore volume and $C_{\text{recovered}}$

The specific surface area and pore volume of the raw materials used and HTC-chars produced at 230 °C and 15 h using citric acid (c) as catalyst were listed in Table 6. Reed as raw material had the highest specific surface area and pore volume of 2.31 m² g⁻¹ and 0.0048 cm³ g⁻¹, respectively, while juncus had the lowest ones with 1.57 m² g⁻¹ and 0.0034 cm³ g⁻¹.

Table 6: Surface area, pore volume and $C_{\text{recovered}}$ of raw materials and their HTC-chars

Material	Surface area [m ² g ⁻¹]	Pore volume [cm ³ g ⁻¹]	$C_{\text{recovered}}$ [%]
Reed	2.31	0.0048	-
R _c	24.66	0.1247	61.40
Typha	2.29	0.0041	-
T _c	18.69	0.0862	55.20
Juncus	1.57	0.0034	-
J _c	8.61	0.0191	55.57
Carex	2.26	0.0037	-
Ca _c	11.58	0.0541	53.30

The specific surface areas of HTC-chars produced were 5-10 times higher than those were of the raw materials used. Additionally, there was five to 26 fold increase in the measured pore volumes after HTC indicating that HTC-chars had higher specific surface areas and greater pore volumes, which were observed with a considerable increment in the portion of adsorbed nitrogen gas during the measurement process.

The influence of the reaction temperature on the development of the specific surface area for HTC-chars showed that the porosity was increased considerably after HTC.

HTC-char from reed and typha produced showed higher surface area than those of HTC-chars produced from juncus and carex.

Figure 23 shows that the specific surface area of the HTC-chars from reed increased by the increment of reaction temperatures between 180-230 °C, and it was more than it was for the raw material reed. Increasing the reaction temperature from 180 to 230 °C resulted in an increase of 66.75 % in the specific surface area of the HTC-char produced.

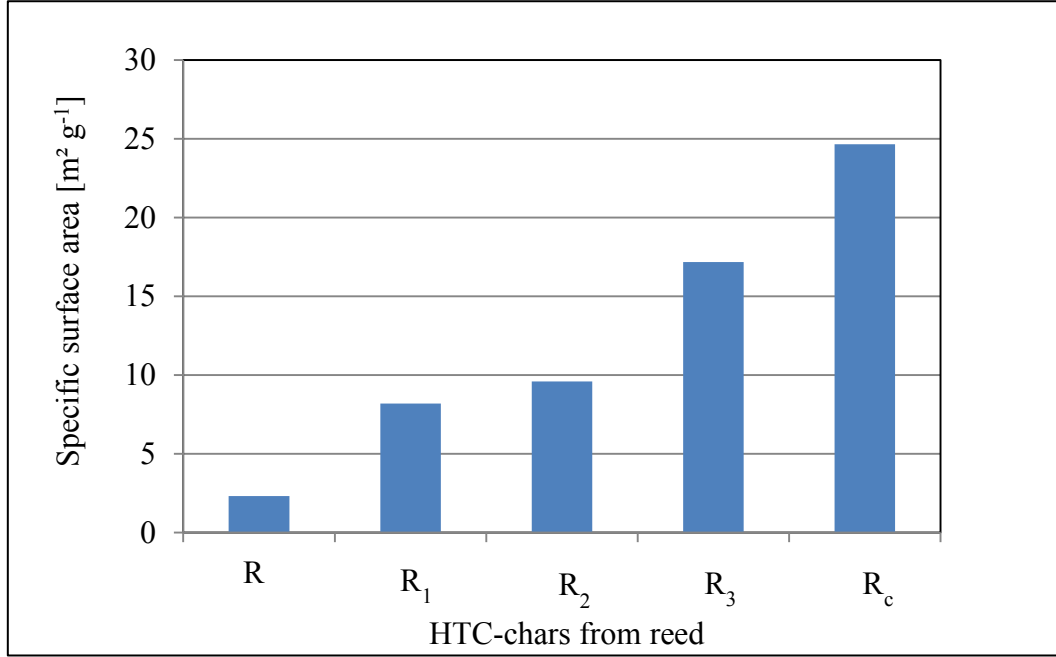


Figure 23: Effect of the variation of reaction temperatures between 180-230 °C on the specific surface area of HTC-chars produced from reed

Using the Brunauer-Emmett-Teller analysis (nitrogen absorption isotherms), typical surface areas of HTC-char produced from treated maize silage at 190 °C and 2 h was $12.30 \text{ m}^2 \text{g}^{-1}$ (Mumme et al., 2011) and 10.79 or $11.33 \text{ m}^2 \text{g}^{-1}$ for HTC-chars produced at 250 °C and 4 h from corn stalk and tamarix ramosissima (Xiao et al., 2012).

The highest carbon recovered ($C_{\text{recovered}}$ [%]) was found with HTC-char from reed (Table 6). It could be seen that the recovered carbon in HTC-chars were ranging from 53.30 % to 61.40 % pointing that a major proportion of the carbon in the biomass was stored, similar observation was confirmed by Xiao et al. (2012). The rest carbon (39.60 to 46.70 %) was found mainly in the organic compounds containing in the aqueous phase (furfural, 5-methylfurfural hydroxyl, organic acids, aldehydes, etc.).

The main element of biomass and HTC-char is carbon. The solid carbon values are actually more important for HTC-char with regard to their use. Apart of it is a solid carbon with respect to quantitative analysis and another part is present as a volatile portion (Brownsort, 2009).

Figure 24 shows the adsorption-desorption isotherms using BET-method (nitrogen absorption isotherms) of raw materials used and HTC-chars produced at a reaction temperature of 230 °C.

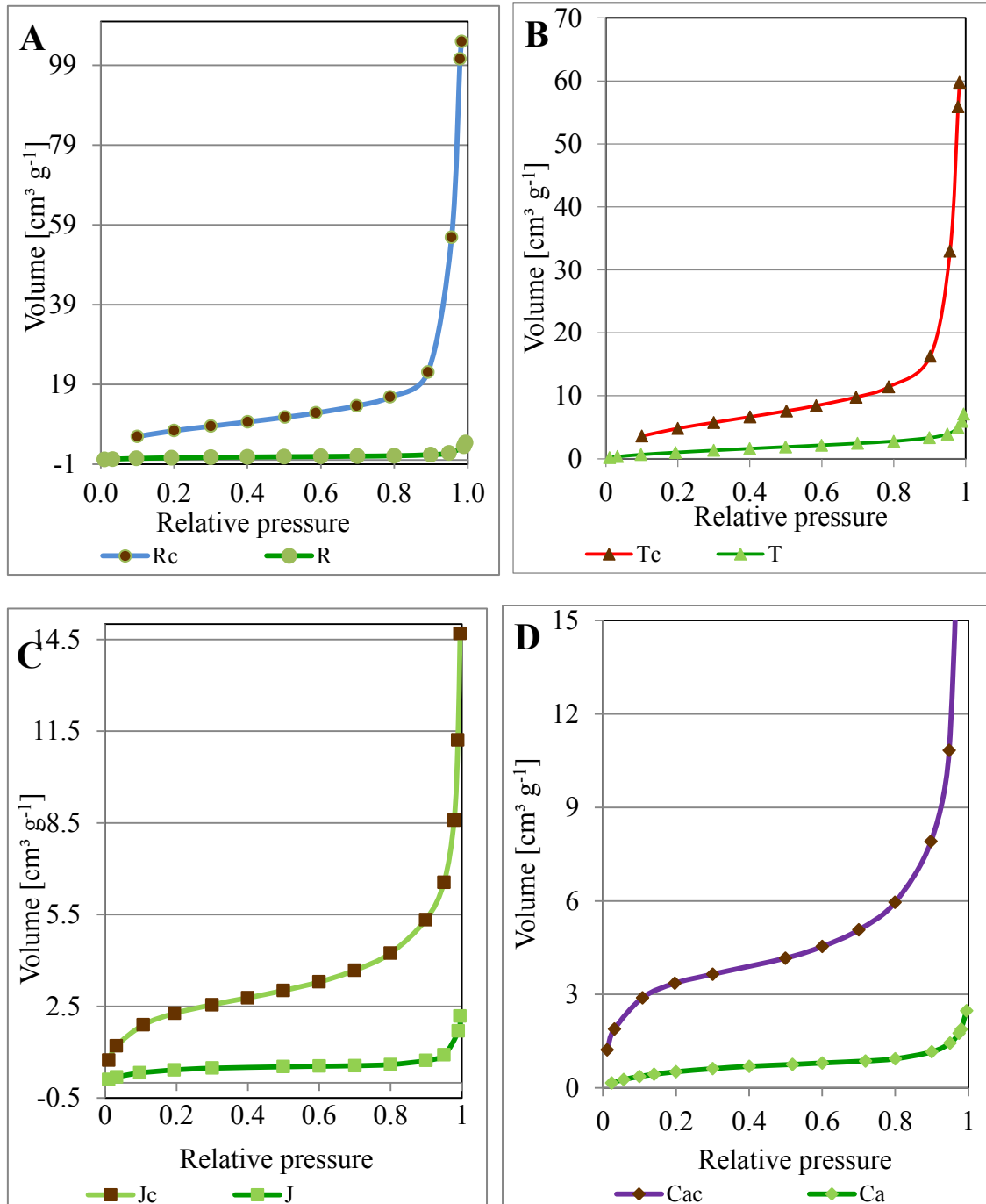


Figure 24: Adsorption/desorption isotherm of reed (A), typha (B), juncus (C) and carex (D) and their HTC-chars produced at 230 °C

The adsorption at lower relative pressure appeared to be negative in Figure 24 (A and C), which is not the case in reality. In this respect, it is worth mentioning that gas sorption can never be negative and all curves must start at 0 ml g⁻¹ intake.

The difference between the curves before and after HTC indicated that the carbonization of biomass developed its surface area. The largest nitrogen intake was with the HTC-char from reed (Figure 24 A), which absorbed about 107 cm³ of nitrogen gas per gram of sample at a relative pressure of about one. The nitrogen sorption isotherms of all samples shared the same shape. All HTC-chars go with type IV corresponding to IUPAC Classification of adsorption Isotherm, indicating the existence of large fractions of mesoporous (Sevilla and Fuertes, 2009a).

4.1.2.5 Bulk density

Figure 25 presents the modification of the bulk density of biomass after hydrothermal carbonization at different reaction temperatures. Generally, the HTC-char from juncus had the highest bulk density at all HTC-reaction temperatures used. Comparison with the raw materials, the reductions of the bulk density of HTC-chars produced at 180 °C were between 11.11 % (for carex) and 33.45 % (for juncus) of the raw material bulk density. The reduction in the bulk density was higher by increasing the reaction temperature to 230 °C; it was between 39.88 % (for typha) and 61.04 % (for juncus).

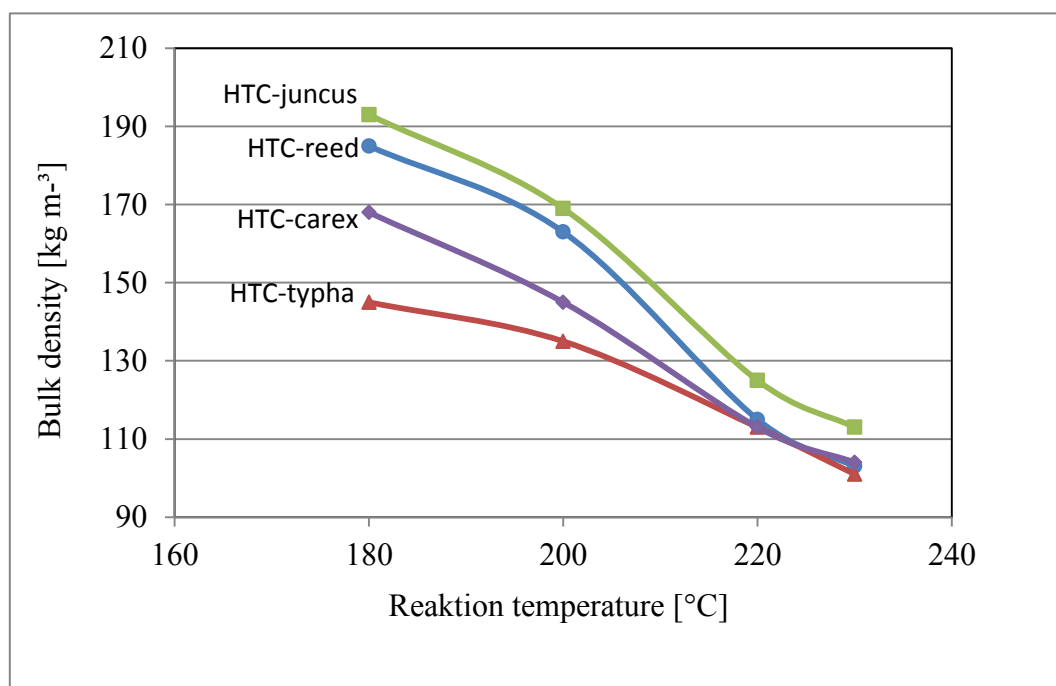


Figure 25: Effect of the variation of reaction temperatures between 180-230 °C on the bulk density of HTC-chars

The results showed that the difference in the bulk densities of HTC-chars produced at 180 °C were more than those of HTC-chars produced at higher reaction temperatures. From the results presented in Figure 25, it is noticeable that the bulk densities of HTC-

chars from reed, typha and carex produced at reaction temperatures 220 °C were similar, that was also the case for these HTC-chars produced at 230 °C.

Changes in the density depended on the HTC-process parameters as well as the type of raw materials, which indicated that the composition of the raw materials influenced the bulk density of their HTC-chars. Depending on the reaction severity; the decomposition of the raw material during HTC resulted in the dissolve of hemicellulose, cellulose and lignin. So that, the varying the reaction temperatures resulted in compositional changes that led to corresponding bulk density changes. Comparable bulk density changes (e.g., between 98 and 82 % of original bulk density) were reported with the carbonization of switchgrass at temperature up to 400 °C (Sadaka et al., 2014).

Similarly, there was a 14 % reduction in its bulk density compared to raw bulk density while using mild carbonization (torrefaction) of eucalyptus at 280 °C (Rodrigues and Rousset, 2009).

4.1.2.6 Biochar acidity/Alkalinity levels

The pH values of HTC-chars produced were in the acidic area in the range 3.70-4.70. The results showed that there were no significant changes in the pH value by changing the reaction temperatures. The process waters were also acidic, it could be because of the presence of organic acids resulting from the decomposition of monosacharides (Sevilla and Fuertes, 2009a; Sevilla and Fuertes, 2009b), where most hemicellulose decomposes between 180 and 200 °C producing acetic, formic, propionic acids and water. The pH of raw material has been reported as a parameter that has a significant effect on reaction mechanisms (Libra et al., 2011; Titirici et al., 2007a).

4.1.2.7 Statistical testing of significance of the effect of HTC-reaction temperature

Table 7 presents the results of the ANOVA table (as described in item 3.4). Each group contains HTC-chars from reed, typha, juncus and carex produced at reaction temperatures of 180 °C (first group), 200 °C (second group), 220 °C (third group) and 230 °C (fourth group), respectively.

The results showed that the variation of the reaction temperatures had generally a high significant influence ($P < 0.01$) on each of the yield, the proportion of carbon, oxygen and nitrogen, or rather the O/C and H/C atomic ratio. It had also a high significant influence on the specific surface area and the bulk density of HTC-chars produced.

On the other hand, the variation of reaction temperatures had no significant effect on the hydrogen proportion ($P= 0.54$) and the ash content ($P= 0.82$). F-value between 3.629 and 211.516 presented that these models were significant.

Table 7: Analysis of variance and lack of fit test for the influence of the reaction temperatures on the properties of HTC-chars produced

Parameter	Unit	Groups	Sum of squares	Degree of freedom	Mean square	F-value	P-value
Yield	[%]	Between groups	2175.62	3.00	725.21	64.66	Sig.
		Within groups	493.47	44.00	11.22		
		Total	2669.09	47.00			
Carbon	[%]	Between groups	1930.36	3.00	643.45	211.52	Sig.
		Within groups	133.85	44.00	3.04		
		Total	2064.21	47.00			
Oxygen	[%]	Between groups	2382.61	3.00	794.20	211.51	Sig.
		Within groups	165.21	44.00	3.75		
		Total	2547.82	47.00			
Hydrogen	[%]	Between groups	0.49	3.00	0.16	0.73	0.54
		Within groups	9.86	44.00	0.22		
		Total	10.35	47.00			
Nitrogen	[%]	Between groups	10.54	3.00	3.51	3.63	Sig.
		Within groups	42.58	44.00	0.97		
		Total	53.12	47.00			
O/C	[-]	Between groups	0.78	3.00	0.26	247.61	Sig.
		Within groups	0.05	44.00	0.00		
		Total	0.83	47.00			
H/C	[-]	Between groups	0.36	3.00	0.12	15.93	Sig.
		Within groups	0.33	44.00	0.01		
		Total	0.69	47.00			
Ash	[%]	Between groups	1.14	3.00	0.38	0.31	0.82
		Within groups	54.65	44.00	1.24		
		Total	55.79	47.00			
BET	[m ² g ⁻¹]	Between groups	231.46	3.00	77.15	2.79	Sig.
		Within groups	470.47	17.00	27.67		
		Total	701.93	20.00			
Bulk density	[kg m ⁻³]	Between groups	35674.50	3.00	11891.50	74.12	Sig.
		Within groups	7059.50	44.00	160.44		
		Total	42734.00	47.00			

However, the P-values of all these responses were less than 0.01, which pointed out that the model terms regarded here for response analysis were high significant (Karacan et al., 2007). The detailed effects of the variation of the reaction temperatures on some factors were presented in Table 8. It could be seen that the yield of HTC-chars receded steadily from 52.83 % at 180 °C (first group) with rising the reaction temperature and

was 35.47 % at 230 °C (fourth group). The results showed that increasing the reaction temperatures from 180-220 °C had a significant effect on the yield of HTC-chars, where the increasing from 220-230 °C had no significant effect. On the other hand, increasing the reaction temperatures in the range 180, 200, 220 and 230 °C had a significant effect on the proportions of carbon, oxygen and the bulk density.

Table 8: Means and standard error (SNK method) of different terms for the influence of reaction temperature on the properties of HTC-chars produced at 15 h using citric acid as catalyst

Reaction temperature [°C]	Yield [%]	Carbon proportion [%]	Oxygen proportion [%]	Bulk density [kg m ⁻³]
180	52.38±4.03 ^a	52.73±1.10 ^a	39.08±1.26 ^a	172.92±19.29 ^a
200	46.18±3.44 ^b	58.00±1.77 ^b	33.19±1.79 ^b	153.17±14.62 ^b
220	37.85±2.56 ^c	65.79±2.03 ^c	24.35±2.46 ^c	116.67±5.55 ^c
230	35.47±3.21 ^c	68.81±1.93 ^d	21.34±2.04 ^d	105.25±5.01 ^d

^{a,b,c,d} Values with different superscripts were significantly ($P < 0.05$) different (the comparison between values only applied to the same term)

The higher standard errors could be interpreted because of the fact that in each group HTC-chars from the four raw materials (reed, typha, juncus and carex) with different characteristics are included. For example, the difference in the bulk density between HTC-chars from juncus and typha produced at 180 °C was 24.87 %, which explained the high standard errors for this group.

These results supported the research hypothesis about the effect of HTC-process parameters, especially the reaction temperature on the properties of HTC-chars produced. The effect of the reaction temperature was noteworthy; higher reaction temperatures led to more liquid and gaseous products, which resulted in a decrease in the solid phase. On the other hand, HTC-chars became richer in carbon proportion by increasing the reaction temperature.

The composition of the HTC-char is influenced by the removal of water and carbon dioxide during HTC-process (Libra et al., 2011; Funke and Ziegler, 2010). A release of moisture will be also happen that may create wide range of pore sizes within HTC-chars and as a result, the HTC-char produced will have a lighter and porous structure as well as a lower bulk density.

Boxplots presented in Figure 26 show that the yield of HTC-chars produced from the four raw materials used at reaction temperature of 180 °C (first group) appeared to be

higher than those produced at reaction temperatures between 200-230 °C, which affirmed that the reaction temperatures had an effect on the yield of HTC-chars used. They also suggested that there was more variability in the yield at this reaction temperature.

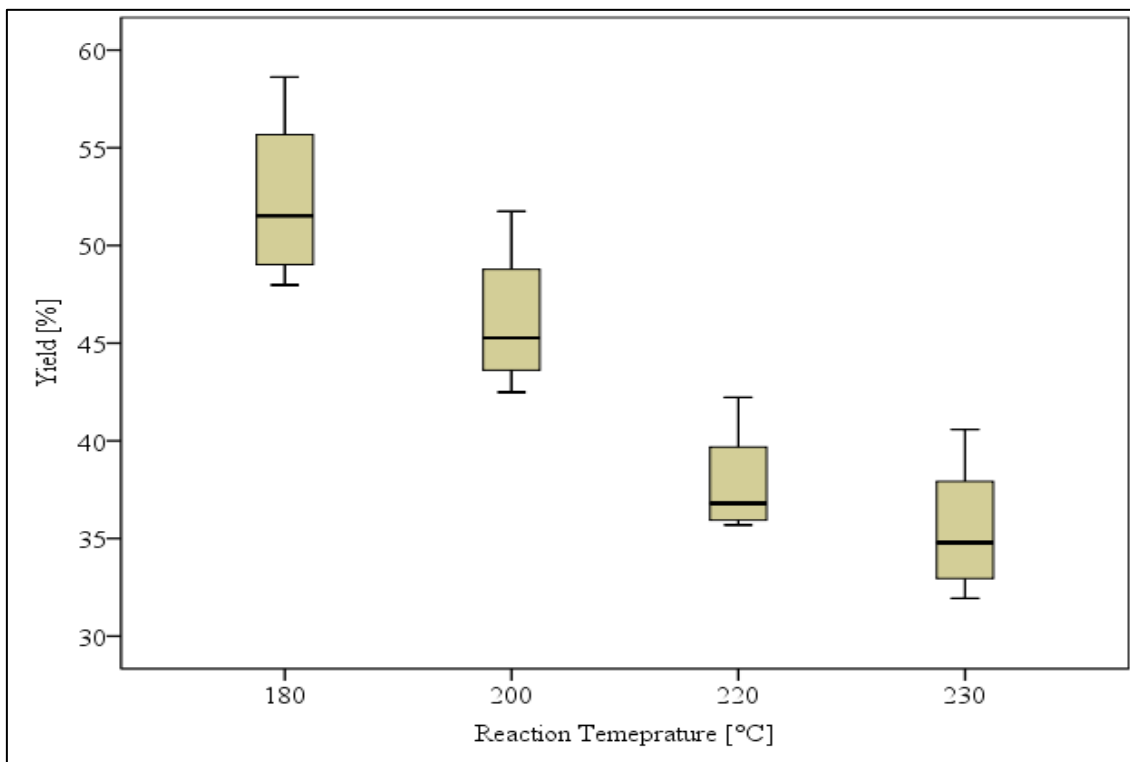


Figure 26: The yield of the HTC-chars produced at different reaction temperatures 180-230 °C and 15 h using citric acid as catalyst as boxplots

The medians across the boxplots varied considerably at reaction temperatures between 180-220 °C and there was no overlap in spreads, which reflected a difference between these groups. That was also proved with the results presented in Table 8.

At reaction temperatures 220 and 230 °C, boxes overlapped but not both medians were noticed for the yield of HTC-chars produced, so there was likely to be a difference between these two groups, but the difference was not significant (Table 8).

All boxplots skewed to the right. The top whisker was longer than the bottom whisker and the line median was gravitating towards the lower portion of the box, which showed a positive skewness and indicated the wider range of observations were in the upper quartile as compared to the lower quartile. The boxplots for some of the other terms were presented in the Appendix V.

4.1.3 Effect of the HTC-reaction time on HTC-char

4.1.3.1 HTC-char yields

The yields of HTC-chars produced from reed, typha, juncus and carex were shown in Figure 27. The results show that the yields were high at short reaction times (between 1-5 h) and decreased with increasing the reaction time.

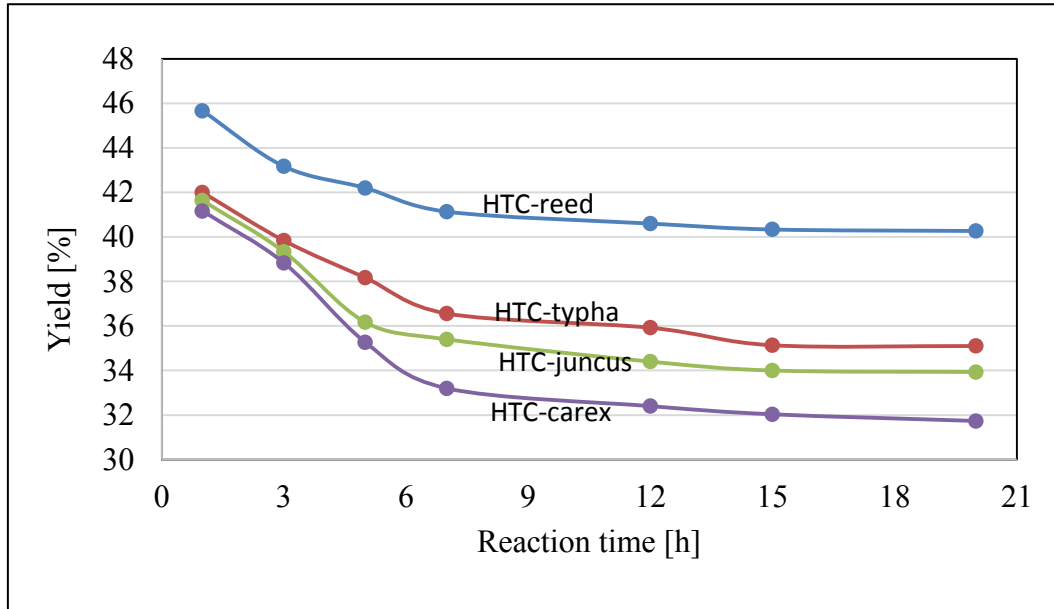


Figure 27: Effect of the variation of reaction times between 1-20 h on the yield of HTC-chars produced at 230 °C using citric acid as catalyst

The yield of HTC-char produced from reed was the highest at the different reaction times, while HTC-chars of carex had the lowest yields. A reduction of about 9.39, 12.95, 14.97 and 19.35 % in HTC-char yields produced from reed, typha, juncus and carex, respectively, was found while increasing the reaction time from 1-7 h.

HTC-char yields did not appreciably change by increasing the reaction time in the range between 7-20 h. Low reaction times gave a higher yield of HTC-char, but these HTC-chars had low quality in terms of carbon and oxygen proportions as well as the specific surface area. Increasing the reaction time reduced the total solid yields and promoted the formation of higher amounts of water-soluble compounds. This decrease in the yield was also accompanied with an increase in the pressure at the end of the process, which indicated that the lower the yield, the higher the gas production. This behavior was consistent with other results in the literature (Castello et al., 2014).

Generally, higher mass loss occurs with biomass that contains high hemicellulose composition because of least thermal stability among other polymers in biomass (Garrote et al., 1999). The fiber analysis of biomasses used showed that carex had the

highest percentage of hemicellulose composition in it and therefore had the high mass loss and the lowest yield compared to the other HTC-chars produced.

4.1.3.2 Elemental compositions

The influence of the reaction times on the elemental composition of the HTC-chars produced was shown in Figure 28. The highest carbon proportions or rather lowest oxygen proportions were found in the HTC-chars from juncus and carex.

The different HTC-chars were designated as R_N, T_N, J_N and Ca_N, where N= 5, 6, 7, 8, 9, c, 10 indicated to chars produced at 1 h, 3 h, 5 h, 7 h, 12 h, 15 h and 20 h

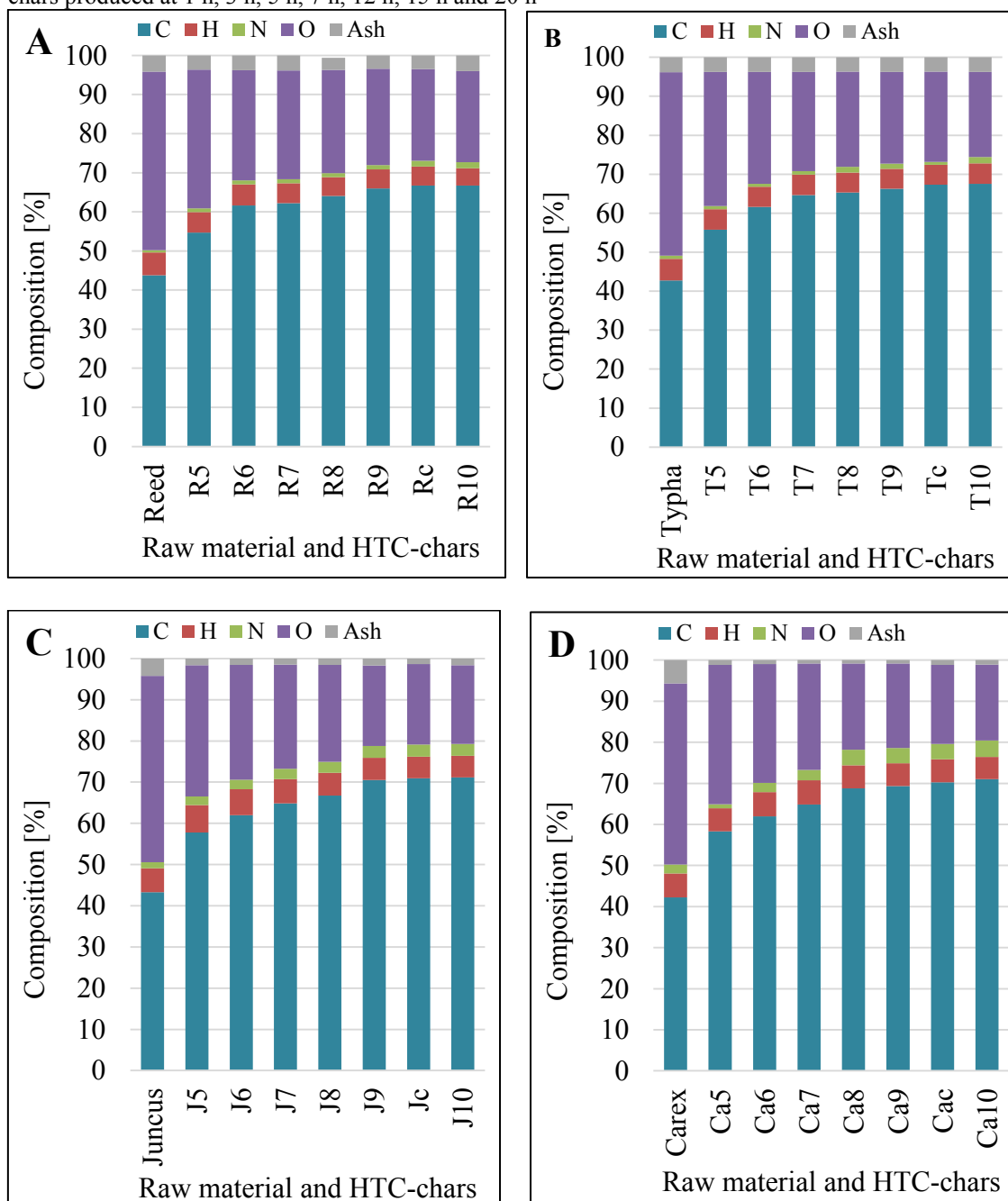


Figure 28: Effect of the variation of reaction times on the elemental compositions of HTC-chars produced from reed (A), typha (B), juncus (C) and carex (D)

For all raw materials used, the increase in reaction times resulted in an enrichment in the carbon proportions and a reduction in the oxygen proportions of HTC-chars produced. The carbon proportions in HTC-chars produced at reaction time of 1 h were about 17 % lower than those were produced at reaction time of 15 h. There were noteworthy reductions in the oxygen proportion for the HTC-chars compared with the raw materials. A reduction of more than 34.30 % of the oxygen proportions by increasing the reaction time from 1-15 h was obtained. The increase of the reaction time in the range 12-20 h had no considerable influence on the carbon and oxygen proportions. There were slight changes of hydrogen and nitrogen proportions as well as ash contents of HTC-chars produced at the different reaction times. Low reaction times gave low carbon proportions and high oxygen proportions, which indicated that the reaction time affected the degree of the reaction. All changes were smaller than those were obtained by the variation of reaction temperatures, which indicated that the reaction time had a lower effect compared with the reaction temperature. The influences of the reaction times were clearly presented in the Van Krevelen diagram (Figure 29).

The different HTC-chars were designated as R_N , T_N , J_N and Ca_N , where $N = 5, 6, 7, 8, 9, c, 10$ indicated to chars produced at of 1 h, 3 h, 5 h, 7 h, 12 h, 15 h and 20 h, respectively.

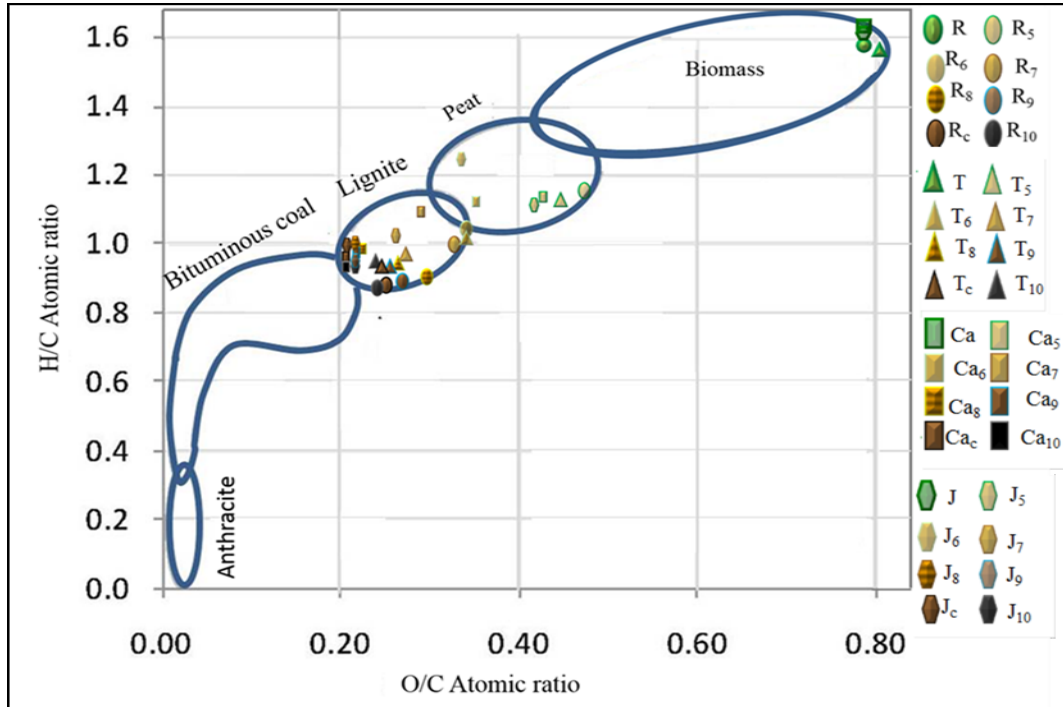


Figure 29: Van Krevelen diagram based on O/C and H/C atomic ratios of the raw materials used and HTC-chars produced at different reaction times

The O/C and H/C atomic ratios were decreased by increasing the reaction times. Interestingly, at reaction times 5 h and 7 h, there was very little change in O/C atomic

ratios, while a considerable reduction in H/C atomic ratios was occurred. Increasing the reaction time from 12-20 h had almost no influence on the H/C and O/C atomic ratios, where the variations on both ratios were less pronounced.

It seemed to be that at reaction times up to 3 h, the main reaction was physical dewatering of the biomass, which was also reported by Funke and Ziegler (2010).

The considerable reduction in H/C atomic ratios at reaction times 5 h and 7 h might be because of the solution of sugars (like glucose and fructose) within the reaction water as proposed by Funke and Ziegler (2011).

Reaction time affects both the dehydration and decarboxylation reactions. Increasing the reaction time resulted in HTC-chars produced with lower H/C and O/C atomic ratios. Similar observations about the effect of reaction times on the properties of HTC-chars have been investigated by others (Funke and Ziegler, 2010; Yan et al., 2010; Kleinert and Wittmann, 2009; Yan et al., 2009).

4.1.3.3 Specific surface areas

BET measurements of HTC-chars produced at reaction times between 12-20 h were determined because they were of good quality regarding their elemental composition and the results were presented in Figure 30 (some values were not available as HTC-char from juncus at 12 h and HTC-char from carex at 20 h).

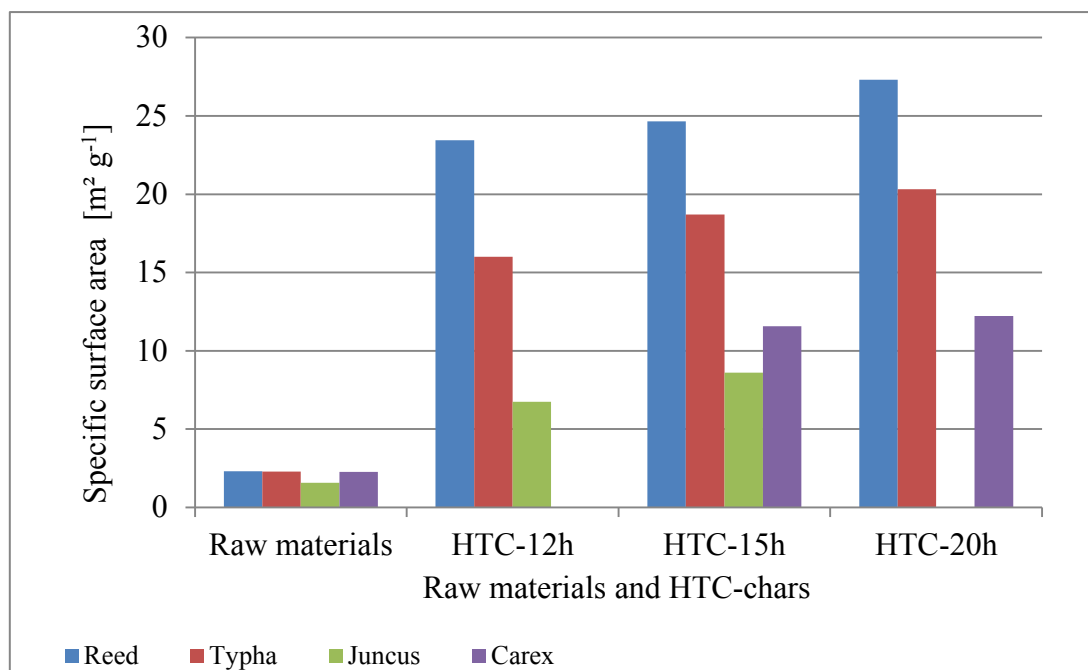


Figure 30: Effect of the variation of reaction times on the specific surface area of the HTC-chars produced at 230 °C using citric acid as catalyst

The results showed that the variation of reaction time in the range of 12-20 h had a little effect, where the specific surface areas increased only slightly with an increase in the reaction time in this range. Specific surface areas of HTC-chars produced at reaction time of 20 h were the highest and were about 5-12 times greater than those were of raw materials used. HTC-chars from reed showed higher surface areas than the other HTC-chars. Surface areas of HTC-chars from typha were lower than those were of HTC-chars from reed. HTC-chars produced from juncus had higher surface areas than those of HTC-chars from carex and lower than those of HTC-chars produced of reed and typha, HTC-chars from carex had the lowest ones at all reaction times. It was due to that longer reaction time led to higher reaction severity, which resulted in an increase in the porosity and the surface area.

4.1.3.4 Bulk density

As shown in Figure 31, the bulk density of HTC-chars produced from all raw materials used decreased with increasing the reaction time.

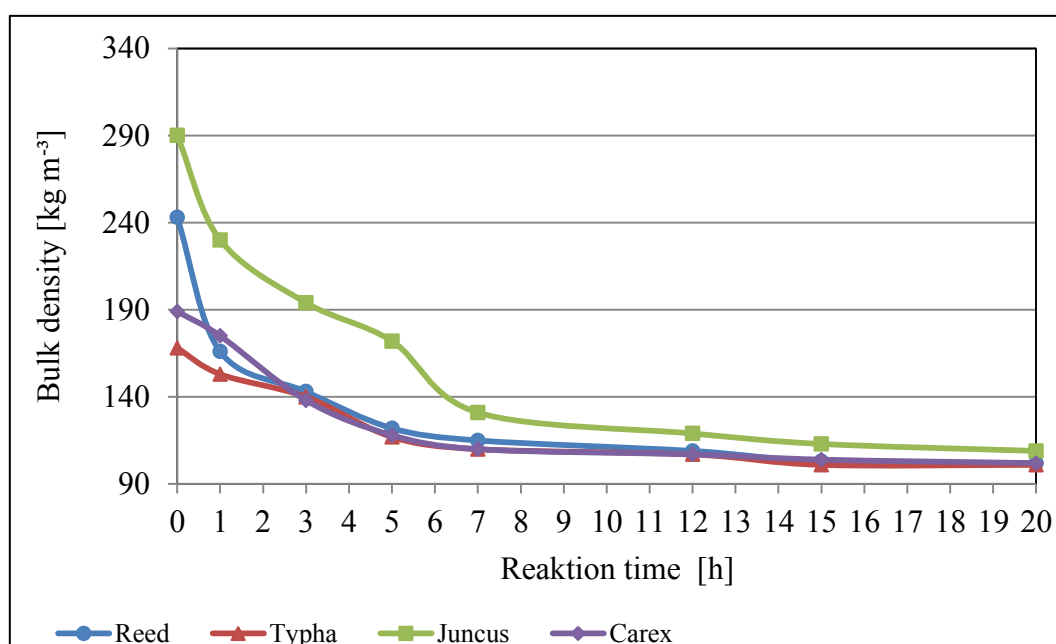


Figure 31: Effect of the variation of reaction times on the bulk density HTC-chars produced at 230 °C

At the reaction time of 1 h, there were reductions in bulk densities of 31.69, 8.93, 20.69 and 7.41 % of HTC-chars produced from reed, typha, juncus and carex compared with the raw materials, respectively. Further reductions took place by increasing the reaction time in the range 1-7 h and were between 34.52 % (HTC-char from typha) and 54.83 % (HTC-char from juncus) compared with the raw materials. After that there was a

slightly reduction in the bulk density by increasing the reaction time in the range of 12-20 h. On the other hand, bulk densities of all HTC-chars of reed, typha and carex were similar at reaction times 3-20 h.

The escape of volatiles during carbonization process built voids, which resulted in a reduction in the bulk density of the HTC-chars produced. The higher-degree decomposition during HTC improved the formation of the porous structure, which in its role reduced the bulk density of biomass used.

The result showed that changes in the density depended on the type of raw materials used as well as the carbonization parameters. The density of HTC-chars is necessary for designing the biomass processing and the transport systems.

4.1.3.5 Statistical testing of significance of the effect of HTC-reaction time

The statistical analysis indicated that the yield of HTC-char was significantly affected by increasing the reaction time from 1-5 h, further increase of the reaction time between 7-20 h had no significant influence on the change of the yield (Table 9).

Table 9: Means and standard error (SNK method) of different terms for the influence of reaction time on the properties of HTC-chars produced at 230 °C using citric acid as catalyst

Reaction time [h]	Yield [%]	Carbon proportion [%]	Oxygen proportion [%]	Hydrogen proportion [%]	Bulk density [kg m ⁻³]
1	42.62±1.88 ^a	56.64±1.55 ^a	33.93±1.40 ^a	5.68±0.65 ^a	181.33±30.74 ^a
3	40.29±1.78 ^b	61.80±0.29 ^b	28.43±0.50 ^b	5.70±0.55 ^a	153.83±24.55 ^b
5	37.95±2.79 ^c	64.17±1.21 ^c	26.10±1.07 ^c	5.52±0.42 ^{ab}	131.17±24.93 ^c
7	36.57±3.03 ^c	66.22±1.84 ^d	23.84±2.03 ^d	5.24±0.41 ^{ab}	115.50±9.82 ^d
12	35.83±3.16 ^c	68.05±2.03 ^e	22.06±2.20 ^e	5.21±0.36 ^{ab}	110.75±5.75 ^d
15	35.47±3.21 ^c	68.81±1.93 ^e	21.34±2.04 ^e	5.08±0.43 ^b	105.25±5.01 ^d
20	35.23±3.28 ^c	69.11±2.08 ^e	20.67±2.09 ^e	5.09±0.49 ^b	103.75±3.89 ^d

^{a,b,c,d} Values with different superscripts were significantly ($P < 0.05$) different (the comparison between values only applied to the same term)

On the other hand, the variation of reaction time in the range between 1-12 h played a significant role in the developing of both carbon and oxygen proportions, where the hydrogen proportions were not significantly affected. The change of the bulk density was significant at reaction times between 1-7 h. The higher standard errors were due to that each group contained HTC-chars produced from the four types of the raw materials used with different properties of HTC-chars produced at each reaction time.

As a result, HTC-reaction times in the range between 12-20 h had no significant influence on the properties of HTC-chars produced (Values with similar superscripts were not significantly ($P > 0.05$) different), where the variations of the properties of HTC-chars were less pronounced. These findings may be important during designing HTC-stations.

Compared to the effect of reaction temperatures, varying reaction times had a little influence on the changes of the properties of HTC-char especially in the reaction times between 12-20 h, higher reaction temperatures and longer reaction times enhanced the reaction severity and developed the properties of HTC-chars produced. Longer reaction time had an influence on surface morphology and composition of HTC-chars because cellulose and hemicellulose did not react completely at shorter reaction time. With an increase in reaction time, a further decomposition of cellulose and hemicellulose might be occurred, which could increase the number of microspheres.

Boxplots presented in Figure 32 show that the oxygen proportions in HTC-chars produced at reaction times 1-5 h appeared to be higher than those were produced at other reaction times. The medians across these boxplots varied also considerably and there was no overlap in spreads between these boxplots and the others at reaction time (12-20 h), which reflects a difference between these groups. Boxplots for other terms were presented in the Appendix V.

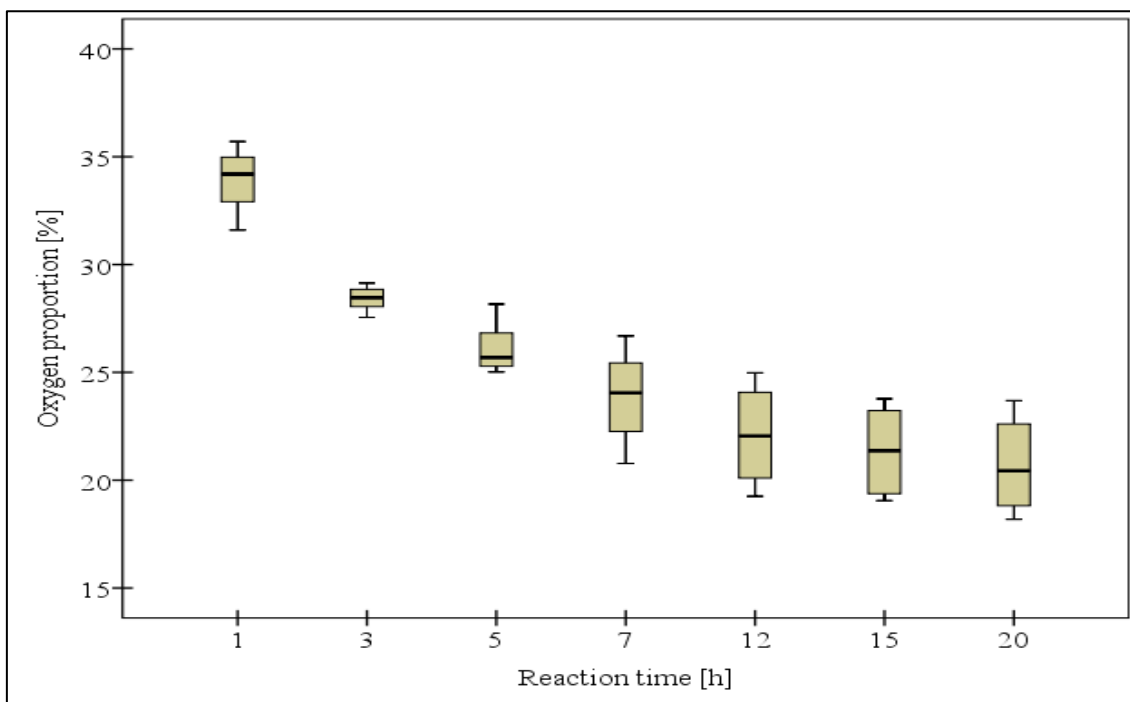


Figure 32: Oxygen proportion in HTC-chars produced at different reaction times 1-20 h and 230 °C using citric acid as catalyst as boxplots

4.1.4 Effect of the amount of biomass (solid load) on HTC-char

4.1.4.1 Yield and specific surface area of HTC-char

In this study, two solid loads 6 % and 9 % (30 and 50 g of raw material and 500 mg water) were used. As seen in Figure 33 (A), the yields of HTC-chars produced at 230 °C and 15 h using citric acid as catalyst were increased by raising the amount of biomass used from 30 g to 50 g.

Figure 33 (B) shows that BET values were affected by changing the solid load, where HTC-chars produced using solid load of 9 % had greater specific surface area.

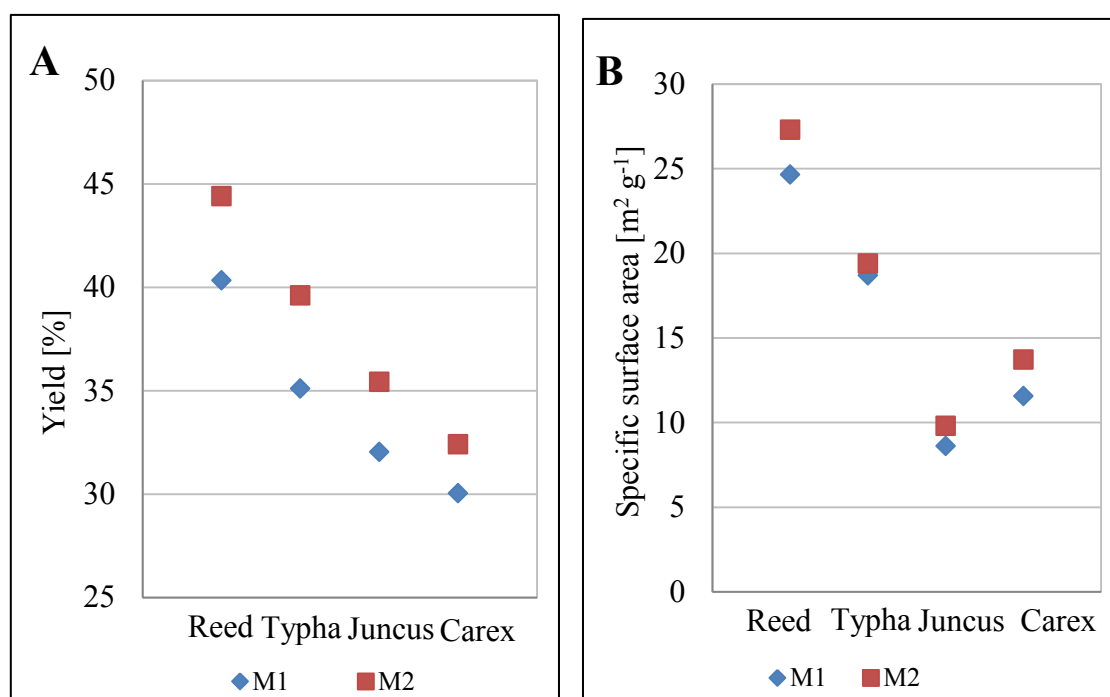


Figure 33: Effect of the variation of solid load on the yield (A) and BET-measurement (B) of HTC-chars produced, biomass amount: M₁= 30 g, M₂= 50 g

HTC-chars produced from reed at the two solid loads had the highest yield and specific surface area. On the other hand, the obtained results exhibited no considerable change in the elementary composition of the HTC-chars produced, especially with regard to the carbon proportion, although that the calculated percentage of carbon recovered increased by increment the solid load. It was also found that there was no change in the bulk density of the HTC-chars produced. As a result, the change of solid load had a little effect on the properties of HTC-char-produced compared with the effect of reaction temperature and time.

It is supposed that the solid load plays also a crucial role in the hydrothermal carbonization of biomass. The obtained results could be explained by the fact that water

enhanced the hydrolysis reactions while using less biomass quantity. However, the used solid loads in this range may were not sufficient to influence considerably on the properties of HTC-chars. Heilmann et al. (2011) has proposed an effect of the solid load on the yield of HTC-char. The lower the solid load, the lower was the total carbon and the energy properties of HTC-chars (Fiori and Volpe, 2017).

The data reported of pressure measuring during HTC-process showed that the measured process pressure was increased by increasing the solid load, which might be as indicator that higher solid load promoted the gas formation.

4.1.4.2 Statistical testing of significance of the effect of solid load

The results of the significant analysis for the effect of the solid load (the amount of biomass used) were presented in Table 10.

Table 10: Means and standard error of different terms for the influence of solid load ($M_1 = 30$ g, $M_2 = 50$ g) on the properties of HTC-chars produced at 230 °C and 15 h using citric acid as catalyst

Term	Unit	Amount of biomass g		P-value
		M_1	M_2	
Yield	[%]	35.47±3.21	39.07±3.59	0.017
Carbon proportion	[%]	68.81±1.93	68.63±1.93	0.818
Oxygen proportion	[%]	21.34±2.05	21.61±2.51	0.770
Hydrogen proportion	[%]	5.18±0.36	5.11±0.54	0.678
Specific surface area	[m ² g ⁻¹]	15.88±6.54	17.56±6.88	0.545
Bulk density	[kg m ⁻³]	105.25±5.01	105.17±4.84	0.967

Yields of HTC-chars were the only significantly affected term with $P = 0.017$. On the hand, each of the carbon, oxygen and hydrogen proportions as well as specific surface areas and bulk densities of HTC-chars produced were not significantly changed ($P > 0.05$). The results showed that the variation of solid load in this study had a lower influence on the properties of HTC-chars produced than those were by the variation of both reaction times and reaction temperatures.

4.1.5 Effect of the catalyst and oxidation on HTC-char

4.1.5.1 Elemental compositions and yield

Table 11 lists the proportions of carbon, hydrogen, nitrogen and oxygen nitrogen as well as the ash content and the yield of HTC-chars produced at reaction temperature 230 °C

using citric and phosphoric acids as catalysts as well as of HTC-chars after oxidation with nitric acid.

HTC-chars produced using citric acid (0.05 g) as catalyst had lower carbon proportions, higher oxygen proportions and higher ash content as lower HTC-char yields compared with HTC-chars produced using higher amount (0.50 g) of citric acid as catalyst. There were slightly changes in the proportions of hydrogen and nitrogen, but no clear tendency was found for their changes.

No clear tendency was observed for the changes of the proportion of carbon and hydrogen as well as ash contents in HTC-chars produced using citric acid (0.50 g) or phosphoric acid as catalysts. Carbon proportions increased for HTC-chars produced from reed and typha and decreased with those produced from juncus and carex while using phosphoric acid as catalyst. On the other hand, no consider changes were found in the oxygen proportions for each of HTC-chars produced from reed and typha, but these were increased by carbonization of juncus and carex. Moreover, the yield of HTC-chars produced increased between 6 % and 9 % while using phosphoric acid as catalyst.

The oxidation of HTC-chars using nitric acid reduced the carbon proportion. The hydrogen proportion decreased slightly, but there was a markedly increase in the nitrogen and oxygen proportion after oxidation (Ibrahim et al., 2018). O/C atomic ratios were increased for all HTC-chars after oxidation and H/C ratio increased for the oxidation of HTC-chars from typha, juncus and carex.

The changes while using higher concentration of citric acid with may be explained because acidic conditions catalyzed the carbonization of the raw materials and the dehydration reactions seemed to be more favored than those were in the absence of catalyst or by used lower concentration of it (Titirici et al., 2007a).

Quesada-Plata et al. (2016) found that the addition of phosphoric acid during HTC increased each of the carbon proportion and the fixed carbon contents for all biomasses used and promoted the dehydration reaction during HTC. The lower change in the properties of HTC-chars using citric acid (0.50 g) and phosphoric acid as catalyst could be because both catalysts promoted the dehydration reaction during HTC.

The obtained change in the elemental composition after oxidation indicated that the oxidation process make a decarburization compared with the HTC-char used, which could be related to the dissolve of organic compounds from HTC-chars. That might be an indication that the oxidation affected the chemical structure of HTC-chars and introduced the oxygen functional groups onto the surface.

Table 11: Effect of catalyst used and oxidation on the properties of HTC-chars produced at 230 °C and 15 h

Parameter	Unit	Raw material	HTC-chars			
		Reed	R _c	R ₁₂	R _p	R _n
C	[%]	43.82	66.71	65.59	66.80	57.77
H	[%]	5.82	4.55	4.46	4.49	3.88
N	[%]	0.54	1.53	1.37	0.69	3.90
O	[%]	45.67	23.41	24.57	23.54	29.90
Ash	[%]	4.15	3.50	4.02	4.48	4.55
Yield	[%]	-	40.30	39.70	42.27	-
		Typha	T _c	T ₁₂	T _p	T _n
C	[%]	42.74	67.30	66.00	68.32	59.02
H	[%]	5.58	5.09	4.99	4.79	4.51
N	[%]	0.78	0.78	1.71	0.82	4.32
O	[%]	47.08	23.15	23.51	23.19	27.31
Ash	[%]	3.82	3.68	3.80	2.89	4.32
Yield	[%]	-	35.10	33.75	38.33	-
		Juncus	J _c	J ₁₂	J _p	J _n
C	[%]	43.27	70.95	70.16	70.17	57.63
H	[%]	5.85	5.25	5.41	4.90	4.78
N	[%]	1.41	2.92	2.59	2.12	5.88
O	[%]	45.23	19.54	19.72	21.98	29.86
Ash	[%]	4.24	1.34	2.12	1.36	3.65
Yield	[%]	-	34.00	32.67	36.67	-
		Carex	Ca _c	Ca ₁₂	Ca _p	Ca _n
C	[%]	42.24	70.28	67.62	69.09	57.59
H	[%]	5.86	5.57	5.38	4.83	4.86
N	[%]	2.17	3.76	3.67	2.63	5.28
O	[%]	44.09	19.25	21.01	22.58	28.06
Ash	[%]	5.64	1.15	2.12	1.46	2.40
Yield	[%]	-	32.03	31.37	34.97	-

The different HTC-chars were designated as R_N, T_N, J_N and Ca_N, where N= c, 12, p and n indicated to chars produced using citric acid (0.50 g), citric acid (0.05 g), phosphoric acid (6.50 g) and after oxidation with nitric acid, respectively

The still higher content of oxygen and hydrogen in HTC-chars produced indicated the availability of activated sites on their surface, which could affect the adsorption performance of HTC-chars.

4.1.5.2 Specific surface areas

The specific surface areas were measured for the most HTC-chars produced in this series and presented in Figure 34. As seen in Figure 34, HTC-char produced from reed had the highest surface area compared with that of other corresponding HTC-chars, respectively. The results showed that using phosphoric acid as catalyst increased the surface area for all HTC-chars produced compared with those produced using citric acid (0.50 g) as catalyst. The oxidation of HTC-chars from reed and typha showed positive effect, where the surface areas of these chars were found to increase after treatment with nitric acid compared with the raw HTC-char used. This can be because nitric acid may dissolve organic compounds from HTC-chars.

The different HTC-chars were designated as R_N , T_N , J_N and Ca_N , where $N=c, p$ and n indicated to chars produced using citric acid (0.50 g), phosphoric acid (6.50 g) and after oxidation with nitric acid, respectively

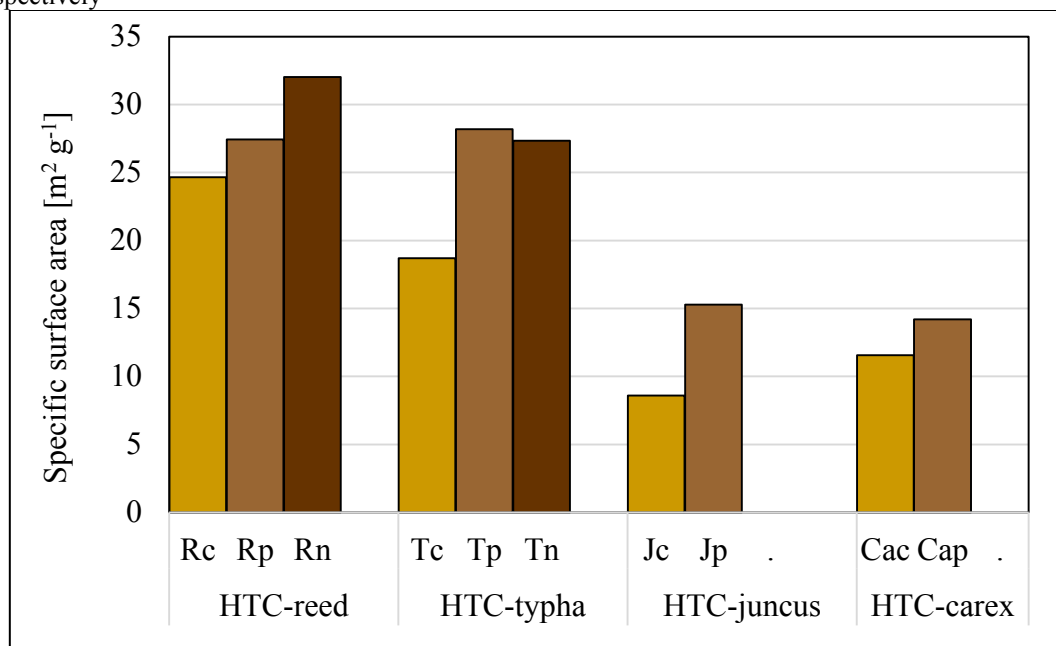


Figure 34: Effect of catalyst and oxidation on specific surface area of HTC-chars produced at 230 °C and 15 h

4.1.5.3 Bulk density

The results presented in Figure 35 show that using phosphoric acid as catalyst during HTC had a similar effect on the bulk density of HTC-chars produced while using citric acid as catalyst. On the other hand, the bulk density of HTC-chars after oxidation with

nitric acid seemed to be increased of more than 34 % compared with the bulk density of HTC-chars produced before oxidation. This can be because the HTC-chars possibly gained weight after oxidation with nitric acid.

The different HTC-chars were designated as R_N , T_N , J_N and Ca_N , where $N = c, p$ and n indicated to chars produced using citric acid (0.50 g), phosphoric acid (6.50 g) and after oxidation with nitric acid, respectively

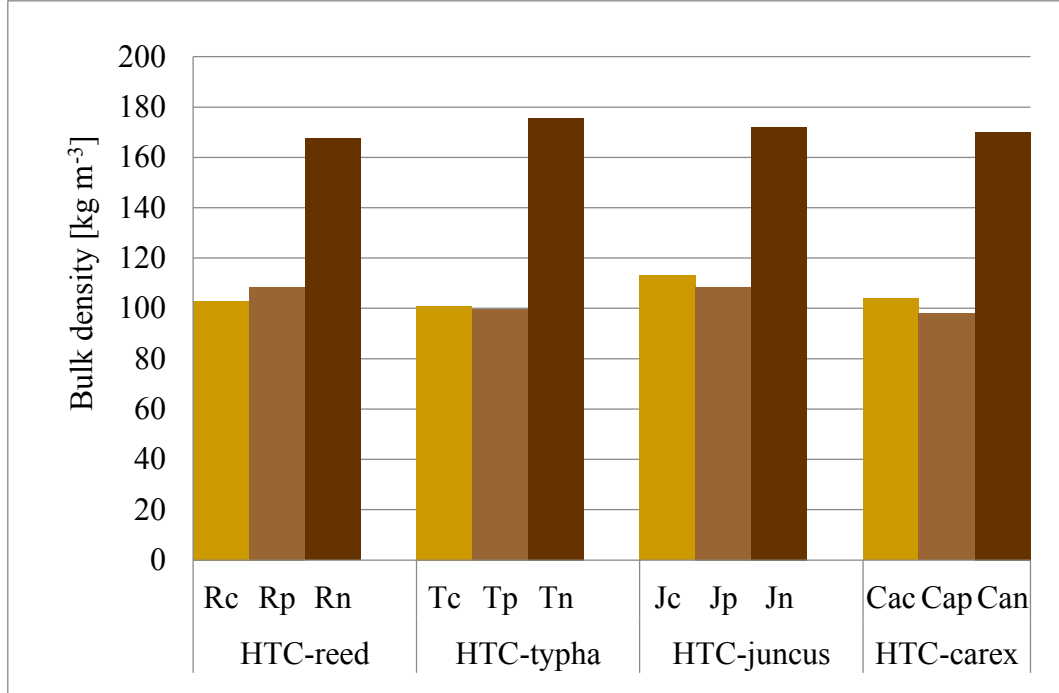


Figure 35: Effect of catalyst and oxidation on bulk density of HTC-Chars produced at 230 °C and 15 h

4.1.5.4 pH value and point of zero charge

The pH values of HTC-chars produced were seen to vary in the range 2-5.19 as listed in Table 12. HTC-chars produced using citric acid (0.05 g) had the highest pH values, while HTC-chars after oxidation had the lowest ones. The results showed that all HTC-chars had acidic pH values.

Table 12: The pH value of HTC-chars produced at 230 °C and 15 h

Parameter	R_c	R_{12}	R_p	R_n	T_c	T_{12}	T_p	T_n
pH	3.80	4.01	2.60	2.00	4.40	5.19	2.70	2.20
Parameter	J_c	J_{12}	J_p	J_n	Ca_c	Ca_{12}	Ca_p	Ca_n
pH	4.60	5.15	2.90	2.40	4.60	5.03	2.80	2.30

The different HTC-chars were designated as R_N , T_N , J_N and Ca_N , where $N = c, 12, p$ and n indicated to chars produced using citric acid (0.50 g), citric acid (0.05 g), phosphoric acid (6.50 g) and after oxidation with nitric acid, respectively

Table 13 shows pH_{pzc} values of HTC-chars produced from reed and typha. The pH_{pzc} values were found in the range between 2.92 and 5.49. Obviously, there was a decrease in pH_{pzc} values of HTC-chars after oxidation with nitric acid.

Compared with HTC-chars produced from reed using citric acid and phosphoric acid as catalyst, a reduction of about 35 % in pH_{pzc} of HTC-chars after oxidation was found. On the other hand, the reduction was between 19.56 and 35.52 % for HTC-chars produced from typha.

Table 13: Point of zero charge of HTC-chars of reed and typha produced at 230 °C

Parameter	R_c	R_p	R_n	T_c	T_p	T_n
pH_{pzc}	4.48	3.63	2.92	5.49	5.04	3.25

The use of different catalysts or the oxidation of HTC-chars affected their pH values, which led to an effect on their morphology and specific surface area. The lower pH could be because of the existence of acid functional groups such as carboxyl, lactone, and phenol on their surface.

The obtained results showed that the type of used biomass, the process parameters and the oxidation of HTC-chars affected pH_{pzc} values. The values of pH of the aqueous solution in the adsorption study should be maintained above this value to ensure a negatively charged surface of HTC-chars and favor the adsorption.

Liu et al. (2012) reported that pH_{pzc} of biochar from pyrolysis of wheat straw was approximately 7.80. On the other hand, pH_{pzc} values of biochar produced at different pyrolysis temperatures were between 3.04 and 10.10 (Uchimiya et al., 2011).

4.1.5.5 Statistical testing of significance of the effect of the catalyst

The significant analysis was made in order to study the effect of the catalyst used on the properties of HTC-chars produced. The results in Table 14 showed that the variation of catalyst during HTC-process had a significant effect on each of the yield and hydrogen proportion ($P < 0.05$). Actually, the yield was not considerably affected ($P = 0.047$). Oxygen proportions as well as specific surface area and bulk density were not significantly affected by the change of catalyst during HTC. That could be explained that acidic acid and phosphoric acid had a similar effect on HTC-process, especially regarding to the promoting of dehydration reactions.

Table 14: Means and standard error of different terms for the influence of the catalyst used on the properties of HTC-chars produced at 230 °C and 15 h

Term	Unit	Catalyst		P-value
		Citric acid	Phosphoric acid	
Yield	[%]	35.47±3.21	38.06±2.83	0.047
Carbon proportion	[%]	68.81±1.93	68.60±1.31	0.751
Oxygen proportion	[%]	21.34±2.05	22.54±0.92	0.076
Hydrogen proportion	[%]	5.18±0.36	4.753±0.26	0.003
Specific surface area	[m ² g ⁻¹]	15.88±6.54	21.28±6.85	0.061
Bulk density	[kg m ⁻³]	105.25±5.01	103.42±4.94	0.377

4.1.6 Effect of the particle sizes of raw materials on HTC-char

4.1.6.1 Yield and elemental compositions of HTC-char

Table 15 lists the yield of HTC-chars produced while using two different particle sizes (0.50 mm and 4 mm) at a reaction temperature of 230 °C and a reaction time of 15 h. A reduction of 9.01, 9.49, 6.97 and 6.34 % in the yield of HTC-chars produced from reed, typha, juncus and carex, respectively, were found while using smaller particle size of the raw materials.

Table 15: Effect of the particle size of raw materials on the yield of HTC-chars produced at 230 °C and 15 h

HTC-char	R _c	R ₁₃	T _c	T ₁₃	J _c	J ₁₃	Ca _c	Ca ₁₃
Yield [%]	40.30	36.67	35.10	31.77	34.00	31.63	32.03	30.00

The different HTC-chars were designated as R_N, T_N, J_N and Ca_N, where N= c, 13, indicated to HTC-chars produced using particle size 4 mm and 0.50 mm, respectively

A larger particle possesses less surface area per unit mass, which can reduce the convective heat transfer rate. The heterogeneous properties of the biomass with large particle size results in an irregular heat distribution. Compared with large Particles, smaller particles have higher heat transfer and lower resistances to the diffusion of volatiles that results in a higher mass loss than that is in the larger, so that the yields of HTC-chars were lower. Similar results were obtained by using different thermochemical conversion process (Yan et al. 2014; Peng et al., 2012; Medic et al., 2011).

Interestingly, no influence of the particle size on the elemental composition of HTC-chars in this test were recognized (Figure 36). However, the ash content increased with a reduction in the particle size. It seemed difficult from obtained results to predict how the particle size of the raw material affected the degree of reaction.

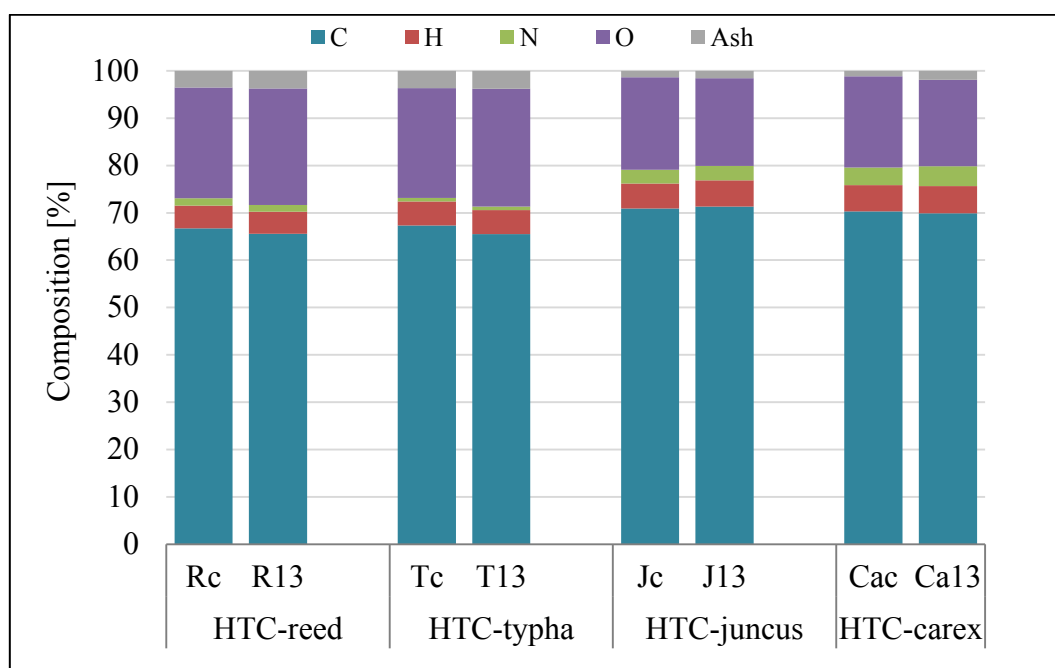


Figure 36: Effect of the particle size on the elemental analysis of HTC-chars

4.1.6.2 Statistical testing of significance of the effect of particle sizes

The significant analysis showed that the significant effect of the variation of particle size was similar to that was by the variation of the solid load. The results in Table 16 showed that only the yields of HTC-chars were significantly affected (with $P = 0.022$).

Table 16: Means and standard error of different terms for the influence of the particle size on the properties of HTC-chars produced at 230 °C and 15 h using citric acid as catalyst

Term	Unit	Particle size [mm]		P-value
		4.00	0.50	
Yield	[%]	35.47±3.21	32.52±2.62	0.022
Carbon proportion	[%]	68.81±1.93	68.48±2.35	0.706
Oxygen proportion	[%]	21.34±2.05	21.28±3.02	0.961
Hydrogen proportion	[%]	5.18±0.36	5.15±0.59	0.833
Nitrogen proportion	[%]	2.25±1.22	2.46±1.28	0.683
Ash content	[%]	2.42±1.25	2.63 ±0.97	0.646

Where the changes of carbon, oxygen, hydrogen and nitrogen proportions as well as ash content were not significant (with $P > 0.05$). The size, shape and biomass properties influence both the conductive and convective heat transfer rate to the biomass and within the raw materials themselves during HTC.

4.1.7 Fourier transform infrared spectroscopy analysis

Fourier transform infrared spectroscopy analysis (FTIR) indicated the presence of several surface functional groups such as hydroxyl, carboxyl, carbonyl or phenol groups on the surface of HTC-chars produced as shown in Table 17.

Table 17: Functional groups of HTC-char samples according to the FTIR spectrum

Functional groups	Absorbance [cm^{-1}]
O–H (hydroxyl or carboxyl)	3100-3400
C–H (methyl and methylene)	2850-2922
C=C (aromatic)	1500-1615
C–H (out-of-plane)	760-795
C=O (Carbonyl)	1695-1700
C–O (hydroxyl, ether or ester)	1000-1300

Figure 37 shows an example of FTIR of HTC-chars produced from reed and typha using different reaction temperatures and presents these changes. The FTIR results of the raw materials and HTC-chars at 180 °C and 200 °C were similar, which indicated that the raw materials did not completely decompose under these mild HTC-reaction conditions. HTC-chars produced under more severe conditions (reaction temperature of 220 °C and 230 °C) had FTIR spectrums with features that were different from those of the raw materials. The band near 1160 cm^{-1} could be attributed to stretching vibrations to C-O-C in the cellulose and hemicellulose, this band was not found at higher reaction temperature or after oxidation, which indicated to the decomposition of the raw materials under the higher HTC reaction conditions. The aliphatic C–H stretching vibrations from the methyl and methylene groups (Mohan et al., 2011) were attributed by absorption band near 2900 cm^{-1} . Hydroxyl group (adsorption at 3100-3400 cm^{-1}) correspond to the O–H stretching vibration (hydroxyl or carboxyl) was quite flat (Araujo-Andrade et al., 2005) and found in all samples except of these after oxidation. The bands at 760-795 cm^{-1} , which related to aromatic character were assigned as C-H out-of-plane bending vibrations and were observed by the carbonization of typha at all reaction temperatures, which were stronger by increasing the reaction temperature, but they were found around 790 cm^{-1} by the carbonization of reed at 220 and 230 °C (Figure 37). The peak at 1512 cm^{-1} may be corresponded to a C=C stretching vibration caused by the aromatic structure (Ozcimen and Karaosmanoglu, 2004).

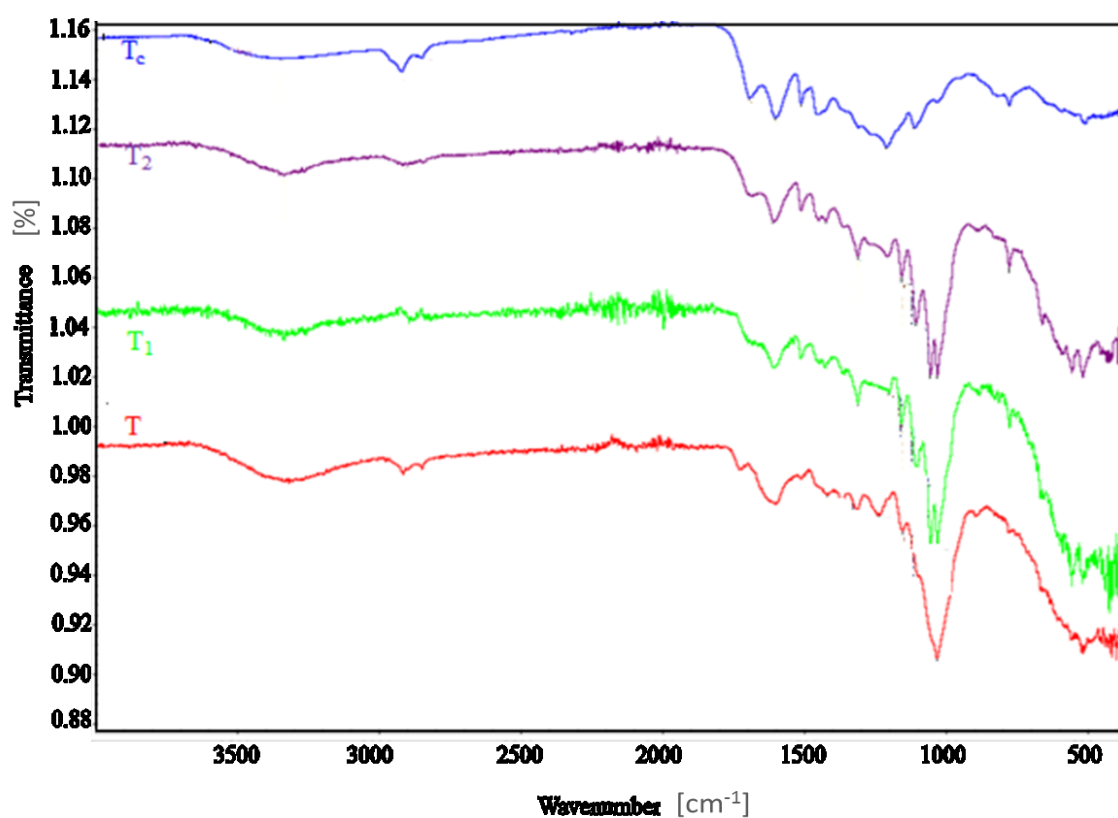
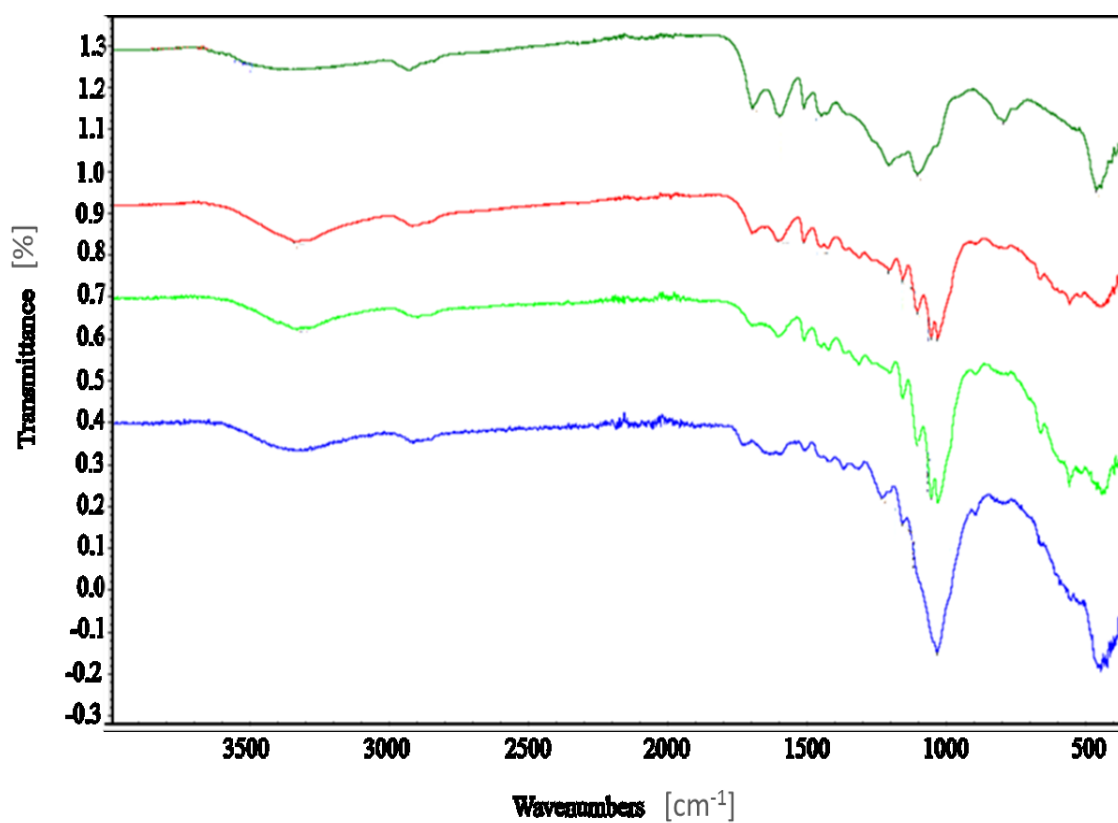


Figure 37: FTIR of HTC-chars from reed and typha produced at 15 h using citric acid as catalyst at different reaction temperature (180-230 °C)

Compared with the raw material, the adsorption band at around 1450 cm^{-1} correspond to carboxylic group (C (O) OH stretching) increased by increasing the hydrothermal reaction temperature, this band were not found with HTC-chars after oxidation with nitric acid. Carbonyl group (C=O) reflected by band at $1695\text{-}1700\text{ cm}^{-1}$ (Kabyemela et al., 1999) became stronger after hydrothermal carbonization especially at higher reaction temperatures, this band was not observed with raw material or with HTC-chars produced at reaction temperature $180\text{ }^{\circ}\text{C}$, while the content of C-O bands (hydroxyl, ether or ester) between near 1000 cm^{-1} and 1300 cm^{-1} was decreased. FTIR spectrums of the reed and typha were similar to that of the juncus and carex. There were some differences in the intensity of some bands, which can be explained by the different lignin, cellulose and hemicellulose contents of the raw materials (Ibrahim et al., 2018).

The analyses showed that HTC-chars consisted of several surface functional groups, which contributed positively to their adsorption performances. In general, FTIR of the raw materials and HTC-chars were different in intensity and shape. Some bands became stronger after carbonization, especially during higher reaction temperatures indicated that different thermal decomposition processes occurred during HTC.

Reaction temperatures and the variation of catalysts or the oxidation of HTC-chars with nitric acid affected the existence of functional groups on the surface of HTC-chars because they affected their chemical structure and the reaction mechanism occurred during HTC as dehydration and decarboxylation, which in their rolls affected the decomposition of hemicellulose, cellulose and lignin during HTC.

The results obtained were consistent with previous reports while using other types of biomasses (Sevilla et al., 2011; Titirici et al., 2008).

4.1.8 Conclusion

Reed, typha, juncus and carex were used as a reference for wetland biomasses to produce higher value carbonaceous products using HTC. The effect of HTC-process parameter on the properties of HTC-chars produced were investigated.

In conclusion, the following statements can be formulated for the influence of the process parameters:

- The properties of HTC-chars produced from different raw materials at the same process parameter differed from each other. Higher reaction temperatures and longer reaction times resulted in more liquid and gaseous products. As a result, lower yields of HTC-char were obtained.

- Higher reaction temperatures and longer reaction times resulted in a significantly increase in carbon proportion, specific surface area, and a significantly decrease in each of oxygen proportion and bulk density as well as H/C and O/C atomic ratios. These HTC-chars were increasingly more similar to those associated with lignite and bituminous coal. However, HTC-reaction times in the range between 12-20 h had no significant influence on the properties of HTC-chars produced.
- The variation of catalyst, solid load and particle size had lower effect on the properties of HTC-chars produced than those were by the variation of both reaction temperatures and reaction times.
- At all process parameter, HTC-chars and process waters were acidic.
- Several surface functional groups such as hydroxyl, carboxyl, carbonyl or phenol groups were found on the surface of HTC-chars. The nature of the raw materials and HTC-conditions as well as the oxidation of HTC-chars with nitric acid influenced the surface functional groups presented on HTC-chars.

4.2 Batch adsorption study

4.2.1 Effect of HTC-reaction temperature on the adsorption performance

4.2.1.1 Individually comparison between adsorbents

The adsorption capacities of HTC-chars of different adsorbents were plotted against the applied carbonization reaction temperatures in HTC-process and presented in Figure 38. The adsorption capacities of the raw materials were 0.55, 0.42, 0.36 and 0.33 mg l⁻¹ for reed, typha, juncus and carex, respectively. It is clear that all the HTC-chars tested successfully removed ammonia from aqueous solutions. The adsorption capacities of HTC-chars produced at 180 °C were similar and 83.55, 86.90, 87.93 and 89.84 % more than those of their raw materials of reed, typha, juncus and carex, respectively.

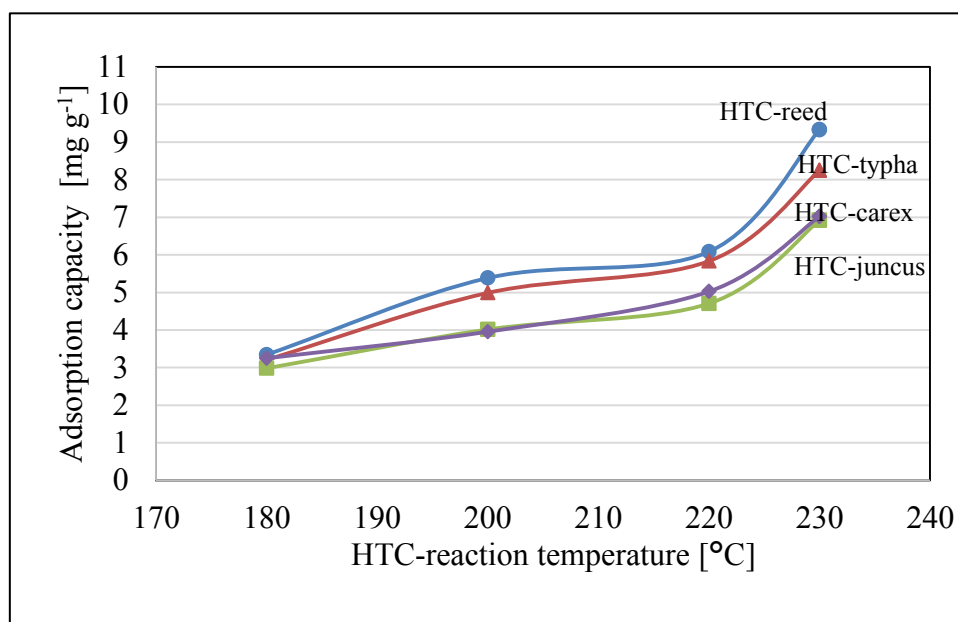


Figure 38: Effect of the variation of HTC-reaction temperature on the adsorption capacity of HTC-chars (Ibrahim et al., 2018).

The adsorption capacities of HTC-chars produced at higher HTC-reaction temperature were more than the adsorption capacities of the raw material and HTC-chars produced at lower reaction temperatures indicating that increasing the carbonization reaction temperature enhanced the adsorption of HTC-chars. For example, the adsorption capacity of HTC-char of reed produced at 180 °C was 3.34 mg g⁻¹, whilst it was increased for those HTC-chars produced at 200, 220 and 230 °C by a factor of 1.61, 1.82 and 2.79, respectively.

The fact that the adsorption capacity was the highest for HTC-chars produced at 230 °C might be attributed to develop the surface properties, specific surface area and the

properties of HTC-chars produced at higher reaction temperature (Ibrahim et al., 2014; Qian et al., 2006). The essential advantage of HTC is the enhancement of functional groups such as hydroxyl, aldehyde and carboxyl groups on the surface of HTC-chars produced. These functional surface groups have shown remarkable reactivity related to the adsorption process. HTC-chars of reed produced at all carbonization reaction temperatures had the highest adsorption capacities in comparison with all other adsorbents, which indicated that the adsorption capacity, depending on the biomass, differed stronger at higher carbonization reaction temperatures.

The reason might be in the different content of cellulose, hemicellulose and lignin. Carbonization reaction temperatures and type of raw materials can also affect the properties of HTC-chars, which vary depending on raw materials even when the reaction temperatures are similar (Ibrahim et al., 2014). Libra et al. (2011) reported that a variety of nanostructured carbon materials can be produced using HTC-process designed to meet a specific function.

4.2.1.2 Statistical testing of significance for the groups of adsorbents

In this study, each group of adsorbents contained HTC-chars of reed, typha, juncus and carex produced at a certain reaction temperature. The variation of HTC-reaction temperatures affected the properties of HTC-chars produced from all raw materials used, the adsorption performance of HTC-chars used as adsorbents for the removal of ammonia in aqueous solution were also significantly influenced as shown in Table 18.

Table 18: Means and standard error (SNK method) of the adsorption capacities of the groups of adsorbents containing HTC-chars produced at different HTC-reaction temperatures using citric acid as catalyst

HTC-reaction temperature	[°C]	180	200	220	230
Adsorption capacity	[mg g ⁻¹]	3.20±0.26 ^a	4.59±0.68 ^b	5.41±0.64 ^c	7.88±1.05 ^d

^{a,b,c,d} Values with different superscripts were significantly (P< 0.05) different (the comparison between values only applied to the same term)

Boxplots presented in Figure 39 illustrate that the group of adsorbents containing HTC-chars produced at 180 °C had the lowest adsorbent capacity. On the other hand, the best adsorption capacity was found with the group of adsorbents containing HTC-chars produced at 230 °C. More variability in the adsorption capacities was found in the last group, which could be explained with the fact that the differences in the characterization of adsorbents related to the adsorption performance as specific surface area and

functional groups were more affected with those adsorbents prepared from HTC-chars produced at higher reaction temperatures during HTC.

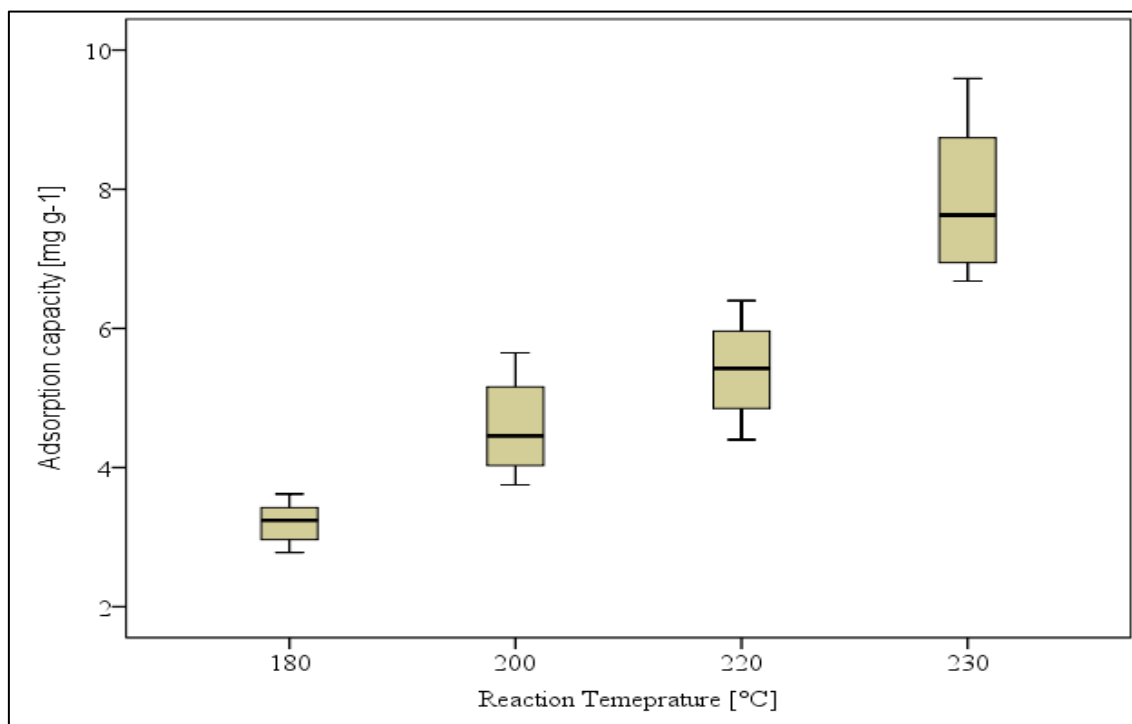


Figure 39: Adsorption capacity of the groups of adsorbents containing HTC-chars produced at different HTC-reaction temperatures as boxplots

4.2.2 Effect of HTC-char type on the adsorption performance

4.2.2.1 Individually comparison between adsorbents

The lowest removal efficiency rate (R [%]) was found with HTC-chars produced using citric acid as catalyst as shown in Table 19, among them R_c had the highest one with 39.72 %, while the lowest one was for J_c with 23.91 %.

Table 19: Effect of the variation of the adsorbents prepared from different HTC-char types on the ammonia removal efficiency rate (R [%]) of HTC-chars

Parameter	Adsorbent used											
	Citric acid as catalyst				Phosphoric acid as catalyst				Oxidation with nitric acid			
	R_c	T_c	J_c	Ca_c	R_p	T_p	J_p	Ca_p	R_n	T_n	J_n	Ca_n
R [%]	39.7	36.2	23.9	25.3	44.9	42.1	32.6	33.9	67.0	55.7	42.2	45.8
pH	3.8	4.4	4.6	4.6	2.6	2.7	2.9	2.8	2.0	2.2	2.4	2.3

The different HTC-chars were designated as R_N , T_N , J_N and Ca_N , where $N = c, p$ and n indicated to chars produced using citric acid, phosphoric acid as catalyst and after oxidation with nitric acid, respectively

The oxidation of HTC-chars with nitric acid improved distinctly the removal efficiency rates, which were 40.75, 35.01, 43.36 and 44.76 % more than those of adsorbent before oxidation, which were produced from reed, typha, juncus and carex, respectively.

The results showed that the adsorbents produced from reed had the highest removal efficiency rates. Comparison the removal efficiency rate of J_n and Ca_n with those were of R_p and T_p indicated that the modification of adsorbents produced from Juncus and carex enhanced their adsorption capacity only compared with their other types of HTC-chars. That must be taken in consideration for the further tests in the column study (Ibrahim et al., 2018).

The results indicated that the adsorption characteristics depended also on other parameters such as the type of raw materials used and the specific surface area of HTC-chars. Zeng et al. (2013) found similar results about the effect of raw materials, process used and activation parameters for different adsorbents produced through pyrolysis, which supported our results.

The effect on the chemical nature of HTC-chars surface was related to the hydrothermal carbonization parameter and the oxidation of these chars. Lower pH values of the adsorbents favor higher uptake of ammonia, this suggests a significant increase of adsorption sites with the surface acidity. The oxidized HTC-chars became more acidic and had the highest removal efficiency rate.

4.2.2.2 Statistical testing of significance for the groups of adsorbents

The results of statistical testing of significance for the effect of the use of different raw materials or catalysts during the production of the adsorbents or the oxidation of the adsorbents produced on their ammonia removal efficiency was presented in Table 20. Regarding the type of the raw materials used and regardless the oxidation of HTC-chars or the catalysts used during HTC, there was a significant effect (with $P= 0.001$) of the type of HTC-chars used on the ammonia removal efficiency rate (R [%]).

On the other hand the catalyst used during HTC-process or the oxidation of the HTC-chars after production had also a high significant effect on the adsorption process (with $P< 0.0001$). The oxidation with nitric acid enhanced significantly the ammonia adsorption, because it affected the chemical nature of the adsorbent.

Table 20: Means and standard error (SNK method) of different terms for the effect of HTC-char type on the adsorption performance of the groups of adsorbents used

Raw materials	Removal efficiency [%]	Adsorption capacity [mg g ⁻¹]
R	50.45±12.64 ^a	11.35±2.84 ^a
T	44.68±8.63 ^a	10.05±1.94 ^a
J	32.92±7.94 ^b	7.41±1.78 ^b
Ca	34.98±8.92 ^b	7.87±2.01 ^b
Catalyst/ Oxidation	Removal efficiency [%]	Adsorption capacity [mg g ⁻¹]
Citric acid	31.29±7.12 ^a	7.04±1.61 ^a
Phosphoric acid	38.31±5.38 ^b	8.62±1.21 ^b
Nitric acid	52.68±10.09 ^c	11.85±2.27 ^c

^{a,b,c} Values with different superscripts were significantly ($P < 0.05$) different (the comparison between values only applied to the same term)

Concerning the significant change of both the removal efficiencies and the adsorption capacities, the adsorbents in this test were classified in two groups, the first one contained HTC-chars produced from reed, typha, juncus and carex at 230 °C and 15 h using citric acid or phosphoric acid as catalyst and the second group contained adsorbents oxidizing with nitric acid. Therefore, in the following statistical testing of significance, the effects of the variation of adsorption parameters were performed taking in consideration these two groups.

4.2.3 Effect of contact time on the adsorption performance

4.2.3.1 Individually comparison between adsorbents

The optimum time required to reach equilibrium for ammonia- HTC-char system was determined by investigating the rate of ammonia uptake by HTC-chars from aqueous solution. The results in Figure 40 (A and B) presents that the removal efficiency rates (R [%]) for all adsorbents used were increased with an increase in the contact time.

The adsorption of ammonia was initially fast during the first 15-30 min, thereafter increasing the contact time led to a slowly increase in the ammonia uptake and eventually approached zero, when equilibrium was reached (Ibrahim et al., 2018). Compared with the removal efficiency rates of the adsorbents at contact time of 15 min, there was an increase in the range of 68.90-81.80 % and 63.75-77.05 % in the removal efficiency rates at contact time of 60 min of the adsorbents produced using citric acid

and phosphoric acid as catalysts during HTC, respectively. The increase for adsorbents after oxidation with nitric acid was 18.23-36.34 %. However, the contact time with quite good ammonia removal was 60 min.

The different adsorbents were designated as R_N , T_N , J_N and Ca_N , where $N= c, p$ and n indicated to chars produced using citric acid, phosphoric acid and after oxidation with nitric acid, respectively

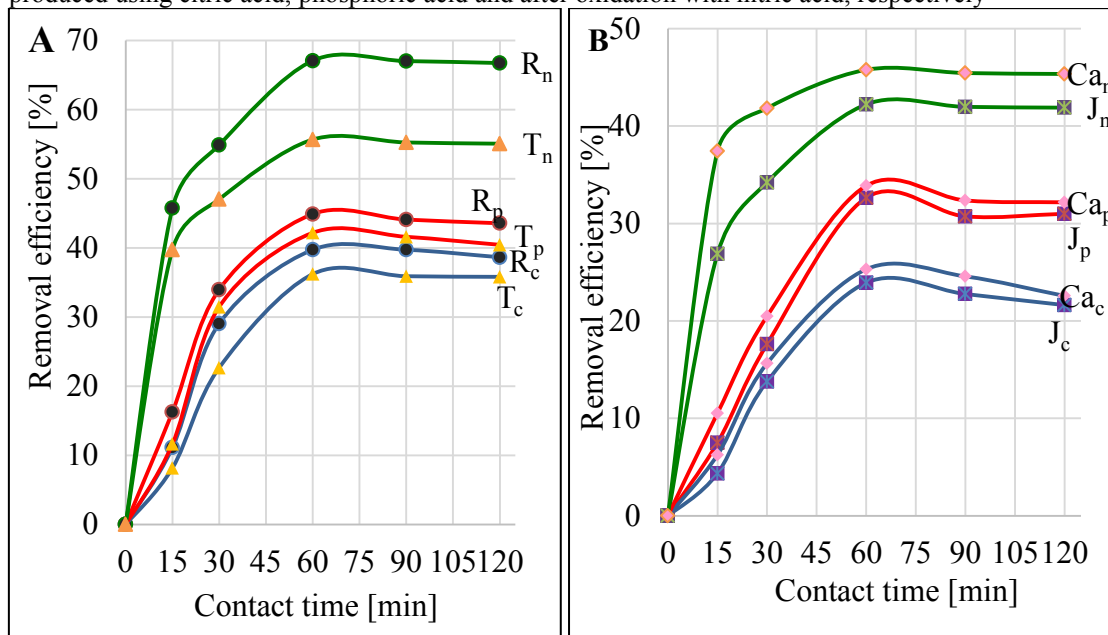


Figure 40: Effect of contact time on the removal efficiency rate of HTC-chars

It was observed that the removal efficiency rates of HTC-chars after oxidation at all contact times used were higher than those of HTC-chars were produced while using phosphoric acid during HTC. However, the last ones had higher removal efficiency rates at the studied contact times than those of HTC-chars produced while using citric acid as catalyst during HTC. HTC-chars produced from reed had the highest removal efficiency rates at all contact times compared with the other adsorbents.

The change in contact times had a considerable effect on adsorbents produced while using citric acid and phosphoric acid during HTC compared with those after oxidation that could be because the last ones had rapidly bond ammonia from solution to their surface-active side.

The results of the effect of contact time on the adsorption performance were in accordance with results reported in the literature (Ghauri et al., 2012). Vassileva et al. (2008) found that the optimum time to establish adsorption equilibrium between activated carbons modified by oxidation and the ammonium was 2 h that could be related to the nature of the adsorbents used, which affected the time reach equilibrium.

These changes in the removal efficiency rate of adsorption might be because at the beginning, all active sites were unoccupied and the dissolved concentration gradients were high. Thereafter, the ammonia adsorption rate was significantly decreased due to the reduction of unsaturated and active sites over the adsorption process (Huang et al., 2008; Karadag et al., 2006).

4.2.3.2 Statistical testing of significance for the groups of adsorbents used

The results presented in Table 21 indicate that the variation of contact times between 15-60 min for the adsorbents before oxidation had a significant effect concerning the significant change of both the removal efficiency rates and the adsorption capacities.

Table 21: Means and standard error (SNK method) of different terms for the effect of the contact time on the adsorption performance of adsorbents before and after oxidizing with nitric acid

Contact time [min]	Adsorbents before oxidation		Adsorbents oxidizing with nitric acid	
	Removal efficiency [%]	Adsorption capacity [mg g ⁻¹]	Removal efficiency [%]	Adsorption capacity [mg g ⁻¹]
15	9.47±3.57 ^a	2.13±0.80 ^a	37.44±7.12 ^a	8.41±1.58 ^a
30	23.08±7.26 ^b	5.19±1.63 ^b	44.73±8.23 ^{ab}	10.07±1.85 ^{ab}
60	34.84±7.20 ^c	7.84±1.62 ^c	52.68±10.09 ^b	11.85±2.27 ^b
90	33.96±7.45 ^c	7.64±1.68 ^c	52.32±10.27 ^b	11.77±2.31 ^b
120	33.23±7.66 ^c	7.48±1.72 ^c	52.50±10.48 ^b	11.82±2.36 ^b

^{a,b,c} Values with different superscripts were significantly ($P < 0.05$) different (the comparison between values only applied to the same term)

The results showed that there was a high significant effect of the contact times on the adsorption performance (with $P < 0.0001$) for all adsorbents used. However, no significant change was found while increasing the contact time in the range between 60-120 min. On the other hand, the variation of contact time between 30-120 min while using the adsorbents oxidizing with nitric acid had no significant effect on the adsorption process (Values with similar superscripts were not significantly ($P > 0.05$) different). The results confirmed that the optimum time required to reach equilibrium for ammonia-HTC-char system was 60 min. This contact time has been chosen for the further adsorption test in this study. The research hypothesis about the significantly effect of adsorption process parameters, here contact time, on the adsorption performances of adsorbents used was proved for the adsorbents before oxidation but only in the range between 15-60 min.

4.2.4 Effect of initial ammonia concentration on the adsorption performance

4.2.4.1 Individually comparison between adsorbents

The results in Figure 41 (A and B) suggested that the removal efficiency rate of HTC-chars decreased with the initial ammonia concentrations in the aqueous solutions.

The different adsorbents are designated as R_N , T_N , J_N and Ca_N , where $N = c, p$ and n indicates to chars produced using citric acid, phosphoric acid as catalyst and after oxidation with nitric acid, respectively

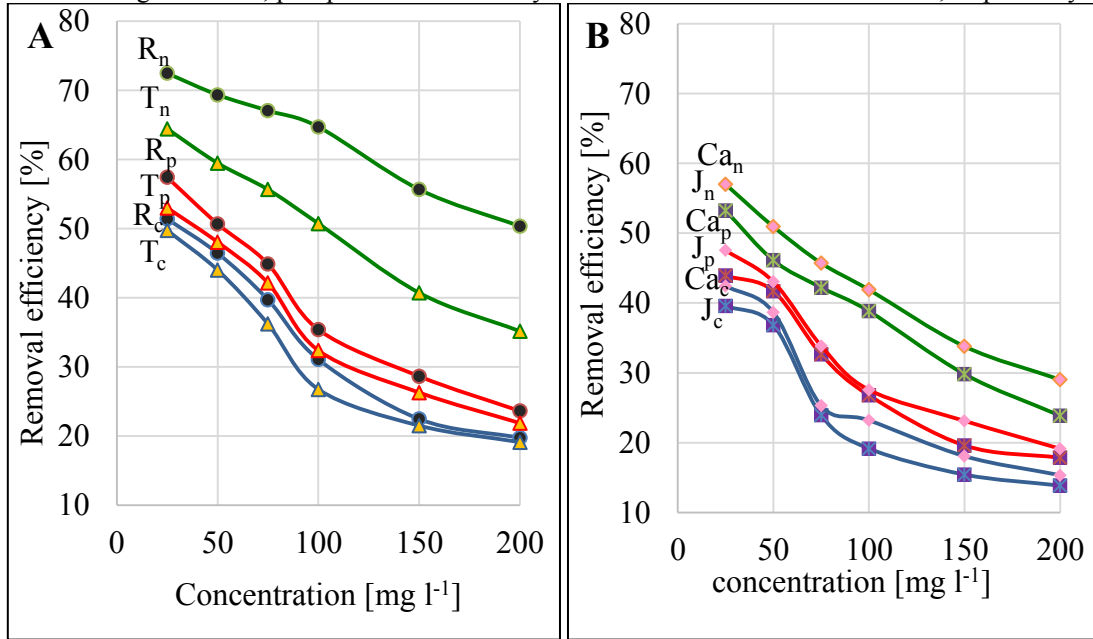


Figure 41: Effect of initial ammonia concentration on the removal efficiency rate of HTC-chars (Ibrahim et al., 2018)

Compared with the removal efficiency rates of the adsorbents at initial ammonia concentration of 25 mg l^{-1} , there was an decrease in the range of 61.56-65.04 % and 58.73-59.78 % in the removal efficiency rates obtained at initial ammonia concentration of 75 mg l^{-1} of the adsorbents produced using citric acid and phosphoric acid as catalysts during HTC, respectively. The decrease was 30.52-55.19 % for adsorbents after oxidation with nitric acid.

The removal efficiency rates of HTC-chars after oxidation at all initial ammonia concentration used were higher than those were of HTC-chars produced while using phosphoric acid as catalyst during HTC. However, the last ones had higher removal efficiency rates at the studied initial ammonia concentrations than those of HTC-chars produced while using citric acid as catalyst during HTC. On the other hand, HTC-chars produced from reed had the highest removal efficiency rates at all initial ammonia concentration compared with the other adsorbents.

By increasing the initial concentration, the removal efficiency rate will be decreased because of the limited number of adsorption sites on the adsorbent, which be saturated above a certain concentration. Furthermore, the high initial concentration of ammonia molecules leads to the lack of available active sites on the surface. The ratio of total number of moles of ammonia to the adsorbent surface area is low at lower initial concentration, therefore its uptake increases. The initial concentration provides the requested driving force to overcome all mass-transfer resistances between aqueous bulk and the surface of solid phases that is why a higher initial concentration of ammonia may enhance the adsorption capacity (Ibrahim et al., 2018; Lalhruitluanga et al., 2010; Long et al., 2008). The equilibrium of ammonia in the solution and on the surface of the adsorbent may increase with its concentration in the solution (Long et al., 2008).

4.2.4.2 Statistical testing of significance for the groups of adsorbents

The results in Table 22 showed a decrease in the removal efficiency rate with its concentration in the aqueous solutions for all adsorbents used. However, there was an increase in their adsorption capacities.

Table 22: Means and standard error (SNK method) of different terms for the effect of ammonia concentration on the adsorption performance of adsorbents before and after oxidizing

initial ammonia concentration [mg l ⁻¹]	Adsorbents before oxidation		Adsorbents oxidizing with nitric acid	
	Removal efficiency [%]	Adsorption capacity [mg g ⁻¹]	Removal efficiency [%]	Adsorption capacity [mg g ⁻¹]
25	48.14±5.67 ^a	3.61±0.43 ^a	61.79±7.70 ^a	4.64±0.58 ^a
50	43.69±4.46 ^b	6.55±0.67 ^b	56.48±9.24 ^{ab}	8.64±1.39 ^b
75	34.84±7.20 ^c	7.84±1.62 ^c	52.68±10.09 ^{ab}	11.85±2.27 ^c
100	27.79±4.96 ^d	8.34±1.49 ^c	49.05±10.50 ^b	14.72±3.15 ^c
150	21.89±4.11 ^e	9.85±1.85 ^d	40.00±10.31 ^c	18.00±4.64 ^d
200	18.82±3.06 ^f	11.29±1.8 ^e	34.60±10.38 ^c	20.71±6.23 ^d

^{a,b,c,d,e,f} Values with different superscripts were significantly (P< 0.05) different (the comparison between values only applied to the same term)

In general, there was a high significant effect of the change of initial ammonia concentrations on the adsorption performance (with P< 0.0001) for adsorbents before oxidation. In comparison with the adsorbents oxidizing with nitric acid, the adsorption performance, in terms of removal efficiency rates and adsorption capacities, of the adsorbents before oxidation was more significantly affected by changing the initial

ammonia concentrations. Regarding the adsorbents oxidizing with nitric acid, the change of the initial concentrations in the range 25-75 mg l⁻¹ and 150-200 mg l⁻¹ had no significant effect on their removal efficiency rate (Values with similar superscripts were not significantly ($P > 0.05$) different). The tendency of their adsorption capacities was a little different. In this term, the change of the initial ammonia concentrations between 75 and 100 mg l⁻¹ or between 150 and 200 mg l⁻¹ had no significant effect.

4.2.5 Effect of solution pH on the adsorption performance

4.2.5.1 Individually comparison between adsorbents

The results presented in Figure 42 (A and B) showed that increasing the solution pH led to an increase in the ammonia removal efficiency of all adsorbents used. This test was made for the adsorbents of reed and typha with the highest adsorption of ammonia in the initial evaluation.

The different adsorbents were designated as R_N and T_N where $N = c, p$ and n indicated to chars produced using citric acid, phosphoric acid and after oxidation with nitric acid, respectively

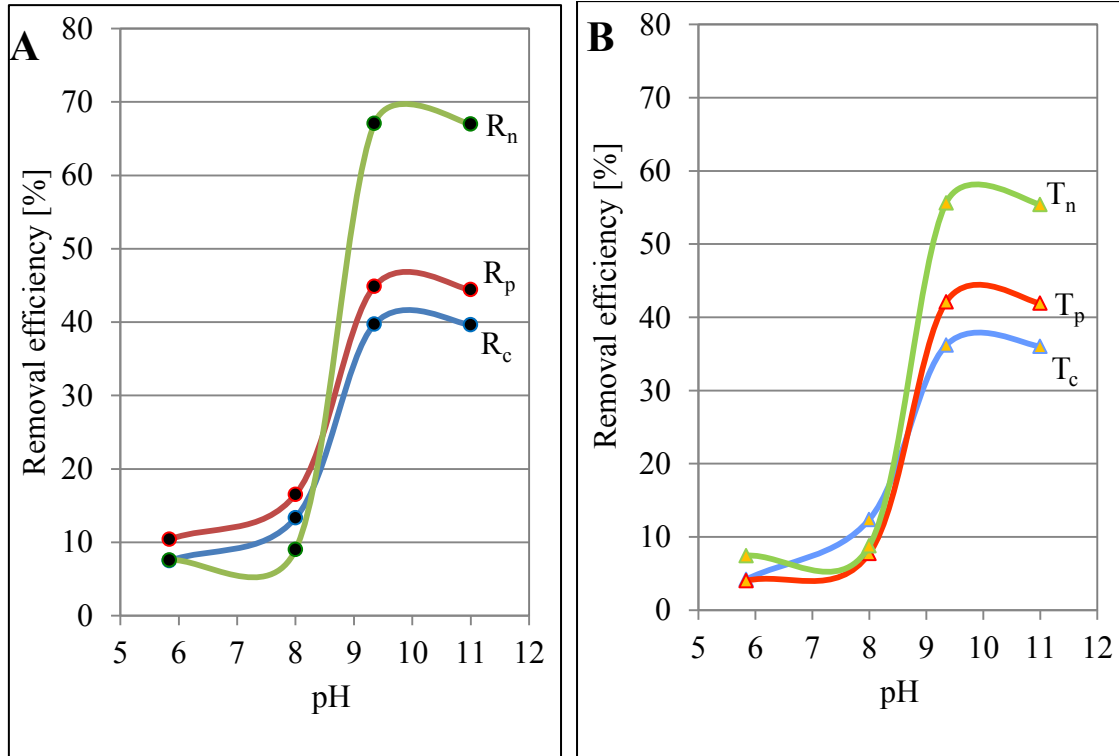


Figure 42: Effect of solution pH on the removal efficiency rate (Ibrahim et al., 2018)

The removal efficiency rates at solution pH values 5.84 and 8 were low for all adsorbents used. As pH increased, ammonia adsorption onto HTC-char increased.

At solution pH 9.35, the ammonia removal efficiency rates of the adsorbents used were 76.90-90.67 % more than those were at solution pH 5.84.

A little decrease in the removal efficiency rates was found at pH 11. So that, the optimum pH for the adsorption of ammonia in aqueous solution in this study was found to be at solution pH 9.35, where the removal efficiency rate reached 67.06 % and the adsorption capacity was 15.09 mg g⁻¹ for R_n, which had the best adsorption performance among the other adsorbents at all solution pH values used. It was found from the results that pH value had much more influence on the removal efficiency rate of adsorbents oxidizing with nitric acid.

It was observed that at the initial pH values of solution 5.84 and 8, the pH values for the mixture solution-solid were close to the pH_{pzc} of the most adsorbents used (Table 13). Therefore, the removal efficiency rates were small and these pH values did not enhance the ammonia uptake at equilibrium for the most HTC-chars used, especially for those after oxidation.

The solution pH is an important factor that influences the adsorption of anions and cations at the solid-liquid interface. At a pH ≤ 8, NH₄⁺ could be competed with other cations such as H⁺ for exchangeable sites, which results in the decrease in the removal efficiency rate. Higher pH values of solution could increase the negative charges on the adsorbent surfaces, which means more attractive to cations on their surfaces.

A little decrease in the removal efficiency at alkaline pH, beyond 9.35 could be because of the partially transformation of NH₄⁺ into electrically neutral NH₄OH (NH₃.H₂O) and the volatilization of NH₃, which leads to the loss of ammonia nitrogen.

This parameter has been reported to exhibit a significant influence on the adsorption of ammonia due to its effect on the surface chemistry and surface charge of the adsorbent and the solubility of ammonia (Yusof et al., 2010). Abdul Halim et al. (2013) reported that the optimum conditions for adsorption in batch study using activated carbon modified with organic acid occurred at solution pH ranged between 8-9.

Zhou et al. (2014) reported that the maximum adsorption capacity of barbecue bamboo charcoal for removing ammonium from aqueous solutions was achieved at solution pH 6-10. Solution pH values 5-8 and 5-7 were reported by other researchers (Liu et al., 2010; Ji et al., 2007).

4.2.5.2 Statistical testing of significance for the groups of adsorbents

The statistical analysis was made for the adsorption test using groups containing HTC-chars of reed and typha before and after oxidation at each solution pH value used.

The results in Table 23 showed that the variation of solution pH in some ranges had a significant influence on the adsorption of ammonia for all adsorbents used.

Table 23: Means and standard error (SNK method) of different terms for the effect of the solution pH on the adsorption performance of adsorbents before and after oxidizing with nitric acid

pH	Adsorbents before oxidation		Adsorbents oxidizing with nitric acid	
	Removal efficiency [%]	Adsorption capacity [mg g ⁻¹]	Removal efficiency [%]	Adsorption capacity [mg g ⁻¹]
5.84	6.53±2.77 ^a	1.47±0.63 ^a	7.52±0.37 ^a	1.69±0.09 ^a
8.00	12.50±3.30 ^b	2.81±0.74 ^b	8.90±0.43 ^a	2.01±0.10 ^a
9.35	40.75±3.35 ^c	9.17±0.76 ^c	61.36±6.25 ^b	13.80±1.40 ^b
11.00	40.20±3.13 ^c	9.08±0.70 ^c	61.01±5.66 ^b	13.68±1.28 ^b

^{a,b,c,d} Values with different superscripts were significantly ($P < 0.05$) different (the comparison between values only applied to the same term)

It was observed that the variation of solution pH in the range of 5.84-9.35 had a significant effect on the ammonia adsorption while using all adsorbents before oxidation with nitric acid (Values with different superscripts were significantly ($P < 0.05$) different). However, there was no significant effect on the adsorption process when the solution pH-values were changed from 9.35 to 11. On the other hand, the variation of solution pH had a little effect while using adsorbents oxidizing with nitric acid, this variation of between 5.84 and 8 as well as between 9.35 and 11 had no significant effect on each of removal efficiency rates and adsorption capacities (Values with similar superscripts were not significantly ($P > 0.05$) different).

The Boxplots presented in Figure 43 for the removal efficiency of adsorbents before oxidation at different solution pH-values indicates that the higher solution pH-values enhanced the removal efficiency of all adsorbents used, which affirmed that the solution pH had an effect on the adsorption process.

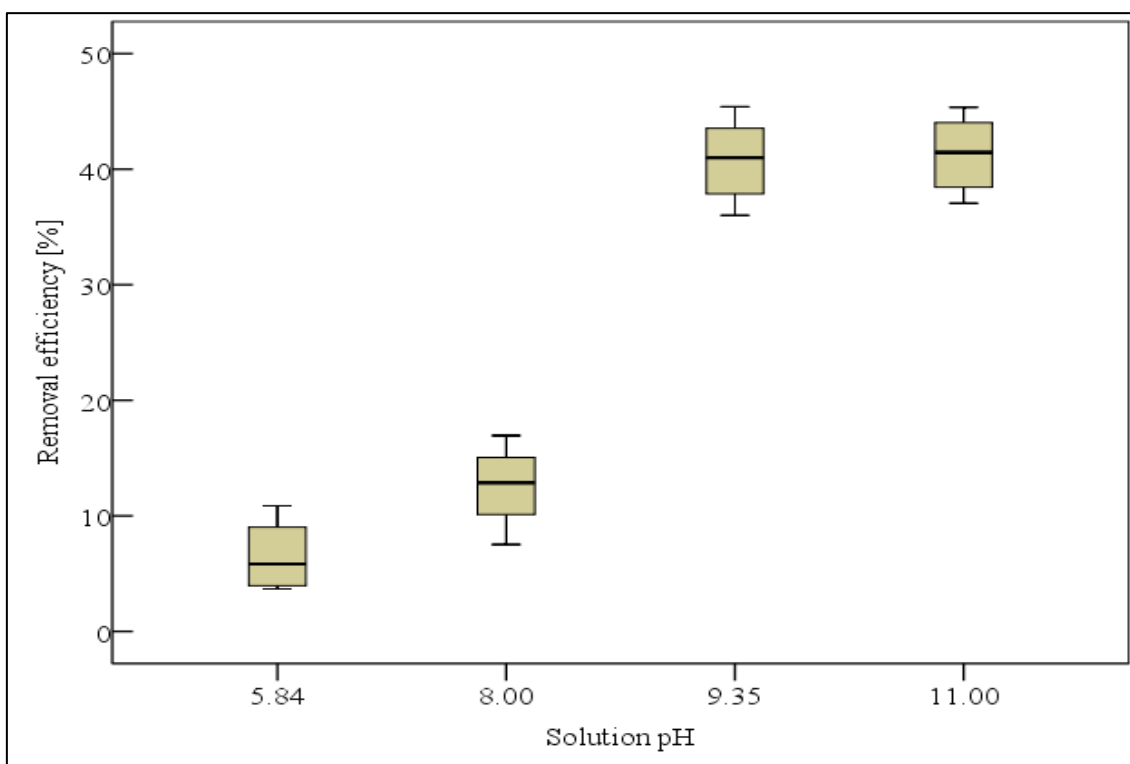


Figure 43: Removal efficiency at different solution pH for adsorbents before oxidation with nitric acid as boxplots

4.2.6 Effect of adsorbent dosage on the adsorption performance

4.2.6.1 Individually comparison between adsorbents

The results in Table 24 showed that the increase in adsorbent dosage from 0.15-1 g developed the removal efficiency.

Table 24: Effect of the variation of the adsorbent dosage on the ammonia removal efficiency rate (R [%]) and the adsorption capacity (q_e)

Parameter	HTC-char mass (Adsorbent dosage) [g]							
	0.15		0.25		0.50		1.00	
	q_e [mg g ⁻¹]	R [%]	q_e [mg g ⁻¹]	R [%]	q_e [mg g ⁻¹]	R [%]	q_e [mg g ⁻¹]	R [%]
R_c	9.15	24.41	8.94	39.72	7.17	44.62	5.27	46.85
T_c	8.44	22.49	8.15	36.21	6.64	41.33	5.06	45.02
R_p	10.46	27.88	10.10	44.89	8.04	50.05	6.51	57.84
T_p	9.37	25.92	9.49	42.14	7.49	46.58	6.13	54.50
R_n	15.43	41.15	15.09	67.06	11.10	69.06	8.20	72.89
T_n	11.32	30.20	12.52	55.66	9.39	58.42	7.12	63.27

The different adsorbents were designated as R_N and T_N where $N = c, p$ and n indicated to chars produced using citric acid and phosphoric acid as catalyst and after oxidation with nitric acid, respectively

Increasing the adsorbent dosage from 0.15 to 0.25 g resulted in a rapid increment in the ammonia removal rates; further increase of the adsorbent did not provide a considerable effect. Furthermore, it was noticeable that increasing the adsorbent dosage in the solution resulted in a decrease of the adsorption capacity per gram of chars (Ibrahim et al., 2018). The results showed that increasing the adsorbent dosage from 0.25 to 1 g led to an increase of 15.21 and 19.58 %, 22.40 and 22.68 % as well as 8.01 and 12.03 % in the removal efficiency rates of R_c and T_c , R_p and T_p as well as R_n and T_n , respectively. On the other hand, there was a reduction of 41.04 and 37.83 %, 35.57 and 35.38 % as well as 45.65 and 43.61 % in the adsorption capacities of the above-mentioned adsorbents, respectively. Moreover, it was observed that adsorbents produced from reed had the best adsorption performance, or rather the adsorbent after oxidation with nitric acid. These results were similar to studies reported by other researchers (Ghauri et al., 2012; Li et al., 2012, Long et al., 2008). However, the increase in the removal efficiency rate did not seem enough to justify doubling the adsorbent dosage, which could interpret that the adsorbent dosage of 0.25 g was the best one in this study. Therefore, 0.25 g dosage of the adsorbents was used in all tests.

The actual number of active sites or adsorption sites per gram of adsorbent will not be proportionately increased while increasing adsorbent dosage and hence therefore, there is a regular decrease in adsorbate uptake, which suggests that after a certain adsorbent dosage, the maximum adsorption is attained. This decrease can be also explained by overlapping of active sites because of overcrowding of adsorbent particles. The inter-particle interaction resulting from high adsorbent dose may be a reason for such reduction, such as aggregation would result in a reduction in the total surface area of the adsorbent (Shukla et al., 2002).

4.2.6.2 Statistical testing of significance for the groups of adsorbents used

The results in Table 25 presented an increase in the removal efficiency rates of adsorbents used by increasing the adsorbent dosage. However, there was a decrease in their adsorption capacities. In general, there was a high significant effect of the change adsorbent dosage on the adsorption performance (with $P < 0.0001$) for all adsorbents.

The increase in adsorbent dosage from 0.15-0.50 g developed the removal efficiency of the adsorbents before oxidation, while no significant effect was observed by further increase in the adsorbent dosage from 0.50 to 1 g. The adsorption capacities of these

adsorbents were significantly affected while increasing the adsorbent dosage from 0.25-1 g (Values with similar superscripts were significantly ($P > 0.05$) different).

Table 25: Means and standard error (SNK method) of different terms for the effect of the adsorbent dosage on the adsorption performance of adsorbents before and after oxidizing

adsorbent dosage [g]	Adsorbents before oxidation		Adsorbents oxidizing with nitric acid	
	Removal efficiency [%]	Adsorption capacity [mg g ⁻¹]	Removal efficiency [%]	Adsorption capacity [mg g ⁻¹]
0.15	25.18±2.09 ^a	9.44±0.78 ^a	35.68±6.01 ^a	13.38±2.26 ^a
0.25	40.75±3.35 ^b	9.17±0.76 ^a	61.36±6.25 ^b	13.08±1.40 ^a
0.50	45.65±3.32 ^c	7.34±0.53 ^b	63.74±5.84 ^b	10.20±0.94 ^b
1.00	51.05±5.54 ^c	5.74±0.62 ^c	68.08±5.29 ^b	7.65±0.59 ^c

^{a,b,c} Values with different superscripts were significantly ($P < 0.05$) different (the comparison between values only applied to the same term)

On the other hand, the increase of adsorbent dosage from 0.25-1 g did not provide a significant effect on the removal efficiency while using adsorbents oxidizing with nitric acid (Values with similar superscripts were not significantly ($P > 0.05$) different). Furthermore, it was noticeable that the adsorption capacity decreased significantly by increasing the adsorbent dosage from 0.25-1 g for those adsorbents.

4.2.7 Sorption isothermes

The corresponding Langmuir and Freundlich isotherms estimated model parameters and correlation coefficients (R^2) were given in Table 26. The correlation coefficients for the linear plots were in most cases high. The correlation coefficients of Langmuir model were comparable to those of the Freundlich model. The maximum adsorption capacity (q_m) of adsorbents produced from reed while using citric acid and phosphoric acid as catalysts during HTC were similar to those of corresponding adsorbents produced from typha and higher than those of HTC-chars produced from juncus and carex.

The highest Langmuir maximum adsorption capacity was found with R_n (after oxidation with HNO₃), which was about 3.40 times as large as the corresponding value for this HTC-chars before oxidation.

Table 26: Parameters obtained from Langmuir and Freundlich isotherms for the adsorbents used (Ibrahim et al., 2018)

Adsorbent	Langmuir			Freundlich		
	R^2 [-]	q_m [mg g ⁻¹]	b [l mg ⁻¹]	R^2 [-]	K [mg g ⁻¹]	n [-]
R _c	0.9880	13.423	0.036	0.9017	1.681	2.522
R _p	0.9954	16.835	0.032	0.9470	1.760	2.321
R _n	0.9961	45.045	0.020	0.9763	1.769	1.565
T _c	0.9757	13.158	0.030	0.9279	1.545	2.518
T _p	0.9914	16.694	0.026	0.9409	1.664	2.391
T _n	0.9981	27.624	0.024	0.9652	1.666	1.843
J _c	0.9598	9.434	0.027	0.8743	1.268	2.776
J _p	0.9794	12.469	0.027	0.9320	1.271	2.366
J _n	0.9960	18.450	0.024	0.9540	1.274	1.845
Ca _c	0.9841	10.571	0.028	0.9188	1.272	2.581
Ca _p	0.9891	14.025	0.025	0.9553	1.284	2.268
Ca _n	0.9984	23.256	0.020	0.9792	1.291	1.847

The different adsorbents were designated as R_N, T_N, J_N and Ca_N, where N= c, p and n indicated to chars produced using citric acid and phosphoric acid as catalyst and after oxidation with nitric acid, respectively

In this study, the values of the separation factor (R_L), which expressed the favorability of the Langmuir isotherm (equation 14); of all HTC-chars used as adsorbents were in the range between 0.27-0.40. From the result, it was apparent that the values of R_L were in the range between 0-1 and hence, adsorption of the adsorbate on HTC-chars seemed to be favorable. Based on the Freundlich affinity coefficient (K), the best affinity for ammonia was found with R_n, which was consistent with the maximum adsorption capacity obtained from Langmuir model.

Values of Freundlich constants (n) in the range 1-10 ($1/n < 1$) represent favorable adsorption (Vassileva et al., 2008). In this study, these values were lower than three. A relatively high R^2 showed that the both models successfully illustrated the kinetics of ammonia adsorption by HTC-chars.

This finding was in accordance with reported results by Liu et al. (2010). For all adsorbents used, the removal of ammonia was more corresponding to Langmuir model because of highest R^2 value (Ibrahim et al., 2018).

Calculation of adsorbent loading at equilibrium has a major impact on designing the adsorption process. The results presented in Figures 44 were prepared in order to predict the relative performance of different types of HTC-chars used at initial ammonia concentrations in the range 25-200 mg l⁻¹.

The different adsorbents were designated as R_N, T_N, J_N and Ca_N, where N= c, p and n indicated to chars produced using citric acid and phosphoric acid as catalyst and after oxidation with nitric acid, respectively

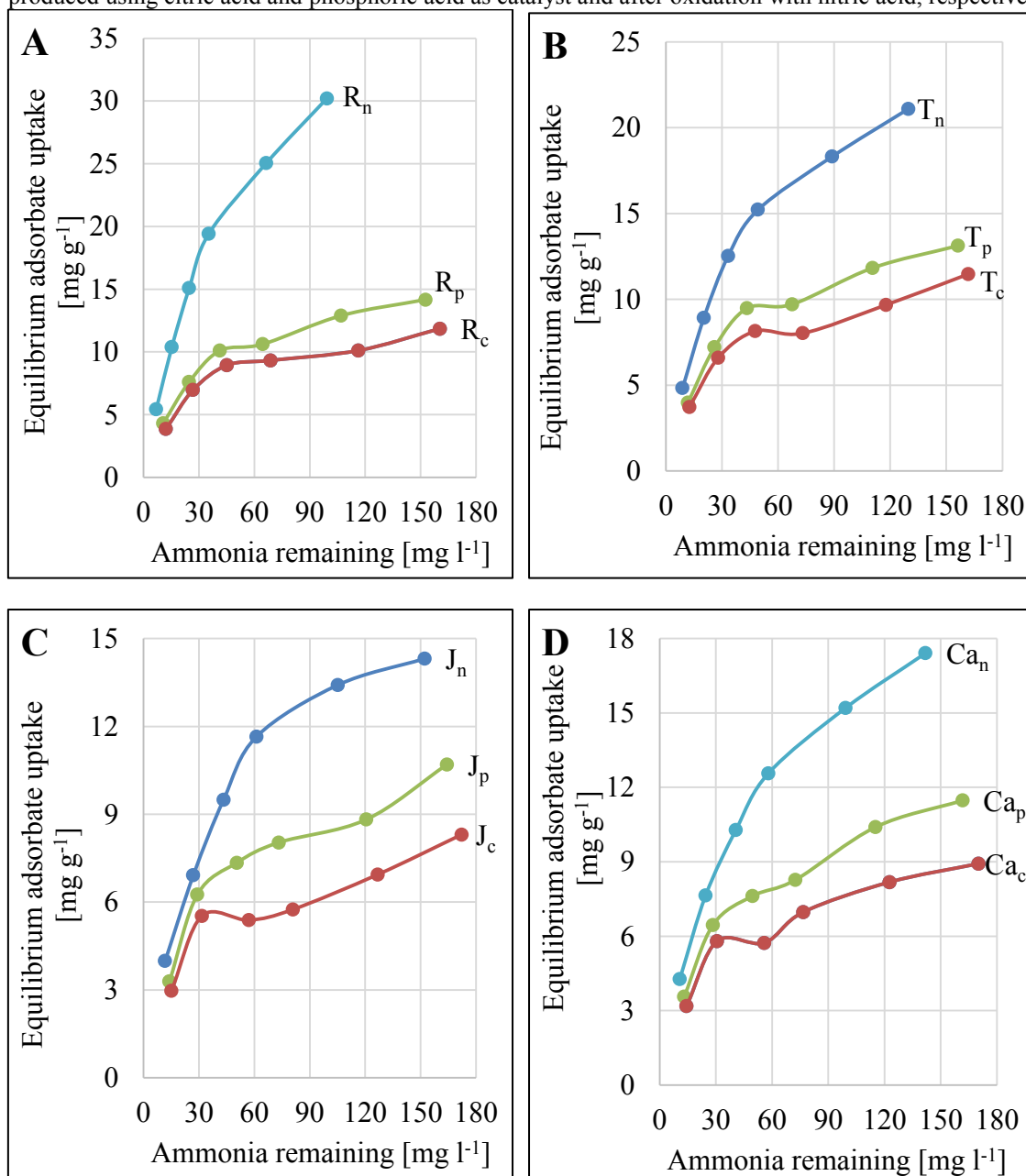


Figure 44: Adsorption isotherm for adsorbents prepared from HTC-chars produced from reed (A), typha (B), juncus (C) and Carex (D)

It was clear from the adsorption isotherms that R_c, R_p and R_n had the highest equilibrium adsorbate uptake of ammonia than the other corresponding adsorbents, respectively.

Compared with adsorbent produced using citric acid and phosphoric acid as catalyst during HTC, adsorbents after oxidation with nitric acid were the best performing adsorbents because at all ammonia concentrations the amount of ammonia adsorbed per unit weight of adsorbent (q_e) was higher than those of their corresponding adsorbents.

Interestingly, the adsorption properties of HTC-chars after oxidization at higher initial concentrations ammonia (150 and 200 mg l⁻¹) were better than ones were while using lower initial concentrations (25 and 50 mg l⁻¹). For example, the adsorption capacity of R_n was about 30 % and 60 % more than those were of R_c at initial ammonia concentrations of 25-50 mg l⁻¹ and 150-200 mg l⁻¹, respectively.

In general, adsorbent with a higher isotherm line indicates that it has a better adsorption capacity than one with a lower isotherm line. The slope of isotherm lines reveals also the performance of each adsorbent. A nearly vertical isotherm line represents poor adsorption properties at lower ammonia concentration. A nearly horizontal isotherm line means that the adsorbent has a good adsorption of ammonia over a wide range of ammonia concentration.

Moreover, the adsorption isotherms can help to calculate the needed adsorbent dosage used to attain the same adsorption performance of different adsorbents. Suggesting that the desired ammonia remaining was 24.70 mg l⁻¹ at initial ammonia concentration of 75 mg l⁻¹. In this case, the amount of ammonia removal (50.30 mg l⁻¹) was same for all adsorbents used. The amount of ammonia adsorbed per unit weight of adsorbent (q_e) for each type could be determined from the isotherm plots.

The needed adsorbent dosage was determined by dividing the amount of ammonia removed by the adsorption capacity. The needed adsorbent dosages were 3.33, 4.91, 6.52 and 7.68 g l⁻¹ for R_n , T_n , Ca_n and J_n , respectively. The calculated results showed that 32.06, 48.84 and 56.59 % more adsorbent dosage of T_n , Ca_n and J_n were needed, respectively, to attain the same adsorption performance as achieved with R_n .

Moreover, the yield of HTC-char from reed was higher than those were for the other HTC-chars. Furthermore, HTC-chars of typha had lower yield and lower removal of ammonia than those are of reed. HTC-chars of juncus and carex had a comparable yield and lower removal efficiency rates as compared with HTC of reed and typha.

Therefore, HTC-char of reed or rather R_n may be more economical for application of ammonia removal in aqueous solution among the tested HTC-chars.

4.2.8 Regeneration and reusable ability studies

4.2.8.1 Regeneration test using different regeneration agents

The adsorption capacity of different adsorbents in the first use and after regeneration using different regeneration agents were presented in Figure 45.

Compared with the adsorption capacities of adsorbents used for the first time, the results indicated that using HCl as regeneration agent resulted in a little reduction in the adsorption capacity of about 5 % after regeneration for the adsorbent produced from reed while using citric acid (R_c) as catalyst during HTC. However, the adsorption capacity remained constant for adsorbents produced from reed while using phosphoric acid (R_p) as catalyst during HTC. Furthermore, adsorbent after oxidation with nitric acid (R_n) had an increase of about 15 % in the adsorption capacity after regeneration.

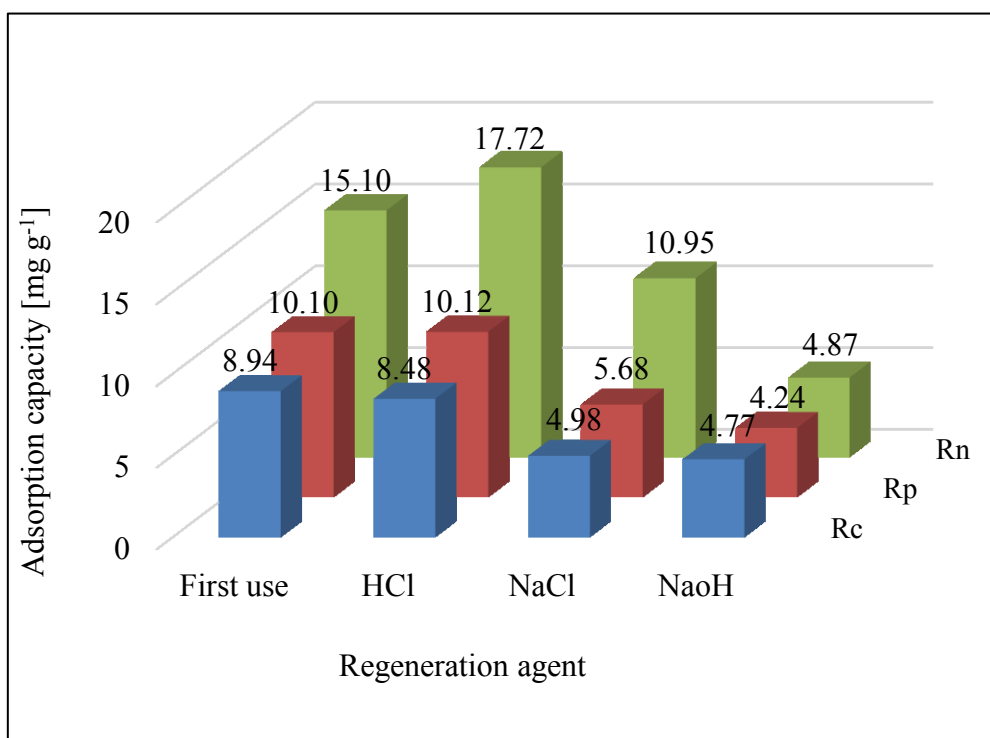


Figure 45: Effect of different regeneration agents on the adsorption capacity of adsorbents used

On the other hand, using NaCl resulted in a reduction of about 45 % in the ammonia adsorption capacity after regeneration for all HTC-chars used. In addition, using NaOH led to reductions of 46.62, 58.02 and 67.74 % in the ammonia adsorption capacity for R_c , R_p and R_n , respectively.

Table 27 presents the regeneration ratios for each of the regeneration agent used. As a result, high regeneration efficiencies of 94.84, 100.21 and 117.76 % were obtained while using HCl as regenerant for each of R_c , R_p and R_n , respectively.

Table 27: Effect of different regeneration agents on the regeneration ratios of the adsorbents produced

HTC-char	Regeneration ratio [%]		
	0.1 M HCl	1 M NaCl	1 M NaOH
R_c	94.84	55.73	53.38
R_p	100.21	56.26	41.98
R_n	117.38	72.53	32.26

Lower regeneration ratios were achieved while using NaCl for all adsorbents used. On the other hand, the lowest regeneration ratios (< 55 %) were found while using NaOH as regeneration agents. Interestingly, after regeneration using NaOH, adsorbents were harsh and formed a coherent mass, which might be probably indicated that some chemical reactions were occurred to form another compound. No further investigation for these changes was performed in the presented study.

The efficiency of a regeneration agent is judged on the extent that it influences a recovery of the adsorptive powers of the adsorbent. Compared with HCl, both NaCl and NaOH were not able to regenerate exhausted adsorbents because of their worse performance. That is an indicator that HCl had the most efficiency to regenerate the exhausted adsorbents used and could enhance the adsorption capacities of the exhausted adsorbents R_p and R_n .

4.2.8.2 Regeneration tests

Four loading and three regeneration cycles in batch experiments using 0.1 M HCl, the best regeneration agent used in this study, were carried out in order to evaluate the possibility of the reuse of the exhausted adsorbents. The adsorption capacity at consecutive adsorption-regeneration cycles were presented in Figure 46. The results showed that the adsorption capacity of R_c decreased steadily after each regeneration cycle and were ultimately at the third regeneration cycle 21.74 % lower than it was for the adsorbent used for the first time.

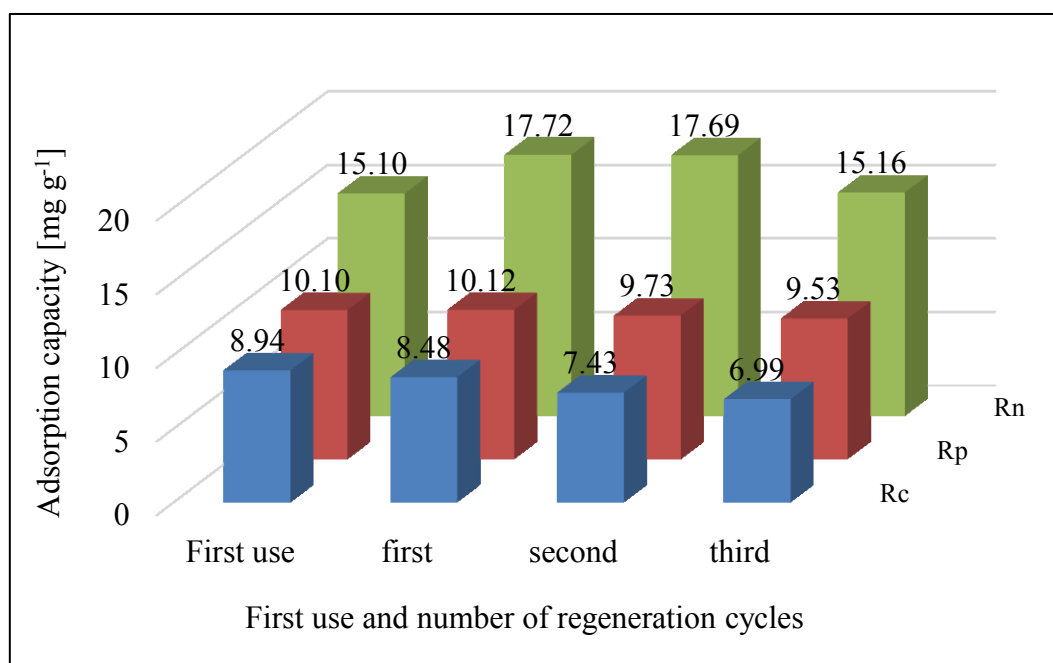


Figure 46: Effect of number of regeneration cycles on the adsorption capacity

On the other hand, in the first adsorption-regeneration cycle, the adsorption capacity of R_p was more than it was for the virgin one (first use). There was a slight reduction in the amount adsorbed with cyclic regeneration with only about 5.65 % after the third regeneration cycle. Furthermore, it can be seen that perfect regeneration was achieved while using R_n as adsorbent, especially in the first two regenerations, where the average adsorption capacity increased by around 14.70 % and was more than it was for the virgin one. A reduction in the adsorption capacity was found after the third regeneration cycle, but it was still more than the adsorption capacity of the virgin one.

The regeneration ratios during the cyclic regenerations were calculated and presented in Table 28. The regeneration ratio with R_c was found to be 94.84 % after the first regeneration cycle. As the adsorption capacity of R_c after regeneration decreased, the regeneration ratio was found to be 78.26 % after the third cycle.

Table 28: Effect of number of regeneration cycles on the regeneration ratios

HTC-char	Regeneration ratio [%]		
	First cycle	Second cycle	Third cycle
R_c	94.84	83.13	78.26
R_p	100.21	97.42	94.35
R_n	117.38	117.18	100.40

The regeneration ratio with R_p was 100.21 % after the first regeneration cycle, which indicated that the adsorption performance was developed. The results showed that the regeneration ratios were maintained well over 94 % through all the three adsorption-regeneration cycles. Furthermore, all the adsorption-regeneration cycles for the exhausted adsorbent of R_n in this study led to develop its regeneration ratios, which was about 117 % in the first two cycles and 100.40 % in the third one.

Compared with the regeneration results of R_p and R_n , it could be concluded that R_c was not suitable for reuse more than three cycles in the adsorption experiments due to the decrease of its adsorption capacity by increasing the number of regeneration cycles.

As a result, HCl could efficiently regenerate exhausted adsorbents used and even after the third regeneration cycle, especially for R_p and R_n and high regeneration efficiency over 94 % could be achieved. The results submitted that the regeneration solution activated R_n , and additional active sites could be created during the regeneration process in the first two regenerations. Some authors while using other adsorbents (Zheng and Wang, 2009) also reported similar results.

The results presented the availability of the regeneration of the exhausted adsorbents and that the efficiency of regeneration could depend clearly on the type of adsorbent used. The adsorbents used were not damaged while using HCl as regeneration agent. High regeneration adsorption capacity after the first regeneration cycle could be because of the almost desorption of ammonia, but in the subsequent cycles, the ammonia was not completely desorbed. This could be an appropriate illustration of the reduction in the adsorption capacity after several cycles despite the activation of adsorbent surface while using HCl as a regeneration agent.

In general, the research hypothesis that the exhausted HTC-chars are regenerable and can be reused several times was proved. However, there was a decreasing in the adsorption performance after regeneration of some adsorbents used.

HTC-chars of reed as adsorbents are attractive because they have several advantages such as low-cost, higher yield, easy preparation and ease of regeneration. In this respect, HTC-char of reed after oxidation offers certain advantages over other adsorbents; it can be regenerated at room temperature for reuse without any loss in ammonia adsorption capacity. Undoubtedly, these tests afford a novel route for the advancement of high-performance adsorbents and extend the application of low-value biomasses in the removal of ammonia from aqueous solution.

4.2.9 Conclusion

HTC-chars produced from reed, typha, juncus and carex were used as adsorbents for the removal of ammonia in aqueous solution using a batch approach. The effect of various adsorption parameters on the adsorption performance was reported and the regeneration efficiency of exhausted adsorbents was studied using different regeneration agents.

In conclusion, the following statements can be formulated for the influence of the adsorption parameters on the adsorption performance of HTC-chars used:

- Adsorbents produced at different reaction temperatures during HTC showed different adsorption performances. The highest ones were with those produced at HTC-reaction temperature of 230 °C, especially those produced from reed.
- The type of raw material, the catalyst used during HTC or the oxidation of the HTC-chars after production affected significantly the adsorption performances.
- During the first 15 to 30 min was the adsorption of ammonia initially fast. The contact time with quite good ammonia removal was 60 min.
- Increasing the initial concentration of ammonia led to a significantly decrease in the removal efficiency rate.
- The best adsorption performance was found at solution pH with 9.35.
- After a certain adsorbent dosage (0.25 g), no significant increase was found in the adsorption capacity.
- The highest adsorption performances were found with adsorbents prepared from HTC-chars produced from reed, especially after oxidation.
- The adsorption performances in the batch study of adsorbents before and after oxidation with nitric acid were significantly affected by the variation of adsorption parameters, which supported the research hypothesis in terms of adsorption study.
- For all adsorbents used, the removal of ammonia was more corresponding to Langmuir model. The highest Langmuir maximum adsorption capacity was found with the oxidized HTC-char produced from reed.
- The exhausted HTC-char was regenerable. The best regeneration results were achieved using HCl solution as a regenerant. The highest regeneration efficiency was found with the oxidized HTC-chars, especially with those produced from reed. A decrease in the adsorption performance after regeneration was found with some adsorbents used.

4.3 Adsorption process in fixed-bed column study

4.3.1 Effect of flow rate on the adsorption performance

4.3.1.1 Individually comparison between adsorbents

The results in Table 29 showed that higher flow rates resulted in shorter breakthrough time and lower breakthrough capacity for all adsorbents used. Increasing the flow rate from 0.75 ml min^{-1} to 3.30 ml min^{-1} led to a decrease in breakthrough times (T_b) of about 80 % for adsorbents prepared from HTC-chars produced from reed and typha while using phosphoric acid as catalyst (R_p and T_p) during HTC. Moreover, the reductions were between 77.35 and 83.06 % for adsorbents prepared from HTC-char produced from reed and typha after oxidation (R_n and T_n), respectively.

On the other hand increasing the flow rate from 3.30 ml min^{-1} to 6.60 ml min^{-1} resulted in a reduction in breakthrough times of 55.82, 57.02, 47.18 and 49.60 % for each of R_p , T_p , R_n and T_n , respectively.

Table 29: Breakthrough time (T_b) and breakthrough capacity ($Q_{0.5}$) at different flow rates

Flow rate [ml min ⁻¹]	T _b (at C _t /C ₀ = 0.5) [h]				Q _{0.5} (at C _t /C ₀ = 0.5) [mg g ⁻¹]			
	R _p	T _p	R _n	T _n	R _p	T _p	R _n	T _n
0.75	23.70	23.01	104.47	32.85	7.27	6.75	25.18	7.69
3.30	4.64	4.56	17.70	7.44	6.26	5.89	18.97	7.65
6.60	2.05	1.96	9.35	3.75	5.54	5.06	18.84	7.62

An average reduction of about 13 % was found in the breakthrough capacity of R_p and T_p through the variation of the flow rates between 0.75 and 6.60 ml min^{-1} . The breakthrough capacity of R_n was only influenced by increasing the flow rates from 0.75 to 3.30 ml min^{-1} . On the other hand, there was no significant influence of the variation of the flow rates on the breakthrough capacity of T_n .

The overall removal efficiency rates of ammonia at different flow rates with time were plotted in Figure 47. The tests while using HTC-chars of reed after oxidation were stopped after 108 h and that met $C_t/C_0 \approx 0.6$. The ammonia removal remained at relatively high initial levels

The results showed that rapid adsorption of ammonia is noticed in the initial stages. It decreased thereafter and finally reached saturation. The overall removal efficiency rates of adsorbents used were slightly affected at flow rate 0.75 ml min^{-1} .

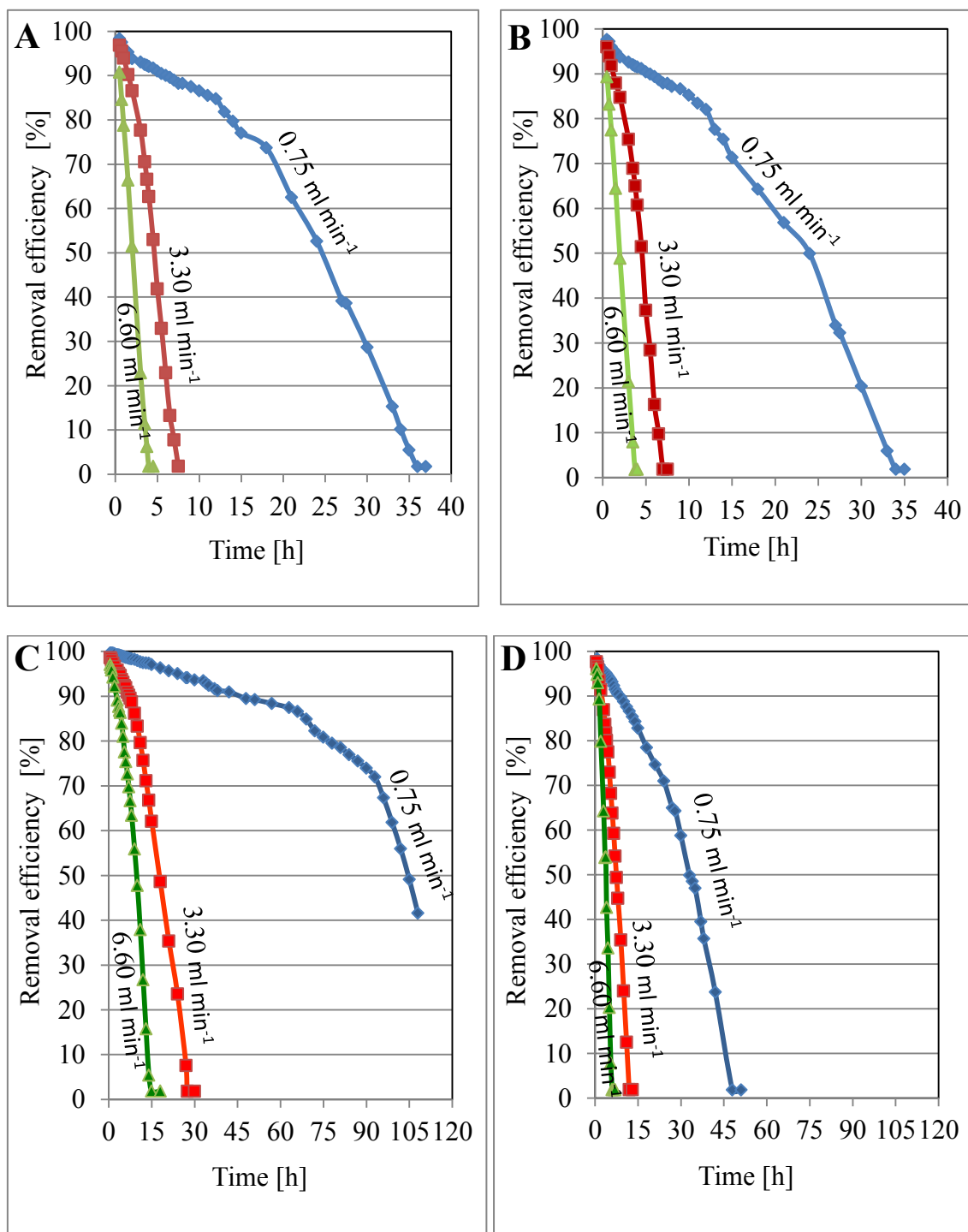


Figure 47: Effect of the flow rate on the removal efficiency of adsorbents prepared from reed (A) and typha (B) while using phosphoric acid as catalyst and from reed (C) and typha (D) after oxidation with nitric acid

It was even more than 90 % at 6 h, 5 h, 7 h and 42 h for R_p and T_p , T_n and R_n respectively. At flow rate 3.30 ml min^{-1} , the removal efficiency rate was about 85 % for R_p and T_p in the first two hours. After that, there was a sharp reduction in the removal efficiency rate, which was about 50 % at 4.50 h and lower than 10 % at 6.50 h.

T_n and R_n had better removal efficiency rates with time. They were even more than 90 % at 2 h and 7 h, respectively. The removal efficiency rates decreased rapidly after 3 h and 17 h, and was lower than 50 % at about 7.50 h and 17.70 h, respectively.

A flow rate of 6.60 ml min^{-1} had a considerable effect on the overall removal efficiency rate of all adsorbents used, which were about 90 % at 0.50 h for R_p and T_p , at 1.50 h for T_n and at about 2.50 h for R_n .

Flow rate is an important parameter for evaluating the effectiveness of adsorbents in a continuous industrial scale fixed bed operation. The higher flow rate was designed to evaluate the ammonia removal capacity of the HTC-chars in situations where the solution would pass more rapidly through the fixed-bed. The results showed that the lower flow rate resulted in better initial removal efficiency than the higher one. Increasing the flow rate led to quicker column saturation and to lower residence time in the bed indicating rapidly increment in the saturated adsorption sites over the adsorption process, this is because that at high flow rate, ammonia has lower time to be in contact with adsorbent.

The breakthrough time developed faster with a higher flow rate and the breakthrough curves became steeper. This is because that mass transfer zone is shortened and the contact time between the adsorbent and the adsorbate is minimized, which resulting in an early breakthrough, which is as an indicator for more effective intra-particle diffusion effects (Sivakumar and Palanissamy, 2009; Uddin et al., 2009).

At lower flow rates (0.75 and 3.30 ml min^{-1}), more favorable adsorption conditions were achieved, because decreasing the flow rate gives rise to longer time to saturation. These results were in agreement with the result obtained by other researchers (Nwabanne and Igbokwe, 2012; Goel et al., 2005). HTC-chars after oxidation showed an increase in the breakthrough time compared with those produced using phosphoric acid as catalyst, which supported that the oxidation of HTC-chars improved distinctly the adsorption capacity. The oxidized HTC-chars might greatly increase adsorption sites and enhance their adsorption capacity, which was confirmed by the higher breakthrough capacity and longer breakthrough time of R_n compared with the other adsorbents used.

4.3.1.2 Statistical testing of significance for the groups of adsorbents

The results of the statistical testing of significance for the effect of the variation of flow rates on the adsorption performance regarding breakthrough time (T_b), breakthrough capacity ($Q_{0.5}$) and time required for bed exhaustion (T_e) were presented in Table 30. The adsorbents used were classified in two groups, the first one included HTC-chars produced from reed and typha while using phosphoric acid as catalyst and the second group included the HTC-chars produced from reed and typha after oxidation with nitric acid. The time required for bed exhaustion at flow rate 0.75 ml min^{-1} for the second group was not available because the tests while using HTC-chars of reed after oxidation were stopped at $C_t/C_0 \approx 0.6$.

Table 30: Means and standard error (SNK method) of breakthrough time (T_b), breakthrough capacity ($Q_{0.5}$) and time required for bed exhaustion (T_e) at different flow rates

Flow rate [ml min ⁻¹]	First group (HTC-chars produced using phosphoric as catalyst acid)		
	T_b (at $C_t/C_0 = 0.5$) [h]	$Q_{0.5}$ [mg g ⁻¹]	T_e (at $C_t/C_0 = 0.9$) [h]
0.75	23.36±0.41 ^a	7.01±0.29 ^a	33.05±1.05 ^a
3.30	4.60±0.11 ^b	6.08±0.24 ^b	6.63±0.19 ^b
6.60	2.00±0.08 ^c	5.35±0.31 ^c	3.50±0.11 ^c
Flow rate [ml min ⁻¹]	Second group (HTC-chars after oxidation with nitric acid)		
	T_b (at $C_t/C_0 = 0.5$) [h]	$Q_{0.5}$ [mg g ⁻¹]	T_e (at $C_t/C_e = 0.9$) [h]
0.75	68.66±39.23 ^a	16.41±9.61 ^a	N.A.
3.30	12.57±5.62 ^b	13.20±6.11 ^a	18.83±8.35 ^a
6.60	6.55±3.07 ^b	13.76±6.67 ^a	9.31±4.29 ^b

^{a,b,c} Values with different superscripts were significantly ($P < 0.05$) different (the comparison between values only applied to the same term)

The results showed that the adsorption performance of the first group of adsorbents was significantly affected by the variation of flow rates between $0.75\text{-}6.60 \text{ ml min}^{-1}$ (Values with similar superscripts were significantly ($P < 0.05$) different).

That was not the case for the second group, in which the breakthrough time was not significantly affected by increasing the flow rate from $3.30\text{-}6.60 \text{ ml min}^{-1}$. On the other hand, the breakthrough capacity was not significantly affected by the variation of flow rates between 0.75 and 6.60 ml min^{-1} . The high standard deviations in the second group were because the oxidation with nitric acid enhanced the adsorption performance of HTC-chars produced from reed much more than those were produced from typha.

4.3.2 Effect of initial ammonia concentrations on the adsorption performance

4.3.2.1 Individually comparison between adsorbents

The variation in initial concentration had a considerable impact on the breakthrough curve as shown in Figure 48.

The different adsorbents were designated as R_N and T_N , where $N = p$ and n indicated to chars produced using phosphoric acid as catalyst and after oxidation with nitric acid, respectively

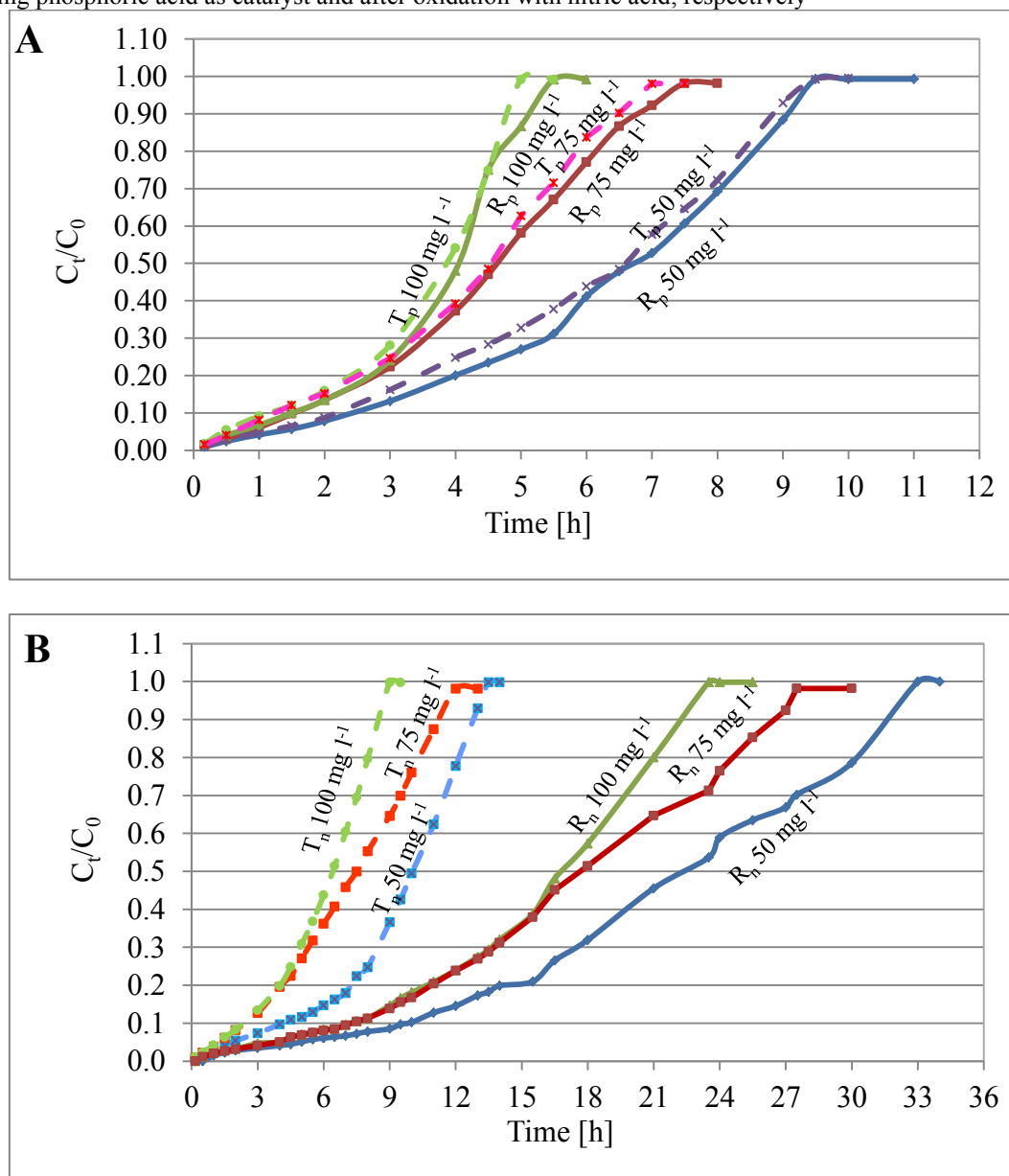


Figure 48: Effect of initial ammonia concentrations on the breakthrough curves for ammonia removal on R_p and T_p (A), R_n and T_n (B)

An increase in the initial concentration led to a shortening in the breakthrough time and therefore a rapid column saturation. A significantly reductions of 39.31, 41.64 and 37.01 % in the breakthrough time while using R_p , T_p and T_n as adsorbents were

observed as the initial concentration increased from 50 to 100 mg l⁻¹. However, it was only 24.48 % while using R_n. Breakthrough times for R_n were 22.02, 17.70 and 16.63 h at initial ammonia concentrations of 50, 75 and 100 mg l⁻¹, respectively, which were more than those of R_p, T_p and T_n.

On the other hand, there was an increase in the breakthrough capacity by increasing the initial ammonia concentration. Figure 49 shows the effect of the variation of initial ammonia concentrations on the breakthrough capacities of different adsorbents used. Increasing the initial concentration from 50 to 75 mg l⁻¹ resulted in an increase of 3.80, 4.60, 9.68 and 17.06 % in the breakthrough capacity of R_p, T_p, T_n and R_n, respectively. It was seen that increasing the initial concentration from 75 to 100 mg l⁻¹ had a higher influence on the change of the breakthrough capacity, which was increased by 13.65, 10.94, 12.13 and 20.17 % using R_p, T_p, T_n and R_n, respectively. In general, the results showed that the change of initial concentration had more effect on the adsorption capacity of R_n than it was for R_p, T_p and T_n.

The different adsorbents were designated as R_N and T_N, where N= p and n indicated to chars produced using phosphoric acid as catalyst and after oxidation with nitric acid, respectively

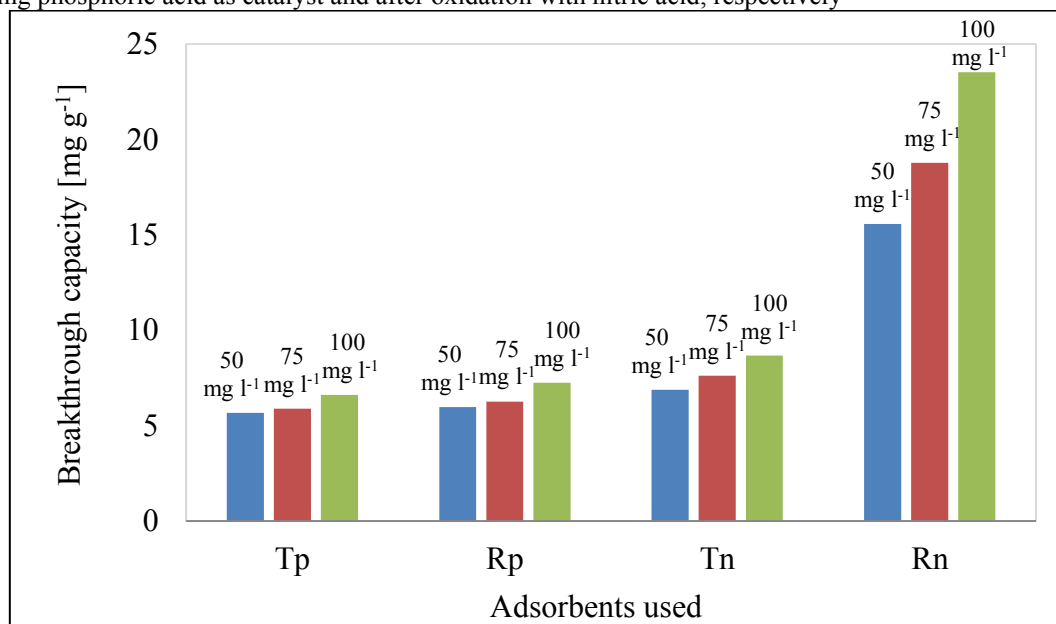


Figure 49: Breakthrough capacity at different initial ammonia concentrations

The breakthrough time decreased for all adsorbents used by increasing the initial ammonia concentration because of the lower mass-transfer rate between the aqueous bulk and the surface of solid phases due to the higher concentration gradient causing a faster transport (Sivakumar and Palanisamy, 2009; Baek et al., 2007).

At higher concentration, the availability of the ammonia for the adsorption sites is more, which leads to a higher and then rapid saturation of the adsorbent as well as higher breakthrough capacity (Han et al., 2007). Increasing the initial concentration results in an increase in ammonia loading rate, this leads to a decrease in the adsorption zone length. The net effect is an increase in the breakthrough capacity (Ko et al., 2003).

4.3.2.2 Statistical testing of significance for the groups of adsorbents

The results presented in Table 31 showed that breakthrough times and times required for bed exhaustion of the first group of adsorbents were significantly affected by the variation of initial ammonia concentrations (Values with similar superscripts were significantly ($P < 0.05$) different). On the other hand, the breakthrough capacities were not significantly affected while increasing the initial ammonia concentration from 50 to 75 mg l⁻¹.

Table 31: Means and standard error (SNK method) of breakthrough time (T_b), breakthrough capacity ($Q_{0.5}$) and time required for bed exhaustion (T_e) at different initial ammonia concentrations

Ammonia concentration [mg l ⁻¹]	First group (HTC-chars produced using phosphoric acid as catalyst acid)		
	T_b (at $C_t/C_0 = 0.5$) [h]	$Q_{0.5}$ [mg g ⁻¹]	T_e (at $C_t/C_0 = 0.9$) [h]
50	6.61±0.12 ^a	5.82±0.18 ^a	9.00±0.21 ^a
75	4.60±0.11 ^b	6.08±0.24 ^a	6.63±0.19 ^b
100	3.94±0.15 ^c	6.94±0.40 ^b	4.95±0.23 ^c
Ammonia concentration [mg l ⁻¹]	Second group (HTC-chars after oxidation with nitric acid)		
	T_b (at $C_t/C_0 = 0.5$) [h]	$Q_{0.5}$ [mg g ⁻¹]	T_e (at $C_t/C_0 = 0.9$) [h]
50	16.05±6.54 ^a	11.22±4.75 ^a	22.18±10.25 ^a
75	12.57±5.62 ^a	13.20±6.11 ^a	18.83±8.35 ^a
100	11.49±5.63 ^a	16.10±8.14 ^a	15.30±7.51 ^a

^{a,b,c} Values with different superscripts were significantly ($P < 0.05$) different (the comparison between values only applied to the same term)

The second group showed another behavior, in which no significant change was found (with $P = 0.40$, 0.44 and 0.42 for T_b , $Q_{0.5}$ and T_e , respectively) at all initial ammonia concentrations that could be because of the high adsorption performance of the adsorbents after oxidation with nitric acid.

4.3.3 Effect of the bed height on the adsorption performance

4.3.3.1 Individually comparison between adsorbents

The results presented in Table 32 indicated that ammonia uptake increased with an increment in the bed height. There was an increase of about 48.10, 45.65, 32.31 and 39.56 % in the breakthrough time by the increment of the bed height between 20-30 cm while using R_p , T_p , R_n and T_n , respectively.

Table 32: Predicted breakthrough times (T_b), breakthrough capacity ($Q_{0.5}$) and time required for bed exhaustion (T_e) for adsorbents used with different bed heights

Adsorbent	Bed height [cm]	20	30	20	30	20	30
	Parameter	T_b (at $C_t/C_0 = 0.5$) [h]		$Q_{0.5}$ [mg g ⁻¹]		T_e (at $C_t/C_e = 0.9$) [h]	
R_p		4.64	8.94	6.26	8.05	6.76	11.86
T_p		4.56	8.39	5.89	7.22	6.50	11.09
R_n		17.7	26.15	18.77	18.94	26.45	35.15
T_n		7.44	12.31	7.62	8.40	11.21	16.14

The different adsorbents are designated as R_N and T_N , where $N = p$ and n indicates to chars produced using phosphoric acid as catalyst and after oxidation with nitric acid, respectively

Regarding the breakthrough capacity, there was an increase of 18.47, 22.15, 0.89 and 9.34 % while using R_p , T_p , R_n and T_n , respectively. The breakthrough capacities of oxidized samples of T_n and R_n were on average roughly 14.06 % and 55.63 % higher than the values for their untreated adsorbents. An increase of 43, 41.39, 24.75 and 30.55 % in the time required for bed exhaustion was found by the increment of the bed height from 20 to 30 cm while using R_p , T_p , R_n and T_n , respectively. It was observed that the change of the bed height had more effect on the adsorption performance while using R_p and T_p than it was while using R_n and T_n .

Furthermore, varying the bed height resulted in a change on breakthrough curves, which were more flat and the column saturation times were longer by increasing the bed height. Various researchers (Xu et al., 2013; Han et al., 2007) reported similar observation about the effect of bed height on the ammonia removal. For the higher bed, the exhaustion approached slower; hence, the adsorption performance will be developed. The oxidation of HTC-chars with nitric acid increased their adsorption performances in terms of the parameters mentioned in Table 32; therefore, they were not considerably affected by the variation of bed heights from 20 to 30 cm.

Figure 50 shows that the length of unused bed (LUB) values at each bed height were similar for all adsorbents used. There was an increase in LUB of 15.08, 18.72, 13.87 and 5.52 % by increasing of the bed height from 20 to 30 cm while using R_p , T_p , T_n and R_n , respectively. However, 21.49, 18.42, 29.44 and 22.61 % decreased the fraction equivalent length of unused bed (FLUB) by increasing the bed height from 20 to 30 cm.

The different adsorbents were designated as R_N and T_N , where $N = p$ and n indicated to chars produced using phosphoric acid as catalyst and after oxidation with nitric acid, respectively

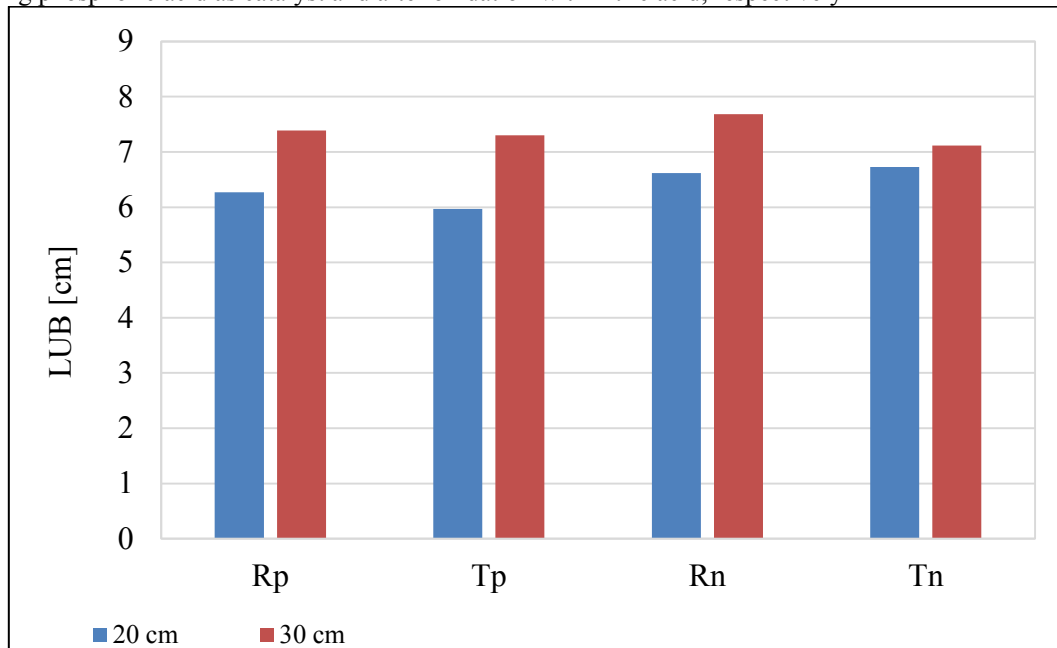


Figure 50: Effect of the bed height on the length of unused bed of adsorbents

The increase in bed height corresponds identically more amount of adsorbent in the column, which results in the availability of increasing the adsorption sites, therefore the breakthrough time and the total adsorption capacity of the adsorbent bed increase (Sivakumar and Palanisamy, 2009).

The saturation takes more time at higher bed height, which leads to the availability of operating the bed for a longer period. The adsorbate concentration at the column outlet increases more slowly than that at a smaller bed height due to the fact that the adsorbate has more time to be in contact with the adsorbent by increasing the bed heights because more adsorbent surface are exposed to flow, which results in a greater removal efficiency of ammonia and longer breakthrough time.

LUB represents the distance that is not saturated at the breakthrough time, which means that the adsorbent is not completely used. It is important to minimize the length of unused bed while designing of an adsorption column. On the other hand, the decrease of

FLUB by increasing the bed height means that increasing the bed height can make the column more efficient.

4.3.3.2 Statistical testing of significance for the groups of adsorbents

As presented in Table 33, The increase of the bed height in the range 20-30 cm had a significant effect on the breakthrough time, breakthrough capacity and time required for bed exhaustion changes while using the first group of adsorbents while the second group was not significantly affected (with $P= 0.11$, 0.89 and 0.24 for T_b , $Q_{0.5}$ and T_e , respectively). The results indicated that the lifetime of adsorbents used was enhanced with an increment in the bed height. At the same bed height, adsorbents after oxidation with nitric acid (second group) had better adsorption performance than the first group, which assured that the oxidation with nitric acid enhanced the adsorption performance. The more enhancement of the adsorption performance of adsorbent prepared from HTC-chars produced from reed after oxidation led to high standard deviations in the second group.

Table 33: Means and standard error of breakthrough time (T_b), breakthrough capacity ($Q_{0.5}$) and time required for bed exhaustion (T_e) for the effect of bed height on the adsorption performance of adsorbents

Bed height [cm]	First group (HTC-chars produced using phosphoric as catalyst acid)		
	T_b at ($C_t/C_0= 0.5$) [h]	$Q_{0.5}$ [mg g ⁻¹]	T_e (at $C_t/C_0= 0.9$) [h]
20	4.60±0.11 ^a	6.08±0.24 ^a	6.63±0.19 ^a
30	8.66±0.34 ^b	7.63±0.47 ^b	11.47±0.44 ^b
Bed height [cm]	Second group (HTC-chars after oxidation with nitric acid)		
	T_b (at $C_t/C_0= 0.5$) [h]	$Q_{0.5}$ [mg g ⁻¹]	T_e (at $C_t/C_0= 0.9$) [h]
20	12.57±5.62 ^a	13.20±6.11 ^a	18.83±8.35 ^a
30	19.23±7.58 ^a	13.67±5.77 ^a	25.65±10.41 ^a

^{a,b} Values with different superscripts were significantly ($P < 0.05$) different (the comparison between values only applied to the same term)

In general, the research hypothesis about the significantly effect of adsorption process parameters on the adsorption performances of adsorbents used in fixed bed column study, in the ranges used in this study, was proved for the adsorbents used before oxidation. That was not the case for adsorbents after oxidation.

4.3.4 Modelling of fixed-bed column breakthrough

4.3.4.1 Thomas model

Using linear regression, adsorption capacity of the column (q_0) and adsorption rate constant (K_{th}) were determined from the slope and intercept from the plot of $\ln(C_0/C_t-1)$ against t as shown in Figure 51 (A, B, C, D).

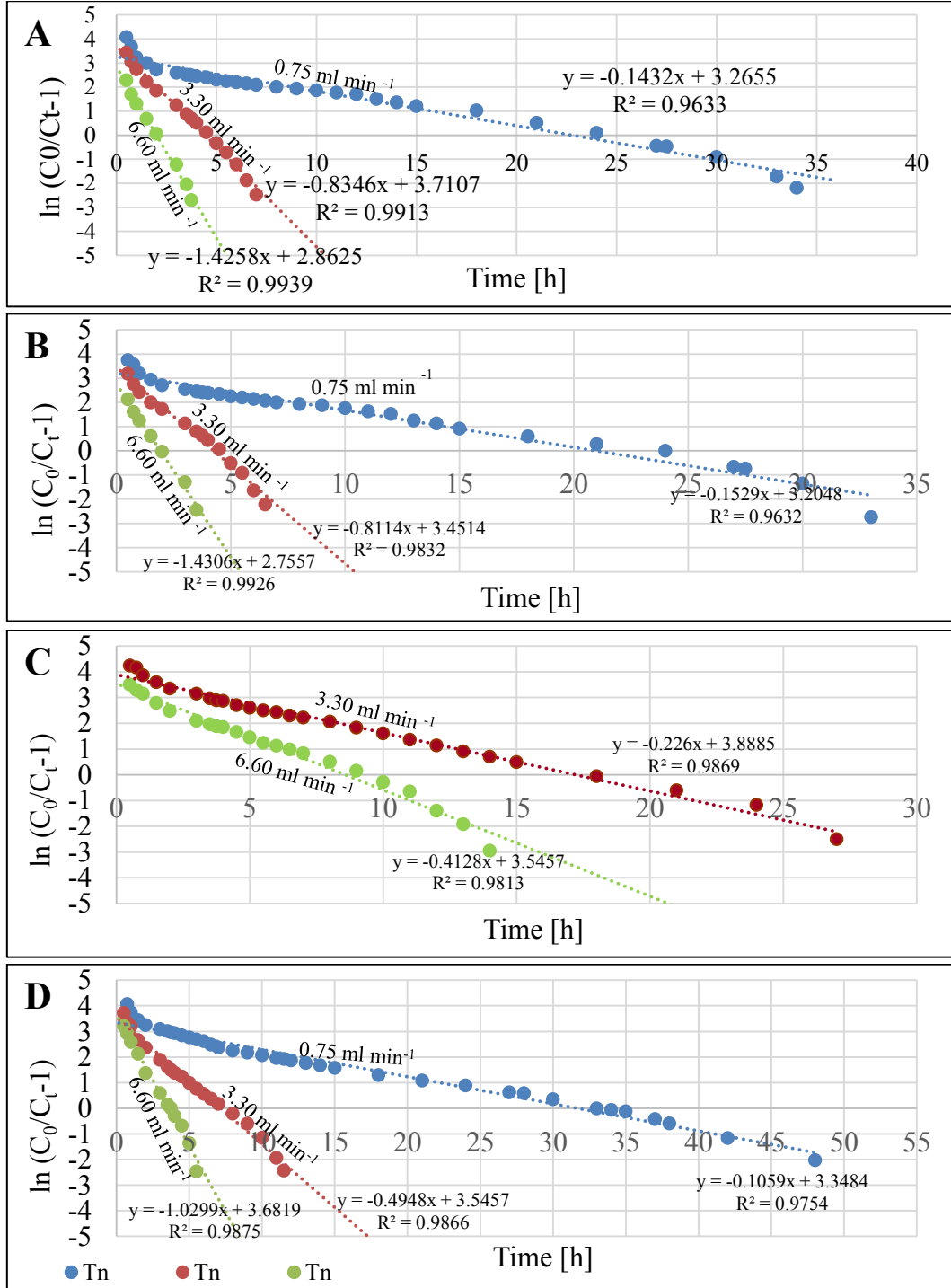


Figure 51: Thomas model at different flow rates for adsorbents produced using phosphoric acid as catalyst R_p (A) and T_p (B) and after oxidation with nitric acid R_n (C) and T_n (D)

Increase the flow rate resulted in a decrease in the adsorption capacity of the bed (q_0) of 23.95 and 19.13 % while using R_p and T_p , respectively. However, the variation of the flow rate from 0.75-6.60 ml min⁻¹ had no considerable effect, with a decrease of lower than 1 %, on the adsorption capacity of the bed while using adsorbents after oxidation. On the other hand, there was an increase in the adsorption rate (K_{th}) value by increasing the flow rate. The linear regression coefficient R^2 values under all flow rates were more than 0.9632.

The contact between the adsorbate and adsorbent was remarkably affected by the flow rate. The contact times were relatively short at higher flow rates. Hence, the adsorption processes were not complete and resulted in lower adsorption capacities. The higher regression coefficient indicating a good fit of using Thomas model.

The results of K_{th} , q_0 and R^2 by varying initial concentration of ammonia were given in Table 34. The results showed that increasing the initial ammonia concentration resulted in a decrease in the adsorption rate (lower K_{th} values) of 8.65, 16.32, 30.71 and 21.52 % while using R_p and T_p , R_n and T_n , respectively. On the other hand, there was an increase in the adsorption capacities (q_0) of 11.341, 8.01, 31.87 and 18.87 % of the same adsorbents. The linear regression coefficient R^2 values under all initial concentrations were more than 0.9582.

Table 34: Parameters predicted by Thomas model for different adsorbents at different initial concentrations of ammonia

Adsorbent	50 [mg l ⁻¹]			75 [mg l ⁻¹]			100 [mg l ⁻¹]		
	R^2	K_{th}	q_0	R^2	K_{th}	q_0	R^2	K_{th}	q_0
	[-]	[ml mg ⁻¹ min ⁻¹]	[mg g ⁻¹]	[-]	[ml mg ⁻¹ min ⁻¹]	[mg g ⁻¹]	[-]	[ml mg ⁻¹ min ⁻¹]	[mg g ⁻¹]
R_p	0.9809	0.0116	96.99	0.9913	0.0111	100.04	0.9687	0.0106	109.40
T_p	0.9741	0.0121	87.30	0.9832	0.0108	91.55	0.9634	0.0101	94.91
R_n	0.9939	0.0035	263.29	0.9869	0.0030	304.17	0.9824	0.0024	386.45
T_n	0.9582	0.0081	112.19	0.9866	0.0066	122.31	0.9840	0.0064	138.28

The different adsorbents were designated as R_N and T_N , where $N= p$ and n indicated to chars produced using phosphoric acid as catalyst and after oxidation with nitric acid, respectively

The obtained results could be explained because that the increase in the initial ammonia concentration increases the driving force and the competition between adsorbate molecules for the adsorption site (Han et al., 2007; Aksu and Gonen, 2004).

Therefore, high driving force because of the higher ammonia concentration leads to a better column performance. The results suggested that an increase in the initial concentration increased the fixed-bed adsorption capacity that was also found by other researchers (Kizito et al., 2016; Han et al., 2007).

The assumption of Thomas model is that the adsorption process follows Langmuir kinetics of adsorption–desorption. The relatively high values of R^2 suggested that the linear regression analysis of Thomas model had a good fit with the experimental data. The results obtained from fixed-bed experiments were correspond with those from batch study, in which the results illustrated that the removal of ammonia was convenient more to Langmuir model.

The results showed that HTC-chars after oxidation, especially those produced from reed had a better performance than the other HTC-chars tested, which indicated the effectively use of HTC-chars of wetland biomasses for treatment of solution contaminated with ammonia. The obtained results with modelling the continuous adsorption process can be scaled to an actual industrial fixed-bed column operation.

4.3.4.2 Yoon-Nelson model

Through plotting $\ln(C_t/(C_0-C_t))$ versus t , the rate constants (K_{YN}) and the time required for 50 % ammonia breakthrough (τ) while using different flow rates were obtained from the slope and intercept respectively. The presented results in Figure 52 (A, B, C, D) showed that an increase in the flow rate led to an increase in K_{YN} , which presented an increase in the fixed-bed adsorption rate.

However, the breakthrough time (τ) at 50 % decreased. It was noted that increasing the flow rate from 0.75 to 3.30 ml min⁻¹ resulted in an increase in K_{YN} of 82.06, 81.17, 80.74 and 78.45 % while using R_p , T_p , R_n and T_n , respectively. Furthermore, there was a decrease in the breakthrough time of 79.88, 79.70, 83.62 and 77.29 % for the adsorbent used in the same previous order.

On the other hand, increasing the flow rate from 3.30 to 6.60 ml min⁻¹ had a little effect on these parameters comparing with the effect of the variation of flow rates from 0.75 to 3.30 ml min⁻¹. There was an increase in K_{YN} of 41.46, 43.28, 48.73 and 57.95 %. The breakthrough time decreased in this case by 54.84, 54.72, 51.60 and 52.96 % while using R_p , T_p , R_n and T_n , respectively.

As presented in Figure 52, the regression coefficient (R^2) was more than 0.9143 under all used flow rates.

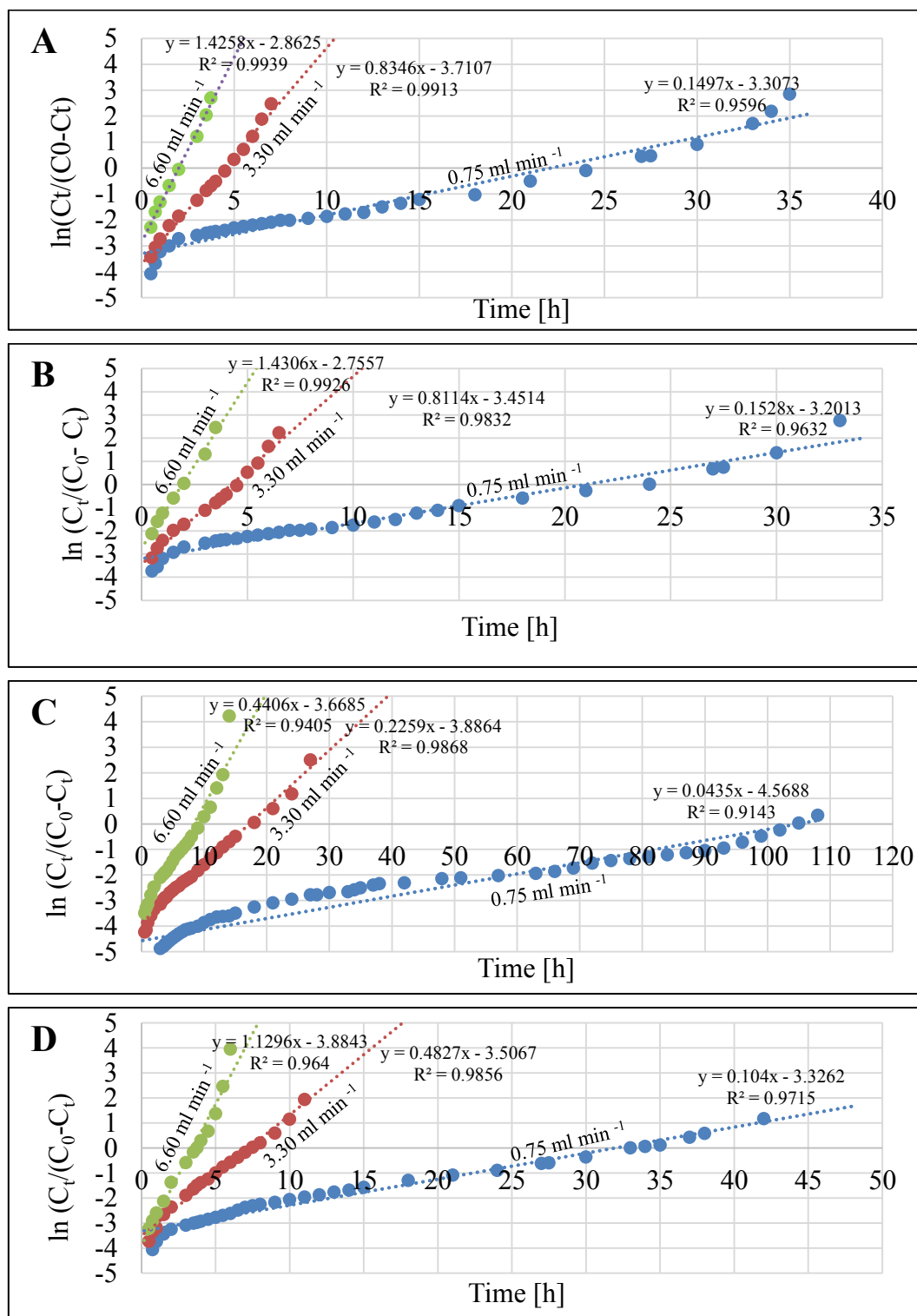


Figure 52: Yoon-Nelson model at different flow rates for adsorbents produced using phosphoric acid as catalyst R_p (A) and T_p (B) and after oxidation with nitric acid R_n (C) and T_n (D)

The results of regression coefficient (R^2) rate constants (K_{YN}) and the breakthrough times (τ) by varying initial concentration of ammonia were given in Table 35. Increasing the initial concentration led to an increase in the adsorption rate of the bed in terms of higher values of K_{YN} . It was noted that increasing the flow rate from 50 to 100 mg l^{-1} resulted in an increase in K_{YN} of 44.44, 39.76, 25.58 and 34.42 % while using R_p , T_p , R_n and T_n , respectively. Furthermore, there was a decrease in the breakthrough time of 43.93, 42.59, 26.19 and 37.55 % for the adsorbent used in the same previous order. Increasing the initial concentration developed the competition between adsorbates for the adsorption sites, which led to an increase in the uptake rate.

Table 35: Parameters predicted by Yoon-Nelson model at different initial concentrations

Adsorbent	50 [mg l^{-1}]			75 [mg l^{-1}]			100 [mg l^{-1}]		
	R^2	K_{YN}	τ	R^2	K_{YN}	τ	R^2	K_{YN}	τ
	[-]	[l min^{-1}]	[h]	[-]	[l min^{-1}]	[h]	[-]	[l min^{-1}]	[h]
R_p	0.9755	0.5888	6.503	0.9913	0.8346	4.446	0.9687	1.0597	3.647
T_p	0.9727	0.6107	6.060	0.9832	0.8114	4.254	0.9634	1.0137	3.480
R_n	0.9745	0.1860	21.801	0.9868	0.2260	17.204	0.9790	0.2500	16.093
T_n	0.9599	0.4220	9.695	0.9772	0.5010	7.311	0.9785	0.6430	6.055

The results showed that at different flow rates and initial concentration, the predicted breakthrough times (τ) from Yoon-Nelson seemed to agree well with the experimental breakthrough times in the entire fixed-bed adsorption system. In addition, the high linear regression coefficient R^2 values more than 0.9143 supported that the Yoon-Nelson model was in a good agreement with the experimental data and the results could be used in design estimation. Similar observations supported that the model proposed by Yoon-Nelson had a good correlation of the effects of flow rate and initial concentration in the experiments for the removal of lead or for biosorption of phenol by immobilized activated sludge (Nwabanne and Igbokwe, 2012; Aksu and Gönen, 2004).

In relation to the values of R^2 , Thomas and Yoon-Nelson models provided the perfect fit to the experimental data at various adsorption conditions. They can be applied to estimate the adsorption performance for the adsorption of ammonia in a fixed-bed column.

4.3.5 Column regeneration studies

The regeneration results of the exhausted adsorbent R_n , prepared by oxidizing HTC-char produced from reed with nitric acid), which had the highest adsorption capacity in fixed-bed-experiments, using 0.1 M HCl under flow rate of 4.50 ml min^{-1} , ammonia concentration 150 mg l^{-1} and adsorbent bed height of 20 cm were shown in Figure 53.

The regeneration curves for each of the first (R_{n1}), second (R_{n2}) and third (R_{n3}) regeneration cycles of the adsorbent indicated that the amount of ammonia in the effluent increased in the first 10 min up to an ammonia concentration of 2050.69, 1536.52 and 1396.96 mg l^{-1} , respectively, which was 92.69, 90.24 and 89.26 % higher than the influent ammonia concentration.

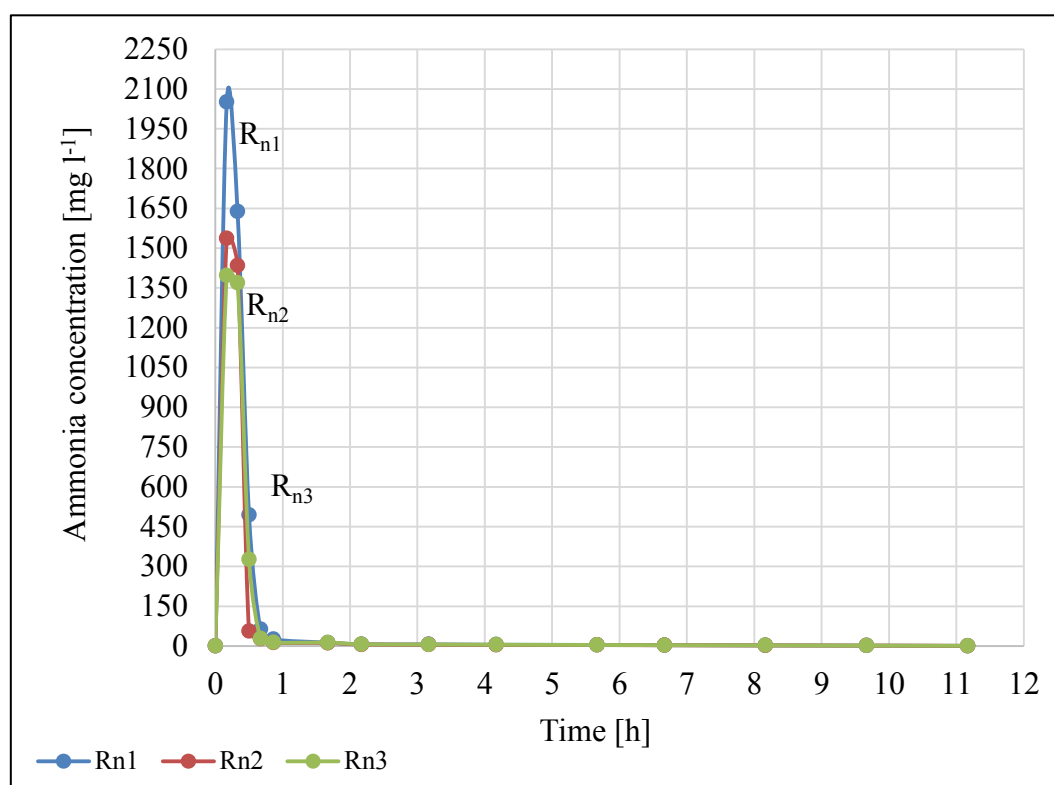


Figure 53: Profiles of three regeneration cycles of the exhausted adsorbent

This increase followed by a steep decline after 20 min and then practically becomes lower than 1 mg l^{-1} at 670 min, after which further regeneration was negligible.

The high ammonia concentration in the initial regeneration effluent led to an increase in pH value. As the regeneration process was carried, the pH would be equal to it of the regeneration effluent, which indicated that the regeneration process was completed. About three liters of the regeneration agent was sufficient for complete regeneration.

Almost complete ammonia elution was achieved and the use of 0.1 M HCl appeared to be effective. It could be concluded that HCl solution can be used repeatedly for regeneration of HTC-char. Usually, the higher the effectiveness of the regeneration is measured by the earlier and higher ammonia elution peak occurred as well as the lower volume requested of the regenerant volume for a complete elution.

After each regeneration cycle, the regenerated adsorbent was washed with bi-distilled water. Then they loaded again with ammonia concentration of 150 mg l^{-1} under the identical conditions as used before regeneration (flow rate 3.3 ml min^{-1} , bed height 20 cm) in order to check the regeneration efficiency. The adsorption conditions for each experiment were constant. The results from adsorption cycles for the regenerated adsorbents compared with the virgin one were presented in Figure 54.

The breakthrough curves obtained for all cycles were nearly identical and were compared to that of virgin adsorbent using the same adsorption parameter.

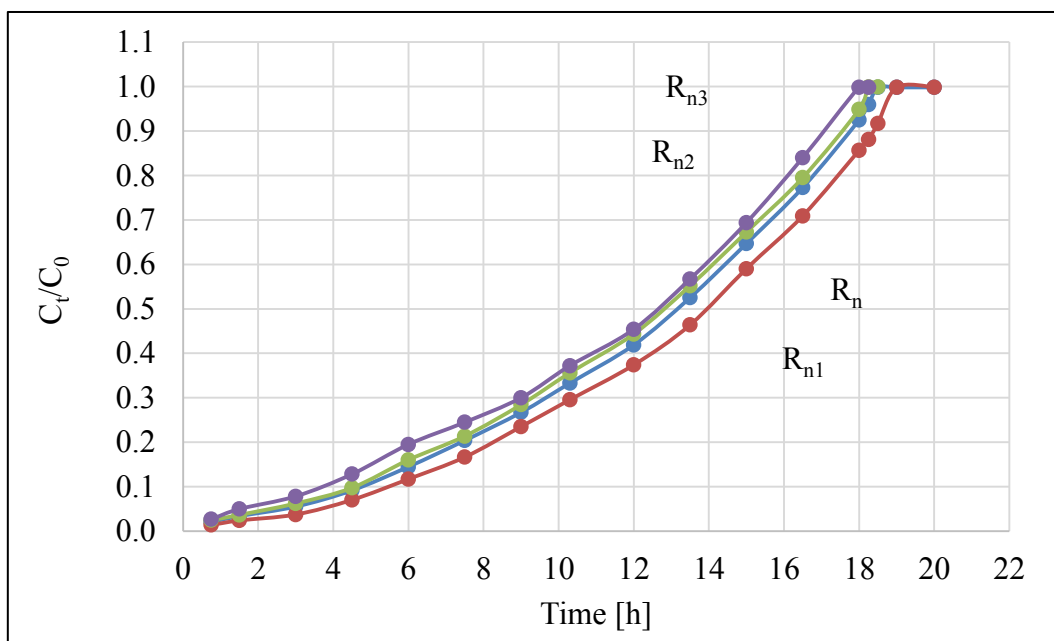


Figure 54: Breakthrough curves for ammonia adsorption using adsorbent before and after regeneration

The results showed that the efficiency of the regenerated adsorbent for the second and third regeneration cycles was a little less than it was of the virgin adsorbent.

The removal efficiency rates of adsorbents decreased a little when they were used for long period. It was mainly because fixed-bed columns were exhausted with ammonia.

Breakthrough time, adsorption capacity and exhausted times for adsorbents used before and after regeneration were presented in Table 36.

For virgin adsorbent, the breakthrough time was 13.13 h and the breakthrough capacity was 27.85 mg g⁻¹. However, they were increased with about 6 % after the first regeneration. After the second and third regenerations, the loading process was repeated and it was found that the breakthrough times and breakthrough capacities were between about 2 % and 4 % lower than the virgin adsorbent.

Adsorption-desorption cycles were carried out with a small increase by 3.48 % in the bed exhaustion time in the first cycle, which was decreased by 1.18 and 3.99 % in the second and third cycles. HCl solution probably activated the adsorbents and developed adsorption performance in the first regeneration cycle.

Table 36: Predicted time required for breakthrough times (T_b), breakthrough capacity ($Q_{0.5}$) and bed exhaustion time (T_e) for adsorbents used before and after regeneration

Adsorbent	T_b (at $C_t/C_0=0.5$) [h]	$Q_{0.5}$ [mg g ⁻¹]	T_e (at $C_t/C_0=0.9$) [h]
R_n	13.13	27.85	17.76
R_{n1}	13.92	29.53	18.4
R_{n2}	12.81	27.18	17.55
R_{n3}	12.62	26.77	17.05

A related point to consider is that no important decrease of regeneration efficiency was noticed for the first three cycles, indicating that the adsorbent has good potential to adsorb ammonia after reuse for a few times. Thus, it can be determined that the exhausted column could be efficiently regenerated by using HCl, which indicated that using HCl to regenerate exhausted adsorbents was performed efficiently and without damage to mechanical and adsorptive properties of the adsorbent used.

Regeneration is necessary for long-term efficiency and cost reduction in adsorption process. HTC-char presented a good potential to adsorb ammonia in aqueous solution and can be employed as an effective and alternative treatment technique.

4.3.6 Conclusion

Four different adsorbents with the best adsorption performances in batch study were used for the removal of ammonia in aqueous solution in fixed-bed column study.

The effects of various adsorption parameters such as flow rate, initial ammonia concentration and bed height on the adsorption performance as well as the regeneration efficiency of exhausted adsorbents using HCl solution as a regenerant were studied.

In conclusion, the following statements can be formulated for the influence of the adsorption parameters on the adsorption performance of HTC-chars used:

- Increasing the flow rate from 0.75-6.60 ml min⁻¹ led to a reduction in the breakthrough times and breakthrough capacities of the adsorbents used.
- Increasing the inlet concentration from 25-150 mg l⁻¹ led to a rapid column saturation and a reduction in the breakthrough times of the adsorbents used.
- Increasing the bed height from 20 to 30 cm led to an increase in the breakthrough capacities and the breakthrough times of the adsorbents used.
- Adsorbents prepared from HTC-chars produced from reed, especially after oxidation showed the highest adsorption performances.
- The variation of adsorption parameters in fixed-bed column had significantly effects only on the adsorbents used before oxidation. That was not the case while using adsorbents after oxidation.
- The relatively high values of correlation coefficients (R^2) suggested that the linear regression analysis of Thomas and Yoon-Nelson models had a good fit with the experimental data. Both models can be applied to estimate the adsorption performance for the adsorption of ammonia in a fixed-bed column.
- The research hypothesis related to the regeneration of the exhausted adsorbent was proved. The exhausted HTC-char was regenerable and the fixed-bed column can be reused even many times.

5 Summary and future work

5.1 Background of the work

The purpose was to develop an alternative, sustainable and competitive adsorbents synthesized from wetland biomasses using the hydrothermal carbonization process for the removal of ammonia in aqueous solution.

The existence of toxic pollutants in water is one of the most important environmental issues. Water contamination by ammonia and ammonium presents a serious pollution problem. Various technologies are available for the removal of ammonia and ammonium from water. However, high costs and associated operational and technical maintenance problems of these methods limit their application on a large industrial scale. When adsorption is considered for water treatment, commercial activated carbon is usually the chosen adsorbent. High production and regeneration costs of activated carbons restrict their applicability, so that it is requested to investigate and develop alternative effective and cheaper adsorbents synthesized from cheap natural or raw agricultural materials.

The underlying motivation of this work was a move towards using more sustainable and environmentally beneficial technologies as hydrothermal carbonization (HTC) to produce a variety of high-value carbonaceous material from widespread but little used biomasses as wetland biomasses (reed, typha, juncus and carex).

5.1.1 Hydrothermal carbonization of wetland biomasses

Hydrothermal carbonization of wetland biomasses resulted in the production of HTC-char, HTC-liquid and HTC-gas. The highest HTC-char yields were found by the carbonization of reed. The HTC-char yields from reed as well as from the other raw materials were significantly affected by the variation of all HTC-process parameters used in this study.

Depending on the process parameters, HTC-chars produced were carbon rich and chemically similar to lignite or bituminous coal. The characteristics of HTC-char varied with both raw materials used and hydrothermal carbonization parameters as well as the follow-up treatment of HTC-chars produced. Using different raw materials during HTC resulted in chars with different properties, which supported the first research hypothesis. Reaction temperatures and reaction times affected significantly the composition of HTC-chars produced. Higher reaction temperatures and longer reaction times generally

resulted in an increase in carbon proportion. On the other hand, the amount of oxygen decreased steadily and significantly indicating the elimination of this element during HTC-process; the hydrogen proportion varied only slightly with reaction severity. These results supported the research hypothesis that the reaction temperatures and times significantly affect HTC-chars properties.

The respective addition of different catalysts (citric and phosphoric acid) influenced the HTC process and should lead to an acceleration. In addition, the absorption capacity should be increased. The change of the properties of HTC-chars after oxidation with nitric acid could be because of the dissolving of the organic compounds, which led to a change in the elemental composition and the specific surface area.

However, the variation of catalyst, solid load and particle size in the ranges used in this study affected the properties of HTC-chars produced, but their effects were actually not significant and lower than those were by the variation of both reaction temperatures and reaction times.

5.1.2 Adsorption process in batch study

HTC-chars were characterized and investigated as an adsorbent for the removal of ammonia in aqueous solution using a batch approach.

HTC-chars from reed and typha had higher adsorption capacities than the commercial activated carbon samples used. Hydrothermal treatment at higher reaction temperatures improved significantly the removal efficiency rates of HTC-chars used. All adsorbents produced at reaction temperature 230 °C had the higher adsorption performances compared with those produced at lower reaction temperatures.

A quite good removal was achieved with a contact time of one hour. However, no significant change was found while increasing the contact time between 60-120 min. The variation of contact times had a more considerable effect on adsorbents before oxidation compared with those after oxidation.

Increasing the initial ammonia concentration decreased significantly the removal efficiency rates because of the limited number of adsorption sites on the adsorbent.

The variation of solution pH had a significant effect on adsorption performances while using adsorbents before oxidation with nitric acid. This effect was lower while using those oxidizing with nitric acid. The best adsorption performance was achieved at pH of solution with 9.35.

The removal efficiency rate of ammonia increased with the increase of adsorbent dosage but the adsorption capacity decreased. At a certain adsorbent dosage, the maximum adsorption was achieved.

The catalyst used during HTC-process or the oxidation of the HTC-chars after production affected their chemical structures and might create adsorption sites, which enhanced significantly their adsorption performances. The oxidized HTC-chars became more acidic and their adsorption capacities were developed.

Statistical testing of significance confirmed that the adsorption performances of adsorbents used in batch study were significantly affected by the variation of adsorption parameters. In general, this effect was lower while using those oxidizing with nitric acid. These results supported the research hypothesis that HTC-chars have a high efficiency for ammonia removal in aqueous solution and their adsorption performances are significantly affected by the adsorption process parameters.

The exhausted HTC-char was regenerable and high regeneration adsorption capacity was observed after the first regeneration cycle. A decrease in the adsorption performance after regeneration was found with some adsorbents used, which supported partly the research hypothesis related to the regeneration of the exhausted adsorbent.

5.1.3 Adsorption process in fixed-bed column study

The experiments were set up in order to test and compare four different filter materials, which had the best adsorption performances in the batch study.

A slower flow rate provided better ammonia removal efficiency and the breakthrough times increased by decreasing the flow rates. In general, lower flow rates resulted in a longer breakthrough times and times required for bed exhaustion, which increased the lifetime of the adsorbents. The variation of flow rates had a significant effect on the adsorption performances of all adsorbents used.

Furthermore, increasing initial ammonia concentrations resulted in lower breakthrough times and sharper breakthrough curves for all adsorbents used, but the breakthrough capacities were increased.

It was seen that varying the bed heights exhibited a change on breakthrough curves. The column saturation times were longer by increasing the bed heights, which enabled a longer lifetime of the column.

However, the variation of initial ammonia concentrations and the bed heights had no significant effect on adsorbents oxidizing with nitric acid.

The regeneration results showed that the ammonia removal efficiency of the regenerated adsorbent in the first adsorption cycle was better than it was while using the virgin adsorbent. A little decrease in the ammonia removal efficiency in the second and third regeneration cycles was observed, which indicated that the adsorption capacity was restored after regeneration and the fixed-bed column can be reused even many times, which supported the hypothesis related to the regeneration of the exhausted adsorbent.

The results of this work confirmed that it was possible to transform these wetland biomasses into higher value carbonaceous products with a sufficiently high efficiency for ammonia removal in aqueous solution, which could be designed as a filter.

The advantage of using HTC-char of reed as adsorbent for ammonia removal exists is not only because of its highest adsorption performance, but also of its highest char yield and its higher affinity for regeneration. In this respect, recent HTC-chars produced from wetland biomasses, especially those from reed are giving promising results in terms of regenerative ability, because it can be reused several times without a significant decreasing in its removal capacity after regeneration process. The regeneration of adsorbents extends their lifetimes and makes them ecologically and economically feasible. The potential regeneration and reuse of adsorbents used can minimize the need of raw material, which make them more sustainable for the environment and result in a less energy consumption for producing new adsorbents.

5.2 Short review of future work

This work can present the basis for the development of projects and business plans for implementations of the HTC-process as a large scale industrial HTC-plant. One of the most crucial challenges in the biochar industry is the inability to measure and characterize its quality during the carbonization process continuously, which is a key property and open an enormous potential for carbonization engineering.

Furthermore, controlling how to produce a particular quality of HTC-char for a specific application is of importance in the process engineering design, especially because the researches aim to develop new technologies. The achievement of this objective will be through a planned future project realized. The predicated method for this purpose (DE 102016125286A1) is patent-pending process. The main goal of our future works is a product with a wide range of uses, storage stability and transportable.

6 Zusammenfassung und zukünftige Arbeit

6.1 Hintergrund der Arbeit

Ziel der Arbeit war die Entwicklung alternativer, nachhaltiger und wettbewerbsfähiger Adsorbentien aus Moorbiosmassen mittels der Technik hydrothermale Karbonisierung zur Entfernung von Ammoniak in wässriger Lösung.

Das Vorhandensein toxischer Schadstoffe im Wasser ruft Umweltprobleme hervor. Die Verunreinigung von Wasser durch Ammoniak und Ammonium ist eines der ernstesten Verschmutzungsprobleme. Für die Entfernung von Ammoniak und Ammonium aus Wasser stehen verschiedene Technologien zur Verfügung. Hohe Kosten und damit verbundene Probleme begrenzen jedoch die Anwendung dieser Verfahren in einem industriellen Maßstab.

Wenn das Verfahren der Adsorption für die Wasserbehandlung in Betracht gezogen wird, ist handelsübliche Aktivkohle gewöhnlich das Adsorptionsmittel der Wahl. Hohe Herstellungs- und Regenerierungskosten von Aktivkohlen beschränken jedoch ihre Anwendbarkeit, so dass es erforderlich ist, alternative wirksame und billigere Adsorptionsmittel, die aus billigen natürlichen oder rohen landwirtschaftlichen Materialien synthetisiert werden, zu untersuchen und zu entwickeln.

Die zugrundeliegende Motivation dieser Arbeit war das Anwenden einer nachhaltigen und umweltfreundlichen Technologie, wie die hydrothermale Karbonisierung (HTC), um kohlenstoffhaltige Materialien aus weit verbreiteten, aber wenig genutzten Moorbiosmassen (Schilf, Rohrkolben, Binsen und Seggen) zu produzieren.

6.1.1 Hydrothermale Karbonisierung von Moorbiosmassen

Die hydrothermale Karbonisierung von Moorbiosmassen führte zur Produktion von HTC-Kohle, HTC-Flüssigkeit und HTC-Gas. Die höchsten HTC-Kohleausbeuten wurden durch die Karbonisierung von Schilf gefunden. Die Kohleausbeuten von Schilf wie auch von den anderen Moorbiosmassen wurden signifikant durch die Variation aller in dieser Untersuchung verwendeten HTC-Prozessparameter beeinflusst. Abhängig von den Prozessparametern waren die hergestellten HTC-Kohlen kohlenstoffreich und chemisch ähnlich wie Braunkohle oder Steinkohle.

Die Eigenschaften der HTC-Kohle variierten sowohl entsprechend der jeweilig eingesetzten Moorbiosmasse auch mit den HTC-Prozessparametern als auch entsprechend der Nachbehandlungsvariante. Die Verwendung verschiedener

Moorbiomassen zur HTC führte zu Kohlen mit unterschiedlichen Eigenschaften, was die erste Forschungshypothese bestätigt.

Reaktionstemperaturen und Reaktionszeiten beeinflussten signifikant die Zusammensetzung von HTC-Kohlen. Höhere Reaktionstemperaturen und längere Reaktionszeiten führten im Allgemeinen zu einer Erhöhung des Kohlenstoffanteils. Andererseits nahm die Menge an Sauerstoff stetig und signifikant ab, was auf die Eliminierung dieses Elements während des HTC-Prozesses hinweist; der Wasserstoffanteil variierte nur geringfügig mit den Reaktionstemperaturen und -zeiten. Diese Ergebnisse bestätigen die Forschungshypothese, dass die Eigenschaften der HTC-Kohlen durch die Reaktionstemperaturen und -zeiten signifikant beeinflusst werden.

Die jeweilige Zugabe von verschiedenen Katalysatoren (Zitronen- und Phosphorsäure) beeinflusste den HTC-Prozess und sollte zu einer Beschleunigung führen. Darüber hinaus sollte die Absorptionsleistung erhöht werden.

Die Veränderung der Eigenschaften (Verringerung des Kohlenstoffgehalts) von fertig hergestellten HTC-Kohlen nach einer Oxidation mit Salpetersäure konnte festgestellt werden. Als Grund ist anzunehmen, dass Kohlematerial aufgelöst wurde, was auch zu einer Veränderung der Elementzusammensetzung und der spezifischen Oberfläche führte.

Die Variation des Katalysators, der Feststoffbeladung und der Partikelgröße in den in dieser Untersuchung verwendeten Bereichen beeinflusste zwar die Eigenschaften der hergestellten HTC-Kohlen, aber ihre Wirkungen waren nicht signifikant und niedriger als diejenigen der Reaktionstemperaturen und Reaktionszeiten hervorgerufen wurden.

6.1.2 Adsorptionsuntersuchungen in einem Batch-Verfahrensansatz

Die HTC-Kohlen wurden als Adsorptionsmittel für die Entfernung von Ammoniak in wässriger Lösung mit einem Batch-Ansatz charakterisiert und untersucht.

HTC-Kohlen aus Schilf und Rohrkolben hatten eine höhere Adsorptionskapazität als die kommerziell vertriebenen Aktivkohleproben. Die hydrothermale Behandlung bei höheren Reaktionstemperaturen verbesserte signifikant die Entfernungseffizienzrate von verwendeten HTC-Kohlen. Alle HTC-Kohlen, die bei einer Reaktionstemperatur von 230 °C hergestellt wurden, hatten höhere Adsorptionsleistungen, verglichen mit denen, die bei niedrigeren Reaktionstemperaturen hergestellt wurden.

Eine gute Entfernung von Ammoniak wurde mit einer Kontaktzeit von einer Stunde erreicht. Es wurde jedoch keine signifikante Veränderung gefunden, wenn die

Kontaktzeit im Bereich zwischen 60-120 min erhöht wurde. Die Variationen der Kontaktzeiten hatten eine starke Wirkung auf die Adsorbentien vor der Oxidation als auf die nach der Oxidation.

Eine Erhöhung der Ausgangskonzentration von Ammoniak verringerte signifikant die Effizienz der Entfernung. Der Grund dafür kann in der begrenzten Anzahl von Adsorptionsstellen auf dem Adsorptionsmittel, der HTC-Kohle, vermutet werden.

Bei der Verwendung von Adsorptionsmitteln vor der Oxidation mit Salpetersäure, hatte die Variation von Lösungs-pH einen signifikanten Effekt auf die Adsorptionsleistung. Dieser Effekt war geringer unter Verwendung derjenigen, die mit Salpetersäure oxidierten. Die beste Adsorptionsleistung wurde bei pH 9,35 erreicht.

Die Effizienz der Entfernung von Ammoniak stieg mit der Zunahme der Adsorptionsmitteldosierung, aber die Adsorptionskapazität nahm ab. Bei einer bestimmten Adsorptionsmitteldosierung wurde die maximale Adsorption erreicht.

Der Katalysator, der während des HTC-Prozesses verwendet wurde, oder die Oxidation der HTC-Kohlen nach deren Herstellung beeinflussten ihre chemische Struktur und konnten Adsorptionsstellen erzeugen, die ihre Adsorptionsleistung signifikant verbesserten. Die mit Salpetersäure oxidierten HTC-Kohlen wurden saurer. Daraufhin konnte nachgewiesen werden, dass Ammoniak an der Kohlenoberfläche stark adsorbiert wurde.

Statistische Tests auf Signifikanz bestätigten, dass die Adsorptionsleistung von Adsorbentien signifikant durch die Variation der Adsorptionsparameter beeinflusst wurde. Im Allgemeinen war dieser Effekt geringer, wenn die mit Salpetersäure oxidierten Adsorptionsmittel (HTC-Kohlen) verwendet wurde. Diese Ergebnisse bestätigen die diese Richtung gleichlautende Forschungshypothese, dass HTC-Kohlen eine hohe Effizienz für die Ammoniakentfernung in wässriger Lösung aufweisen, und dass ihre Adsorptionsleistung signifikant durch die Parameter des Adsorptionsprozesses beeinflusst wird.

Die beladene HTC-Kohle war regenerierbar und es wurde eine hohe Regenerationsadsorptionskapazität nach dem ersten Regenerationszyklus beobachtet. Bei einigen verwendeten Adsorptionsmitteln wurde eine Abnahme der Adsorptionsleistung nach der Regeneration festgestellt, was teilweise die in diese Richtung gleichlautende Forschungshypothese.

6.1.3 Adsorptionsuntersuchungen in einem Festbett-Säulenansatz

Die Experimente wurden durchgeführt, um jene vier verschiedenen Filtermaterialien zu testen und zu vergleichen, die die besten Ammoniakentfernungskapazitäten in der Batch-Studie aufwiesen.

Eine langsamere Durchflussrate ergab eine bessere Ammoniakentfernungseffizienz und die Durchbruchzeit verlängerte sich durch das Verringern der Durchflussraten. Im Allgemeinen führte eine niedrigere Durchflussrate zu späteren Durchbruchzeiten und Zeiten, die für die Erschöpfung des Betts erforderlich war. Das erhöhte die Lebensdauer des Adsorptionsmittels. Die Variation der Durchflussraten hatte eine signifikante Wirkung auf die Adsorptionsleistung aller verwendeten Adsorptionsmittel.

Darüber hinaus führte eine Erhöhung der Ausgangskonzentration der Ammoniak zu einer früheren Durchbruchzeit aller verwendeten Adsorbentien. Die Durchbruchskapazität wurde jedoch erhöht.

Es wurde festgestellt, dass das Variieren der Betthöhe eine Veränderung der Durchbruchkurven zeigte. Die Säulensättigungszeit war später, indem die Betthöhe erhöht wurde, das ermöglichte eine längere Lebensdauer der Festbettsäule.

Die Variation der Ausgangskonzentration von Ammoniak und der Betthöhen hatte keine signifikante Wirkung auf die Adsorptionsleistung der mit der Salpetersäure oxidierten Adsorptionsmittel.

Die Ergebnisse zur Ammoniakentfernungseffizienz zeigten bei regenerierten Adsorptionsmitteln im ersten Adsorptionszyklus bessere Ergebnisse als bei neuen, noch nicht regenerierten Adsorptionsmitteln (HTC-Kohlen). Es wurde danach eine geringe Abnahme der Ammoniakentfernungseffizienz im zweiten und dritten Regenerationszyklus beobachtet. Es kann vorsichtig verallgemeinert werden, dass die Adsorptionskapazität der HTC-Kohlen nach der Regeneration wiederhergestellt wurde. Das bedeutet, dass die Festbettsäule sogar mehrfach wiederverwendet werden konnte, was die dahingehende Forschungshypothese bezüglich der Regeneration von dem beladenen Adsorptionsmittel bestätigt.

Die Ergebnisse dieser Arbeit bestätigten, dass es möglich war, Moorbioasse in kohlenstoffhaltige Produkte von höherem Wert mit einer ausreichend hohen Effizienz für die Ammoniakentfernung in wässriger Lösung umzuwandeln, um sie potenziell als Filtermaterial nutzen zu können.

Der Vorteil der Verwendung von HTC-Kohle aus Schilf als Adsorptionsmittel für die Ammoniakentfernung besteht nicht nur in seiner höchsten Adsorptionsleistung, sondern auch in seiner höchsten Kohleausbeute und seiner höheren Eignung zur Regeneration. In dieser Hinsicht liefern HTC-Kohlen, die aus Moorbiosmassen, insbesondere aus Schilf, hergestellt wurden, vielversprechende Ergebnisse in Bezug auf die Regenerationsfähigkeit, da sie mehrfach wiederverwendet werden können, ohne dass ihre Entfernungskapazität nach dem Regenerationsprozess wesentlich abnimmt. Die Regenerierung von Adsorptionsmitteln verlängert deren Lebensdauer und macht sie ökologisch und ökonomisch interessant. Die potenzielle Regeneration und Wiederverwendung von Adsorptionsmitteln kann den Bedarf an Rohmaterial minimieren, was sie für die Umwelt nachhaltiger macht und zu einem geringeren Energieverbrauch für die Herstellung neuer Adsorptionsmittel führt.

6.2 Kurzbetrachtung zu zukünftigen Arbeiten

Diese Arbeit kann die Grundlage für die Entwicklung von Projekten und Geschäftsplänen zur Umsetzung des HTC-Prozesses als großtechnische HTC-Anlage liefern. Eine der wichtigsten Herausforderungen in der Biokohle-Industrie ist die Messung von solchen Parametern, die eine permanente Abbildung der Kohlequalität während der Verkohlungs sichtbar machen. Dies wäre ein Schlüssel für die Steuerung der HTC-Prozesse und eröffnet ein enormes Potenzial für die hydrothermale Karbonisierung.

Darüber hinaus ist es für das verfahrenstechnische Design wichtig zu kontrollieren, wie eine bestimmte Qualität von HTC-Kohle für eine bestimmte Anwendung hergestellt werden kann, insbesondere, weil die Forschungen darauf abzielen, neue Technologien zu entwickeln. Die Erreichung dieses Ziels wird durch ein geplantes zukünftiges Projekt realisiert. Das zu diesem Zweck vorgeschlagene Verfahren befindet sich im Patentierungsverfahren patentiert (DE 102016125286A1).

Das Hauptziel unserer zukünftigen Arbeiten ist ein Produkt mit einer breiten Palette von Anwendungen, Lagerstabil und transportabel.

7 References

- Abdul Halim, A., Latif, M.T., Ithnin, A. (2013): Ammonia removal from aqueous solution using organic acid modified activated carbon. *World Applied Sciences Journal*, 24(1): 01-06.
- Acharjee, T.C., Coronella, C.J., Vasquez, V.R. (2011): Effect of thermal pretreatment on equilibrium moisture content of lignocellulosic biomass. *Bioresource Technology*, 102: 4849-4854.
- Afonso, C.A.M., Crespo, J.G. (2005): *Green separation processes*. Wiley VCH, 323-337.
- Ahmedna, M., Johns, M.M., Clark, S.J., Marshall, W.E., Rao, R.M. (1997): Potential of agricultural byproduct-based activated carbons for use in raw sugar decolourisation. *Journal of the Science of Food and Agriculture*, 75: 117-124.
- Ailstock, M.S., Norman, C.M., Bushmann, P.J. (2001): Common reed phragmites australis: Control and effects upon biodiversity in freshwater nontidal wetlands. *Restoration Ecology*, 9: 49-59.
- Aksu, Z., Gonen, F. (2004): Biosorption of phenol by immobilized activated sludge in a continuous packed bed: prediction of breakthrough curves. *Process Biochem*, 39: 599-613.
- Allen, A.G., Harrison, R.M., Wake, M.T. (1988): A meso-scale study of the behavior of atmospheric ammonia and ammonium. *Atmospheric Environment*, 22: 1347-1353.
- Allen, S.J., McKay, G., Porter, J.F. (2004): Adsorption isotherm models for basic dye adsorption by peat in single and binary component systems. *Journal of Colloid and Interface Science*, 280: 322-333.
- Alonso, D.M., Wettstein, S.G., Dumesic, J.A. (2012): Bimetallic catalysts for upgrading of biomass to fuels and chemicals. *Chemical Society Reviews*, 41(24): 8075-8098.
- Aneja, V.P., Chauhan, J.P., Walker T.J. (2000): Characterization of atmospheric ammonia from swine waste storage and treatment lagoons. *Journal of Geophysical Research*, 105: 11535-11545.
- Araujo-Andrade, C., Ruiz, F., Martinez-Mendoza, J.R., Terrones, H. (2005): Infrared and Raman spectra, conformational stability, ab initio calculations of structure, and vibrational assignment of alpha and beta glucose. *Journal of Molecular Structure: THEOCHEM*, 714: 143-146.
- Arogo, J., Westerman, P.W., Heber, A.J., Robarge, W.P., Classen, J.J. (2006): Ammonia emissions from animal feeding operations. In: *Animal Agriculture and the Environment: National Center for Manure and Animal Waste Management White Papers*. (p. 41-88. Edited by J. M. Rice, D. F. Caldwell, and F. J. Humenik. ASABE, St. Joseph, MI. 776 pages).
- ASTM D3172 (2013): A standard practice for proximate analysis of coal and coke according to American Society for Testing and Materials (ASTM) established procedures.

- Atia, A., Haugen-Kozyra, K., Amrani, M. (2004): Ammonia and hydrogen sulfide emissions from livestock production. Alberta Agriculture, Food and Rural Development.
- ATSDR (Agency for Toxic Substances and Disease Registry) (1990): Toxicological profile of ammonia. NITS order number PB/91/180315/AS.CDC. Atlanta, Ga. USA.
- ATSDR (2004): Toxicological profile for ammonia (Update). Atlanta, GA: Public Health Service.
- Aydincak, K., Yumak, T., Sinag, A., Esen, B. (2012): Synthesis and characterization of carbonaceous materials from saccharides (glucose and lactose) and two waste biomasses by hydrothermal carbonization. *Industrial and Engineering Chemistry Research*, 51: 9145-9152.
- Baek, K., Song, S., Kang, S., Rhee, Y., Lee, C., Lee, B., Hudson, S., Hwang, T. (2007): Adsorption kinetics of boron by anion exchange resin in packed column bed. *Journal of Industrial and Engineering Chemistry*, 13(3): 452-456.
- Balat, M., Balat, M., Kırtay, E., Balat, H. (2009): Main routes for the thermo-conversion of biomass into fuels and chemicals. Part 1: Pyrolysis systems. *Energy Conversion and Management*, 50: 3147-3157.
- Balci, S., Dince, Y. (2002): Ammonium ion adsorption with sepiolite: Use of transient uptake method. *Chemical Engineering and Processing*, 41: 79-85.
- Bargmann, I., Rillig, M.C., Kruse, A., Greef, J.M., Kücke, M. (2014): Effects of hydrochar application on the dynamics of soluble nitrogen in soils and on plant availability. *Journal of Plant Nutrition and Soil Science*, 177: 48-58.
- Belderok, H.J.M. (2007): Experimental investigation and modeling of the pyrolysis of biomass. Master thesis, Eindhoven University of Technology, Eindhoven.
- Berge, N.D., Kammann, C., Ro, K., Libra, J. (2013): Environmental applications of hydrothermal carbonization technology: Biochar production, carbon sequestration, and waste conversion. In: *Sustainable carbon materials from hydrothermal processes*. John Wiley and Sons, Ltd, 295-340.
- Berge, N.D., Ro, K.S., Mao, J., Flora, J.R.V., Chappell, M.A., Bae, S. (2011): Hydrothermal carbonization of municipal waste streams. *Environmental Science and Technology*, 45: 5696-5703.
- Bergius, F. (1928): Beiträge zur Theorie der Kohleentstehung. *Naturwissenschaften*, 16: 1-10.
- Bergius, F., Specht, H. (1913): Die Anwendung hoher Drücke bei chemischen Vorgängen und eine Nachbildung des Entstehungsprozesses der Steinkohle, Wilhelm Knapp Verlag, Halle a. S.
- Bernardo, M., Lapa, N., Gonçalves, M., Mendes, B., Pinto, F., Fonseca, I., Lopes, H. (2012): Physico-chemical properties of chars obtained in the co-pyrolysis of waste mixtures. *Journal of Hazardous Materials*, 219-220: 196-202.
- Blaschek, H.P., Ezeji, T.C. (2007): Science of alternative feedstock, corn-based ethanol in Illinois and the U.S.: A report from the Department of Agricultural and Consumer Economics, University of Illinois.

- Boerjan, W., Ralph, J., Baucher, M. (2003): Lignin biosynthesis, annual review of plant biology. Flanders Interuniversity Institute for Biotechnology, Ghent University, 519-546.
- Bogucka-Kockaa, A., Fatty, M.J. (2010): Acids composition of fruits of selected Central European sedges, *Carex L.* (Cyperaceae). *Grasas y Aceites*, 61(2): 165-170.
- Boopathy, R., Karthikeyan, S., Mandal, A.B., Sekaran, G. (2013): Adsorption of ammonium ion by coconut shell activated carbon from aqueous solution: kinetic, isotherm, and thermodynamic studies. *Environmental Science and Pollution Research*, 20(1): 533-542.
- Brownsort, P.A. (2009): Biomass pyrolysis processes: Performance parameters and their influence on biochar system benefits. Master thesis, the University of Edinburg.
- Brunauer, S., Emmett, P.H., Teller, E. (1938): Adsorption of gases in multimolecular layers. *Journal of American Chemical Society*, 60: 309-319.
- Butt, H.J., Graf, K., Kappl, M. (2003): Physics and chemistry of interfaces. Wiley-VCH GmbH & Co. KGaA, Weinheim, 177-204.
- Cao, X., Ro, K.S., Chappell, M., Li, Y., Mao, J. (2011): Chemical structure of swine-manure chars with different carbonization conditions using advanced solid-state ^{13}C NMR spectroscopy. *Energy Fuels*, 25(1): 388-397.
- Castello, D., Kruse, A., Fiori, L. (2014): Supercritical water gasification of glucose/phenol mixtures as model compounds for lignocellulosic biomass. *Chemical Engineering Transactions*, 37: 193-198.
- CEFIC (1986): European Council of Chemical Manufacturers Federations. Test method for the measurement of pH.
- Cheng, C.H., Lehmann, J., Thies, J.E., Burton, S.D., Engelhard, M.H. (2006): Oxidation of black carbon by biotic and abiotic processes. *Organic Geochemistry* 2006, 37(11): 1477-1488.
- Cheremisinoff, N.P. (2002): An overview of water and wastewater treatment, handbook of water and wastewater treatment technologies. Woburn: Butterworth-Heinemann, 1-61.
- Chun, Y., Sheng, G.Y., Chiou, C.T., Xing, B.S. (2004): Compositions and sorptive properties of crop residue-derived chars. *Environmental Science and Technology*, 38: 4649-4655.
- Chung, Y.C., Lin, Y., Tseng, C.P. (2005): Removal of high concentration of NH_3 and coexistent H_2S by biological activated carbon. *Bioresource Technology*, 96(16): 1812-1820.
- Cotana, F., Cavalaglio, G., Pisello, A., Gelosia, M., Ingles, D., D'Antonio, S. (2015): Sustainable ethanol production from common reed (*phragmites australis*) through simultaneous saccharification and fermentation. *Sustainability*, 7: 12149-12163.
- Crini, G. (2006): Non-conventional low-cost adsorbents for dye removal: A review. *Bioresource Technology*, 97: 1061-1085.

- Cruz-Olivares, C., Pérez-Alonso, C., Barrera-Díaz, C., Ureña-Nuñez, F., Chaparro-Mercado, M., Bilyeu, B. (2013): Modeling of lead (II) biosorption by residue of allspice in a fixed-bed column. *Chemical Engineering Journal*, 228: 12-27.
- Dahlgren, R.M.T., Clifford, H.T., Yeo, P.F. (1985): *The families of the monocotyledons, structure, evolution and taxonomy*. Berlin: Springer-Verlag.
- Dastgheib, S.A., Karanfil, T., Cheng, W. (2004): Tailoring activated carbons for enhanced removal of natural organic matter from natural waters. *Carbon N Y*, 42: 547-557.
- Davis, M.L. (2010): *Water and wastewater engineering-design principles and practice*. Michigan, USA: McGraw-Hill, 30(3): 266-267.
- Dea Marchetti, P. (2009): *Hydrothermal carbonization (HTC) of food waste-testing of a HTC prototype research unit for developing countries*. PhD thesis, the Università Degli Studi Di Pavia Facoltà Di Ingegneria.
- Demirbas, E., Kobya, M., Konukman, A.E.S. (2008): Error analysis of equilibrium studies for the almond shell activated carbon adsorption of Cr (VI) from aqueous solutions. *Journal of Hazardous Materials*, 154: 787-794.
- Dinjus, E., Kruse, A., Tröger, N. (2011): Hydrothermal carbonization-1. Influence of lignin in lignocelluloses. *Chemical Engineering and Technology*, 34(12): 2037-2043.
- DIN 51 718 (1995): *Bestimmung des Wassergehaltes und der Analysenfeuchtigkeit*. Deutsches Institut für Normung e. V. Berlin, Stand: September 1995, Beuth Verlag GmbH, Berlin.
- Du, Z., Mohr, M., Ma, X., Cheng, Y., Lin, X., Liu, Y., Zhou, W., Chen, P., Ruan, R. (2012): Hydrothermal pretreatment of microalgae for production of pyrolytic bio-oil with a low nitrogen content. *Bioresource Technology*, 120: 13-18.
- Düll, R., Kutzelnigg, H. (2011): *Taschenlexikon der Pflanzen Deutschlands und angrenzender Länder*, 7. Aufl. –Wiebelsheim.
- Erlach, B.T., Tsatsaronis, G. (2010): In upgrading of biomass by hydrothermal carbonization: Analysis of an industrial-scale plant design, ECOS 2010- 23rd International Conference on Efficiency, Cost, Optimization, simulation and environmental impact of energy systems.
- Eurich-Menden, B., Döhler, H., Grimm, E. (2003): *Abschlussbericht zum Projekt Umweltgerechte Tierhaltung: Entwicklung von Lösungsvorschlägen für die Implementierung der besten verfügbaren Techniken (BVT) in Deutschland Teil: Intensive livestock farming*, Kuratorium für Technik und Bauwesen in der Landwirtschaft. Darmstadt.
- Ezeji, T., Qureshi, N., Blaschek, H.P. (2007): Butanol production from agricultural residues: Impact of degradation products on *Clostridium beijerinckii* growth and butanol fermentation. *Biotechnology and Bioengineering*, 97: 1460-1469.
- Fiori, L., Volpe, M. (2017): Agro-waste to solid biofuel through HTC: The role of process variables on secondary char formation and hydrochar energy properties. First International Symposium on Hydrothermal Carbonization: Possibilities and limits for feedstock, processes and applications 3-4 April 2017 | Queen Mary, University of London, UK.

- Florio, G. (2014): Agronomic and environmental evaluation of perennial herbaceous plants fertilized with slurry to obtain biomass for bioenergy. PhD thesis, Sede Amministrativa: Università degli Studi di Padova.
- Freundlich, H. (1906): Über die Adsorption in Lösungen. Z. The Journal of Physical Chemistry, 57: 385-470.
- Frosch, W. (2004): Experimentelle Untersuchungen zum Einsatz von Flüssigmist-Additiven zur Emissionsminderung umweltrelevanter Gase und Verbesserung der Fließeigenschaften des Flüssigmistes. Dissertation. Martin-Luther Universität Halle-Wittenberg.
- Fuertes, A.B., Arberstain, M.C., Sevilla, M., Macia-Agullo, J.A., Fiol, S., Lopez, R.J., Smernik, R.J., Aitkenhead, W.P., Arce, F., Macias, F. (2010): Chemical and structural properties of carbonaceous products obtained by pyrolysis and hydrothermal carbonization of corn stover. Australian Journal of Soil Research, 48: 618-626.
- Funke, A. (2012): Hydrothermale Karbonisierung von Biomasse-Reaktionsmechanismen und Reaktionswärme. Dissertation, Technischen Universität Berlin, Berlin.
- Funke, A., Ziegler, F. (2011): Heat of reaction measurements for hydrothermal carbonization of biomass. Bioresource Technology, 102(16): 7595-7598.
- Funke, A., Ziegler, F. (2010): Hydrothermal carbonization of biomass: A summary and discussion of chemical mechanisms for process engineering. Society of Chemical Industry and John Wiley Sons, Ltd. Biofuels, Bioproducts and Biorefining, 4: 160-177.
- Garrote, G., Dominguez, H., Parajo, J. (1999): Hydrothermal processing of lignocellulosic materials. European Journal of Wood and Wood Products, 57(3): 191-202.
- Ghauri, M., Tahir, M., Abbas, T., Khurram, M.S. (2012): Adsorption studies for the removal of ammonia by thermally activated carbon. Science International (Lahore), 24(4): 411-414.
- Ghiaci, M., Abbaspur, A., Kia, R., Seyedeyn-Azad, F. (2004): Equilibrium isotherm studies for the sorption of benzene, toluene, and phenol onto organo-zeolites and as-synthesized MCM-41. Separation and Purification Technology, 40: 217-229.
- Glasner, C., Deerberg, G., Lyko, H. (2011): Hydrothermale Carbonisierung: Ein Überblick. Chemie Ingenieur Technik, 83: 1932-1943.
- Goering, H.K., Van Soest, P.J. (1970): Forage fiber analysis, USDA Agric. Handbook no. 379, Agricultural research service, USDA, Washington DC, 1-9.
- Goel, J., Kadirvelu, K., Rajagopal, C., Garg, V.K. (2005): Removal of lead (II) by adsorption using treated granular activated carbon: Batch and column studies. Journal of Hazardous Materials, B125: 211-220.
- Greve, T. (2016): Hydrothermale Carbonisierung von Landschaftspflegematerial Parameteranalyse und Methodenentwicklung in Richtung einer Prozessmodellierung. Dissertation. Fakultät für Mathematik und Naturwissenschaften der Carl von Ossietzky Universität Oldenburg

- Gue, J., Shengxu, W., Chen, Y., Chang, A. (2004): Adsorption of NH_3 on to activated carbon prepared from palm shells impregnated with H_2SO_4 . *Colloid and Interface Science*, 1(24): 1-6.
- Guo, J., Xu, W.S., Chen, Y.L., Lua, A.C. (2005): Adsorption of NH_3 onto activated carbon prepared from palm shells impregnated with H_2SO_4 . *Journal of Colloid and Interface Science*, 281: 285-290.
- Gupta, V.K., Sadegh, H., Yari, M., Ghoshekandi, R.S., Maazinejad, B., Chahardori, M. (2015): Removal of ammonium ions from wastewater. A short review in development of efficient methods. *Global Journal of Environmental Science and Management*, 1(2): 149-158.
- Han, R., Wang, Y., Yu, W., Zou, W., Shi, J., Liu, H. (2007): Biosorption of methylene blue from aqueous solution by rice husk in a fixed-bed column. *Journal of Hazardous Materials*, 141: 713-718.
- Harmsen, P., Huijgen, W., Bermudez, L., Bakker, R. (2010): Literature review of physical and chemical pretreatment processes for lignocellulosic biomass. Wageningen UR Food and Biobased Research, institute within the legal entity Stichting Dienst Landbouwkundig Onderzoek 2.
- Harper, L.A., Sharpe, R.R., Parkin, T.B. (2000): Gaseous nitrogen emissions from anaerobic swine lagoons: Ammonia, nitrous oxide and dinitrogen gas. *Journal of Environmental Quality*, 29: 1356-1365.
- Hartung, E. (2001): Ammoniak-Emissionen der Rinderhaltung und Minderungsmaßnahmen. In: *Emissionen der Tierhaltung Grundlagen, Wirkungen, Minderungsmaßnahmen*, Landwirtschaftsverlag Münster.
- Hashaikeh, R., Fang, Z., Butler, I.S., Hawari, J. Kozinski, J.A. (2007): Hydrothermal dissolution of willow in hot compressed water as a model for biomass conversion. In: *Fuel*, 86: 1614-1622.
- Haslam, S.M. (2010): A book of reed: (*Phragmites australis* (Cav.) Trin. ex Steudel, formerly *phragmites communis* trin.). Forrest Text, Cardigan, GB.
- Hatcher, P.G., Wenzel, K.A., Cody, G.D. (1994): The coalification reactions of vitrinite derived from coalified wood. Transformations to the rank of bituminous coal, in vitrinite reflections as a maturity parameter, P. K. Mukhopadhyay and W. G. Dow, eds., *Am. Chem. Soc. Symp. Series 570*, Am. Chem. Soc., Washington, D.C., 112-135.
- Heber, A.J., Ni, J.Q., Haymore, B.L., Duggirala, R.K., Keener, K.M. (2001): Air quality and emission measurement methodology at swine finishing buildings. *Transactions of the ASAE*, 44: 1765-1778.
- Heilmann, S.M., Davis, H.T., Jader, L.R., Lefebvre, P.A., Sadowsky, M.J., Schendel, F.J., von Keitz, M.G., Valentas, K.J. (2010): Hydrothermal carbonization of microalgae. *Biomass and Bioenergy*, 34: 875-882.
- Heilmann, S.M., Jader, L.R., Sadowsky, M.J., Schendel, F.J., von Keitz, M.G., Valentas, K.J. (2011): Hydrothermal carbonization of distiller's grains. *Biomass and Bioenergy*, 35(7): 2526-2533.

- Hillinger, H.G. (1990): Stallgebäude, Stallluft und Lüftung. Ferdinand Enke Verlag, Stuttgart.
- Hristov, A.N., Hanigan, M., Cole, A., Todd, R., McAllister, T.A., Ndegwa, P.M., Rotz, A. (2011): Review: Ammonia emissions from dairy farms and beef feedlots. *Animal Science Journal*, 91: 1-35.
- Hoekman, S.K., Broch, A., Robbins, C., Zielinska, B., Felix, L. (2013): Hydrothermal carbonization (HTC) of selected woody and herbaceous biomass feedstocks. *Biomass Conversion and Biorefinery*, 3: 113-126.
- Hoekman, S.K., Broch, A., Robbins, C. (2011): Hydrothermal carbonization (HTC) of lignocellulosic biomass. *Energy Fuels*, 25: 1802-1810.
- Hu, B., Yu, S.H., Wang, K., Liu, L., Xu, X.W. (2008): Functional carbonaceous materials from hydrothermal carbonization of biomass: An effective chemical process. *Dalton Transactions*, 40: 5414-5423.
- Hu, B., Wang, K., Wu, L., Yu, S.H., Antonietti, M., Titirici, M.M. (2010): Engineering carbon materials from the hydrothermal carbonization process of biomass. *Advanced Materials*, 22: 813-828.
- Huang, C., Li, H., Chen, C. (2008): Effect of surface acidic oxides of activated carbon on adsorption of ammonia. *Journal of Hazardous Materials*, 159: 523-527.
- Huber, G.W., Iborra, S., Corma, A. (2006): Synthesis of transportation fuels from biomass: Chemistry, catalysts, and engineering. *Chemical Reviews*, 106: 4044-4098.
- Hung, C.M., Lou, J.C., Lin, C.H. (2003): Removal of ammonia solutions used in catalytic wet oxidation processes. *Chemosphere*, 52: 989-995.
- Hwang, I.H., Aoyama, H., Matsuto, T., Nakagishi, T., Matsuo, T. (2012): Recovery of solid fuel from municipal solid waste by hydrothermal treatment. *Waste Management*, 32: 410-416.
- Ibrahim, B., Schlegel, M., Kanswohl, N. (2018): Effectiveness of biochar from hydrothermal carbonization of wetland biomass for sorption of ammonia. *Chemie Ingenieur Technik*, 90(3): 340-347.
- Ibrahim, B., Schlegel, M., Kanswohl, N. (2014): Investigation of applicability of wetland biomass for producing biochar by hydrothermal carbonization (HTC). *Landbauforschung Applied Agricultural and Forestry Research*, 2(64): 119-124.
- Ilies, P., Mavinic, D.S. (2001): The effect of decreased ambient temperature on the biological nitrification and denitrification of a high ammonia landfill leachate. *Water Research*, 35: 2065-2072.
- Jamari, S.S., Howse, J.R. (2012): The effect of the hydrothermal carbonization process on palm oil empty fruit bunch. *Biomass Bioenergy*, 47: 82-90.
- Ji, Z.Y., Yuan, J.S., Li, X.G. (2007): Removal of ammonium from wastewater using calcium form clinoptilolite. *Journal of Hazardous Materials*, 141: 483-488.
- Jorgensen, T.C., Weatherley, L.R. (2003): Ammonia removal from wastewater by ion exchange in the presence of organic contaminants. *Water Research*, 37: 1723-1728.

- Kabyemela, B.M., Adschiri, T., Malaluan, R.M., Arai, K. (1999): Glucose and fructose decomposition in subcritical and supercritical water: Detailed reaction pathway, mechanisms, and kinetics. *Industrial and Engineering Chemistry Research*, 38: 2888-2895.
- Kaczmarek-Derda, W.A., Brandsæter, L.O., Netland, J. (2014): The effect of soil moisture and soil type on growth of juncus spp. and poapratensis. NJF Seminar 471. Recent advances in IWM of perennial and annual weeds, with a special emphasis on the role of crop-weed interactions. Uppsala, Sweden.
- Kaltschmitt, M., Hartmann, H., Hofbauer, H.H. (2009): *Energie aus Biomasse: Grundlagen, Techniken und Verfahren* Springer-Verlag, Berlin, Heidelberg.
- Kaltschmitt, M., Krewitt, W., Heinz, A., Bachmann, T., Gruber, S. (2000): Endbericht Gesamtwirtschaftliche Bewertung der Energiegewinnung aus Biomasse unter Berücksichtigung externer und makroökonomischer Effekte (Externe Effekte der Biomasse). Universität Stuttgart, Institut für Energiewirtschaft und Rationelle Energieanwendung.
- Karacan, F., Ozden, U., Karacan, S. (2007): Optimization of manufacturing conditions for activated carbon from Turkish by chemical activation using response surface methodology. *Applied Thermal Engineering Journal*, 27: 1212-1218.
- Karadag, D. Koc, Y. Turan, M., Armagan, B. (2006): Removal of ammonium ion from aqueous solution using natural Turkish clinoptilolite. *Journal of Hazardous Materials*, 136: 604-609.
- Karunarathnea, H.D.S.S., Amarasinghea, B.M.W.P.K (2013): Fixed bed adsorption column studies for the removal of aqueous phenol from activated carbon prepared from sugarcane bagasse. *Energy Procedia*, 34: 83-90.
- Khan, A., De Jong, W., Jansens, P., Spliethoff, H. (2009): Biomass combustion in fluidized bed boilers: Potential problems and remedies. *Fuel processing technology*, 90(1): 21-50.
- Kim, J.S., Ha, S.Y., Nam, J.B., Choi, M.S., Yang, J.K. (2015): Evaluation of chemical pretreatment on steam exploded reed (*Phragmites australis*) for bioethanol production. 37th Symposium on Biotechnology for Fuels and Chemicals. San Diego, CA.
- Kizito, S., Wu, S., Wandera, S.M., Dong, R. (2016): Evaluation of ammonium adsorption in biochar-fixed beds for treatment of anaerobically digested swine slurry: Experimental optimization and modeling. *Science of the Total Environment*, 563-564: 1095-1104.
- Kleinert, M., Wittmann, T. (2009): Carbonization of biomass using a hydrothermal approach: State-of-the-art and recent developments, In: *Proceedings of the 17th European Biomass Conference and Exhibition* (29 June- 3 July 2009, Hamburg, Germany).
- Knezevic, D., van Swaaij, W., Kersten, S. (2010): Hydrothermal conversion of biomass. II. Conversion of wood, pyrolysis oil, and glucose in hot compressed water. *Industrial and Engineering Chemistry Research*, 49: 104-112.

- Ko, D.C.K., Porter, J.F., McKay, G. (2003): Fixed bed studies for the sorption of metal ions onto peat. *Transactions of the Institution of Chemical Engineers, Part B*, 81: 78-86.
- Kobayashi, N., Okada, N., Hirakawa, A., Sato T., Kobayashi, J., Hatano, S., Itaya, Y., Mori, S. (2010): Characteristics of solid residues obtained from hot-compressed-water treatment of woody biomass. *Industrial and Engineering Chemistry Research*, 48: 373-379.
- Koerkamp, P.W.G., Metz, J.H.M., Uenk, G.H., Phillips, V.R., Holden, M.R., Sneath, R.W., Short, J.L., White, R.P., Hartung, J., Seedorf, J., Schroder, M., Linkert, K.H., Pedersen, S., Takai, H., Johnsen, J.O., Wathes, C.M. (1998): Concentration and emission of ammonia in livestock buildings in northern Europe. *Journal of Agricultural Engineering Research*, 70: 79-85.
- Kritzer, P. (2004): Corrosion in high-temperature and supercritical water and aqueous solutions: a review. *The Journal of Supercritical Fluids* 29: 1-29.
- Krause, A. (2010): Hydrothermale Carbonisierung organischer Reststoffe Machbarkeitsbetrachtung der technischen Realisierungsmöglichkeiten in der Region Kagera/Tansania. Diplomarbeit, Technische Universität Berlin.
- Krus, M., Theuerkorn, W., Grosskinsky, T. (2014): Typha cultivation in agriculture, 2nd International Conference - Water resources and wetlands. 11-13 September 2014 Tulcea (Romania); Editors: Petre Gâstescu; Włodzimierz Marszelewski; Petre Bretcan; ISSN: 2285-7923: 301-306.
- Kruse, A., Funke, A., Titirici, M. (2013): Hydrothermal conversion of biomass to fuels and energetic materials. *Current Opinion in Chemical Biology*, 17(3): 515-521.
- Kruse, A., Dinjus, E. (2007): Hot compressed water as reaction medium and reactant. Degradation reactions. *The Journal of Supercritical Fluids*, 41: 361-379.
- Kubo S. (2011): Nanostructured carbohydrate-derived carbonaceous materials. Dissertation. University of Potsdam, Potsdam, Germany.
- Kuehn, K.A., Lemke, M.J., Suberkropp, K., Wetzel, R.G. (2000): Microbial biomass and production associated with decaying leaf litter of the emergent macrophyte *Juncus effusus*. *Limnology and Oceanography*, 45(4): 862-870.
- Kumar, S., Loganathan, V.A., Gupta, R.B., Barnett, M.O. (2011): An assessment of U (VI) removal from groundwater using biochar produced from hydrothermal carbonization. *Journal of environmental management*, 92(10): 2504-2512.
- Kurvits, T., Marta, T. (1998): Agricultural NH₃ and NO_x emissions in Canada. *Environmental Pollution*, 102(SI): 187-194.
- Lalhruaitluanga, H., Jayaram, K., Prasad, M.N.V., Kumar, K. (2010): Lead (II) adsorption from aqueous solutions by raw and activated charcoals of *Melocanna baccifera* Roxburgh (bamboo) a comparative study. *Journal of Hazardous Materials*, 175: 311-318.
- Langmuir, I. (1918): Adsorption of gases on plane surfaces of glass, mica and platinum. *Journal of the American Chemical Society*, 40: 1361-1403.

- Lau, F.S., Roberts, M.J., Rue, D.M., Punwani, D.V., Wen, W.W., Johnson, P.B. (1987): Peat beneficiation by wet carbonization. *International Journal of Coal Geology*, 8: 111-121.
- Lebedynets, M., Sprinsky, M., Sakhnyuk, I., Zbytniewsky, I., Golembiewsky, R., Buszewsky, B. (2004): Adsorption of ammonium ions onto a natural zeolite: Transcarpathian clinoptilolite. *Adsorption Science and Technology*, 22(9): 731-741.
- Leger, S., Chornet, E., Overend, R.P. (1987): Characterization and quantification of changes occurring in the low-severity dewatering of peat. In: *International Journal of Coal Geology*, 8: 135-146.
- Lehmann, J., Joseph, S. (2009): *Biochar for environmental management: science and technology earthscan*. London, Sterling.
- Le Leuch, L.M., Bandosz, T.J. (2007): The role of water and surface acidity on the reactive adsorption of ammonia on modified activated carbons. *Carbon*, 45: 568-578.
- Li, C.Y., Li, W.G., Wie, L. (2012): Research on absorption of ammonia by nitric acid modified bamboo charcoal at low temperature. *Desalination and Water Treatment*, 47: 3-10.
- Li, F., Xie, Y., Shi, L. (2015): Adsorption of ammonia nitrogen in wastewater using rice husk derived biochar. *Chinese Journal of Environmental Engineering*, 9(3): 1221-1226.
- Libra, J.A., Ro, K.S., Kammann, C., Funke, A., Berge, N.D., Neubauer, Y., Titirici, M.M., Fühner, C., Bens, O., Kern, J., Emmerich, K.H. (2011): Hydrothermal carbonization of biomass residuals: A comparative review of the chemistry, processes and applications of wet and dry pyrolysis. *Biofuels*, 2: 71-106.
- Lim, B.R., Ahn, K.H., Songprasert, P., Lee, S.H., Kim, M.J. (2004): Microbial community structure in an intermittently aerated submerged membrane bioreactor treating domestic wastewater. *Desalination*, 2: 145-153.
- Limousin, G., Gaudet, J.P., Charlet, L., Szenknect, S., Barthès, V., Krimissa, M. (2007): Sorption isotherms: A review on physical bases, modeling and measurement. *Applied Geochemistry*, 22: 249-275.
- Liu, B., Giannis, A., Zhang, J., Chang, V.W.C., Wang, J.Y. (2015): Air stripping process for ammonia recovery from source-separated urine: modeling and optimization. *Journal of Chemical Technology and Biotechnology*, 90: 2208-2217.
- Liu, Y., Zhao, X., Li, J., Ma, D., Han, R. (2012): Characterization of bio-char from pyrolysis of wheat straw and its evaluation on methylene blue adsorption. *Desalination Water Treat*, 46(1-3): 115-123.
- Liu, Z., Balasubramanian, R. (2012): Hydrothermal carbonization of waste biomass for energy generation. *Procedia Environmental Sciences*, 16: 159-166.
- Liu, Z., Zhang, F.S., Wu, J. (2010): Characterization and application of chars produced from pinewood pyrolysis and hydrothermal treatment. *Fuel*, 89: 510-514.
- Long, X.L., Cheng, H., Xin, Z.L., Xiao, W.D., Li, W., Yuan, W.K. (2008): Adsorption of ammonia on activated carbon from aqueous solutions. *Environmental Progress*, 27(2): 224-233.

- Lowell, S., Shields, J.E., Thomas, M.A., Thommes, M. (2004): Characterization of porous solids and powders: Surface area, pore size and density. Kluwer Academic Publishers, the Netherlands.
- Lu, L., Namioka, T., Yoshikawa, K. (2011): Effects of hydrothermal treatment on characteristics and combustion behaviors of municipal solid wastes. *Applied Energy*, 88(11): 3659-3664.
- Lu, X., Jordan, B., Berge, N.D. (2012): Thermal conversion of municipal solid waste via hydrothermal carbonization: comparison of carbonization products to products from current waste management techniques. *Waste Management*, 32(7): 1353-1365.
- Marañón, E., Ulmanu, M., Fernandez, Y., Anger, I., Castrillon, L. (2006): Removal of ammonium from aqueous solutions with volcanic tuff. *Journal of Hazardous Materials*, 137: 1402-1409.
- McCrory, D.F., Hobbs, P.J. (2001): Additives to reduce ammonia and odour emissions from livestock waste: A review. *Journal of Environmental Quality*, 30: 345-355.
- McGinn, S.M., Janzen, H.H. (1998): Ammonia sources in agriculture and their measurements. *Canadian Journal of Soil Science*, 78: 139-148.
- McNaughton, D.J., Vet, R.J. (1996): Eulerian model evaluation field study (EMEFS): A summary of surface network measurements and data quality. *Atmospheric Environment*, 30: 227-238.
- Meda, B., Hassouna, M., Aubert, C., Robin, P., Dourmad, J.Y. (2011): Influence of rearing conditions and manure management practices on ammonia and greenhouse gas emissions from poultry houses. *World's Poultry Science Journal*, 67: 441-456.
- Medic, D., Darr, M., Shah, A., Potter, B., Zimmerman, J. (2011): Effects of torrefaction process parameters on biomass feedstock upgrading. *Fuel*, 91(1): 147-154.
- Mohan, D., Rajput, S., Singh, V.K., Steele, P.H., Charles, U., Pittman, J.r. (2011): Modeling and evaluation of chromium remediation from water using low cost bio-char, a green adsorbent. *Journal of Hazardous Materials*, 188: 319-333.
- Mohan, D., Pittman, C.U., Steele, P.H. (2006): Pyrolysis of wood/biomass for bio-oil: A Critical Review. *Energy and Fuels*, 20(3): 848-889.
- Mok, W.S.L., Antal, M.J.J., Szabo, P., Varhegyi, G., Zelei, B. (1992): Formation of charcoal from biomass in a sealed reactor. *Industrial and Engineering Chemistry Research*, 31(4): 1162-1166.
- Montgomery, D.C., Runger, G.C. (2003): Applied statistics and probability for engineers, John Wiley and Sons.
- Mudliar, S., Giri, B., Padoley, K., Satpute, D., Dixit, R., Bhatt, P., Pandey, R., Juwarkar, A., Vaidya, A. (2010): Bioreactors for treatment of VOCs and odours- A review. *Journal of Environmental Management*. 91: 1039-1054.
- Mukherjee, D.K., Sengupta, A.N., Choudhury, D.P., Sanyal, P.K., Rudra, S.R. (1996): Effect of hydrothermal treatment on caking propensity of coal. In: *Fuel*, 4: 477-482.
- Mumme, J., Eckervogt, L., Pielert, J., Diakit , M., Rupp, F., Kern, J.r. (2011): Hydrothermal carbonization of anaerobically digested maize silage. *Bioresource Technology*, 102: 9255-9260.

- Neftel, A., Blatter, A., Stadelmann, F.X. (1990): Ammoniak in der bodennahen Luftschicht von landwirtschaftlichen Produktionsbetrieben. Schlussbericht des nationalen Forschungsprogramms 14+ "Waldschäden und Luftverschmutzung in der Schweiz" Eidgenössische Forschungsanstalt für Agrikulturchemie und Umwelthygiene, Liebefeld - Bern.
- Nelson, D.A., Molton, P.M., Russell, J.A., Hallen, R.T. (1984): Application of direct thermal liquefaction for the conversion of cellulosic biomass. *Industrial and Engineering Chemistry Product Research and Development*, 23: 471-475.
- Neubarth, J., Kaltschmitt, M. (2000): Erneuerbare Energien in Österreich. Systemtechnik, Potenziale, Wirtschaftlichkeit, Umweltaspekte. Springer-Verlag, Wien, New York.
- Nwabanne, J.T., Igbokwe, P.K. (2012): Adsorption performance of packed bed column for the removal of lead (ii) using oil palm fiber. *International Journal of Applied Science and Technology*, 2(5): 106-115.
- Nguyen, M.V., Lee, B.K. (2015): Removal of dimethyl sulfide from aqueous solution using cost-effective modified chicken manure biochar produced from slow pyrolysis. *Sustainability*, 7: 15057-15072.
- Okoniewska, E., Lach, J., Kacprzak, M., Neczaj, E. (2007): The removal of manganese, iron and ammonium nitrogen on impregnated activated carbon, *Desalination*, 206: 251-258.
- Ogink, N.W., Aarnink, A.J. (2003): Managing emissions from swine facilities: Current situation of Netherlands and Europe. In proceedings of the University of Illinois Pork. Industry Conference, Champaign, USA, 285-302.
- Orem, W.H., Neuzil, S.G., Lerch, H.E., Cecil, C.B. (1996): Experimental early-stage coalification of a peat sample and a peatified wood sample from Indonesia. Conference Paper. *Organic Geochemistry*, 24(2): 111-125.
- Ostertagová, E., Ostertag, O. (2013): Methodology and application of one-way ANOVA. *American Journal of Mechanical Engineering*, 1(7): 256-261.
- Ozcimen, D., Karaosmanoglu, F. (2004): Production and characterization of bio-oil and biochar from rapeseed cake. *Renewable Energy*, 29: 779-787.
- Özbay, N., Pütün, A.E., Uzun, B.B., Pütün, E. (2001): Biocrude from biomass: pyrolysis of cottonseed cake. *Renewable Energy*, 24(3-4): 615-625.
- Padmesh, T., Sekaram, G. (2005): Batch and column studies on biosorption dyes on fresh water macro alga. *Journal of Hazardous Materials*, 125: 121-129.
- Pagans, E., Font, X., Sánchez, A. (2005): Biofiltration for ammonia removal from composting exhaust gases. *Chemical Engineering Journal*, 113: 105-110.
- Pala, M., Kantarli, I.C., Buyukisik, H.B., Yanik, J. (2014): Hydrothermal carbonization and torrefaction of grape pomace: A comparative evaluation. *Bioresource Technology*, 161: 255-262.
- Parkash, B., Velan, M. (2005): Adsorption of bismark brown dye on the activated carbons prepared from rubber wood sawdust using different activation methods. *Journal of Hazardous Materials*, 126: 63-70.

- Peng, J.H., Bi, H.T., Sokhansanj, S., Lim, J.C. (2012): A study of particle size effect on biomass torrefaction and densification. *Energy and Fuels*, 26: 3826-3839.
- Peterson, A.A., Vogel, F., Lachance, R.P., Froling, M., Michael J.A.J., Tester, J.W. (2008): Thermochemical biofuel production in hydrothermal media: A review of sub- and supercritical water technologies. *Energy and Environmental Science*, 1: 32-65.
- Plomion, C., Leprovost, G., Stokes, A. (2001): Wood formation in trees. *Plant Physiol*, 127: 1531-1523.
- Qian, H.S., Yu, S.H., Luo, L.B., Gong, J.Y., Fei, L.F., Liu, X.M. (2006): Synthesis of uniform Te@Carbon-rich composite nanocables with photoluminescence properties and carbonaceous nanofibers by the hydrothermal carbonization of glucose. *Chemistry of Materials*, 18: 2102-2108.
- Quesada-Plata, F., Ruiz-Rosas, R., Morallón, E., Cazorla-Amorós, D. (2016): Activated carbons prepared through H₃PO₄-assisted hydrothermal carbonization from biomass wastes: porous texture and electrochemical performance. *ChemPlusChem*, 81(12): 1349-1359.
- Ramke, H.G., Blöhse D., Lehmann H.L., Antonietti, M., Fettig, J. (2010): Machbarkeitsstudie zur Energiegewinnung aus organischen Siedlungsabfällen durch hydrothermale Carbonisierung, Abschlussbericht. Deutsche Bundesstiftung Umwelt, Osnabrück.
- Ramke, H.G., Blöhse, D., Lehmann, H.L., Antonietti, M., Fettig, J. (2009): Hydrothermal carbonization of organic waste, Sardinia 2009: Twelfth International Waste Management and Landfill Symposium, S. Margherita di Pula – Cagliari, Sardinia, Italy.
- Rathore, N.S., Panwar, N.L., Kurchania, A.K. (2008): Renewable energy: Theory and practices. Udaipur, India: Himanshu Publications.
- Reza, M.T., Lynam, J.G., Vasquez, V.R., Coronella, C.J. (2012): Pelletization of biochar from hydrothermally carbonized wood. *Environmental Progress and Sustainable Energy*, 31(2): 225-234.
- Reza, M.T. (2011): Hydrothermal Carbonization of Lignocellulosic Biomass. Master Thesis. University of Nevada.
- Reymond, J.P., Kolenda, F. (1999): Estimation of the point of zero charge of simple and mixed oxides by mass titration. *Powder Technology*, 103(1): 30-36.
- Rillig, M.C., Wagner, M., Salem, M., Antunes, P.M., George, C., Ramke, H.G., et al. (2010): Material derived from hydrothermal carbonization: Effects on plant growth and arbuscular mycorrhiza. *Applied Soil Ecology*, 45: 238-242.
- Rodrigues, T.O., Rousset, P.L.A. (2009): Effects of torrefaction on energy properties of *Eucalyptus grandis* wood. *Cerne*, 15: 446-452.
- Rogers M.D.S. (2003): Tissue culture and wetland establishment of the freshwater monocots *Carex*, *Juncus*, *Scirpus*, and *Typha*. *In Vitro Cellular and Developmental Biology-Plant*, 39(1): 1-5.

- Roman, S., Valente Nabais, J., Ledesma, B., González, J., Laginhas, C., Titirici, M. (2013): Production of low-cost adsorbents with tunable surface chemistry by conjunction of hydrothermal carbonization and activation processes. *Microporous and Mesoporous Materials*, 165: 127-133.
- Rousset, P., Davrieux, F., Macedoc, L., Perréd, P. (2011): Characterization of the torrefaction of beech wood using NIRS: Combined effects of temperature and duration. *Biomass and Bioenergy*, 35: 1219-1226.
- Ruyter, H.P. (1982): Coalification model. *Fuel*, 61: 1182-1187.
- Sabine L., Everitt, B.S. (2004): A handbook of statistical analyses using SPSS, Chapman and Hall/CRC Press LLC. Printed in the United States of America.
- Sadaf, S., Bhatti, H.N. (2014): Evaluation of peanut husk as a novel, low cost biosorbent for the removal of indosol orange RSN dye from aqueous solutions: Batch and fixed bed studies, *Clean Technologies and Environmental Policy*, 16: 527-544.
- Sadaka, S., Sharara, M.A., Ashworth, A., Keyser, P., Allen, F. Wright, A. (2014): Characterization of biochar from switchgrass carbonization. *Energies*, 7: 548-567.
- Sathitsuksanoh, N., Zhu, Z., Templeton, N., Rollin, J.A., Harvey, S.P., Zhang, Y.H.P. (2009): Saccharification of a potential bioenergy crop, *phragmites australis* (common reed), by lignocellulose fractionation followed by enzymatic hydrolysis at decreased cellulase loadings. *Industrial and Engineering Chemistry Research*, 48: 6441-6447.
- Sawyer, C.N., McCarty, P.L. (1978): *Chemistry for environmental engineering* (third ed.). New York. McGraw-Hill Book Co.
- Schimmelpfennig, S., Glaser, B. (2012): One-step forward toward characterization: some important material properties to distinguish biochars. *Journal of Environmental Quality*, 41: 1001-1013.
- Schneider, F., Escala, M., Supawittayayothin, K., Tippayawong, N. (2011): Characterization of biochar from hydrothermal carbonization of bamboo. *International Journal of Energy and Environment*, 2(4): 647-652.
- Schuhmacher, J.P., Huntjens, F.J., van Krevelen, D.W. (1960): Chemical structure and properties of coal XXVI – studies on artificial coalification. *Fuel*, 39: 223-234.
- Schüth, F. (2003): Endo- and exotemplating to create high-surface-area inorganic materials. *Angewandte Chemie International Edition*, 42: 3604-3622.
- Sepulveda, L., Fermamdez, K., Contreras, E., Palina, C. (2004): Adsorption of dyes using peat: Equilibrium and kinetic studies. *Environmental Technology*, 25: 987-996.
- Sevilla, M., Macia-Agullo, J.A., Fuertes, A.B. (2011): Hydrothermal carbonization of biomass as a route for the sequestration of CO₂: Chemical and structural properties of the carbonized products. *Biomass Bioenergy*, 35: 3152-3159.
- Sevilla, M., Fuertes, A.B. (2009a): The production of carbon materials by hydrothermal carbonization of cellulose. *Carbon*, 47: 2281-2289.
- Sevilla, M., Fuertes, A.B. (2009b): Chemical and structural properties of carbonaceous products obtained by hydrothermal carbonization of saccharides. *Chemistry- A European Journal*, 15: 4195-4203.

- Sharma, R.K., Wooten, J.B., Baliga, V.L., Lin, X., Geoffrey Chan, W., Hajaligol, M.R. (2004): Characterization of chars from pyrolysis of lignin. *Fuel*, 83(11-12): 1469-1482.
- Shukla, A., Zhang, Y.H., Dubey, P., Margrave, J.L., Shukla, S.S. (2002): The role of sawdust in the removal of unwanted materials from water. *Journal of Hazardous Materials*, B95: 137-152.
- Sing, K.S.W., Everett, D.H., Haul, R.A.W., Moscou, L., Pieroti, R.A., Rouquerol, I., Siemieniewska, T. (1985): Reporting physisorption data for gas-solid systems. *Pure and Applied Chemistry*, 57: 603-619.
- Sivakumar, P., Palanisamy, P.N. (2009): Adsorption studies of basic Red 29 by a non-conventional activated carbon prepared from *Euphorbia antiquorum* L. *International Journal of ChemTech Research*, 1(3): 502-510.
- Stach, E., Teichmüller, R., Teichmüller, M., Mackowsky, M.T., Taylor, G.H., Chandra, D. (1982): *Coal petrology*. third ed., Stach E. Gebrüder Bornträger, Berlin, 38-86.
- Stemann, J., Putschew, A., Ziegler, F. (2013): Hydrothermal carbonization: Process water characterization and effects of water recirculation. *Bioresource Technology*, 143: 139-146.
- Tan, I.A.W., Ahmad, A.L., Hameed, B.H. (2008): Adsorption of basic dye using activated carbon prepared from oil palm shell, batch and fixed bed studies. *Desalination*, 225(1): 13-28.
- Terzyk, A.P., Rychlicki, G., Biniak, S., Łukaszewicz, J.P. (2003): New correlations between the composition of the surface layer of carbon and its physicochemical properties exposed while paracetamol is adsorbed at different temperatures and pH. *Journal of Colloid and Interface Science*, 257(1): 13-30.
- Thommes, M., Kaneko, K., Neimark, A.V., Olivier, J.P., Rodriguez-Reinoso, F., Rouquerol, J., Sing, K.S.W. (2015): Physisorption of gases, with special reference to the evaluation of surface area and pore size distribution (IUPAC Technical Report). *Pure Appl. Chem. Pure and Applied Chemistry*. 87(9-10): 1051-1069.
- Titirici, M.M., Antonietti, M. (2010): Chemistry and materials options of sustainable carbon materials made by hydrothermal carbonization. *Chemical Society Reviews*, 39: 103-116.
- Titirici, M.M., Antonietti, M., Baccile, N. (2008): Hydrothermal carbon from biomass: A comparison of the local structure from poly- to monosaccharides and pentoses/hexoses. *Green Chemistry*, 10: 1204-1212.
- Titirici, M.M., Thomas, A., Antonietti, M. (2007a): Back in the black: Hydrothermal carbonization of plant material as an efficient chemical process to treat the CO₂ problem? *New Journal of Chemistry*, 31: 787-789.
- Titirici, M.M., Thomas, A., Yu, S.H., Muller, J.O., Antonietti, M. (2007b): A direct synthesis of mesoporous carbons with bicontinuous pore morphology from crude plant material by hydrothermal carbonization. *Chemistry of Materials*, 19: 4205-4212.

- Uchimiya, M., Wartelle, L.H., Klasson, K.T., Fortier, C.A., Lima, I.M. (2011): Influence of pyrolysis temperature on biochar property and function as a heavy metal sorbent in soil. *Journal of Agricultural and Food Chemistry*, 59: 2501-2510.
- Uddin, M.T., Rukanuzzaman, M., Khan, M.M.R., Islam, M.A. (2009): Adsorption of methylene blue from aqueous solution by jackfruit (*Artocarpusheteropyllus*) leaf powder: A fixed-bed column study. *Journal of Environmental Management*, 90: 3443-3450.
- Unur, E. (2013): Materials functional nanoporous carbons from hydrothermally treated biomass for environmental purification. *Microporous and Mesoporous Materials*, 168: 92-101.
- Van de Weerdhof, M.W. (2010): Modeling the pyrolysis process of biomass particles. Master Thesis, Eindhoven University of Technology.
- Van Krevelen, D.W. (1993): Coal, typology- physics- chemistry- constitution. Amsterdam; New York, Elsevier Science.
- Van Krevelen, D.W. (1950): Graphical-statistical method for the study of structure and reaction processes of coal. *Fuel*, 29: 269-284.
- Vassileva, P., Tzvetkova, P., Nickolov, R. (2008): Removal of ammonium ions from aqueous solutions with coal-based activated carbons modified by oxidation. *Fuel*, 88: 387-390.
- Wang, H., Huang, H., Jiang, J. (2011): The effect of metal cations on phenol adsorption by hexadecyl-trimethyl-ammoniumbromide (hdtma) modified clinoptilolite (Ct.). *Separ. Separation and Purification Technology*, 80: 658-662.
- Wang, L.H., Lin, C.I. (2008): Adsorption of chromium (III) ion from aqueous solution using rice hull ash. *Journal of the Chinese Institute of Chemical Engineers*, 39: 367-373.
- Wang, L.K., Hung, Y.T., Shammas, N.K. (2006): Handbook of Environmental Engineering, Volume 4: Advanced Physicochemical Treatment Processes. © The Humana Press Inc., Totowa, NJ. ISBN: 978-1-58829-361-9 (Print) 978-1-59745-029-4 (Online).
- Werner, A. (2003): Untersuchungen zum Adsorptionsverhalten von Salizylsäure in GEH-Festbettfiltern, Prozesswissenschaften TU Berlin, Berlin.
- WHO (1986): Environmental Health Criteria No 54: Ammonia. (IPCS International Program on Chemical Safety). 210.
- Wichtmann, W., Tanneberger, F., Wichmann, S., Joosten, H. (2010): Paludiculture is paludifuture: Climate, biodiversity and economic benefits from agriculture and forestry on rewetted wetland. *Peatlands International*, 1: 48-51.
- Wiedner, K., Naisse, C., Rumpel, C., Pozzi, A., Wieczorek, P., Glaser, B. (2013): Organic geochemistry chemical modification of biomass residues during hydrothermal carbonization- what makes the difference, temperature or feedstock? *Organic Geochemistry*, 54: 91-100.

- Wilderer, P.A., Bungartz, H.J., Lemmer, H., Wagner, M., Keller, J., Wuertz, S. (2002): Single and multi-component adsorption of cadmium and zinc using activated carbon derived from bagasse-an agricultural waste. *Water Research*, 36: 370-393.
- Wirth, B., Mumme, J. (2013): Anaerobic digestion of wastewater from hydrothermal carbonization of corn silage. *Applied Bioenergy* 1: 1-10.
- Worch, E. (2012): Adsorption technology in water treatment: Fundamentals, processes, and modeling. Germany: Walter de Gruyter & Co.
- Xiao, L.P., Shi, Z.J., Xu, F., Sun, R.C. (2012): Hydrothermal carbonization of lignocellulosic biomass: Chemical and structural properties of the carbonized products. *Bioresource Technology*, 118: 619-623.
- Xu, X., Gao, B., Tan, X., Zhang, X., Yue, Q., Wang, Y., Li, Q. (2013): Nitrate adsorption by stratified wheat straw resin in lab-scale columns. *Chemical Engineering Journal*, 226: 1-6.
- Yan, W., Kent Hoekman, S., Broch, A., Coronella, C.J. (2014): Effect of hydrothermal carbonization reaction parameters on the properties of hydrochar and pellets. *Environmental Progress and Sustainable Energy*, 33(3): 676-680.
- Yan, W., Hastings, J.T., Acharjee, T.C., Coronella, C.J., Vasquez, V.R. (2010): Mass and energy balance of wet torrefaction of lignocellulosic biomass. *Energy Fuels*, 24: 4738-4742.
- Yan, W., Acharjee, C.T., Coronella, J.C., Vásquez, R.V. (2009): Thermal pretreatment of lignocellulosic biomass. *Environmental Progress and Sustainable Energy*, 28(3): 435-440.
- Yoon, Y.H., Nelson, J.H. (1992): Breakthrough time and adsorption capacity of respirator cartridges. *American Industrial Hygiene Association Journal*, 45: 509-516.
- Yu, S.H., Cui, X., Li, L., Li, K., Yu, B., Antonietti, M., Cölfen, H. (2004): From starch to metal/carbon hybrid nanostructures: Hydrothermal metal-catalyzed carbonization. *Advanced Material*, 16(18): 1636-1641.
- Yu, Y., Lou, X., Wu, H. (2008): Some recent advances in hydrolysis of biomass in hot-compressed water and its comparisons with other hydrolysis methods. *Energy Fuels*, 22: 46-60.
- Yusof, A.M., Keat, L.K., Ibrahim, Z., Majid, Z.A., Nizam, N.A. (2010): Kinetic and equilibrium studies of the removal of ammonium ions from aqueous solution by rice husk ash-synthesized zeolite Y and powdered and granulated forms of mordenite. *Journal of Hazardous Materials*, 174: 380-385.
- Zeitz, J., Folger, H., Roßkopf, N. (2011): Moorböden in Mecklenburg-Vorpommern: Verbreitung, Zustand und Funktionen. *Telma, Beiheft*, Hannover, 4: 107-132.
- Zeng, Z., Zhang, S.D., Li, T.Q., Zhao, F.L., He, Z.L., Zhao, H.P. et al. (2013): Sorption of ammonium and phosphate from aqueous solution by biochar derived from phytoremediation plants. *Journal of Zhejiang University Science B*, 14(12): 1152-1161.

- Zeymer, M., Meisel, K., Clemens, A., Klemm M. (2017): Technical, economic, and environmental assessment of the hydrothermal carbonization of green waste. *Chemical Engineering and Technology*, 40(2): 260-269.
- Zhang, B., Shahbazi, A., Wang, L., Diallo, O., Whitmore, A. (2011): Hot-water pretreatment of cattails for extraction of cellulose. *Journal of Industrial Microbiology and Biotechnology*, 38(7): 819-824.
- Zhang, L., Xu, C., Champagne, P. (2010): Overview of recent advances in thermo-chemical conversion of biomass. *Energy Conversion and Management*, 51: 969-982.
- Zhao, Y., Zhang, B., Zhang, X., Wang, J., Liu, J., Chen, R. (2010): Preparation of highly ordered cubic NaA zeolite from halloysite mineral for adsorption of ammonium ions. *Journal of Hazardous Materials*, 178: 658-664.
- Zheng, H., Han, L., Ma, H., Zheng, Y., Zhang, H., Liu, D., Liang, S. (2008): Adsorption characteristics of ammonium ion by zeolite 13X. *Journal of Hazardous Materials*, 158: 577-584.
- Zheng, Y., Wang, A. (2009): Evaluation of ammonium removal using a chitosan-g-poly (acrylic acid)/ rectorite hydrogel composite. *Journal of Hazardous Materials*, 171: 671-677.
- Zhou, Z., Yuan, J., Hua, M. (2014): Adsorption of ammonium from aqueous solutions on environmentally friendly barbecue bamboo charcoal: characteristics and kinetic and thermodynamic studies. *Environmental Progress and Sustainable Energy*, 34(3): 655-662.
- Zürcher, F. (2004): Möglichkeiten zur Minderung der Ammoniakverluste aus der Landwirtschaft. Amt für Umweltschutz Appenzell A.Rh., 9100 Herisau.

8 Appendix

Appendix I

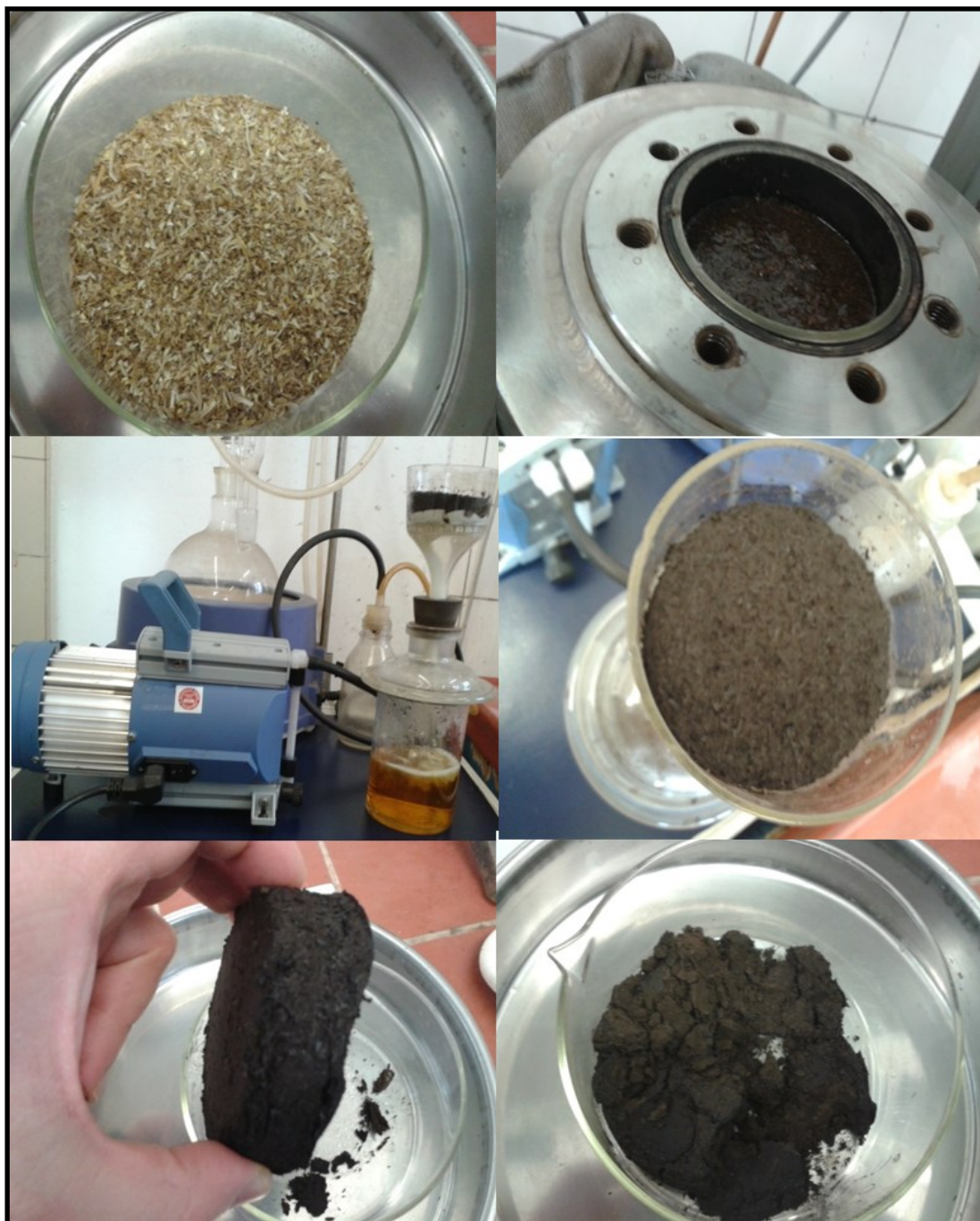
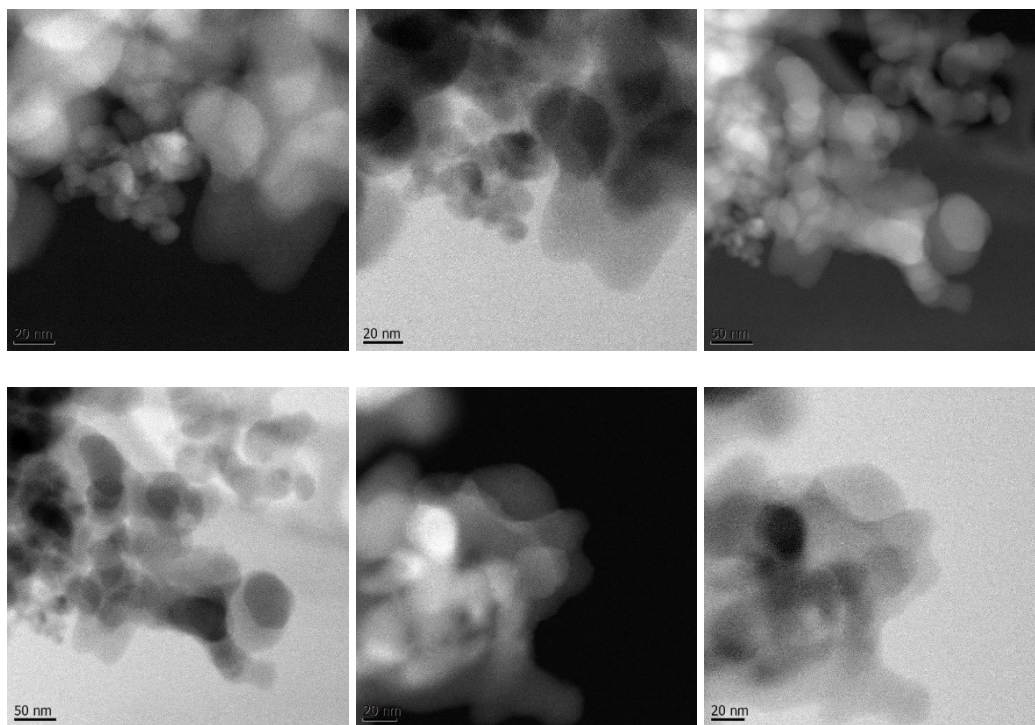


Figure I.1: From raw material to HTC-char

Appendix II

A: Reed



B: Typha

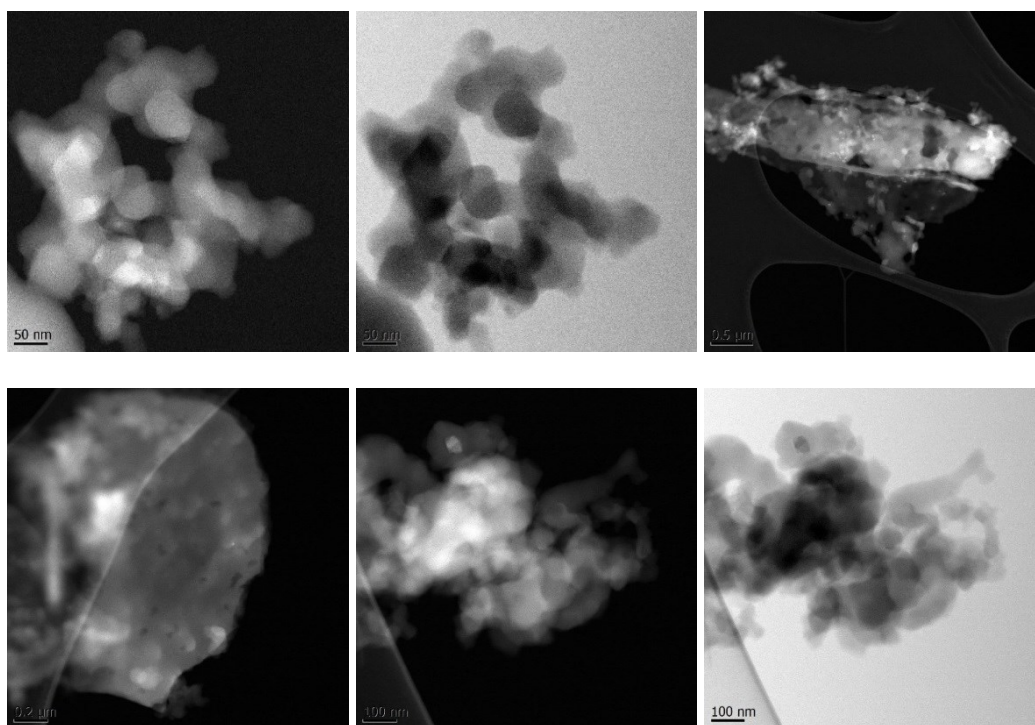


Figure II.1: Supplementary information about transmission electron microscopy (TEM) images for HTC- chars produced from reed (A) and typha (B) at 230 °C and 15 h using citric acid as catalyst

Appendix III

An example on determining of BET analysis

ASAP 2010 V4.00 C Unit 1 Serial # 602

Sample: 5, powder
File Name: C:\ASAP2010\BASSEL\004-477.SMP

Started: 31.05.12 17:32:05 Analysis Adsorptive: N₂
Completed: 31.05.12 21:31:22 Analysis Bath: 77.35 K
Report Time: 31.07.13 13:33:42 Thermal Correction: No
Sample Weight: 0.2940 g Smoothed Pressures: No
Warm Free space: 26.5000 cm³ Cold Free space: 94.0000 cm³
Equil. Interval: 10 secs Low Pressure Dose: None

Analysis Log

Relative Pressure	Pressure [mmHg]	Vol Adsorbed [cm ³ g ⁻¹ STP]	Elapsed Time [HR:MN]	Saturation Press. [mmHg]
			00:16	771.65869
0.010975612	8.46943	3.4102	00:29	
0.031165313	24.04898	4.5455	00:33	
0.108130087	83.43952	6.1828	00:37	
0.196544713	151.66544	7.1429	00:40	
0.300054197	231.53943	7.9446	00:43	
0.399525788	308.29755	8.6791	00:46	
0.499932254	385.77707	9.4792	00:49	
0.599898393	462.91681	10.4415	00:53	
0.699729080	539.95203	11.7569	00:56	
0.799248050	616.74670	13.8383	01:00	
0.895745313	691.20966	18.7438	01:06	
0.954403894	736.47406	32.8472	01:23	
0.980277953	756.44000	62.4242	01:42	
0.983692451	759.07483	77.3024	01:55	
0.988821039	763.03235	103.1612	02:17	
0.980765659	756.81635	99.3939	02:22	
0.975433794	752.70197	93.4930	02:28	
0.947784583	731.36621	48.9798	03:05	
0.899668081	694.23669	21.5682	03:25	
0.805623508	621.66638	12.8188	03:32	
0.692344198	534.25342	10.2033	03:36	
0.588482500	454.10764	9.0462	03:40	
0.502303554	387.60690	8.3811	03:43	
0.402303522	310.44101	7.7395	03:46	
0.306233062	236.30740	7.1654	03:49	
0.201626021	155.58647	6.4640	03:53	
0.100338751	77.42727	5.4696	03:59	

ASAP 2010 V4.00 C

Unit 1

Serial # 602

Sample: 5, powder
File Name: C:\ASAP2010\BASSEL\004-477.SMP

Started: 31.05.12 17:32:05 Analysis Adsorptive: N2
Completed: 31.05.12 21:31:22 Analysis Bath: 77.35 K
Report Time: 31.07.13 13:33:42 Thermal Correction: No
Sample Weight: 0.2940 g Smoothed Pressures: No
Warm Free space: 26.5000 cm³ Cold Free space: 94.0000 cm³
Equil. Interval: 10 secs Low Pressure Dose: None

BET Surface Area Report

BET Surface Area: 25.9694 ± 0.2531 m² g⁻¹
Slope: 0.165972 ± 0.001623
Y-Intercept: 0.001656 ± 0.000184
C: 101.199319
VM: 5.965584 cm³ g⁻¹ STP
Correlation Coefficient: 9.999043e-01
Molecular Cross-section: 0.1620 nm²

Relative Pressure	Vol Adsorbed [cm ³ g ⁻¹ STP]	1/ [VA*(Po/P - 1)]
0.010975612	3.4102	0.003254
0.031165313	4.5455	0.007077
0.108130087	6.1828	0.019609
0.196544713	7.1429	0.034247

ASAP 2010 V4.00 C

Unit 1

Serial # 602

Sample: 5, powder
File Name: C:\ASAP2010\BASSEL\004-477.SMP

Started: 31.05.12 17:32:05 Analysis Adsorptive: N2
Completed: 31.05.12 21:31:22 Analysis Bath: 77.35 K
Report Time: 31.07.13 13:33:42 Thermal Correction: No
Sample Weight: 0.2940 g Smoothed Pressures: No
Warm Free space: 26.5000 cm³ Cold Free space: 94.0000 cm³
Equil. Interval: 10 secs Low Pressure Dose: None

BJH Desorption Pore Distribution Report

$$t = 3.5400 \times [-5.0000 / \ln (P/P_o)] 0.3330$$

Diameter Range: 10.0000 to 1000.0000 A
 Adsorbate Property Factor: 9.530000 A
 Density Conversion Factor: 0.001547
 Fraction of Pores Open at Both Ends: 0.000

Pore Diameter Range [A]	Average Diameter [A]	Incremental Pore Volume [cm ³ g ⁻¹]	Cumulative Pore Volume [cm ³ g ⁻¹]	Incremental Pore Area [m ² g ⁻¹]	Cumulative Pore Area [m ² g ⁻¹]
1024.5- 805.8	888.7	0.009958	0.009958	0.448	0.448
805.8- 385.6	460.4	0.078513	0.088471	6.822	7.270
385.6- 204.0	241.4	0.049316	0.137787	8.172	15.442
204.0- 106.5	125.5	0.013116	0.150903	4.180	19.622
106.5- 66.8	77.1	0.001589	0.152492	0.824	20.446
66.8- 21.0	22.9	0.000006	0.152498	0.010	20.456
21.0- 16.2	17.8	0.001204	0.153701	2.708	23.164

ASAP 2010 V4.00 C Unit 1 Serial # 602
 Sample: 5, powder
 File Name: C:\ASAP2010\BASSEL\004-477.SMP

Started: 31.05.12 17:32:05 Analysis Adsorptive: N2
 Completed: 31.05.12 21:31:22 Analysis Bath: 77.35 K
 Report Time: 31.07.13 13:33:42 Thermal Correction: No
 Sample Weight: 0.2940 g Smoothed Pressures: No
 Warm Free space: 26.5000 cm³ Cold Free space: 94.0000 cm³
 Equil. Interval: 10 secs Low Pressure Dose: None

Summary Report

Area

Single Point Surface Area at P/Po 0.19654471: 24.9832 m² g⁻¹
 BET Surface Area: 25.9694 m² g⁻¹
 BJH Desorption Cumulative Surface Area of pores
 between 10.000000 and 1000.000000 A Diameter: 23.1636 m² g⁻¹

Volume

BJH Desorption Cumulative Pore Volume of pores
 between 10.000000 and 1000.000000 A Diameter: 0.153701 cm³ g⁻¹

Pore Size

BJH Desorption Average Pore Diameter (4V/A): 265.4192 A

Appendix IV

Photometric analysis methods (Scientific publishing company mbH Stuttgart)

Determination range: 0.05-2.50 µg (in 0.50 ml sample)

Detection limit: 0.02 µg (in 2.50 ml measuring solution)

Basics

Reaction:

Phenol forms an intense blue-colored indophenol complex in alkaline solution with ammonia and sodium hypochlorite. Catalysts such as Sodium nitroprussiate or manganese sulfate determine the sensitivity.

Method:

For a sample solution, a phenolate solution and a sodium hypochlorite solution are added successively and shaken using Thermo Scientific Espresso Centrifuge and Scientific Vortex Shaker Genie. The photometric measurement is carried out after 45 min at 625 nm against a blank solution.

Reference

- Gerlach A. (1980): Ein Vergleich von Methoden zur Bestimmung von Ammonium- und Nitratstickstoff in Böden: Acta Oecol. Ser. J: Oecol. Plant 1(2): 185-200.
- Reusch Berg B.; Abdullah M.J. (1977): An Automatic method for the determination of ammonia in seawater. Water Research 11: 637-638.
- Zöltzer D. (1985): Photometrische Analysenverfahren Wissenschaftliche Verlagsgesellschaft mbH. Stuttgart.

Reagents:

1. Phenol- 2. Sodium nitroprussiate 3. Sodium hypochlorite solution (5 %)- 4. Sodium hydroxide 5. Ammonia stock solution

Methods of determination:

Sample solution: 0.50 ml with 0.05-2.50 µg NH_4^+

Analytical vessel: 25 ml beaker

Reagent solutions + 1 ml phenolate solution

+ 1 ml hypochlorite solution

shake after each reagent addition

Measurement against blank test: after 45 min at 625 nm in 1cm cuvettes

Appendix V

Statistical testing of significance of HTC-experiments

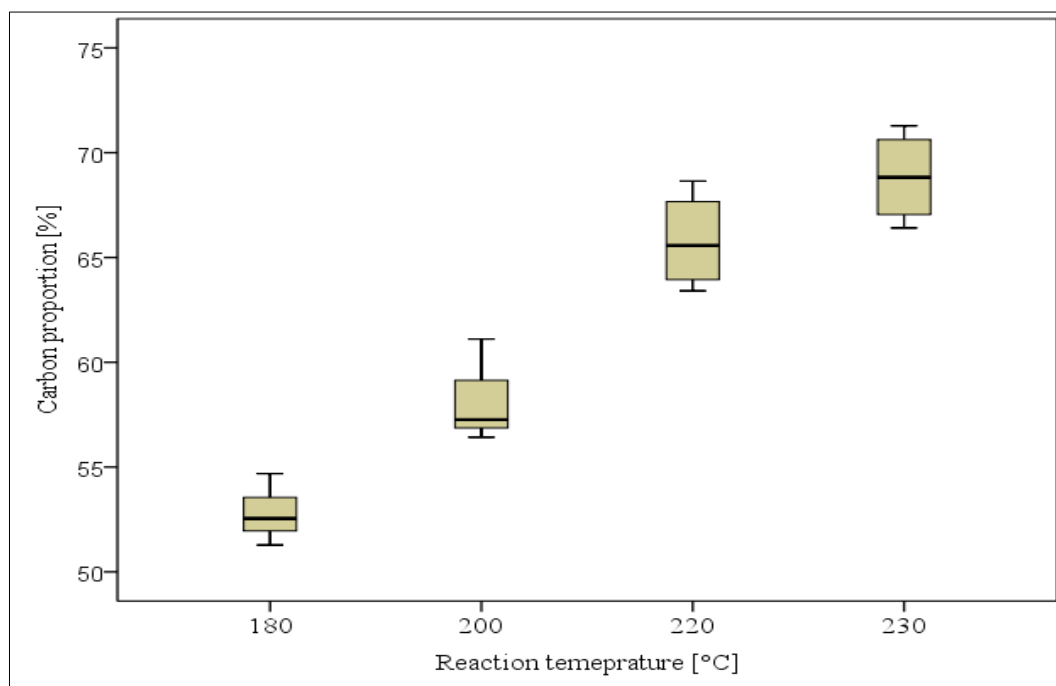


Figure V.1: Boxplots for the carbon proportion in HTC-chars produced at different reaction temperatures 180-230 °C and at 15 h using citric acid as catalyst

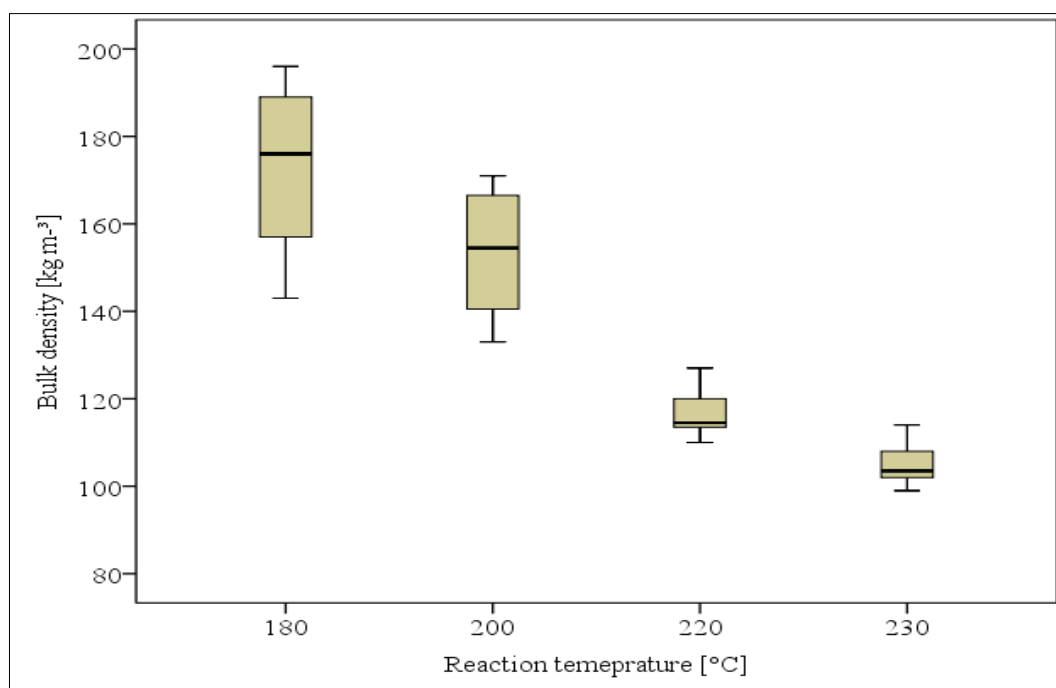


Figure V.2: Boxplots for the bulk density of HTC-chars produced at different reaction temperatures 180-230 °C and at 15 h using citric acid as catalyst

Table V.1: Analysis of variance and lack of fit test for the influence of the variation of reaction times (1-20 h) on the characterization of HTC-chars produced at 230 °C using citric acid as catalyst

Parameter		Sum of squares	Degree of freedom	Mean square	F-value	Significant
Yield [%]	Between groups	561.67	6	93.612	11.968	< 0.0001
	Within groups	602.26	77	7.822		
	Total	1163.93	83			
Carbon proportion [%]	Between groups	1474.93	6	245.821	88.063	< 0.0001
	Within groups	214.94	77	2.791		
	Total	1689.87	83			
Oxygen proportion [%]	Between groups	1614.99	6	269.165	90.153	< 0.0001
	Within groups	229.90	77	2.986		
	Total	1844.89	83			
Hydrogen proportion [%]	Between groups	4.54	6	0.757	3.377	0.005
	Within groups	17.26	77	0.224		
	Total	21.81	83			
Nitrogen proportion [%]	Between groups	15.58	6	2.596	2.676	0.021
	Within groups	74.70	77	0.970		
	Total	90.28	83			
Atomic ratio O/C [-]	Between groups	0.46	6	0.077	111.101	< 0.0001
	Within groups	0.05	77	0.001		
	Total	0.51	83			
Atomic ratio H/C [-]	Between groups	1.02	6	0.170	29.025	< 0.0001
	Within groups	0.45	77	0.006		
	Total	1.48	83			
Ash proportion [%]	Between groups	0.37	6	0.062	0.036	1.000
	Within groups	133.27	77	1.731		
	Total	133.64	83			
Specific surface area [m ² g ⁻¹]	Between groups	110.52	2	55.262	1.223	0.310
	Within groups	1220.38	27	45.199		
	Total	1330.90	29			
Bulk density [kg m ⁻³]	Between groups	60921.81	6	10153.635	30.393	< 0.0001
	Within groups	25723.75	77	334.075		
	Total	86645.56	83			

Table V.2: Statistical testing of significance of the effect of the solid load on the characterization of the groups of HTC-char produced

Parameter		N	Mean	Std. deviation	Std. error	95 % confidence interval for mean		Minimum	Maximum
						Lower bound	Upper bound		
Yield [%]	30	12	35.47	3.21	0.93	33.43	37.51	31.94	40.58
	50	12	39.07	3.58	1.03	36.79	41.35	35.25	44.67
	Total	24	37.27	3.80	0.78	35.66	38.87	31.94	44.67
Carbon proportion [%]	30	12	68.81	1.93	0.56	67.59	70.04	66.41	71.28
	50	12	68.63	1.93	0.56	67.40	69.86	65.92	71.30
	Total	24	68.72	1.89	0.39	67.92	69.52	65.92	71.30
Oxygen proportion [%]	30	12	21.34	2.05	0.59	20.04	22.64	19.05	23.78
	50	12	21.61	2.50	0.72	20.03	23.20	18.68	24.98
	Total	24	21.47	2.24	0.46	20.53	22.42	18.68	24.98
Hydrogen proportion [%]	30	12	5.19	0.36	0.10	4.96	5.42	4.58	5.88
	50	12	5.11	0.54	0.16	4.76	5.45	4.08	5.79
	Total	24	5.15	0.45	0.09	4.96	5.34	4.08	5.88
Nitrogen proportion [%]	30	12	2.25	1.22	0.35	1.47	3.02	0.68	3.89
	50	12	2.19	1.48	0.43	1.25	3.13	0.71	4.29
	Total	24	2.22	1.33	0.27	1.66	2.78	0.68	4.29
Atomic ratio O/C [-]	30	12	0.23	0.03	0.01	0.21	0.25	0.20	0.27
	50	12	0.24	0.03	0.01	0.22	0.26	0.20	0.28
	Total	24	0.24	0.03	0.01	0.22	0.25	0.20	0.28
Atomic ratio H/C [-]	30	12	0.90	0.05	0.01	0.87	0.94	0.83	1.00
	50	12	0.89	0.08	0.02	0.84	0.94	0.74	0.99
	Total	24	0.90	0.06	0.01	0.87	0.92	0.74	1.00
Ash proportion [%]	30	12	2.42	1.25	0.36	1.62	3.21	0.90	3.97
	50	12	2.46	1.28	0.37	1.65	3.27	0.74	4.18
	Total	24	2.44	1.24	0.25	1.92	2.96	0.74	4.18
Specific surface area [m ² g ⁻¹]	30	12	15.88	6.54	1.89	11.73	20.03	8.34	24.95
	50	12	17.56	6.88	1.99	13.19	21.93	9.62	27.68
	Total	24	16.72	6.62	1.35	13.93	19.52	8.34	27.68
Bulk density [kg m ⁻³]	30	12	105.25	5.01	1.45	102.07	108.43	99.00	114.00
	50	12	105.17	4.84	1.40	102.09	108.24	100.00	114.00
	Total	24	105.21	4.82	0.98	103.17	107.24	99.00	114.00

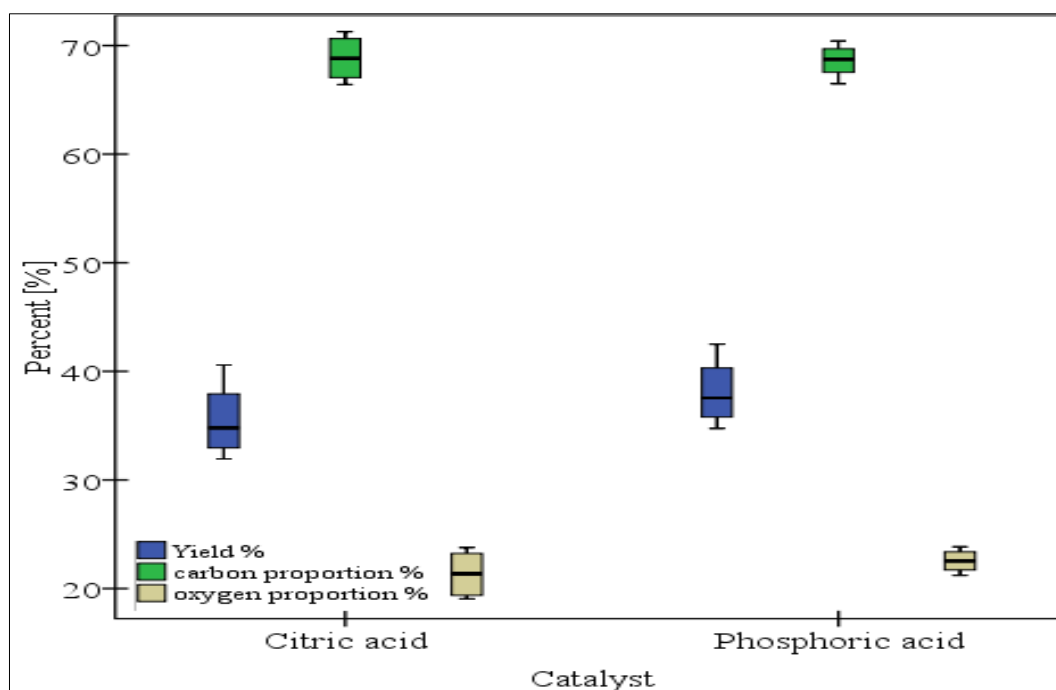


Figure V.3: Boxplots for the effect of the variation of catalysts on the characterization of the groups of HTC-char produced at 230 °C

Table V.3: Statistical testing of significance of the effect of the variation of particle sizes on the characterization of the groups of HTC-char produced

Parameter	N	Mean	Std. deviation	Std. error	95 % confidence interval for mean		Minimum	Maximum	
					Lower bound	Upper bound			
Yield [%]	0.50	12	32.52	2.62	0.76	30.86	34.18	29.82	37.12
	4.00	12	35.47	3.21	0.93	33.43	37.51	31.94	40.58
	Total	24	33.99	3.23	0.66	32.63	35.36	29.82	40.58
Carbon proportion [%]	0.50	12	68.48	2.35	0.68	66.99	69.97	65.39	71.55
	4.00	12	68.81	1.93	0.56	67.59	70.04	66.41	71.28
	Total	24	68.64	2.11	0.43	67.75	69.54	65.39	71.55
Oxygen proportion [%]	0.50	12	21.28	3.02	0.87	19.36	23.21	18.13	24.78
	4.00	12	21.34	2.05	0.59	20.04	22.64	19.05	23.78
	Total	24	21.31	2.53	0.52	20.24	22.38	18.13	24.78
Hydrogen proportion [%]	0.50	12	5.15	0.59	0.17	4.77	5.52	4.38	5.98
	4.00	12	5.19	0.36	0.10	4.96	5.42	4.58	5.88
	Total	24	5.17	0.48	0.10	4.97	5.37	4.38	5.98
Nitrogen proportion [%]	0.50	12	2.46	1.28	0.37	1.65	3.27	1.02	4.24
	4.00	12	2.25	1.22	0.35	1.47	3.02	0.68	3.89
	Total	24	2.35	1.23	0.25	1.83	2.87	0.68	4.24
Atomic ratio O/C [-]	0.50	12	0.23	0.04	0.01	0.21	0.26	0.19	0.28
	4.00	12	0.23	0.03	0.01	0.21	0.25	0.20	0.27
	Total	24	0.23	0.03	0.01	0.22	0.25	0.19	0.28
atomic ratio H/C [-]	0.50	12	0.90	0.08	0.02	0.85	0.95	0.80	1.02
	4.00	12	0.90	0.05	0.01	0.87	0.94	0.83	1.00
	Total	24	0.90	0.06	0.01	0.88	0.93	0.80	1.02
Ash proportion [%]	0.50	12	2.63	0.97	0.28	2.01	3.25	1.45	3.93
	4.00	12	2.42	1.25	0.36	1.62	3.21	0.90	3.97
	Total	24	2.52	1.10	0.22	2.06	2.99	0.90	3.97

Statistical testing of significance of batch adsorption study

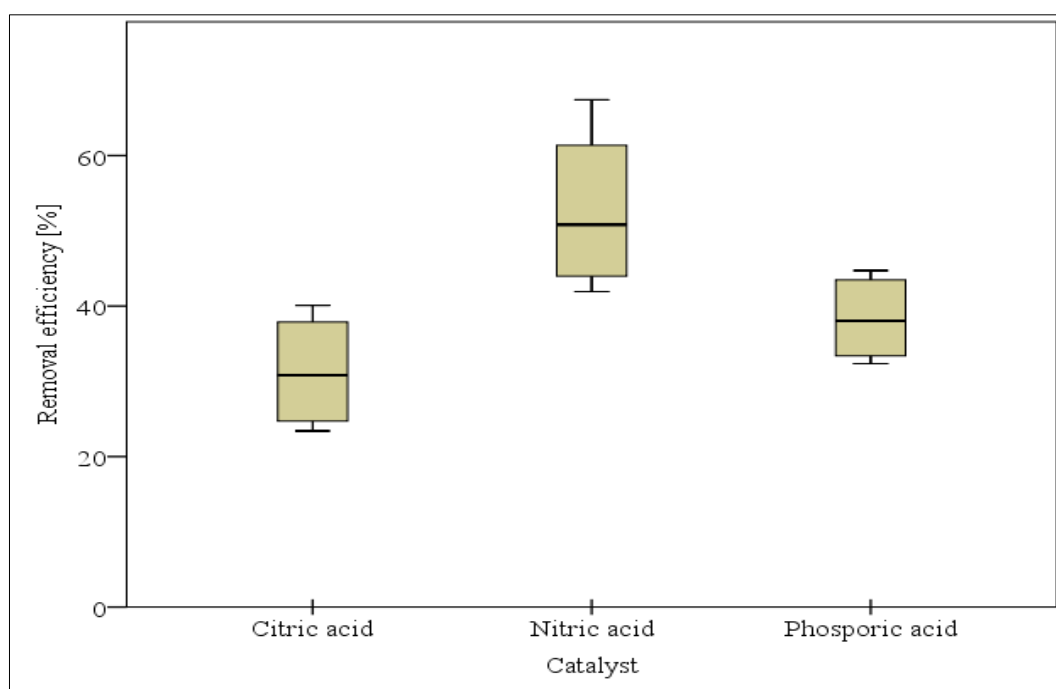


Figure V.4: Boxplots for the effect of the variation of the adsorbents prepared from different HTC-char types on the ammonia removal efficiency rate (R [%]) of HTC-chars

Table V.4: Analysis of variance and lack of fit test for the effect of the contact time on the adsorption performance of adsorbents before oxidizing with nitric acid

Adsorbents before oxidation		Sum of squares	Degree of freedom	Mean square	F-value	Significant
Removal efficiency [%]	Between groups	11308.06	4.00	2827.01	61.10	< 0.0001
	Within groups	5320.56	115.00	46.27		
	Total	16628.62	119.00			
Adsorption capacity [mg g^{-1}]	Between groups	572.16	4.00	143.04	61.08	< 0.0001
	Within groups	269.31	115.00	2.34		
	Total	841.47	119.00			

Table V.5: Analysis of variance and lack of fit test for the effect of the contact time on the adsorption performance of adsorbents after oxidizing with nitric acid

Adsorbents oxidizing with nitric acid		Sum of squares	Degree of freedom	Mean square	F-value	Significant
Removal efficiency [%]	Between groups	2195.83	4.00	548.96	6.30	< 0.0001
	Within groups	4790.05	55.00	87.09		
	Total	6985.87	59.00			
Adsorption capacity [mg g^{-1}]	Between groups	112.30	4.00	28.07	6.39	< 0.0001
	Within groups	241.53	55.00	4.39		
	Total	353.83	59.00			

Table V.6: Analysis of variance and lack of fit test for the effect of the initial ammonia concentration on the adsorption performance of adsorbents before oxidizing with nitric acid

Adsorbents before oxidation		Sum of squares	Degree of freedom	Mean square	F-value	Significant
Removal efficiency [%]	Between groups	16730.04	5.00	3346.01	129.66	< 0.0001
	Within groups	3561.28	138.00	25.81		
	Total	20291.32	143.00			
Adsorption capacity [mg g ⁻¹]	Between groups	857.09	5.00	171.42	83.79	< 0.0001
	Within groups	282.31	138.00	2.05		
	Total	1139.40	143.00			

Table V.7: Analysis of variance and lack of fit test for the effect of the initial ammonia concentration on the adsorption performance of adsorbents after oxidizing with nitric acid

Adsorbents oxidizing with nitric acid		Sum of squares	Degree of freedom	Mean square	F-value	Significant
Removal efficiency [%]	Between groups	6256.32	5.00	1251.26	13.16	< 0.0001
	Within groups	6276.78	66.00	95.10		
	Total	12533.09	71.00			
Adsorption capacity [mg g ⁻¹]	Between groups	2159.39	5.00	431.88	33.38	< 0.0001
	Within groups	853.85	66.00	12.94		
	Total	3013.23	71.00			

Table V.8: Analysis of variance and lack of fit test for the effect of solution pH on the adsorption performance of adsorbents before oxidizing with nitric acid

Adsorbents before oxidation		Sum of squares	Degree of freedom	Mean square	F-value	Significant
Removal efficiency [%]	Between groups	12129.52	3.00	4043.17	408.44	< 0.0001
	Within groups	435.55	44.00	9.90		
	Total	12565.07	47.00			
Adsorption capacity [mg g ⁻¹]	Between groups	614.01	3.00	204.67	408.51	< 0.0001
	Within groups	22.04	44.00	0.50		
	Total	636.06	47.00			

Table V.9: Analysis of variance and lack of fit test for the effect of solution pH on the adsorption performance of adsorbents after oxidizing with nitric acid

Adsorbents oxidizing with nitric acid		Sum of squares	Degree of freedom	Mean square	F-value	Significant
Removal efficiency [%]	Between groups	17196.95	3.00	5732.32	320.92	< 0.0001
	Within groups	357.25	20.00	17.86		
	Total	17554.20	23.00			
Adsorption capacity [mg g ⁻¹]	Between groups	870.15	3.00	290.05	321.72	< 0.0001
	Within groups	18.03	20.00	0.90		
	Total	888.19	23.00			

Table V.10: Analysis of variance and lack of fit test for the effect of adsorbent mass on the adsorption performance of adsorbents before oxidizing with nitric acid

Adsorbents before oxidation		Sum of squares	Degree of freedom	Mean square	F-value	Significant
Removal efficiency [%]	Between groups	4471.35	3.00	1490.45	104.08	< 0.0001
	Within groups	630.09	44.00	14.32		
	Total	5101.43	47.00			
Adsorption capacity [mg g ⁻¹]	Between groups	107.37	3.00	35.79	77.09	< 0.0001
	Within groups	20.43	44.00	0.46		
	Total	127.80	47.00			

Table V.11: Analysis of variance and lack of fit test for the effect of adsorbent mass on the adsorption performance of adsorbents after oxidizing with nitric acid

Adsorbents oxidizing with nitric acid		Sum of squares	Degree of freedom	Mean square	F-value	Significant
Removal efficiency [%]	Between groups	3849.80	3.00	1283.27	37.41	< 0.0001
	Within groups	686.11	20.00	34.31		
	Total	4535.91	23.00			
Adsorption capacity [mg g ⁻¹]	Between groups	150.04	3.00	50.01	24.15	< 0.0001
	Within groups	41.42	20.00	2.07		
	Total	191.46	23.00			

Statistical testing of significance of dynamic fixed-bed column study

Table V.12: Analysis of variance and lack of fit test for the effect of flow rate on the adsorption performance of adsorbents before oxidizing with nitric acid

Adsorbents before oxidation (first group)		Sum of squares	Degree of freedom	Mean square	F-value	Significant
Breakthrough time [h] (at $C_e/C_0 = 0.5$)	Between groups	1629.148	2	814.574	13147.47	< 0.0001
	Within groups	0.929	15	0.062		
	Total	1630.077	17			
Breakthrough capacity $Q_{0.5}$ [mg g^{-1}]	Between groups	8.900	2	4.450	56.365	< 0.0001
	Within groups	1.184	15	0.079		
	Total	10.084	17			
Time required for bed exhaustion T_e [h] (at $C_t/C_e = 0.9$)	Between groups	3161.814	2	1580.907	4096.203	< 0.0001
	Within groups	5.789	15	0.386		
	Total	3167.603	17			

Table V.13: Analysis of variance and lack of fit test for the effect of flow rate on the adsorption performance of adsorbents after oxidizing with nitric acid

Adsorbents oxidizing with nitric acid (second group)		Sum of squares	Degree of freedom	Mean square	F-value	Significant
Breakthrough time [h] (at $C_e/C_0 = 0.5$)	Between groups	14078.719	2	7039.360	13.367	< 0.0001
	Within groups	7899.431	15	526.629		
	Total	21978.150	17			
Breakthrough capacity $Q_{0.5}$ [mg g^{-1}]	Between groups	35.437	2	17.718	0.305	0.741
	Within groups	870.138	15	58.009		
	Total	905.575	17			
Time required for bed exhaustion [h] (at $C_t/C_e = 0.9$)	Between groups	2644.700	2	1322.350	36.028	< 0.0001
	Within groups	440.436	12	36.703		
	Total	3085.136	14			

Table V.14: Analysis of variance and lack of fit test for the effect of initial ammonia concentration on the adsorption performance of adsorbents before oxidizing with nitric acid

Adsorbents before oxidation (first group)		Sum of squares	Degree of freedom	Mean square	F-value	Significant
Breakthrough time [h] (at $C_e/C_0 = 0.5$)	Between groups	23.26	2.00	11.63	747.46	< 0.0001
	Within groups	0.23	15.00	0.02		
	Total	23.50	17.00			
Breakthrough capacity $Q_{0.5}$ [mg g^{-1}]	Between groups	4.14	2.00	2.07	24.92	< 0.0001
	Within groups	1.25	15.00	0.08		
	Total	5.38	17.00			
Time required for bed exhaustion T_e [h] (at $C_t/C_e = 0.9$)	Between groups	49.56	2.00	24.78	572.87	< 0.0001
	Within groups	0.65	15.00	0.04		
	Total	50.21	17.00			

Table V.15: Analysis of variance and lack of fit test for the effect of initial ammonia concentration on the adsorption performance of adsorbents after oxidizing with nitric acid

Adsorbents oxidizing with nitric acid (second group)		Sum of squares	Degree of freedom	Mean square	F-value	Significant
Breakthrough time [h] (at $C_e/C_0 = 0.5$)	Between groups	68.12	2.00	34.06	0.96	0.40
	Within groups	530.46	15.00	35.36		
	Total	598.58	17.00			
Breakthrough capacity $Q_{0.5}$ [mg g ⁻¹]	Between groups	72.25	2.00	36.13	0.86	0.44
	Within groups	631.03	15.00	42.07		
	Total	703.28	17.00			
Time required for bed exhaustion T_e [h] (at $C_t/C_e = 0.9$)	Between groups	141.90	2.00	70.95	0.92	0.42
	Within groups	1155.94	15.00	77.06		
	Total	1297.84	17.00			

Table V.16: Analysis of variance and lack of fit test for the effect bed height on the adsorption performance of adsorbents before oxidizing with nitric acid

Adsorbents before oxidation (first group)		Sum of squares	Degree of freedom	Mean square	F-value	Significant
Breakthrough time [h] (at $C_e/C_0 = 0.5$)	Between groups	49.57	1.00	49.57	785.35	< 0.0001
	Within groups	0.63	10.00	0.06		
	Total	50.20	11.00			
Breakthrough capacity $Q_{0.5}$ [mg g ⁻¹]	Between groups	7.29	1.00	7.29	51.88	< 0.0001
	Within groups	1.40	10.00	0.14		
	Total	8.69	11.00			
Time required for bed exhaustion T_e [h] (at $C_t/C_e = 0.9$)	Between groups	70.42	1.00	70.42	618.71	< 0.0001
	Within groups	1.14	10.00	0.11		
	Total	71.56	11.00			

Table V.17: Analysis of variance and lack of fit test for the effect bed height on the adsorption performance of adsorbents after oxidizing with nitric acid

Adsorbents oxidizing with nitric acid (second group)		Sum of squares	Degree of freedom	Mean square	F-value	Significant
Breakthrough time [h] (at $C_e/C_0 = 0.5$)	Between groups	133.13	1.00	133.13	2.99	0.11
	Within groups	445.46	10.00	44.55		
	Total	578.60	11.00			
Breakthrough capacity $Q_{0.5}$ [mg g ⁻¹]	Between groups	0.68	1.00	0.68	0.02	0.89
	Within groups	353.58	10.00	35.36		
	Total	354.26	11.00			
Time required for bed exhaustion T_e [h] (at $C_t/C_e = 0.9$)	Between groups	139.40	1.00	139.40	1.56	0.24
	Within groups	890.75	10.00	89.07		
	Total	1030.15	11.00			

Eidesstattliche Erklärung

Hiermit erkläre ich durch eigenhändige Unterschrift, die vorliegende Dissertation selbstständig verfasst und keine anderen als die angegebenen Quellen und Hilfsmittel verwendet zu haben. Die aus den Quellen direkt oder indirekt übernommenen Gedanken sind als solche kenntlich gemacht. Die Dissertation ist in dieser Form noch keiner anderen Prüfungsbehörde vorgelegt worden.

Rostock, den 17.10.2018

Unterschrift

Theses of the doctoral thesis

- *The hydrothermal carbonization process can be used to develop the characteristic of biomass and produce a sterile solid product*

Some properties of biomass make it unsuitable for use as energy feedstock, in carbon sequestration or improvement of soil fertility. However, not only does biomass have an interesting internal structure, it also has the advantage of being available in large quantities at low cost. Moreover, non-fossil carbon sources such as biomass present promising renewable energy carrier. Therefore, pre-treatment technologies can be used to develop the characteristic of biomass and convert it into useful and homogenous products, more efficient energy carriers or carbon storage deposits. Hydrothermal carbonization process (HTC) is a thermo-chemical process for the conversion of organic material, which can improve the properties of biomass. Wet biomass can be transformed into carbonaceous materials with no request to be dried before or during HTC-process. When HTC-char is used in heating, large amounts of greenhouse gases emissions can be mitigated compared with the fossil-derived sources of energy. Due to its reaction temperature, HTC-process is seen as an innovative method to convert problematic biomass like bio-waste, sewage sludge and fermentation residue in a renewable, sterile and hygienic solid product.

- *Wetland biomasses can be converted into sustainable carbonaceous materials*

Due to the increasing demand, the supply of biomass for different utilizations is becoming limited. This is reflected in rising prices of biomass as well as in an area competition between food, feed and energy production. From a global perspective, Germany is one of the regions rich in wetland areas. However, the production of biomass from re-wetted or wetland is not in competition with other agricultural products. They are abundant at low costs and their properties can be improved using treatment technologies, which may give them a higher value. Rapidly growing grassy plants, such as, reed, typha, juncus and carex, belong to the promising sources of plant biomasses. Their short rotation period and abundant content give favorable application possibilities. HTC can be used for the treatment of such biomasses to generate sustainable carbonaceous materials with higher carbon content than the original biomasses.

- *HTC-process parameters have an influence on the HTC-char*

Depending on the process parameters, HTC-chars produced were carbon rich and chemically similar to lignite or bituminous coal. The color of biomass changed through HTC-process because of the losses of the moisture and light volatile gases at different stages of HTC depended on the process parameters. The changes in color can be as an indicator of the degree of conversion. The characteristics of HTC-char varied with both raw materials used and hydrothermal carbonization parameters as well as the follow-up treatment of HTC-chars produced. The properties of HTC-chars produced from different raw materials at the same process parameter differed from each other. Reaction temperatures and reaction times affected significantly the composition of HTC-chars produced. Higher reaction temperatures and longer reaction times resulted in lower yields of HTC-chars, a significantly decrease in each of oxygen proportion, bulk density and H/C and O/C atomic ratios. A significantly increase in the carbon proportion and specific surface area were obtained. The variation of catalyst, solid load and particle size had lower effect on the properties of HTC-chars produced than those were by the variation of both reaction temperatures and reaction times. The nature of the raw materials and HTC-conditions as well as the oxidation of HTC-chars with nitric acid influenced the surface functional groups presented on HTC-chars.

- *HTC-chars from wetland biomasses can be used as alternative and competitive adsorbents for the removal of ammonia in aqueous solution*

Air and water pollutants affect human and animal health and their well-being; they contribute also to environmental pollution. Ammonia (NH_3) and ammonium (NH_4^+) are familiar by-products of animal and agriculture waste as well as the industrial activities. They are undesirable contaminants because of their negatively impact on air and water quality. Some traditional techniques are available for water treatment applications, particularly for the removal of ammonia and ammonium ions. However, associated operational and technical maintenance problems, strict monitoring and control of operating conditions and the high costs of these methods restrict their applicability. Adsorption processes using dry adsorbents is estimated as superior to other methods. Nevertheless, the difficulty of the use of commercially synthetic sorbents such as activated carbon

and its regeneration problem requested to investigate and develop alternative effective and cheaper adsorbents synthesized of cheap natural or raw agricultural materials. Such materials can be as potential replacements for the expensive commercial adsorbents and can improve the efficiency of ammonia removal. In recent times, using low cost natural materials, agricultural residue and waste products to produce potential replacements of the expensive commercial adsorbents for the removal of pollutants is a promising approach.

- *The ammonia removal efficiency of HTC-chars is affected by the adsorption parameters in the batch study*

Batch study using ammonia solution as a model compound were used to measure the adsorption performance of ammonia in aqueous solution onto HTC-chars produced. Adsorbents produced at different reaction temperatures during HTC showed different adsorption performances. The highest ones were with those produced at HTC-reaction temperature of 230 °C, especially those produced from reed. The type of raw material, the catalyst used during HTC or the oxidation of the HTC-chars after production affected significantly the adsorption performances. A quite good removal was achieved with a contact time of one hour. Increasing the initial ammonia concentration decreased significantly the removal efficiency rates because of the limited number of adsorption sites on the adsorbent. The best adsorption performance was achieved at pH of solution with 9.35. The removal efficiency rate of ammonia increased with the increase of adsorbent dosage but the adsorption capacity decreased. The catalyst used during HTC-process or the oxidation of the HTC-chars after production affected their chemical structure and might create adsorption sites, which enhanced significantly their adsorption performance. The oxidized HTC-chars became more acidic and ammonia was strongly adsorbed on their surface. As a result, the adsorption performance of the adsorbents used in batch study were significantly affected by the variation of adsorption parameters.

- *The ammonia removal efficiency of HTC-chars is affected by the adsorption parameters in fixed-bed column study*

Dynamic fixed-bed column experiments determine the change in removal efficiency with the time. They are requested to attain basic data for direct applications in industrial systems. The fixed-bed column study was carried out

using HTC-chars that had the best ammonia removal efficiency in the already performed batch study. In general, lower flow rates during the adsorption process resulted in a longer breakthrough times and times required for bed exhaustion, which increased the lifetime of the adsorbents. The variation of flow rates had a significant effect on the adsorption performances of all adsorbents used. Furthermore, increasing initial ammonia concentrations resulted in lower breakthrough times for all adsorbents used, but the breakthrough capacities were increased. It was seen that varying the bed heights exhibited a change on breakthrough curves. The column saturation times were longer by increasing the bed heights, which enabled a longer lifetime of the column. However, the variation of initial ammonia concentrations and the bed heights had no significant effect on adsorbents oxidizing with nitric acid. Adsorbents prepared from HTC-chars produced from reed, especially after oxidation showed the highest adsorption performances.

- *HTC-chars are regenerable adsorbents. They can be reused several times without loss of their adsorption performances after regeneration*

In addition to its high adsorption capacity, a good adsorbent must also present a good ability of reuse during multiple adsorption-regeneration cycles, which is substantial importance in the economic development. Regeneration and reuse of the adsorbent material is a crucial aspect to make it more environments friendly and economical. The investigations of the possibility of the regeneration of the exhausted adsorbents were performed for some adsorbents used in both the batch study and the fixed-bed column study. All regeneration tests were carried out at room temperature. The exhausted HTC-chars were regenerable and could be reused even many times. The best regeneration results were achieved using HCl solution as a regenerant. The highest regeneration efficiency was found with the oxidized HTC-chars, especially with those produced from reed. A decrease in the adsorption performance after regeneration was found with some adsorbents used.

- *HTC-char from wetland biomasses can be used as a filter material as an alternative for activated carbon*

HTC-char is a low-cost adsorbent with many potential environmental applications. The exhausted HTC-char can be applied directly as fertilizer with no need to be regenerated. The results of this work confirmed that it was

possible to transform these wetland biomasses into higher value carbonaceous products with a sufficiently high efficiency for ammonia removal in aqueous solution, which could be designed as a filter. The advantage of using HTC-char of reed as adsorbent for ammonia removal exists not only because of its highest adsorption performance, but also of its highest char yield and its higher affinity for regeneration. In this respect, recent HTC-chars produced from wetland biomasses, especially those from reed are giving promising results in terms of regenerative ability, because it can be reused several times without a significant decreasing in its removal capacity after regeneration process. The regeneration of adsorbents extends their lifetimes and makes them ecologically and economically feasible. The potential regeneration and reuse of adsorbents used can minimize the need of raw material, which make them more sustainable for the environment and result in a less energy consumption for producing new adsorbents.

- *Perspectives and further research needs*

One of the most crucial challenges in the biochar industry is the inability of measuring and characterizing the quality during the carbonization process continuously, which is a key property and will open an enormous potential for carbonization engineering.

Furthermore, controlling how to produce a particular quality of HTC-char for a specific application is of importance in the process engineering design, especially because the researches aim to develop new technologies. The achievement of this objective will be through a planned future project realized. The predicated method for this purpose (DE 102016125286A1) is patent-pending process. The main goal of our future works is a product with a wide

ACKNOWLEDGEMENTS

I would like to express my deepest gratitude to my supervisor Prof. Dr. Norbert Kanswohl for the guidance and active participation during this research. His encouragement and patience were a great help to me.

I would like to thank Prof. Dr. Frank Scholwin and Prof. Dr. Christina Dornack for reviewing my thesis.

I am also grateful to my colleagues in our research group. I would like to appreciate staffs of Leibniz Institute for Catalysis Rostock for the good cooperation and the support during the implementation of some analyses. I thank Ms. Dittmann (AUF, University of Rostock) for the advice regarding the statistical analyses

I would like to acknowledge the financial support from Rosa-Luxemburg-Stiftung. I am also grateful to Prof. Fritz Tack for his support.

And last but certainly not least, I wish to express my deepest gratitude to my family members. My sincere gratitude goes to my wife Yara and my daughter Ghazal. Thank them for all the unconditional love and support to me. Their love has been and will always be a great source of inspiration in my life.

Lebenslauf

Persönliche Angaben

Name: Bassel Ibrahim

Geburtsdatum: 26.09.1975

Schulausbildung

1981-1986 Grundschule

1987-1989 Mittelschule

1990-1993 Sekundarschule/ Gymnasium

Abschluss: Reifezeugnis einer allgemein bildenden Sekundarschule
wissenschaftlicher Zweig

Studium

1993-1998 Bakkalaureus Verfahrenstechnik der Petrolchemie. Fakultät für Chemie u.
Petrolchemie - Al Baath-Universität-Homs-Syrien

2000 Fach- u. Qualifikationsdiplom im Fachgebiet „Computerwissenschaften u.
deren Anwendungen in der Wirtschaft“. Fakultät für Wirtschaft – Aleppo
Universität- Aleppo- Syrien

2002 Diplom des postgradualen Studiums im Fachgebiet „Bohren und
Produktion der Gas- u. Erdölbrunnen“. Fakultät für Chemie u.
Petrolchemie - Al Baath-Universität- Homs-Syrien

2010 Doktorand im Bereich Umwelttechnologie an der Universität Rostock

Sprachkenntnisse

Deutsch: sehr gute Kenntnisse in Wort und Schrift

Arabisch: Muttersprache

Englisch: sehr gute Kenntnisse in Wort und Schrift

EDV-Kenntnisse

Sehr gute MS-Office Kenntnisse

Auslandsaufenthalte für wissenschaftliche und technische Arbeiten

2002 Großbritannien, SCADA und DCS-Systeme zur Erdgas-Druckreduzierung
und Messanlagen

2004 Ägypten, Berechnung der Gastransportkosten

2005 Ägypten, Hydraulische Berechnung von Öl- und Gaspipelines

2007 Großbritannien, Prozessmodellierung mit Varisim-Programm

2008 Ukraine, Prozessmodellierung mit Aspen-Hysys-Programm

Erfahrungen

01.02.2017 Wissenschaftlich Mitarbeiter am Innovations- und Bildungszentrum
- Hohen Luckow

01.01.2016- Projektleiter an der Universität Rostock

30.11.2016 Wissenschaftlicher Mitarbeiter im Bereich Energie- Umwelt- Wirtschaft
an der Universität Rostock

01.04.2015- Wissenschaftlich Mitarbeiter am Innovations- und Bildungszentrum
31.12.2015 Hohen Luckow

2010- Promotionsstudent an der Universität Rostock. Erfahrungen im Bereich
Umwelttechnik

2003- Leiter der wirtschaftlichen und technischen Studienabteilung, Industrie
30.05.2009 Branche in Syrien

2001-2003 Prozessingenieur, Projektingenieur, Projektkoordinator,
Projektmanagement, Industrie Branche

1998 -2001 Prozessingenieur Projektingenieur Industrie Branche

Veröffentlichung

Fachzeitschrift

- **Ibrahim, B.**, Schlegel, M., Kanswohl, N. **(2018)**: Effectiveness of Biochar from Hydrothermal Carbonization of Wetland Biomass for Sorption of ammonia. Chemie Ingenieur Technik. 90(3): 340-347.
- **Ibrahim, B.**, Schlegel, M., Kanswohl, N. **(2014)**: Investigation of applicability of wetland biomass for producing biochar by hydrothermal carbonization (HTC). Landbauforsch Appl Agric Forestry Res. 2(64): 119-124.

Patente

- DE 102016100639.4: Verfahren zur Behandlung einer Biomasse. Anmeldedatum: 15.01.2016. Veröffentlichungsdatum: 20.07.2017. Erfinder: **Ibrahim, B., Schlegel, M.**
- DE 102016100527.4: Herstellung eines Supplementkomplexes, insbesondere für zur Biogaserzeugung verwendbare Biomassen Anmeldedatum: 14.01.2016. Veröffentlichungsdatum: 20.07.2017. Erfinder: **Ibrahim, B., Schlegel, M.**
- DE 102016125286.7: Verfahren zur Herstellung von Biokohle. Intervallkondensation von Gas der hydrothermalen Karbonisierung (HTC) mit nachgeschalteter Prüfung des Kondensats zur Abbildung des Verkohlungsstandes. Anmeldedatum: 21.12.2016. Veröffentlichungsdatum: 21.06.2018. Erfinder: **Ibrahim, B., Schlegel, M.**
- URS-29103 Verfahren zur Herstellung von Biokohle durch HTC. Eingereicht im Juli 2018. Erfinder: **Ibrahim, B., Schlegel, M.**

Tagungen und Fachvorträge

- Schlegel, M., **Ibrahim, B.**, Wohlrab, S., Fras, J., Kanswohl, N., Zosel, J. **(2018)**: Online-Messung des hydrothermalen Karbonisierungsprozesses zur Erhöhung der Kohlequalität. In: Prof. Dr. M. Nelles: Tagungsband 12. Rostocker Bioenergieforum: Schriftenreihe Umweltingenieurwesen. 78. Rostock, 2018. SBN 978-3-86009-473-0, 277-286.
- Hudde, J., Orth, M., **Ibrahim, B.**, König, K., Bröcker, F. **(2017)**: Alternatives Entsorgungssystem für internationale Schiffsabfälle zur Energieerzeugung. 7. Statuskonferenz. Bioenergie. Flexibel und integriert in die nächste Epoche. 20-21 NOV 2017 LEIPZIG.
- Schlegel, M., **Ibrahim, B.**, Kipping-Rössel, D., Ortiz-Laurel, H., Perez Pineda, E. **(2017)**: Verwendung der abgetrennten festen Phase einer mikrobiologischen anaeroben Hydrolyse als Ausgangsstoff für die Erzeugung von Biokohle. In: Hochschule Stralsund: 24. Stralsunder Symposium "Nutzung regenerativer Energiequellen und Wasserstofftechnik".
- Schlegel, M., **Ibrahim, B.**, Fras, J., Kanswohl, N., Zosel, J. **(2017)**: Hydrothermal carbonization processes to increase the transportability of plant biomasses. In: Conference Economy and Efficiency - contemporary solutions in logistics and production, OiE.

- Hudde, J., Orth, M., **Ibrahim, B.**, König, K., Bröcker, F. (2017): Biogaserzeugung aus Schiffsabfällen internationaler Herkunft. In: Tagungsband des 11. Rostocker Bioenergieforum. Schriftenreihe Umweltingenieurwesen Agrar- und Umweltwissenschaftliche Fakultät der Universität Rostock. Band 68 2017.
- Ortíz-Laurel, H., Rössel-Kipping, D., **Ibrahim, B.**, Gonzalez-Muñoz, L., Kanswohl, N., Schlegel, M. (2017): Energiebilanz der Rizinusölpflanze (*Ricinus communis* L.) bei Betrachtung des verfügbaren Energiepotenzials aller Pflanzenbestandteile. In: Schriftenreihe Umweltingenieurwesen; Prof. Dr. Michael Nelles (Hrsg.) Universität Rostock (Hrsg.): Tagungsband 11. Rostocker Bioenergieforum. 68. Rostock, 2017. - ISBN 978-3-86009-455-6, 353-361.
- Schlegel, M., Eltigani, A., Abdelgayoum, S., Kanswohl, N., **Ibrahim, B.**, Orth, M. (2017): Residues of food industry for generating biogas. In: Ministry of Climate Change and Environment in Association with Dubai Chamber (Hrsg.): Symposium on Food Industry and Environment, Dubai Chamber of Commerce. Vereinigte Arabische Emirate, 2017, 6 -7.
- Schlegel, M., Kanswohl, N., **Ibrahim, B.**, Rehl, T. (2016): Energiebilanz der Reststoffe – am Beispiel einer deutschen Region (Deutsch-Slowakische Konferenz, Bratislava). In: Deutsch-slowakische Auslandshandelskammer: Energiewächter/ Exportinitiative Energie d. Bundesministeriums für Wirtschaft und Energie. Bratislava, 2016, 20-21.
- Schlegel, M., Fras, J., Geick, T., Zosel J., Schelter, M., Kritznier, A., Orth, M., **Ibrahim B.**, Kanswoh N. (2016): Logistical advantages due to the use of an innovative sensor unit for controlling optimum biogas processes. Research Paper. Poznan University of Technology. 6(5): 407-418. DOI: 10.21008/j.2083-4950.2016.6.5.
- **Ibrahim, B.**, Schlegel, M., Kanswohl, N. (2014): Charakterisierung der durch hydrothermale Karbonisierung (HTC) aus Moorbiomasse produzierten Biokohle: Auswirkungen des Karbonisierungsprozesses auf die Biokohleneigenschaften. In: HTP-Fachforum „Biobasierte hydrothermale Prozesse –Technologien zur stofflichen und energetischen Nutzung“. Poster und „Speed Präsentation“ der Poster. Leipzig: DBFZ. ISSN 2197-4632.
- **Ibrahim, B.** (2014): Behandlung von hydrothermal karbonisierten Biomassen für die Ammoniakabtrennung: Der hydrothermale Karbonisierungsprozesses (HTC). Doktorand_innen-Jahrbuch 2014 der Rosa-Luxemburg-Stiftung. VSA: Verlag 2014 Hamburg. ISBN 978-3-89965-628-2, 165-174.
- **Ibrahim, B.**, Schlegel, M., Geick, T., Kanswohl, N. (2013): Behandlung von hydrothermal karbonisierten Biomassen für die Ammoniakabtrennung aus Biogas. Tagungsband XX. Energie-Symposium. 7.-9. November 2013, Stralsund.